Gene Expression Profiling of Mesenchymal Stem Cells Aged In Vitro

Malcolm B Will

MBChB, MRCS

A thesis submitted to the University of Glasgow

in partial fulfilment of the requirements

for the Degree of Doctor of Philosophy

June 2010

Section of Experimental Haematology and Haematopoietic Stem Cells

and Department of Medical Oncology,

University of Glasgow

Abstract

Mesenchymal Stem Cells (MSC's) have shown promise as a cell-based therapy for myocardial repair. However, MSC's have a finite replicative lifespan and lose proliferative and differentiation capacity during expansion *in vitro*. Therefore, understanding the molecular mechanisms that regulate ageing and senescence of MSC's should enhance our ability to use these cells in cell-based approaches and give insight into mechanisms of tissue ageing.

We established MSC cultures from the sternal bone marrow of eight donors undergoing coronary artery bypass surgery. After thirty population doublings (nine passages) MSC's displayed morphological abnormalities, expression of senescence associated ß-galactosidase, telomere erosion and decreased adipogenic and osteogenic differentiation capacity. Using serial analysis of gene expression (SAGE) we identified 243 known genes differentially expressed between MSC's at passages two and nine. Analysis of known direct interactions between genes revealed a regulatory signaling network centered on down-regulation of the transcription factor, activator protein 1 (AP-1). Transcriptional changes in MSC's at passage nine included genes associated with inflammation, regulation of cell cycle, metabolism and extracellular matrix re-modelling. The validation studies corroborated the SAGE results and eighteen genes were identified as differentially expressed in late passage MSC's from multiple donors. Furthermore, caveolin 1, cyclin D1, tissue plasminogen activator and olfactomedin-like 3 were able to discriminate MSC's of different culture age.

In addition, we show evidence that the p38 MAPK signalling pathway contributes to the decline in proliferation and differentiation of MSC's during expansion and is critical for the maintenance of genomic stability. The results provide further evidence that MSC's senesce prematurely in response to undefined culture stresses. Our studies have provided novel markers that identify MSC ageing *in vitro* and suggest that identifying factors that activate p38 MAPK signalling should enhance our ability to use MSC's in cell-based therapies.

Acknowledgements

I would like to thank my two scientific supervisors, Jo Mountford and Nicol Keith, for giving me their full support and scientific knowledge that was required to complete this research. It has been an excellent training and I am very grateful to have been given the opportunity.

I would also like to thank my clinical supervisor, Andrew Murday who has always been my advocate and my advisor, Karin Oien for her support during my time in the laboratory as well as her expertise in the SAGE method.

Many thanks to Sharon Burns, Stacey Hoare, Katrina Jackson, Claire Cairney and Alan Bilsland of the O2 research group for the tuition in molecular biology and contribution to this project. I would also like to acknowledge members of Tessa Holyoake's group, past and present for all their help, reagents and general discussion.

I am most grateful for the financial support provided by the British Heart Foundation, Glasgow Royal Infirmary Endowments Fund, Tenovus Scotland and the Scottish Heart Transplant Endowments Fund.

And last and definitely not least, the biggest thanks and love go to my family. Sally, you are a tower of strength and I appreciate your endless nagging to get this thesis finished – yes it took a while! My daughters Gracie, Izzy and Erin – I am so lucky to have you in my life and one day you can read the book that daddy was writing.

Author's Declaration

I am the sole author of this thesis. All the references have been consulted by me in the preparation of this manuscript. Except where otherwise stated, the work presented in this thesis was performed personally.

Abbreviations

Ab	Antibody
ALT	Alternative Lengthening of Telomeres
AP-1	Activator Protein 1
BM	Bone Marrow
CABG	Coronary Artery Bypass Surgery
CD	Cluster Differentiation
CDK	Cyclin-Dependent Kinase
CDKN	Cyclin-Dependent Kinase Inhibitor
CGH	Comparative Genomic Hybridisation
CSC	Cardiac Stem Cell
DGED	Digital Gene Expression Displayer
DNA	Deoxyribonucleic Acid
DNase	Deoxyribonuclease
EPC	Endothelial Progenitor Cell
ESC	Embryonic Stem Cell
FACS	Fluorescent Activated Cell Sorting
FGF	Fibroblast Growth Factor
FITC	Fluorescein Isothiocyanate
GSK3	Glycogen Synthase Kinase 3
H_2O_2	Hydrogen Peroxide
HLA	Human Leukocyte Antigen
HSC	Haematopoietic Stem Cell
hTR	Human Telomerase RNA component
hTERT	Human Telomerase Reverse Transcriptase
ICD	Internal Cardiac Defibrillator
MAPC	Multi-Potent Adult Progenitor Cell
MAPK	Mitogen Activated Protein Kinase
MHC	Major Histocompatibility Complex
MI	Myocardial Infarction
MiRNA	MicroRNA
MSC	Mesenchymal Stem Cell
mRNA	Messenger Ribonucleic Acid
PE	Phycoerythrin
NHSC	Non-Haematopoietic Stem Cell
P/C	Phenol/Chloroform
PCR	Polymerase Chain Reaction
P38I	P38 MAPK Inhibitor
RIN	RNA Integrity Number
RNA	Ribonucleic Acid
RNAi	RNA interference
RT	Reverse Transcriptase
SA ß-GAL	Senescence Associated Beta-Galactosidase
SAGE	Serial Analysis of Gene Expression
SM	Skeletal Myoblast
T/E	Trypsin/EDTA
TRAP	Telomerase Repeat Amplification Protocol
TRF	TTAGGG Repeat Binding Factor
TRITC	Tetramethylrhodamine isothiocyanate
VAD	Ventricular Assist Device
VEGF	Vascular Endothelial Growth Factor

Units

ºC	degrees Celsius
bar	barometric pressure
bp	base pair
Da	dalton
g	gram
G	gravity
hr	hour
k	kilo
l	litre
m	milli
µ	micro
min	minute
n	nano
nt	nucleotide
p	pico
rcf	relative centrifugal force
rpm	revolutions per minute
sec	second
v/v	volume for volume
w/v	weight for volume

1 Introduction

Ischaemic heart disease (IHD) is a major health and economic burden on society in the United Kingdom (UK). The disease is common and results in 146,000 heart attacks, 68,000 new cases of heart failure (HF) and 96,000 deaths each year. One million people in the UK have HF and based on current trends a further 500,000 will suffer from the condition by 2015 (www.heartstats.org). The rapidly increasing prevalence can be attributed to both ageing of the population and improvements in the treatment and survival of patients following myocardial infarction (MI) (1;2). Despite improvements in management, 40% of patients with HF die within a year of diagnosis and novel therapeutic approaches that replace cardiomyocytes and enhance myocardial repair are required.

Encouraging results in animal models has led researchers to evaluate the potential of adult progenitor and stem cells in clinical trials. At present, there is huge expectation from patients and the medical community that cellular therapy may be an effective adjunct to conventional medical and surgical treatments for IHD. Favourable results using bone marrow mono-nuclear cells (BM MNC's) has encouraged researchers to identify cells within this population that confer the most benefit and mesenchymal stem cells (MSC's) have shown the most promise in animal studies to date. This has encouraged the use of MSC's in clinical trials for the treatment of osteogenesis imperfecta (3), metabolic disorders (4), BM failure after chemotherapy (5), graft versus host disease (6;7), stroke (8) and MI (9;10). Since MSC's are present at low frequency in the BM, significant expansion is required *in vitro* in order to generate sufficient cells for these approaches. The expansion process itself induces rapid ageing of MSC's and loss of their stem cell properties as shown by a decline in proliferative and differentiation capacity *in vitro* (11;12). Furthermore, with prolonged culture MSC's show increased susceptibility to genetic events that lead to transformation and although usage appears safe the possibility of cancer formation remains a major concern in clinical trials (13;14).

MSC's are most extensively studied and characterised in BM samples from young, healthy donors and not those with conditions such as IHD. The characteristics of MSC's in these patients and suitability for autologous use remain largely unknown. With links emerging between ageing and a decline in stem cell

function, impaired tissue homeostasis and the onset of age-related diseases it seems crucial that basic research is carried out on MSC's from patient groups that may benefit the most from these therapies. Gene expression profiling should enhance our understanding of the molecular pathways that contribute to ageing and senescence of MSC's and serial analysis of gene expression (SAGE) offers the potential to identify novel genes and molecular mechanisms that regulate this process i*n vitro*. Improved understanding of stem cell ageing should not only enhance the efficiency of cell-based therapies but also increase knowledge of tissue ageing and cancer and this may be of importance.

1.1 Mesenchymal Stem Cells

The bone marrow stroma functions to create a unique micro-environment that regulates the proliferation, differentiation and maturation of HSC's. The cellular composition has been well documented and includes reticular cells, adipocytes, osteoblasts, endothelial cells, smooth muscle cells and macrophages. The existence of stem cells within the bone marrow stroma was first described over twenty years ago although most researchers have focused on their haematopoietic counterparts (15). The term 'Mesenchymal Stem Cell' (MSC) was introduced in 1991 (16) and eight years later it was demonstrated that MSC's had the capacity for multi-lineage differentiation (17). The interest generated by this report and the potential application of MSC's for the treatment of human diseases has made this one of the most intensely researched areas in the last decade.

1.1.1 Isolation and Characterisation of Mesenchymal Stem Cells

MSC's were first identified and primarily characterised *in vitro*. Friedenstein *et al* recognised that bone marrow stromal cells adhered to plastic and formed colonies almost forty years ago (18). This was referred to as the colony forming unit-fibroblast (CFU-F) assay. MSC's are still derived using the same methods today although an additional density gradient separation step using either Percoll or Ficoll is performed to separate the MNC fraction (17;19). After plating in basal media containing serum, MSC's display fibroblast-like (spindle shaped) morphology and expand rapidy to confluence over fourteen days. Although first described in adult bone marrow, it is has been demonstrated that MSC's exist in

almost all organs and tissues of mice (20) and in support MSC's have been isolated from human tissues including periosteum (21), trabecular bone (22), adipose tissue (23), synovium (24), skeletal muscle (25), heart (26), lung (27), teeth (28), placenta (29), amniotic fluid (30) and umbilical cord blood (31). For the purposes of this research, MSC's were isolated from the sternal BM of patients undergoing coronary artery bypass surgery (CABG).

Despite the method used to isolate MSC's, there is unequivocal evidence that cultures are heterogeneous consisting of cells of different size, proliferative and differentiation potential (19;32). Although the plastic adherence technique is entirely suitable for this research, there have been attempts to identify markers that can isolate homogenous populations of MSC's. At present, human MSC's are recognised by the absence of haematopoietic and endothelial surface markers including CD11b, CD14, CD31, CD34 and CD45 and the high expression of non-specific markers including CD73 (ecto 5' nucleotidase and recognised by the monoclonal antibodies SH3 and SH4), CD90 (Thy1) and CD105 (Endoglin and recognised by the monoclonal antibody SH2) (17;33). However, none of these markers uniquely identify MSC's and variable expression is often demonstrated depending on the source of cells and culture methods used. There have been attempts to identify surface markers that alone or in combination achieve higher levels of enrichment of MSC's when compared to cultures established by plastic adherence. One of the most encouraging reports was by Gronthos *et al* using magnetic selection of BM MNC's expressing the markers Stro-1 and CD106 (vascular adhesion molecule-1, VCAM1) (34). This combination identified a small population of MSC's (1.4% of the Stro-1 positive fraction) with a CFU-F incidence of 1 in 2 and was effective in isolating 90% of the CFU-F's from the BM MNC fraction. At the clonal level, Stro-1/CD106 positive MSC's showed enhanced proliferation and differentiation capacity and expressed telomerase which was not detectable in MSC's isolated by plastic adherence. MSC's with similar properties have been described by other researchers when selecting for cells expressing the stem cell markers CD133 and SSEA4 (stage-specific embryonic antigen 4). Tondreau *et al* showed that CD133 positive cells generated adherent MSC-like cultures and expressed the pluripotency marker Oct-4 (Octamer-4) which is found at high levels on undifferentiated embryonic stem cells (ESC's) (35). Gang *et al* found that SSEA4 could select for MSC's with enhanced differentiation capacity in comparison to unselected cells (36). At the clonal

level, almost 80% of MSC's underwent adipogenic, osteogenic and chondrogenic differentiation in comparison to 30% of clones in MSC's isolated by plastic adherence.

In addition to cell morphology and surface marker expression, functional studies remain the gold standard to assess MSC characteristics *in vitro*. The ability to differentiate into bone, fat and cartilage is a defining property described by multiple laboratories (17;19;37-39). As mentioned already, MSC's analysed by clonal assays are heterogenous, with individual cells capable of variable expansion and differentiation capacity (19;32). These studies also demonstrate that very few clones have multilineage differentiation capacity and most are restricted to one or two differentiation pathways. Furthermore, with increasing passage the number of multipotent clones decrease and most become restricted to a single differentiation pathway. Studies suggest the typical default pathway is towards osteogenesis and the this can be induced using media containing β-glycerol-phosphate, ascorbic acid, dexamethasone and serum (11;19;37;40). When MSC's are cultured as a monolayer in media containing these supplements, an osteoblast-like morphology develops and an increase in alkaline phosphatase activity and deposition of calcium-rich extracellular matrix can be detected using Von Kossa and Alizarin Red respectively. A smaller proportion of clones undergo adipogenesis when grown as a monolayer in media containing isobutylmethylxanthine (19). MSC's change morphology and large lipid filled vacuoles accumulate in the cytoplasm that stain positive using the dye, Oil Red O. Very few clones have the capacity to undergo chondrogenic differentiation and specific culture conditions are required to intiate this process (19). MSC's are pelleted by centrifugation and cultured in serum-free nutrient media containing TGF-ß, most commonly the ß3 isoform. MSC's synthesise glycosaminoglycans and the pattern of chondroitin sulphate deposition changes in a way similar to that of maturing human articular cartilage (39). Synthesis of other cartilage related proteins such as aggrecan, decorin, type II collagen and chondroadherin can also be detected.

In addition to the standard lineages, human MSC's have been shown to differentiate into other cell types *in vitro* including cardiomyocytes (41), endothelial cells (42;43) and neural cells (44). However, at present these are not considered defining properties of MSC's because the methods used to

characterise the cells were not robust and functional assays were not always performed. In these studies, cell differentiation was confirmed by the detection of lineage specific transcripts and doubt has arisen over the validity of this approach because similar transcripts have been identified in undifferentiated MSC's at the single cell and colony level (45-47). The findings infer that MSC cultures contain both multi-potent primitive cells and committed cells with restricted lineage potential. Therefore, the detection of lineage specific transcripts alone appears inadequate to confirm that MSC's acquire the functional properties of cells that highly express these transcripts. It has been demonstrated that MSC's co-cultured with cardiomyocytes express cardiac-specific genes although exhibit the electrophysiological properties of stromal cells and not cardiomyocytes (48). Future studies will need to perform rigourous functional assessment of differentiated MSC's before these alternative differentiation pathways can be considered as defining properties of these cells.

Relative to their *in vitro* characteristics, the *in vivo* behaviour of MSC's remains poorly understood. Unlike HSC's and ESC's that are defined by their ability to reconstitute haematopoiesis or generate teratomas *in vivo*, similar assays to charactertise MSC's are not widely performed. The best described method involves loading human MSC's onto fibronectin-coated hydroxyapatite cubes and implanting the cubles subcutaneously into immune-deficient mice (49). Bone and cartilage formation and to a lesser extent fat have been demonstrated on explanted cubes and labelled cells confirmed that those implanted had undergone differentiation rather than infiltration of the cubes with host cells. Site specific or intravenous delivery of MSC's in animal models has provided additional evidence that the cells can migrate to areas of tissue injury and differentiate *in vivo*. However, the majority of cells administered intravenously become entrapped in the pulmonary circulation (50) and the absolute numbers that reach the target tissue and engraft appears low and at levels insufficient to explain the beneficial effects seen on tissue function (51;52). It has been increasingly recognised that the beneficial effects of administering MSC's after MI occur through paracrine mechanisms that enhance neo-angiogenesis, reduce fibrosis and inflammation, and promote the proliferation of endogenous cardiac stem cell populations (53-55). Further understanding of these mechanism is likely to lead to the development of new drugs or growth factors that can be administered to damaged tissues and avoid the need for cell delivery altogether.

A further concern from administering progenitor or stem cells is that they could engraft and differentiate toward undesirable cells types that have detrimental effects on tissue and organ function. Calcification has been identified in the hearts of animals receiving whole BM after MI (56) and injection of MSC's appears to pose an even greater risk (57). Further studies are required to confirm if the administered cells underwent osteogenic differentiation or contributed to increased tissue calcification after injury. These findings highlight the need to use sophisticated imaging techniques in future clinical trials of cell therapy to track administered cells and assess changes in treated organs and tissues. To understand the exact physiological relevance of MSC's *in vivo* and their response after tissue injury, specific surface markers that prospectively identify and isolate MSC's are definitely required. At present, the agreed minimal criteria to define MSC's remains: plastic adherence; fibroblast-like morphology; specific surface marker profile and differentiation into bone, fat and cartilage *in vitro* (33).

1.1.2 Factors Affecting Mesenchymal Stem Cell Proliferation

Although an agreement has been reached on criteria to define MSC's, there is no consensus on the culture protocols used by researchers. To determine optimal culture conditions for clinical scale up, Sotiropolou *et al* investigated the effects of different tissue culture plastic, growth factors, basal media, glucose concentration, glutamine and plating density on the proliferation kinetics of MSC's (58). Importantly, all variables were shown to significantly influence the proliferation of MSC's over the first three passages. MSC's proliferated to the greatest extent in low glucose conditions, in media supplemented with Glutamax and when plated at low density. Earlier studies have demonstrated that low plating densities enrich for primitive MSC's with enhanced proliferative capacity although the absolute number of cells generated using this approach is reduced (32;59). For clinical purposes, a compromise between culture conditions that yield sufficient numbers of cells and those that enrich for MSC progenitors are required.

Like other cell types, MSC's require serum (typically 10-20%) for proliferation and some researchers select batches that sustain the proliferative and differentiation capacity of MSC's (17;32;37). To enhance clinical application,

serum free conditions or even autologous serum has been described to avoid exposure to animal products. Pochampally *et al* demonstrated that serum-free conditions selected for a rare population of MSC's expressing the pluripotency gene, Oct-4 and displayed much longer telomeres when compared to those cultured with serum (60). Despite the fact that these cells generated colonies and underwent multi-lineage differentiation, growth arrest occurred quickly and within ten population doublings. The results infer critical components of serum sustain the self-renewal and long-term proliferation of MSC's and at present it has not been possible to reliably generate cultures using serum-free protocols. In contrast, MSC's cultured in autologous human serum proliferate to a similar extent than those in bovine serum and demonstrate an enhanced capacity for osteogenic differentiation although the differences in the exact components of either serum have not been determined (61). The problem that arises when using autologous serum is that the absolute amounts obtained are limited and appear insufficient for long-term culture protocols and at present clinical application seems unlikely.

Ambient oxygen levels and specific growth factors can also influence the proliferative potential of MSC's. MSC's cultured in low oxygen conditions (2%) are enriched for progenitors that express pluripotency genes and an enhanced capacity for osteogenic differentiation *in vitro* and *in vivo* (62). MSC's with similar properties have been demonstrated using media supplemented with fibroblast growth factor-2 (FGF-2) and these cells achieved 70 population doublings before the onset of growth arrest (63). MSC's cultured in media supplemented with FGF-2 displayed longer telomeres and maintained differentiation capacity for almost 50 population doublings which was twice that seen in MSC's cultured in standard media without the growth factor. FGF-2 has been shown to inhibit the expression of transforming growth factor-ß2 (TGF-ß2) and the activation of downstream tumour suppressor genes confirming an important role in delaying the onset of senescence and maintaining the proliferation of MSC's during prolonged culture (64).

Donor characteristics, particularly age appears to be one of the most important factors influencing the proliferation of MSC's *in vitro*. Studies have confirmed that the proliferative lifespan of MSC's from aged donors is almost half that of their younger counterparts (11;12). In contrast, MSC's derived from foetal

tissues proliferate to a much greater extent than those derived from tissues of young adults (65). Foetal MSC's display increased expression of genes involved in proliferation and DNA repair and decreased expression of genes associated with differentiation when compared to their adult counterparts and this is likely to explain these differences (66). Therefore, ageing affects the characteristics of MSC's at the molecular level although the exact effects on their stem cell properties remains poorly understood. Further study is also required to determine if foetal MSC's have superior capacity to re-generate tissues when used for cell therapy when compared to autologous adult cells as one might predict.

1.1.3 Ageing and Senescence of Mesenchymal Stem Cells

MSC's, like other somatic cells have a finite replicative lifespan and enter a state of irreversible growth arrest called cellular senescence. Senescence was first described in the 1960's in studies on normal human fibroblasts and referred to as the Hayflick limit (67). MSC's have similar growth profile to fibroblasts and undergo 30-40 population doublings before the onset of growth arrest. The replicative lifespan is significantly influenced by donor characteristics and culture conditions as described earlier. MSC's at growth arrest are large, flat and display prominent actin stress filaments (11;12;40). MSC's from aged donors display this phenotype almost immediately upon isolation and proliferate poorly in comparison to cells from young donors (11). A similar phenotype can be found in other senescent cell types and is not specific to MSC's suggesting that increasing cell size could be used as a surrogate marker of MSC ageing *in vitro*.

During prolonged culture, MSC's also display increased expression of senescence-associated ß-galactosidase (SA ß-Gal) (12;40;68). SA ß-Gal was first described in studies of senescent fibroblasts and later shown to reflect the increase in lysosomal activity seen in senescent cells (69;70). Studies have confirmed that the expression of SA ß-Gal increases with each passage and can be visualised in 40 to 80% of late passage MSC's (12;40;68). Importantly, two studies demonstrated that SA ß-Gal is expressed in only a small percentage of MSC's at early passage and therefore expression is a late marker of MSC ageing and senscence *in vitro* and its use appears limited (40;68). Lipofuscin, which is a pigmented residue of lysosomal digestion products and indicative of oxidative

damage to cell membranes is also a marker of cell ageing and Roura *et al* demonstrated that lipofuscin accumulated in MSC's derived from young and old donors cultured for fourteen days (71). Similar levels of expression were seen in cells from both age groups confirming that oxidative damage of MSC's occurs *in vitro* and is a generalised phenomenon of routine culture. The absence of other reports makes it difficult to comment on the ability of lipofuscin to detect ageing and senescence of MSC's and further studies are required.

One of the most widely used markers of cell ageing is a reduction in telomere length. Telomeres are DNA repeats (TTAGGG) that play an essential role in the stable maintenance of eukaryotic chromosomes within a cell by specific binding to structural proteins. Telomeres shorten in dividing cells and these proteins cap the end of linear chromosomes, preventing nucleolytic degradation, end-to-end fusion, irregular combination, and other events that are normally lethal to the cell. The ends of telomeres are maintained by the enzyme telomerase that is composed of an RNA subunit (hTR - human Telomerase RNA template), and a catalytic protein subunit (hTERT - human Telomerase Reverse Transcriptase). Similar to fibroblasts, MSC's lose telomeric DNA at a rate of 50 to 100bp per population doubling and senesce when a critical length is reached (11;12;72). Baxter *et al* confirmed a critical telomere length of approximately 10kB and by comparing young and old donors it was estimated that MSC's lost 17bp of telomeric DNA per year *in vivo*. The heterogeneity in telomere length described in studies of MSC's is difficult to fully explain although the relatively long telomeres seen at growth arrest infer telomere-independent mechanisms of senescence may in fact predominate.

The enzyme telomerase functions to counteract the loss of telomeric DNA during successive cell divisions by the synthesis of TTAGGG repeats. Telomerase is expressed at high levels in cancer cells, ESC's and germ cells and is absent or barely detected in normal human somatic cells (73-75). Although telomerase activity was first demonstrated in MSC's by Pittenger *et al*, other researchers could not reproduce these findings in MSC's cultured in standard conditions (12;17;72;76). The conflicting results may be explained by the existence of rare telomerase positive cells within MSC cultures and also the poor sensitivity of the telomeric repeat amplication protocol (TRAP) itself. The primitive stem cell marker CD133 and combination of markers Stro-1 and CD106 have been used to

isolate telomerase positive cells that can generate MSC cultures indistinguishable to those obtained using the plastic adherence technique (34;35). Furthermore, fibroblasts and more recently MSC's were found to express hTERT using immunoprecipitation and synchronising cells in S-phase when the TRAP assay failed to detect telomerase activity (77;78). Similar to other somatic cells, hTERT is known to be actively repressed in human MSC's via chromatin modifications that can be reversed by treating cells with de-methylating agents and histone deacetylase inhibitors (79;80). Together, the results of these studies highlight that telomerase activity in MSC's is tightly regulated in a cell cycle dependent manner although at levels insufficient to prevent loss of telomeric DNA during extended proliferation.

Lending support to these findings, the onset of senescence in MSC's can be overcome by forced over-expression of hTERT (81). hTERT transduced MSC's displayed increased telomerase activity and long telomeres and proliferated for more than 260 population doublings while maintaining the capacity for osteogenic differentiation *in vitro and in vivo* (81;82). Unfortunately, the transduced cells were shown to accumulate genetic alterations that led to transformation and tumour formation when cells were injected into immune-deficient mice (83). hTERT transduction alone appeared insufficient to result in transformation because multiple genetic events including activating mutations of KRAS, deletion of the tumour suppressor $p16^{INK4\alpha}$ and ARF gene loci and promoter hypermethylation of the cell cycle regulator DBCCR1 were identifed in the transformed cells. Together, the results infer that telomerase activity in MSC's functions to regulate proliferation and lifespan as well as a barrier to cell transformation through its active repression.

In fact, although reports are rare spontaneous transformation of human MSC's *in vitro* has been described and the transformed cells expressed high levels of telomerase activity (13;14). The cells appeared remarkably similar to hTERT transduced MSC's and could generate sarcomas when delivered subcutaneously into immune-deficient mice. Wang *et al* reported that the transformed cells expressed the stem cell marker CD133 raising the possibility that the transformation event occurred in a primitive stem cell population (14). A further communication from Rubio *et al* confirmed that chromosomal abnormalities were present in early passage cultures suggesting the donors

themselves carried genetic abnormalities (84). Providing some reassurance, another study could not demonstrate transformation of ten MSC cultures expanded up to and beyond senescence and in addition the cells displayed normal karyotype by cytogenetic and array-comparative genomic hybridisation (aCGH) techniques (85). Despite this, the confirmation of side-population (SP) cells in both benign and malignant human mesenchymal tumours that have been shown to initiate tumour formation in immune-deficient animals provides further evidence that primitive MSC's are indeed the target of transformation events (86). The overwhelming message is that for clinical trial purposes, MSC's will require robust molecular characterisation and karyotype analysis prior to administration in patients.

A further role of telomerase in MSC's is for the maintenance of normal differentiation as shown from studies on telomerase-deficient mice ($mTR^{-/-}$). Although early generations display a normal phenotype, animals from the fourth generation onwards shown signs of premature ageing including defective haematopoiesis and impaired tissue healing after injury (87-89). In primary cultures derived from $mTR^{-/-}$ animals, MSC's lost their normal differentiation capacity and displayed impaired chondrogenic and adipogenic differentiation in comparison to cells derived from wild type animals (90). Another report linking telomerase activity in MSC's with differentiation *in vitro* was by Zhao *et al* (78). A slight increase in telomerase activity was detected in normal MSC's during adipogenic differentiation in comparison to their undifferentiated counterparts although this was not demonstrated in cells undergoing osteogenic differentiation. Together, the reports highlight a link between telomerase activity *in vitro* and the maintenance of normal stem cell properties of MSC's.

Ageing and senescence of MSC's *in vivo* can contribute to the decline in proliferation and differentiation capacity seen *in vitro*. In MSC's derived from young donors, osteogenic differentiation capacity appears maintained (19;37;38) or increased at late passage when compared to early passage cells (40). At the clonal level it has been demonstrated that the adipogenic differentiation capacity of MSC's is lost earliest during prolonged culture (38). In addition, MSC's from aged donors contained fewer multi-potent clones. In other studies, MSC's from aged donors show a similar decline in adipogenic and osteogenic differentiation capacity at late passage (12;91) whilst in a different study

osteogenic differentiation decreased to a much greater extent (71). Therefore, ageing and senescence of MSC's is associated with a reduction in differentiation capacity and the typical default pathway appears influenced by the age of the donors from which cultures were established. The conflicting results of studies to date makes it impossible to make a definitive statement regarding the exact restriction in lineage fate that occurs with prolonged expansion.

When this research commenced the molecular mechanisms that regulate ageing and senescence of MSC's were largely unknown. In studies of fibroblasts, senescence is associated with the altered expression of numerous genes important for key aspects of cellular physiology (92). The down regulation of cell cycle control genes maintains an irreversible growth arrest that is regarded as a barrier to cell transformation. The two main tumour suppressor pathways, p53 – $p21^{WAF1}$ and $p16^{INK4A}$ –Rb are activated in response to telomere shortening and dysfunction or cellular stress (93;94). Importantly, transgenic animals deficient in these genes displays modest increases in stem cells numbers and function suggesting that tumour suppressor pathways contribute to ageing and loss of function in stem cells (reviewed in (95)). Evidence exists that the same genes contribute to the decline in function and senescence of MSC's during expansion and Park *et al* demonstrated increased expression of p53, $p21^{WAF1}$ and $p16^{INK4A}$ in senescent MSC's (96). Confirming a role of $p16^{INK4A}$ as a tumour suppressor in MSC's , transduction with hTERT resulted in transformation due to a deletion in the $p16^{INK4A}$ gene locus during extended culture (83). The expression of many of these genes are regulated by complex cell signalling pathways including TGF-ß that are themselves regulated by growth factors such as FGF-2 (64).

Recently, a gene expression profile of senescent MSC's has been determined by microarray and validation studies in multiple samples confirmed that replicative senescence was a continuous process with transcriptional changes detected from the first passage (40). In addition, this study identified and validated increased expression of the five micro RNA's (miRNA) has-mir-371, has-mir-369-5P, has-mir-29C, has-mir-499 and has-mir-217 in senescent MSC's. MiRNA's are short non-coding molecules that are highly conserved and regulate protein expression through interactions with the 3' untranslated region of mRNA. There exact role remains poorly understood although they have the potential to regulate the

expression of thousands of genes (97). Lafferty-Whyte *et al* identified twelve miRNA's associated with senescence from review of published literature and target genes for each miRNA were assigned to cellular pathways using systems biology software (98). The pathways most significantly associated with these genes included cytoskeletal re-modelling, cell cycle and metabolism which are characteristic alterations seen in senescent cells. Importantly, two miRNA's (hsa-miR-499 and has-miR-34c) were shown to regulate the onset of senescence regardless of the intiating mechanism and the development of small molecules to manipulate their activity was suggested as a novel approach to modify senescence in MSC's and other cell types.

1.2 Gene Expression Profiling

Comprehensive gene-expression profiling has been utilised to identify novel genes and their function, generate a transcriptome of different cell and tissue types, and to compare the profiles of gene expression between normal and pathological conditions. Techniques such as serial analysis of gene expression (SAGE) and DNA microarray have enabled researchers to identify and determine the expression of thousands of genes simultaneously. Apart from simply identifying gene expression, SAGE and microarrays represent powerful tools that have been used to identify diagnostic and prognostic markers, as well as therapeutic targets in human diseases such as cancer (99-102). In the last decade, the same techniques have been applied to enhance our understanding of developmental (103) and stem cell biology (104;105).

The SAGE technique was first described in 1995 by Velculescu *et al* from the Kinzler and Vogelstein laboratory at John Hopkins University (106). The technique is based on generating clones of short sequence tags (10-27bp) derived from mRNA from cells or tissue of interest. Each tag is sufficiently unique to identify one mRNA transcript and tags are joined to form long DNA fragments called concatamers that can be cloned and sequenced. Each concatamer can contain up to forty tags and therefore efficiency is greatly increased when compared with conventional analysis of expressed sequence tags (EST's) (107). The expression level of each transcript is therefore equal to the number of times a particular tag is observed in a SAGE library and reflects the actual copy number of transcripts in a cell (106). The mRNA transcript

corresponding to the SAGE tag is then identified from publicly available databases and web-based software such as SAGE Map (108) and SAGE Genie (109).

Since the original SAGE protocol, a number of modifications have been developed. Firstly, using different tagging enzymes it has been possible to generate longer SAGE tags (17-27bp) and as a consequence improve tag-to-gene annotation (110;111). Saha *et al* calculated that 17bp and 21bp tags have 64.0% and 99.8% probability of being unique if the genome contained approximately 30 x 10^6 *Nla*III-derived tags and is compromised of random sequences (110). One disadvantage of choosing a longer tag length is a reduction in SAGE efficiency because almost half the number of tags will make up a concatamer of equivalent length (112). Therefore, it has been suggested that researchers consider the need to identify transcripts accurately or identify more differentially expressed tags that have an increased chance of being wrongly annotated.

Other modifications have been described that enhance the applicability of SAGE. For example, if the amount of RNA is limited optimised protocols (113;114) or PCR amplification (115) can be performed prior to the generation of cDNA. In fact, the technique by Datson *et al* was used to generate a SAGE library from a single colony of MSC's (1 x 10^4 cells) using 0.1ng of mRNA (115). Other modifications of SAGE have been developed that include the derivation of tags from the 5'-end rather than the 3'-end (start site) of mRNA to identify transcription initiation sites and alternative polyadenylation sites (116;117). These studies not only allow us to analyse the complete transcriptome but also demonstrate its remarkable complexity.

All the available methods of gene expression profiling are useful in their appropriate context. The greatest advantage of SAGE is that it does not require prior knowledge of the genes to be analysed and therefore allows the detection of truly novel transcripts (118). The technique is therefore attractive when applied to stem cell populations that until recently remained poorly characterised. In its current form, SAGE remains low throughput and labour intensive and hence limited to a small number of experiments. As a result, candidate genes must be validated in a in a larger set of samples and a number of different methods have been previously described (102;106). This is in

contrast to microarrays which are usually performed on multiple experiments and are to an extent self-validating. Another consideration when using SAGE is the demand on sequencing services and the associated cost. These are important considerations for any researcher although new developments in sequencing technology are likely to improve efficiency and reduce costs in the future (119;120).

Apart from these factors SAGE and microarray techniques are fairly comparable in their ability to detect abundant genes and large differences (five to ten fold) in gene expression (112;121). SAGE can outperform microarrays for low abundance genes and small changes in expression if the library is sufficiently large (122). Most studies develop SAGE libraries of approximately fifty thousand tags which are thought to give a 95% chance of detecting a transcript that has at least five copies per cell. Accurate quantitation of transcripts of lower abundance would require library sizes at least five times this number although such studies offer the potential to identify novel genes. On this basis and experience within our research group (123) we used the long-SAGE (17bp) and details of the technique and bioinformatics are discussed further in chapter four.

1.2.1 Insights into Stem Cell Biology through Gene Expression Profiling

Gene expression profiling studies are widely criticised for being fishing expeditions rather than hypothesis driven experiments although the approach has been useful in the comparison of embryonic and adult stem cell populations. The availability of transcriptional signatures of haematopoietic stem cells (HSC's) (124), embryonic stem cells (ESC's) (125) and neural stem cells (NSC's) (126) has led to important findings.

By SAGE, stem cell transcriptomes are complex with a significant proportion of tags either unknown or matching transcripts with poorly defined functions (124;125). Georgantas *et al* showed that SAGE could identify almost 30% more unknown transcripts that microarray when used to profile HSC's obtained from different sources (127). Furthermore, the difference is greater than that expected from sequence error or alternative spliced transcripts combined suggesting these transcripts are in fact novel. The same study also

demonstrated that HSC's were enriched for transcription factors known to be important for haematopoiesis, DNA repair and quiescence confirming the unique characteristics of these cells. In fact, at the gene expression level, leukemic stem cell (LSC's) and normal HSC's are remarkably similar adding further evidence that cancer may in fact be a stem cell disease (128-130). Although this would suggest conventional treatments are not selective for cancer stem cells the study by Gal *et al* was able to identify up regulation of Notch signalling that could be targeted using pharmacological approaches. Therefore, expression profiling can be used to identify novel pathways that can be manipulated using targeted small molecules.

In a similar fashion, gene expression profiling of mouse and human ESC's has improved understanding of mechanisms that regulate pluripotency and cell fate during development (reviewed in (131)). The transcription factors Pou5f1 (Oct-4) and Sox2, signalling molecules Nodal and Lefty and the growth factor FGF-2 have been shown to be markers of ESC's that are maintained in an undifferentiated state. Furthermore, transcripts enriched in ESC's are associated with FGF, TGF-ß and Wnt signalling pathways that can be manipulated by pharmacological approaches to influence cell fate (132). It has been recognised that the same pathways are in fact shared by embryonic and adult stem cells (126;133). The recognition of genes important for maintenance of pluripotency has led to fascinating experiments in recent years. Three studies have demonstrated that embryonic and adult mouse fibroblasts can be reprogrammed into pluripotent stem cells that form viable chimeras that contribute to the germline (134-136). The studies used retroviruses to over express the transcription factors Oct-4, Sox2, c-Myc and Klf4 which are required for the maintenance of pluripotency in ESC's. Interestingly, the cells were similar to ESC's at the epigenetic level and in their ability to form teratomas in immune-deficient animals. Although experimental, Okita *et al* have recently described a virus free approach suggesting it could be possible to reprogram autologous cells for tissue repair or replacement (137). Therefore, understanding mechanism of self-renewal and ageing through gene expression profiling can enhance our ability to use stem cells for future clinical application.

1.2.2 Gene Expression Profiling Studies of MSC's

Compared to the extensive studies performed with ESC's, research into the molecular mechanisms that regulate self-renewal and differentiation of MSC's remains at an early stage. The transcriptome of undifferentiated MSC's from different sources has been well characterised using SAGE (45;105), microarray (46;138-140) and EST analysis (107). Gene expression profiling of MSC's has provided an explanation for their unique biological properties and therapeutic efficiency when used for tissue repair. Phinney *et al* performed SAGE on mouse MSC's derived using immunodepletion to minimise contamination with other cell populations (141). A library of 59,007 tags was produced and almost 3% of assigned tags matched genes known to regulate mesoderm specification and the differentiation pathways typical of MSC's. Furthermore, by assigning tags to gene ontological (GO) descriptions, many of the transcripts were shown to participate in angiogenesis, cell motility and communication, haematopoiesis, immunity, and neural activity which might explain the basis for their effects in animal models of tissue repair. Another finding was that almost a third of SAGE tags encode proteins with indeterminate function and therefore MSC's have additional properties that are yet to be defined.

The most abundant genes in MSC's include collagens (e.g. COL1A1 and COL1A2), vimentin (VIM), connective tissue growth factor (CTGF), transgelin (TAGLN) and eukaryotic translation elongation factor 1, alpha 1 (EEF1A1) (45;105;141;142). Although considered as the molecular foundation of MSC's, they are in fact widely expressed in different cells and tissues, albeit at lower levels. In fact, the inability to identify markers of MSC's remains a limitation of MSC biology. One explanation is that the MSC cultures are heterogeneous and composed of cells with varying proliferative and differentiation capacity (32;143). In fact, this would appear to be the case at the molecular level as well. In a study by Tremain *et al*, micro-SAGE was used to determine the gene expression profile of a single colony of MSC's (45). In addition to the transcripts commonly found in MSC's, epithelial and neural cells markers including cytokeratins and neurofilaments were also detected. A similar finding was reported using microarray to analyse gene expression in a single BM stromal cell isolated by laser capture micro-dissection (46). Transcripts within the cell included those found in epithelial, endothelial, neural and haematopoietic cells including B-cell

progenitors. Together, the results partly explain the broad differentiation capacity of MSC's but also that cultures are composed of cells with varying potential or at different stages of differentiation.

Gene expression profiling of MSC's has confirmed the absence or low expression of genes associated with stemness. Katz *et al* were unable to detect CD133 and ATP binding cassette (ABC) membrane transporter, ABCG2 in a SAGE library generated from adipose-derived MSC's (139). Both are expressed in primitive HSC's and side-population (SP) cells, a rare stem cell population within the BM. Furthermore, a recent study has confirmed that bone marrow-derived MSC's do not express the transcription factors Oct-4, Nanog and Sox2 that are markers of pluripotency in ESC's (144). However, Song *et al* were able match a significant proportion of genes to the JAK-STAT, TGF-ß and Wnt signalling pathways that appear common to both embryonic and adult stem cells (133). Together, the results of these studies highlight important differences in both adult and embryonic stem cells but also the lack of sensitivity of such approaches to detect rare stem cell populations within MSC cultures themselves. Indeed, description of such cells exist and pluripotency genes have been detected in primitive MSC's (35;60;145;146).

The expression profiles of MSC's obtained from bone marrow (105), umbilical cord blood (140;142) and adipose tissue (139) appear remarkably similar. Pannepucci *et al* demonstrated that umbilical cord blood MSC's were enriched for genes that are important for angiogenesisis and bone marrow MSC's those important for osteogenesis (142). This probably reflects the tissue of origin of MSC's and differentiation studies were not performed to confirm differences in MSC properties. A similar study could not demonstrate any difference although their data set was compared to publicly available expression profiles and correlated poorly (140). More recently, an elegant study has identified signalling pathways important for self-renewal and differentiation of MSC's (144). Microarrays were used to compare expression profiles of undifferentiated, differentiated and de-differentiated MSC's (the induction media was withdrawn). Signalling pathways associated with adipogenic, osteogenic and chondrogenic differentiation included NF-κB, p38 MAPK, PPAR and IL-6 and in undifferentiated MSC's, PI3K and Wnt signalling. Interestingly, the profiles of de-differentiated and undifferentiated MSC's were similar and the de-

differentiated MSC's could still differentiate into a different lineage. The importance of these findings is that *in vitro* models of MSC differentiation offer the potential to identify new gene mutations in musculoskeletal disorders and strategies to identify targets of transcription factors that regulate differentiation have been described (147).

Therefore, gene expression profiling of ageing and senescence of MSC's should provide insight into novel strategies to modify stem behaviour and enhance the use of these cells for cell-based therapies.

1.3 Aims

The use of MSC's as an autologous cell-based therapy will require robust characterisation of the cell therapy product at the cellular and molecular level. MSC's have limited proliferative ability although the exact molecular mechanisms of ageing and senescence *in vitro* are not understood. Therefore, our aims were to:

1. Establish a model of MSC isolation and characterisation from the sternal bone marrow of patients undergoing CABG.

2. Understand the transcriptional changes that occur during prolonged expansion of MSC's *in vitro* using SAGE.

3. Identify and validate genes that represent biomarkers of aged MSC cultures.

4. Explore the use of small molecule inhibitors to alter MSC proliferation and ageing *in vitro*.

2 Materials and Methods

2.1 Materials

2.1.1 Equipment

Equipment which is standard in most laboratories and used in this work, but not listed by supplier included: wet and dry ice, water baths, vortex mixers, centrifuges, refrigerators; -20ºC, -70ºC and -150ºC freezers; liquid N_2 cryostorage containers; microwave oven; tissue culture plastics, sterile and non-sterile glass pipettes, bottles, flasks and beakers; plastic bottles, beakers, measuring cylinders and boxes; aluminium foil, cling film and plastic wrapping; rocker platform and shaker; laboratory digital balance and pH meters; magnetic stirrer and hotplate and metal ware including forceps and spatulas.

Agilent Technologies Ltd (West Lothian, UK)

2100 Bioanalyser and Expert 2100 software B.02.03 (including upgrade)

Applied Biosystems Ltd (Warrington, UK)

ABI Prism Automated Sequencer (Models 373 and 377)

7900HT Fast Real-Time PCR system with SDS 2.3 and RQ 1.2 software

Beckman (RIIC) Ltd (High Wycombe, UK)

Avanti™ J-25 centrifuge (high-speed refrigerated centrifuge)

GS-6R centrifuge (low-speed refrigerated centrifuge)

Microfuge® R centrifuge (refrigerated microcentrifuge)

Becton Dickinson (BD) Ltd (Oxford, UK)

BD FACSCalibur™ flow cytometer with BD CellQuest Pro™ software (version 1.a.2f5b)

Carl Zeiss MicroImaging GmbH (Göttingen, Germany)

Axio Observer.A1 inverted microscope with Axio Vision software (version 4.6)

Charles Austin Pumps Ltd (Byfleet, UK)

Capex L2C vacuum pump (for use with QIAvac Multiwell vacuum manifold)

Fisher Scientific (part of ThermoScientific) UK Ltd (Loughborough, UK)

Cell Shock Electroporator electroporation cuvettes

Electro-4 system (for standard and large-scale agarose gel electrophoresis)

HERA Cell 150 Tri-Gas cell culture incubator

Genetic Research Instrumentation (Braintree, UK)

Atto Maxi Slab for vertical PAGE: gel tank and pouring apparatus with 160 x 160 mm glass gel plates, 1.5 mm spacers and 12 and 20 well combs

Labcaire Systems Ltd (North Somerset, UK)

PCR6 Mini Vertical Laminar Flow cabinet

Millipore (Watford, UK)

Milli-Q plus PF water purification system

MJ Research Inc (Watertown, MA, USA)

DYAD Disciple™ Peltier thermal cycler stacked upon a DNA Engine® DYAD Peltier to form a 4 bay system including dual 96 heads with independent block control

PTC-200™ Peltier thermal cycler with dual 48 heads

Nalge (Europe) Ltd (Hereford, UK)

Cryo 1ºC “Mr Frosty” freezing container

NanoDrop Technologies (Wilmington, USA)

ND-1000 spectrophotometer with ND-1000 software (version 3.3)

Novex

XCell SureLock electrophoresis cell

Olympus UK Ltd (London, UK)

CKX41 inverted microscope + Cell^{B} imaging software

Pharmacia Biotech Ltd (St Albans, UK)

GeneQuant RNA/DNA calculator (spectrophotometer)

Qiagen Ltd (Crawley, UK)

QIAvac Multiwell Vacuum Manifold and Regulator (for large scale DNA purification using Qiagen MinElute™ or Edge ExcelaPure™ 96-well UF PCR Purification Kits)

Stratagene Ltd (Cambridge, UK)

UV Stratalinker 2400 (for UV cross-linking)

Syngene Europe Ltd (Cambridge, UK)

Gene Genius Bio Imaging System with GeneSnap Software (version 6.03)

2.1.2 Tissue Culture Reagents

Becton Dickinson (BD) Ltd (Oxford, UK)

Dispase

Matrigel

Fisher Scientific (part of ThermoScientific) UK Ltd (Loughborough, UK)

Hyclone Defined Fetal Bovine Serum (FBS) (U.S Origin)

Invitrogen Ltd (Paisley, UK)

Alpha Minimum Essential Media (α-MEM) (1X)

DMEM/F-12 Media (1:1) (1X)

Dulbecco's Modified Eagle Media (D-MEM) (1X) (low glucose 1000mg/l, sodium pyruvate and GlutaMAX™)

Dulbecco's Phosphate-Buffered Saline (D-PBS) (1X, without Ca2+and Mg2+)

Insulin-Transferrin-Selenium Supplement (ITS) (100X)

Penicillin-Streptomycin-Glutamine (PSG) (100X) solution

RPMI 1640 Media (1X)

Sterile Distilled Water

Trypsin-EDTA (1X), liquid – 0.25% Trypsin 1mM EDTA·4Na

Sigma-Aldrich Company Ltd (Dorset, UK)

Histopaque-1077

2.1.3 Media Formulations, Wash Buffers and Solutions

2.1.3.1MNC Medium

Reagent	Amount	Concentration
RPMI 1640	95ml	95%
FBS	5ml	5%

2.1.3.2MSC Medium

Reagent	Amount	Concentration
D-MEM low glucose (1000mg/l), sodium pyruvate and GlutaMAX™	500ml	83%
FBS	100ml	17%

2.1.3.3α-MEM Basal Medium

Reagents	Amount	Concentration
α-MEM	90ml	90%
FBS	10ml	10%
PSG	1ml	100U/ml Penicillin, 100µg/ml Streptomycin, 2nM L-Glutamine

2.1.3.4D-MEM/F-12 Basal Medium

Reagents	Amount	Concentration
D-MEM/F-12	49ml	99%
ITS	500µl	1%
PSG	500µl	100U/ml Penicillin, 100µg/ml Streptomycin, 2nM L-Glutamine

2.1.3.5Adipogenic Differentiation Medium

Reagents	Amount	Concentration
α-MEM Basal Medium	5ml	99%
Adipogenic supplement (100X solution containing hydrocortisone, isobutylmethylxanthine and indomethacin)	50µl	1%

2.1.3.6Osteogenic Differentiation Medium

Reagents	Amount	Concentration
α-MEM Basal Medium	5ml	95%
Osteogenic supplement (20X solution of dexamethasone, ascorbate-phosphate and ß-glycerolphosphate)	250µl	5%

2.1.3.7Chondrogenic Differentiation Medium

Reagents	Amount	Concentration
D-MEM/F-12 Basal Medium	2.5ml	99%
Chondrogenic supplement (100X solution of dexamethasone, ascorbate-phosphate, proline, pyruvate and TGF-β3	25µl	1%

2.1.3.8MSC Cryopreservation Medium

Reagents	Amount	Concentration
D-MEM low glucose (1000mg/l), sodium pyruvate and GlutaMAX™	6ml	60%
FBS	2ml	20%
DMSO	2ml	20%

2.1.3.9Wash Buffer

Reagent	Amount	Concentration
D-PBS(-Ca^{2+}, -Mg^{2+})	490ml	98%
FBS	10ml	2%

2.1.3.10 FACS Fix

Reagent	Amount	Concentration
D-PBS (-Ca^{2+}, -Mg^{2+})	17.6ml	88%
Formalin solution (37% formaldehyde)	2ml	10% (3.7% formaldehyde)
FBS	400µl	2%

2.1.4 Flow Cytometry Reagents

AbD Serotec Ltd (Oxford, UK)

R-PE-conjugated Mouse Anti-Human CD105 Monoclonal Antibody (MCA1557PE)

Becton Dickinson (BD) Ltd (Oxford, UK)

FITC-conjugated Mouse IgG1, κ Monoclonal Isotype Control (555909)

R-PE-conjugated Mouse IgG1, κ Monoclonal Isotype Control (555749)

R-PE-conjugated Goat Anti-Mouse Immunoglobulin Specific Polyclonal Antibody (Multiple Adsorption) (550589)

R-PE-conjugated Mouse Anti-Human CD13 Monoclonal Antibody (555394)

R-PE-conjugated Mouse Anti-Human CD14 Monoclonal Antibody (555398)

R-PE-conjugated Mouse Anti-Human CD29 Monoclonal Antibody (555443)

FITC-conjugated Mouse Anti-Human CD31 Monoclonal Antibody (555445)

R-PE-conjugated Mouse Anti-Human CD34 Monoclonal Antibody (550761)

FITC-conjugated Mouse Anti-Human CD44 Monoclonal Antibody (555478)

FITC-conjugated Mouse Anti-Human CD45 Monoclonal Antibody (555482)

R-PE-conjugated Mouse Anti-Human CD45 Monoclonal Antibody (555483)

R-PE-conjugated Mouse Anti-Human CD49d Monoclonal Antibody (555503)

R-PE-conjugated Mouse Anti-Human CD49e Monoclonal Antibody (555617)

FITC-conjugated Mouse Anti-Human CD71 Monoclonal Antibody (555536)

R-PE-conjugated Mouse Anti-Human CD73 Monoclonal Antibody (550257)

FITC-conjugated Mouse Anti-Human CD90 Monoclonal Antibody (555595)

FITC-conjugated Mouse Anti-Human CD106 Monoclonal Antibody (551146)

R-PE-conjugated Mouse Anti-Human CD166 Monoclonal Antibody (559263)

FITC-conjugated Mouse Anti-Human HLA-A, B, C Monoclonal Antibody (555552)

FITC-conjugated Mouse Anti-Human HLA-DR, DP, DQ Monoclonal Antibody (555558)

FACSClean™ Solution

FACSFlow™ Sheath fluid

Miltenyi Biotec Ltd (Surrey, UK)

R-PE-conjugated Mouse Anti-Human CD133 Monoclonal Antibody (120-001-243)

Molecular Probes™, Invitrogen Ltd (Paisley, UK)

CellTrace™ CFSE Cell Proliferation Kit

R&D Systems (Oxford, UK)

Mouse Anti-Human STRO-1 Monoclonal Antibody (MAB1038)

Upstate Ltd (now part of Millipore) (Hampshire, UK)

H2A.X Phosphorylation Assay Kit (Flow Cytometry)

2.1.5 MSC Differentiation Reagents

R&D Systems (Oxford, UK)

Human Mesenchymal Stem Cell Functional Identification Kit

2.1.6 Cell Staining Reagents and Antibodies

AbD Serotec Ltd (Oxford, UK)

Normal donkey serum

R&D Systems (Oxford, UK)

Mounting medium

Mouse IgG1 Isotype Control (MAB002)

Normal Goat IgG (AB-108-C)

Sigma-Aldrich Company Ltd (Dorset, UK)

Alcian Blue

Alizarin Red S

(3-Aminopropyl) triethoxysilane

Bovine serum albumin (BSA)

Haematoxylin

Oil Red O

Senescent Cells Staining Kit

Triton X-100

Stratech Scientific Ltd (Soham, UK)

Jackson Immuno Rhodamine (TRITC)-conjugated AffiniPure F (ab') 2 Fragment Donkey Anti-Goat IgG (705-026-147)

Jackson Immuno Fluorescein Isothiocyanate (FITC)-conjugated AffiniPure F (ab') 2 Fragment Donkey Anti-Mouse IgG (715-096-150)

Upstate Ltd (now part of Millipore) (Hampshire, UK)

Anti-phospho-Histone H2A.X (Ser139) (05-636)

Vector Laboratories Ltd (Peterborough, UK)

VECTASHIELD™ Mounting Medium

VECTASHIELD™ Mounting Medium with DAPI

ImmEdge™ Hydrophobic Barrier Pen

VWR International Ltd (Lutterworth, UK)

Giemsa stain improved R66 solution

Rectangular cover glass (24x60mm)

Staining racks

Superfrost™ microscope slides with frosted ends

Whatman Filter Paper

2.1.7 Molecular Biology Reagents and Kits

ABgene (Epsom, UK)

Nucleospin RNA II Kit

Applied Biosystems Ltd (Warrington, UK)

Ambion RNAseZap

Agilent Technologies Ltd (West Lothian, UK)

RNA 6000 Nano LabChip kit

Invitrogen Ltd (Paisley, UK)

DNA molecular markers

I-SAGE™ Long Kit

S.O.C medium

Qiagen Ltd (Crawley, UK)

DNEasy Blood and Tissue Kit

MinElute 96 UF PCR Purification Kit

Taq PCR core kit

Roche Diagnostics Ltd (Sussex, UK)

Glycogen

TeloTAGGG Telomere Length Assay

VH BIO Ltd (Newcastle, UK)

Edge ExcelaPure™ 96-Well UF PCR Purification Kit

2.1.8 Chemicals

Braun Medical Ltd (Sheffield, UK)

Water for injections BP

Fisher Scientific UK Ltd (Loughborough, UK)

Acetic acid, glacial

Ammonium persulphate (10% stock solution)

Chloroform

Glycerol

Hydrochloric acid

Propan-2-ol (isopropanol)

Xylene

Hayman Ltd (James Borrough) (Witham, UK)

Absolute alcohol (ethanol) (analytical reagent grade) (100% and 70% stock solutions)

Invitrogen (Paisley, UK)

Agarose

TRIzol®

Merck Chemicals Ltd (Nottingham, UK)

BIO ((2′Z, 3′E)-6-Bromoindirubin-3′-oxime) (361550)

SB 203580 (4-(4-Fluorophenyl)-2-(4-methylsulfinylphenyl)-5-(4-pyridyl) 1H-imidazole) (559389)

Sigma-Aldrich Company Ltd (Dorset, UK)

Ammonium hydroxide solution (25% NH_3 in water)

ß - Mercaptoethanol

Bromophenol blue

Diethylpyrocarbonate (DEPC)

Dimethyl sulfoxide (DMSO)

Ethidium bromide (10 mg/ml stock solution)

Formalin solution (37% Formaldehyde)

Glycerol

Iron $_{III}$ chloride

Hydrogen peroxide solution (0.98M)

Mitomycin-C

N, N, N', N'-tetramethylethylenediamine (TEMED)

Saturated phenol (25:24:1 phenol: chloroform: iso-amyl alcohol)

Xylene cyanol

2.1.9 Buffers

These were kindly provided by Beatson Institute Central Services.

Sterile phosphate-buffered saline (PBS)

10x Tris-Borate/EDTA (TBE) electrophoresis buffer

2.1.10 Sequencing

PerkinElmer from Applied Biosystems (Warrington, UK)

BigDye Primer Kit

2.1.11 Bioinformatics

Metacore™, GeneGo Inc (St Joseph's, MI, USA)

MetaCore™ is an integrated software suite for functional analysis of experimental data. The scope of data types includes microarray and SAGE gene expression, SNPs and CGH arrays, proteomics, metabolomics, pathway analysis, Y2H and other custom interactions. MetaCore™ is based on a proprietary manually curated database (MetaBase™) of human protein-protein, protein-DNA and protein compound interactions, metabolic and signalling pathways and the effects of bioactive molecules in gene expression. The analytical package includes easy to use, intuitive tools for data visualization, mapping and exchange, multiple networking algorithms and filters. Data analysis was carried out on-line via web portal access requiring annual subscription.

National Centre for Biotechnology Information (NCBI) (Bethesda, MD, USA)

http://www.ncbi.nlm.nih.gov

NCBI is an international resource for molecular biology information.

http://www.ncbi.nlm.nih.gov/SAGE/

SAGE databases, reference files and SAGEmap tools for on-line analysis are available for download or on-line analysis. From September 2006, the website has been undergoing re-structuring and up-dating of tag to gene mappings with limited usability.

http://www.ncbi.nlm.nih.gov/UniGene/

NCBI's UniGene database and tools for on-line analysis clusters all transcripts corresponding to one gene and one name.

http://www.ncbi.nlm.nih.gov/BLAST/

NCBI's BLAST® (Basic Local Alignment Search Tool) for searching DNA or protein similarity through all the available sequence databases and alignment programs.

http://www.ncbi.nlm.nih.gov/PubMed/

The National Library of Medicine's PubMed database, providing access to over 17 million MEDLINE citations back to the 1950's and used for all literature searches.

SAGE Genie, Cancer Genome Anatomy Project (CGAP), National Cancer Institute (NCI) (Bethesda, MD, USA)

http://cgap.nci.nih.gov/SAGE

The SAGE Genie website provides highly intuitive and visual displays of human gene expression and is based on a unique analytical process that reliably matches 10 or 17 bp SAGE tags to known genes. It includes a reference database of single nucleotide polymorphism (SNP) associated alternative tags in order to enhance tag to gene mapping. The website offers multiple functions such as the detailed analysis of individual genes or tags, and also the comparison of SAGE libraries either uploaded by the user or available online. Statistical significance and tag fold differences can be defined by the user and this site was used for the analysis of the MSC SAGE libraries.

SAGE website at John Hopkins University (Baltimore, MD, USA)

http://www.sagenet.org

This is the web-site of the scientists who originally designed SAGE. SAGE 2000 software can be downloaded from the web-site after registration or following the instructions provided with the SAGE kit.

SAGEstat (Version 4) Software from Department of Anatomy and Embryology, Academic Medical Centre (Amsterdam, Netherlands)

Kind gift from Dr J.M.Ruijter (j.m.ruijter@amc.uva.nl). SAGEstat can be used for the evaluation and planning of SAGE analysis and is based on the Z-test which is a test between two proportions and based on the normal approximation of the binomial distribution. The software was used to compare the results to those generated by SAGE Genie.

2.1.12 Software

GraphPad Software (San Diego, CA, USA)

GraphPad Prism® 4 for basic biostatistics and scientific graphing

Microsoft® (Reading, UK)

Microsoft® Office 2003 including Word, Excel, Access and Powerpoint

Tree Star Inc (Ashland, OR, USA)

FlowJo 6.0 flow cytometry analysis software

2.1.13 Taqman® Low Density Array and Reagents

Applied Biosystems Ltd (Warrington, UK)

Taqman® Universal PCR Mastermix

Taqman® low density human endogenous control array (4367563)

Taqman® low density arrays (Format 96b) were custom designed to contain GAPDH as the endogenous control and 95 target assays as shown below:

Gene	Gene Name	Assay ID	Ref Seq ID
ACTB	actin, beta	Hs99999903_m1	NM_001101.2
ADAMTS1	ADAM metallopeptidase with thrombospondin type 1 motif, 1	Hs00199608_m1	NM_006988.3
AKR1C1, AKR1C2	aldo-keto reductase family 1, member C1 (dihydrodiol dehydrogenase 1; 20-alpha (3-alpha)-hydroxysteroid dehydrogenase),aldo-keto reductase family 1, member C2 (dihydrodiol dehydrogenase 2; bile acid binding protein; 3-alpha hydroxysteroid dehydrogenase, type III)	Hs00413886_m1	NM_001353.5 NM_205845.1 NM_001354.4
ANXA2	Annexin A2	Hs00733393_m1	NM_001002857.1
APLP2	Amyloid beta (A4) precursor-like protein 2	Hs00155778_m1	NM_001642.1
ARPC2	actin related protein 2/3 complex, subunit 2, 34kDa	Hs00194852_m1	NM_152862.1 NM_005731.2
ATP5G3	ATP synthase, H+ transporting, mitochondrial F0 complex, subunit C3 (subunit 9)	Hs00266085_m1	NM_001002258.2NM_001689.3
BLVRB	Biliverdin reductase B (flavin reductase (NADPH))	Hs00355972_m1	NM_000713.1
BSCL2, HNRPUL2	Bernardinelli-Seip congenital lipodystrophy 2 (seipin), heterogeneous nuclear ribonucleoprotein U-like 2	Hs00369057_m1	NM_032667.4
CALM1, CALM2	calmodulin 1 (phosphorylase kinase, delta), calmodulin 2 (phosphorylase kinase, delta)	Hs00237233_m1	NM_006888.3
CAV1	caveolin 1, caveolae protein, 22kDa	Hs00184697_m1	NM_001753.3
CCND1	Cyclin D1	Hs00277039_m1	NM_053056.2
CCT7	chaperonin containing TCP1, subunit 7 (eta)	Hs00362446_m1	NM_001009570.1NM_006429.2

CD44	CD44 molecule (Indian blood group)	Hs00153304_m1	NM_001001389.1NM_001001390.1NM_001001391.1NM_001001392.1NM_000610.3
CD63	CD63 molecule	Hs00156390_m1	NM_001040034.1NM_001780.4
CDKN1A	Cyclin-dependent kinase inhibitor 1A (p21, Cip1)	Hs00355782_m1	NM_078467.1, NM_000389.2
CDKN1B	Cyclin-dependent kinase inhibitor 1B (p27, Kip1)	Hs00153277_m1	NM_004064.2
CDKN2A	Cyclin-dependent kinase inhibitor 2A (melanoma, p16, inhibits CDK4)	Hs00233365_m1	NM_058195.2 NM_058197.3 NM_000077.3
CEECAM1	cerebral endothelial cell adhesion molecule 1	Hs00170969_m1	NM_016174.3
CLIC1	chloride intracellular channel 1	Hs00559461_m1	NM_001288.4
COL1A1	collagen, type I, alpha 1	Hs00164004_m1	NM_000088.3
COL1A2	collagen, type I, alpha 2	Hs00164099_m1	NM_000089.3
COL3A1	collagen, type III, alpha 1 (Ehlers-Danlos syndrome type IV, autosomal dominant)	Hs00164103_m1	NM_000090.3
COL5A1	collagen, type V, alpha 1	Hs00609088_m1	NM_000093.3
COTL1	coactosin-like 1 (Dictyostelium)	Hs00332755_m1	NM_021149.2
COX5B	cytochrome c oxidase subunit Vb	Hs00426948_m1	NM_001862.2
CST3	cystatin C (amyloid angiopathy and cerebral haemorrhage)	Hs00264679_m1	NM_000099.2
CTGF	connective tissue growth factor	Hs00170014_m1	NM_001901.2
CTSS	cathepsin S	Hs00175403_m1	NM_004079.3
DEGS1	Degenerative spermatocyte homolog 1, lipid desaturase (Drosophila)	Hs00186447_m1	NM_144780.1 NM_003676.2
DPYSL3	dihydropyrimidinase-like 3	Hs00181665_m1	NM_001387.2

DSP	Desmoplakin	Hs00189422_m1	NM_001008844.1NM_004415.2
DUSP6	dual specificity phosphatise 6	Hs00169257_m1	NM_001946.2
DVL1	dishevelled, dsh homolog 1 (Drosophila)	Hs00182896_m1	NM_004421.2
ELN	elastin (supravalvular aortic stenosis, Williams-Beuren syndrome)	Hs00355783_m1	NM_000501.1
FBXO18	F-box protein, helicase, 18	Hs00262318_m1	NM_032807.3 NM_178150.1
FOS	v-fos FBJ murine osteosarcoma viral oncogene homolog	Hs00170630_m1	NM_005252.2
FOXO3A	forkhead box O3A	Hs00818121_m1	NM_201559.1 NM_001455.2
GARS	Glycyl-tRNA synthetase	Hs00157653_m1	NM_002047.1
GPX4	glutathione peroxidase 4 (phospholipid hydroperoxidase)	Hs00157812_m1	NM_001039847.1NM_002085.3
HMGA1	high mobility group AT-hook 1	Hs00431242_m1	NM_145905.1
HMOX1	Heme oxygenase (decycling) 1	Hs00157965_m1	NM_002133.1
HNF4A	hepatocyte nuclear factor 4, alpha	Hs00230853_m1	NM_178849.1 NM_178850.1 NM_175914.3 NM_001030004.1NM_001030003.1NM_000457.3
HSPA8	heat shock 70kDa protein 8	Hs00852842_gH	NM_006597.3
HTRA1	HtrA serine peptidase 1	Hs00170197_m1	NM_002775.3
IFI30	interferon, gamma-inducible protein 30	Hs00173838_m1	NM_006332.3
IGFBP4	insulin-like growth factor binding protein 4	Hs00181767_m1	NM_001552.2
IL6ST	interleukin 6 signal transducer (gp130, oncostatin M receptor)	Hs00174360_m1	NM_175767.1 NM_002184.2
ITGA11	integrin, alpha 11	Hs00201927_m1	NM_001004439.1NM_012211.3

KDELR2	KDEL (Lys-Asp-Glu-Leu) endoplasmic reticulum protein retention receptor 2	Hs00199277_m1	NM_006854.2
KIAA1199	KIAA1199	Hs00378530_m1	NM_018689.1
KLF9	Kruppel-like factor 9	Hs00230918_m1	NM_001206.2
LMO7	LIM domain 7	Hs00245600_m1	NM_005358.4
LOC401152	HCV F-transactivated protein 1	Hs00386171_m1	NM_001001701.1
LOXL1	lysyl oxidase-like 1	Hs00173746_m1	NM_005576.2
LUM	Lumican	Hs00158940_m1	NM_002345.3
MRC2	mannose receptor, C type 2	Hs00195862_m1	NM_006039.3
MVP	Major vault protein	Hs00245438_m1	NM_017458.2 NM_005115.3
MYL9	myosin, light chain 9, regulatory	Hs00382913_m1	NM_181526.1
MYO10	myosin X	Hs00202485_m1	NM_012334.1
OAZ2	ornithine decarboxylase antizyme 2	Hs00159726_m1	NM_002537.1
OLFML3	Olfactomedin-like 3	Hs00220180_m1	NM_020190.2
PEA15	phosphoprotein enriched in astrocytes 15	Hs00269428_m1	NM_003768.2
PLAT	plasminogen activator, tissue	Hs00263492_m1	NM_033011.1 NM_000930.2 NM_000931.2
POLR2A	polymerase (RNA) II (DNA directed) polypeptide A, 220kDa	Hs00172187_m1	NM_000937.2
PRG1	Proteoglycan 1, secretory granule	Hs00160444_m1	
PRSS23	protease, serine, 23	Hs00359912_m1	NM_007173.3
PSAP	prosaposin (variant Gaucher disease and variant metachromatic leukodystrophy)	Hs00358165_m1	NM_002778.2
PTGS2	Prostaglandin-endoperoxide synthase 2 (prostaglandin G/H synthase and	Hs00153133_m1	NM_000963.1

	cyclooxygenase)		
ROR1	receptor tyrosine kinase-like orphan receptor 1	Hs00178178_m1	NM_005012.1
RPLP0	ribosomal protein, large, P0	Hs99999902_m1	NM_053275.3 NM_001002.3
RTN4	reticulon 4	Hs00199671_m1	NM_207520.1 NM_207521.1 NM_153828.2 NM_020532.4 NM_007008.2
S100A6	S100 calcium binding protein A6	Hs00170953_m1	NM_014624.3
SERPINE1	Serpin peptidase inhibitor, clade E (nexin, plasminogen activator inhibitor type 1), member 1	Hs00167155_m1	NM_000602.1
SERPINE2	Serpin peptidase inhibitor, clade E (nexin, plasminogen activator inhibitor type 1), member 2	Hs00299953_m1	NM_006216.2
SHC1	SHC (Src homology 2 domain containing) transforming protein 1	Hs00427539_m1	NM_183001.3 NM_003029.3
SLC38A2	Solute carrier family 38, member 2	Hs00255854_m1	NM_018976.3
SOD1	superoxide dismutase 1, soluble (amyotrophic lateral sclerosis 1 (adult))	Hs00166575_m1	NM_000454.4
SPARC	secreted protein, acidic, cysteine-rich (osteonectin)	Hs00277762_m1	NM_003118.2
SRM	spermidine synthase	Hs00162307_m1	NM_003132.2
STAT1	Signal transducer and activator of transcription 1, 91kDa	Hs00234829_m1	NM_139266.1 NM_007315.2
STC2	Stanniocalcin 2	Hs00175027_m1	NM_003714.2
TGFBI	transforming growth factor, beta-induced, 68kDa	Hs00165908_m1	NM_000358.1
TGM2	transglutaminase 2 (C polypeptide, protein-glutamine-gamma-glutamyltransferase)	Hs00190278_m1	NM_198951.1 NM_004613.2

THY1	Thy-1 cell surface antigen	Hs00174816_m1	NM_006288.2
TM4SF1	transmembrane 4 L six family member 1	Hs00371997_m1	NM_014220.2
TMEM47	Transmembrane protein 47	Hs00230190_m1	NM_031442.2
TRAM2	translocation associated membrane protein 2	Hs00202213_m1	NM_012288.3
TUBB6	tubulin, beta 6	Hs00603164_m1	NM_032525.1
UBC	ubiquitin C	Hs00824723_m1	NM_021009.3
VCP	valosin-containing protein	Hs00997642_m1	NM_007126.2
VIM	Vimentin	Hs00185584_m1	NM_003380.2
WBSCR1	Williams-Beuren syndrome chromosome region 1	Hs00254535_m1	NM_022170.1
YIPF5	Yip1 domain family, member 5	Hs00229305_m1	NM_030799.6 NM_001024947.1
YWHAB	tyrosine 3-monooxygenase/tryptophan 5-monooxygenase activation protein, beta polypeptide	Hs00793604_m1	NM_139323.2 NM_003404.3

2.1.14 TeloTAGGG Telomere Length Assay Buffers and Solutions

1X TAE buffer

0.04M Tris-Acetate

0.001M EDTA

pH8.0

HCl Solution

0.25M HCl

Denaturation Solution

0.5M NaOH

1.5M NaCl

Neutralisation Buffer

0.5M Tris-HCl

3M NaCl

pH7.5

20X SSC

3M NaCl

0.3M Na-Citrate

pH 7.0

2X SSC

200mls 20 x SSC (solution 5)

1800mls dH2O

DIG Easy Hyb Solution

Add 64mls dH2O to 1 bottle DIG-Easy Hyb granules (provided with TeloTAGGG kit).

Incubate at 37oC until complete reconstitution (prepare in advance).

Stringent Wash Buffer I

2 x SSC

0.1% SDS

Stringent Wash Buffer II

0.2 x SSC

O.1% SDS

1 x Washing Buffer

50mls 10 x washing buffer (provided with TeloTAGGG kit)

450mls dH2O

1 x Blocking Solution

20mls 10 x blocking buffer (provided with TeloTAGGG kit)

180mls Maleic acid buffer

1 x Maleic Acid Buffer

50mls 10 x Maleic acid buffer (provided with TeloTAGGG kit)

450mls dH2O

Anti-DIG-AP

10ul Anti-DIG-AP antibody

100mls 1 x Blocking Solution

1 x Detection Buffer

50mls 10 x Detection Buffer (provided with TeloTAGGG kit)

450mls dH2O

Stripping Buffer

0.8% NaOH

0.1% SDS

2.2 Cell Culture and Flow Cytometry Methods

2.2.1 Cell Culture

Ethical approval for the research was granted from the Local Research and Ethics Committee (LREC) at Glasgow Royal Infirmary (Project number: 02SC005). On the day prior to surgery, informed consent was obtained from patients undergoing CABG within the Department of Cardiac Surgery, Glasgow Royal Infirmary. Copies of the consent and research protocol were kept by me, the patient and filed in the case notes. Thirty of thirty three (91%) patients approached agreed to participate in the research. Patients were excluded from the study if: age >80; osteoporosis; alcoholism; on immunosuppressive medications or previous cardiac surgery.

2.2.1.1Cell Counting and Viability Assessment

All cell counts were performed on a Hawksley BS.748 improved Neubauer counting chamber using the trypan blue exclusion assay. Stock trypan blue solution was diluted at 1:10 with PBS, and 10µl added to 10µl of the cell suspension (1:1 dilution). Approximately 10µl of the mixture was transferred by capillary action to a haemocytometer and viewed under an inverted microscope at 10x magnification. Viable cells exclude the dye and non-viable cells stain blue due to a breakdown in cell membrane integrity. Viable and total cells were counted on two diagonally opposite 16 square ($1mm^2$) grids and averaged. The total number of viable cells is equal to the viable cell concentration multiplied by the dilution factor (e.g. multiply by two if cell: dye ratio is 1:1). Cell viability was calculated by the equation: % cell viability = total viable cells (unstained) / total cells (stained plus unstained) x 100.

2.2.1.2Aspiration of Sternal Bone Marrow

With the patient in theatre and under general anaesthesia, the chest wall was prepared and draped in the usual manner for CABG. A single skin incision was made from the sternal notch to the xiphisternum using a scalpel. Dissection of the subcutaneous tissue down to the pre-sternal fascia was performed using diathermy. A standard 14 gauge BM aspiration needle was assembled and inserted into the manubrium perpendicular to the periosteum, using a twisting motion. Care was taken to avoid excessive force that could push the needle through the sternum and into the anterior mediastinum (with potential injury to the heart or great vessels). The needle stylet was removed and bone marrow aspirated into a 5ml syringe containing 1ml preservative-free heparin (1000units per ml). The syringe was inverted and BM injected through a white needle into a 25ml Universal container containing 14ml BM media and 1ml Heparin (1000units per ml). Two further aspirations were performed in the upper and middle thirds of the sternum. This increased the yield of mononuclear cells and reduced venous blood contamination compared to a large aspiration at one site. The samples are taken immediately to the laboratory for separation of the mononuclear cell fraction.

2.2.1.3Preparation of Human Bone Marrow Mononuclear Cells

Histopaque-1077 is solution of polysucrose and sodium diatrizoate, adjusted to form a density of 1077 ± 0.001 g/ml and is routinely used for the isolation of mononuclear cells from anti-coagulated peripheral blood or bone marrow. During centrifugation, erythrocytes and granulocytes are aggregated by polysucrose and rapidly sediment, whereas, lymphocytes and other mononuclear cells remain at the plasma-Histopaque interface. Erythrocyte contamination is negligible and platelets are removed by subsequent wash steps.

15ml of Histopaque-1077 was transferred to two 50ml tubes and brought to RT (colder temperatures cause clumping and decreased cell recovery). The BM was re-suspended and 30ml carefully layered onto Histopaque-1077 in each tube. The tubes were centrifuged at 400 x g for 30 minutes at RT with the brake turned off. The upper layer was aspirated to within 1cm of the opaque interface and discarded. The opaque interface was transferred into a Universal container

and washed twice by adding 20ml Wash Buffer, then centrifuged at 200 x g for 10 minutes. The supernatant was discarded and the MNC's re-suspended in 10ml MSC media. A 10µl sample was counted using a haemocytometer.

2.2.1.4Colony Forming Unit – Fibroblast (CFU–F) Assay

The CFU-F assay is a well established method for the quantification of MSC's from a human bone marrow sample. CFU-F's represent stem/progenitor cells with non-haematopoietic differentiation potential. Therefore, the assay can be used for quality testing of the MSC source and isolation procedure. The assay can be performed in a dilution series or set up with a defined cell concentration with replicates.

Preparing the CFU-F Assay in a Dilution Series

MSC media was pre-warmed to 37ºC in a waterbath. Re-suspend an aliquot of the MNC suspension at 2 x 10^7 cells per ml in MSC media. Dilute the suspension by pipetting 100µl into a 15ml tube containing 10ml MSC medium to give a concentration of 2 x 10^5 cells per ml. Repeat with 50µl and 25µl to give two further concentrations of 1 x 10^5 and 0.5 x 10^5 cells per ml respectively. Re-suspend the cells and transfer to three labelled 100 mm culture dishes and incubate in a 37ºC incubator with 5% CO_2 and >95% humidity for 2 weeks. The media is not replenished during this period.

Staining and Enumeration of CFU-Fs

MSC media was discarded and cells washed twice with 5ml D-PBS (-Ca^{2+}, -Mg^{2+}). The cells were fixed in 5ml of methanol by incubation at RT for 5 minutes. The methanol was then discarded and the culture dishes allowed to air dry. Dilute the Giemsa staining solution 1:20 with dH_2O and filter through a folded filter paper. Add 5ml Giemsa staining solution to each dish and incubate for 10 minutes. Remove the stain, wash each dish twice with dH_2O and discard. Allow the culture dishes to air dry and perform the scoring procedure. CFU-F colonies containing at least 20 cells were scored macroscopically (typically 1 – 8 mm in diameter). In a dilution series, the correlation between the numbers of MNC's plated and CFU-Fs counted should be linear.

2.2.1.5Expansion and Handling of Human MSC's

MSC's are present a low frequency in human BM samples and require expansion to generate sufficient numbers for further experiments. We used the plastic adherence method and a cell density of 2000 cells per cm^2 although alternative selection methods and plating densities are described.

Set-up of the MSC Expansion Procedure

Reagents were pre-warmed to 37ºC in a waterbath, and BM MNC's re-suspended at a concentration of 1.5 x 10^6 cells per ml in MSC media. 0.32 ml MSC media per cm^2 culture flask (e.g. 8ml media in a T-25, 24ml media in a T-75) were transferred to a culture flask and cultured at 37ºC in an incubator, with 5% CO_2 and > 95% humidity. After 72 hours, the media was aspirated to discard the non-adherent fraction. Cells were replenished with fresh MSC media every 3-4 days and observed daily under an inverted microscope. When the cells reached 80-90% confluence, they were passaged. "Passaging" simply refers to the process of detaching adherent cells from a culture flask and re-plating at the required cell density.

Passaging of Human MSC's

Reagents were pre-warmed to 37ºC in a waterbath. Media was discarded and the cells rinsed with D-PBS (-Ca^{2+}/-Mg^{2+}) equivalent to half the volume of MSC media. Rock the culture flask for 30 seconds to bathe the cell monolayer and discard the D-PBS (-Ca^{2+}, -Mg^{2+}). Add 1ml T/E per 25cm^2 of the culture flask area and incubate for 5 – 10 minutes in an incubator. Gently tapping the flask helps dislodge the monolayer of cells and the cells were viewed under an inverted microscope to ensure detachment. T/E was inactivated by adding 2ml MSC media per ml of T/E, and the cells re-suspend by repetitive pipetting. The cells were transferred to a sterile tube and centrifuged at 200 x g for 5 minutes. The cells were re-suspended in a small volume of MSC media and viable counts assessed using a haemocytometer. MSC's were further expanded by re-plating at 2000 viable cells/cm^2 in a culture flask and changing the MSC media twice a week. The cells were observed daily and passaged when 80-90% confluent. Long-term MSC's cultures were deemed senescent or growth arrested when they failed to reach near confluence after a minimum of three weeks in culture.

Cryopreservation Protocol for MSC's

Passaged MSC's were re-suspended in MSC media at 2 x 10^6 cells per ml and an equal volume of cryopreservation media added to cells and mixed well (final concentration DMSO 10%). 1ml (1 x 10^6 cells) was added to each CryoTube™ and placed in a "Mr Frosty" containing 250ml of fresh propan-2-ol and stored at -70ºC overnight. For long-term storage, the CryoTubes™ were transferred to a liquid N_2 container or ultra low temperature (–150ºC) freezer.

Thawing Protocol for MSC's

CryoTubes™ were removed from storage and thawed in at 37ºC in a waterbath. The vials were disinfected by soaking in 70% ethanol and dried with a paper towel. Cells were transferred to a 15ml tube and 10ml pre-warmed MSC media added drop wise over 5 minutes. Centrifuge at 200 x g for 5 minutes to pellet the cells, re-suspend in fresh media and transfer to a T-75 culture flask. Incubate overnight at 37ºC 5% CO_2 and > 95% humidity for at least 16 hours. The following day, the MSC's are harvested and viability counts assessed by trypan blue exclusion. On occasion, MSC viability was carried out prior to the overnight incubation in order to assess storage and recovery procedures.

2.2.1.6Colony Forming Efficiency – Fibroblast (CFE–F) Assay

The CFE-F assay is a method for the quantification of stem/progenitor cells within established MSC cultures and can be used to assess individual donor differences.

Preparing the CFE-F Assay in Triplicate

Pre-warm the MSC media to 37ºC in a waterbath. Re-suspend an aliquot of the MSC suspension at 57 x 10^3 cells per ml in MSC media. Dilute the suspension by pipetting 100µl into a 15ml tube containing 10ml MSC medium to give a final concentration of 57 x 10^1 cells per ml (this will give a cell density of 10 cells per cm^2 in a 100mm culture dish). Repeat twice , re-suspend the cells carefully and transfer to three 100mm culture dishes and incubate in a 37ºC incubator with 5% CO_2 and >95% humidity for 2 weeks. The media is not replaced during this period.

Staining and Enumeration of CFE-Fs

This procedure is identical to that described for staining and enumeration of CFU–Fs. The percentage CFE-F is calculated by dividing total number of colonies counted in three dishes by the total number of MSC's seeded and multiplying by 100.

2.2.2 Flow Cytometry Analysis of MSC's

Flow cytometry is a quantitative technique that permits the visualisation of cells by multiple parameters using fluorescence. In comparison to spectrophotometers, it is able to measure fluorescence per cell and will allow accurate counting of single cells. All flow cytometry experiments were performed on a BD FACSCalibur™.

Following antibody staining, the cells were visualised with either a linear or log scale, as appropriate, on a Forward Scatter (FSC) versus Side Scatter (SSC) dot plot. FSC detects cell size whilst SSC determines cellular granularity. This view allows a gate to be drawn around the main population of cells and to exclude debris and dead cells that can be seen in the lower left corner of the plot. The cells within this graphical boundary formed the basis for all further analysis.

The cells were visualised in a log scale FL1 vs FL2 dot plot or a histogram. Unstained and isotype controls were used to determine auto-fluorescence and non-specific background staining and the cells were positioned in the first log decade of the parameter(s) by altering the voltage settings. Additionally, positive controls were required to compensate for spectral overlap between fluorochromes using the compensation settings. This was achieved by subtracting as a percentage the fluorescence observed in the detector that should not emit fluorescence. This allocates the cells in the bottom right hand and top left hand corners of the FACS dot plot according to the fluorescent conjugate used. Once optimal compensation was achieved, the test samples were run and the percentage of discrete populations calculated. Ten thousand gated events were collected for each experiment.

2.2.2.1Characterisation of MSC cultures

Passaged MSC's were re-suspended at 1 x 10^6 cells per ml and 100µl of the cell suspension added to each FACS tube containing the following amounts of antibody as recommended by the manufacturer:

Tube No.	FITC Ab	Vol (µl)	PE Ab	Vol (µl)
1	IgG_1	2	IgG_1	2
2	IgG_1	2	CD 13	2
3	CD 90	1	IgG_1	2
4	CD 90	1	CD 13	2
5	CD 90	1	CD 45	2
6	CD 31	2	CD 34	2
7	45	2	CD 34	2
8	CD 31	2	CD 105	1
9	HLA – A, B, C	2	CD 45	2
10	HLA - DR, DP, DQ	2	CD 45	2
11	CD 45	2	CD 13	2
12	CD 45	2	CD 14	2
13	CD 90	1	CD 133	2
14	-	-	Goat Anti Mouse Ig	2
15	Stro1 unconjugated	10	-	
16	Stro1 unconjugated	10	Goat Anti Mouse Ig	5
17	CD 71	2	CD 73	2
18	CD 44	2	CD 29	2
19	HLA – A, B, C	2	CD 49d	2
20	CD 31	2	CD 49e	2
21	CD 106	2	CD 166	2

The tubes were incubated at RT for 30 minutes in the dark. The cells were washed twice with RT wash buffer and centrifuged at 200 x g for 5 minutes. The supernatant was discarded and the cells were re-suspended in FACSFlow™ then analysed immediately on a flow cytometer. Cells were re-suspended in ice-cold FACS Fix solution and stored at 4ºC in the dark if analysis could not be performed on the same day as staining.

2.2.2.2 Carboxy-fluorescein diacetate succinimidyl diester (CFSE) Assay

CFSE is a colourless dye that passively diffuses into cells and remains non-fluorescent until the acetate groups are removed by intracellular esterases. The resulting carboxyfluorescein succinimidyl ester is highly fluorescent and reacts

with intracellular amines to form fluorescent conjugates that are retained by the cell. CFSE is partitioned equally between daughter cells during cell division and as a result high resolution tracking of cell division can be monitored by the reduction in fluorescence seen using flow cytometry. The CellTrace™ CFSE Cell Proliferation Kit (Molecular Probes, Invitrogen) and the manufacturer's protocol with minor modifications were followed for these experiments.

Briefly, passaged MSC's were re-plated at 2000 viable cells per cm^2 in nine wells of two 6-well plates. The following day the media was discarded and replaced with 1ml of wash buffer containing 1μM CFSE and incubated for 15 minutes at 37ºC. Media was again discarded and replaced with 3ml of MSC medium containing either DMSO, 1μM SB203580 or 15nM Mitomycin C. Mitomycin C was used to determine the maximum brightness of cells after uptake of CFSE by inhibiting cell division – referred to as the $CFSE_{Max}$. Cells were analysed at days one, three and five using a flow cytometer. Briefly, MSC's were detached from each well with T/E, washed three times in wash buffer and centrifuged at 200 x g for 5 minutes. The supernatant was discarded and cells re-suspended in FACSFlow™ before analysis on a flow cytometer.

2.2.2.3H2AX DNA Damage Detection Assay

H2AX is a variant of histone H2A protein and is a major substrate of kinases involved in the ATM-initiated signalling cascade in response to DNA damage. H2AX contains several serine residues and phosphorylation of serine 139 occurs in response to DNA double strand breaks, leading to recruitment of DNA repair mechanisms. If damage is too severe, cells will undergo apoptosis leading to fragmentation of the genome and an increase in DNA double strand breaks. Thus, H2AX functions as a marker of DNA damage and its expression occurs before the morphological changes of apoptosis are detectable.

On the previous day, passaged MSC's were re-suspended in MSC media at 1×10^5 viable cells per ml and 3ml added to 3 wells of a 6-well plate. The cells were incubated overnight and the next day positive controls set up by incubating the cells of two wells for 1 hour in 3ml MSC media containing either 75μM H_2O_2 or 300nM Mitomycin C. The media in each well was discarded and the cells washed twice in PBS and allowed to recover over 1 hour in fresh MSC media. The cells

were stained using the Flow Cytometry H2A.X Phosphorylation Assay Kit (Upstate) following the manufacturers instructions.

Briefly, MSC's were detached from each well with T/E, washed three times in wash buffer and centrifuged at 200 x g for 5 minutes. For each well, the cells were re-suspended in 150µl PBS and 50µl (1×10^5) aliquoted into 3 FACS tubes. The cells were fixed on ice, permeabilized and either 3.5µl of PBS, FITC IgG or FITC-anti-phospho-Histone H2A.X antibody added to each tube. The tubes were incubated on ice for 20 minutes in the dark, washed and analysed on a flow cytometer.

2.2.3 Differentiation of MSC's In Vitro

The ability of MSC's to differentiate into multiple mesenchymal lineages is a defining characteristic and can be used to monitor the effects of prolonged expansion on MSC properties. The Human Mesenchymal Stem Cell Functional Identification Kit (R&D Systems) was used following the manufacturers protocols.

2.2.3.1Adipogenic Differentiation and Detection

Passaged MSC's were re-suspended in α-MEM basal medium at 1×10^5 cells per ml and 250µl per well added to two wells (1 control and 1 for differentiation) of a 48-well plate. The cells were incubated overnight and viewed under an inverted microscope to ensure 100% confluence prior to the addition of differentiation medium. 250µl per well of adipogenic differentiation medium or α-MEM basal medium (control) was added and replaced twice a week for 21 days. The cells were observed daily for the appearance of lipid vacuoles in the cytoplasm.

The media was aspirated and discarded and each well washed twice with 0.5ml of D-PBS (-Ca^{2+}, -Mg^{2+}). The cells were fixed by adding 0.5ml of 10% Formalin solution and incubating at RT for 30 minutes. During fixation a working solution of Oil Red O was prepared by adding three parts Oil Red O stock solution (0.5g Oil Red O in 99% isopropanol) to two parts dH_2O and filtering through a folded Whatman #1 filter paper. The formalin was aspirated and 0.5ml of Oil Red O working solution added to each well and incubated at RT for 20 minutes on a plate shaker. The stain was aspirated completely, the cells washed twice with

dH_2O and 0.5ml dH_2O added to each well to keep the cells moist. Lipid vacuoles stain bright red when viewed under an inverted microscope.

The immunofluorescence protocol provided with the Human Mesenchymal Stem Cell Functional Identification Kit was then followed. Briefly, media was discarded and each well washed twice with 0.5ml of D-PBS (-Ca^{2+}, -Mg^{2+}). The cells were fixed by adding 0.5ml of 10% Formalin solution and incubating at RT for 10 minutes. Cells were then washed three times with 1ml 1% BSA D-PBS (-Ca^{2+}, -Mg^{2+}). The cells were permeabilized and blocked using 0.5ml of 0.3% Triton-X 1% BSA 10% Donkey serum D-PBS (-Ca^{2+}, -Mg^{2+}) and incubating at RT for 45 minutes. 300µl of FABP4 Ab (1µg per 100µl) in 1% BSA 10% Donkey serum D-PBS (-Ca^{2+}, -Mg^{2+}) was then added to each well and incubated for 1 hour at RT. Cells were washed three times with 1ml 1% BSA D-PBS (-Ca^{2+}, -Mg^{2+}). 300µl of a TRITC-conjugated donkey anti-goat secondary Ab (15µg per ml) was added to each well and incubated in the dark for 1 hour. Cells were washed a further three times with 1ml 1% BSA D-PBS (-Ca^{2+}, -Mg^{2+}), mounted in DAPI and cover slipped before viewing.

2.2.3.2Osteogenic Differentiation and Detection

Passaged MSC's were re-suspended in α-MEM basal medium at 2 x 10^4 cells per ml and 250µl per well added to two wells (1 control and 1 for differentiation) of a 48-well plate. The cells were incubated overnight and viewed under an inverted microscope to ensure 50-70% confluence prior to the addition of differentiation medium. 250µl of osteogenic differentiation medium was added and replaced twice a week for 21 days. The cells were observed daily for increasing granularity in the cytoplasm.

The media was aspirated and discarded and each well washed twice with 0.5ml of D-PBS (-Ca^{2+}, -Mg^{2+}). The cells were fixed by adding 0.5ml of ice cold 70% Ethanol and incubating a 4ºC for 30 minutes. To prepare the stain, 0.5g of Alizarin Red S was added to 50ml of distilled H_2O and 1% Ammonium Hydroxide solution added drop wise to achieve a pH of 4.2. The fixative was discarded, cells washed twice with distilled H_2O and 0.5ml of the stain added to each well. The cells were incubated at RT for 30 minutes on a rocker platform. The stain

was discarded and the cells washed twice with distilled H_2O. Areas of calcium deposition appeared bright red when viewed under an inverted microscope.

The immunofluorescence protocol provided with the Human Mesenchymal Stem Cell Functional Identification Kit was then followed. Briefly, media was discarded and each well washed twice with 0.5ml of D-PBS (-Ca^{2+}, -Mg^{2+}). The cells were fixed by adding 0.5ml of 10% Formalin solution and incubating at RT for 10 minutes. Cell were then washed three times with 1ml 1% BSA D-PBS (-Ca^{2+}, -Mg^{2+}). The cells were permeabilized and blocked using 0.5ml of 0.3% Triton-X 1% BSA 10% Donkey serum D-PBS (-Ca^{2+}, -Mg^{2+}) and incubating at RT for 45 minutes. 300µl of Osteocalcin Ab (1µg per 100µl) in 1% BSA 10% Donkey serum D-PBS (-Ca^{2+}, -Mg^{2+}) was then added to each well and incubated for 1 hour at RT. Cells were washed three times with 1ml 1% BSA D-PBS (-Ca^{2+}, -Mg^{2+}). 300µl of FITC-conjugated donkey anti-mouse secondary Ab (15µg per ml) was added to each well and incubated in the dark for 1 hour. Cells were washed a further three times with 1ml 1% BSA D-PBS (-Ca^{2+}, -Mg^{2+}), mounted in DAPI and cover slipped before viewing.

2.2.3.3Chondrogenic Differentiation and Detection

Passaged MSC's were re-suspended in MSC medium at 2.5 x 10^5 cells per ml and 1ml transferred to a 15ml conical tube. The cells were centrifuged at 200 x g for 5 minutes and re-suspended in DMEM/F-12 basal medium. The above step was repeated although the cells were not resuspended although media was replaced with either 0.5ml Chondrogenic differentiation medium or DMEM/F-12 basal medium (control). The cell pellets were then cultured for 24 days with media changed twice a week.

At the end of the culture period media was discarded and cell pellets washed once with D-PBS (-Ca^{2+}, -Mg^{2+}). The pellets were fixed by incubating in 0.5ml 10% Formalin solution overnight and processed by an ethanol dilution series and paraffin embedding. The pellets were then cut into 2µM sections and mounted on sialene coated slides. Proteoglycans found in cartilage, such as chondroitin sulphate were detected in the pellets using Alcian blue and a baseline stain with Haematoxylin and Eosin (H+E) was performed to demonstrate basophilic structures purple (nuclei) and eosinophilic structures pink (intra and

extracellular proteins). The protocol was performed by Histology services, Beatson Institute, Glasgow.

To perform immunofluorescence, the paraffin mounted sections were deparaffinised in an ethanol dilution series (provided by Department of Surgery, Glasgow Royal Infirmary) and then rinsed with de-ionised water. Slides were transferred to D-PBS (-Ca^{2+}, -Mg^{2+}) for 5 minutes and permeabilized and blocked using 0.5 ml of 0.3% Triton-X 1% BSA 10% Donkey serum D-PBS (-Ca^{2+}, -Mg^{2+}) and incubating at RT for 45 minutes. Slides were dabbed dry and the section encircled using a hydrophobic pen. 150µl of Aggrecan Ab (1µg per 100µl) in 1% BSA 10% Donkey serum D-PBS (-Ca^{2+}, -Mg^{2+}) was added to each slide and incubated for 1 hour at RT. Slides were washed three times with 1ml 1% BSA D-PBS (-Ca^{2+}, -Mg^{2+}). 150µl of TRITC-conjugated donkey anti-goat secondary Ab (15µg per ml) was added to each slide and incubated in the dark for 1 hour. Slides were washed a further three times with 1ml 1% BSA D-PBS (-Ca^{2+}, -Mg^{2+}) and sections mounted in DAPI and cover slipped before viewing.

2.2.4 Senescence Associated β-Galactosidase Staining of MSC's

Senescence associated ß-galactosidase (SA ß-Gal) activity at pH 6.0 is used as a marker of senescence and is thought to represent the increase in lysosomal mass found in senescent cells. The enzyme is found in lysosomal compartments and has an optimal pH of 4 - 4.5. When ß-galactosidase cleaves the colourless substrate X-gal (5-bromo-4-chloro-3-indolyl-ß–galactopyranoside), galactose and an insoluble blue-coloured dye are produced with the intensity of the blue stain a measure of enzyme expression within cells. The Senescent Cells Staining Kit (Sigma) for the detection of ß-galactosidase activity at pH 6.0 was used following the manufacturers protocol.

Passaged MSC's were re-suspended at 5 x 10^4 cells per ml in MSC medium and 1ml aliquots added to 3 wells of a 24-well plate. Empty wells were filled with D-PBS (-Ca^{2+}, -Mg^{2+}) and the cells were incubated overnight. The following day, media was removed and the cells washed twice with 1ml D-PBS (-Ca^{2+}, -Mg^{2+}). The cells were fixed by adding 300µl 1X Fixation buffer to each well and incubating for 7 minutes at RT. During this time, the staining mixture was made up containing: 500µl 10X staining solution, 62.5µl reagent B, 62.5µl Reagent C,

125µl X-gal solution (pre-warmed for 1 hour in a 37ºC waterbath) and 4.25ml H_20 and passed through a 0.2µm filter. After incubation, fixative was removed and the cells washed 3 times with 1ml D-PBS (-Ca^{2+}, -Mg^{2+}). 300µl of staining mixture was added to each well and the plates were wrapped in foil and incubated at 37ºC without $C0_2$ for 16hours (important as the stain is pH specific). The staining mix was removed and replaced with dH_2O and the cells viewed under an inverted microscope at 10x magnification. At least 300 cells in random fields were counted, and the number cells staining blue and total counted were used to calculate the percentage of senescent (ß-galactosidase positive) cells.

2.2.5 H2AX Detection by Immunofluorescence

Passaged MSC's were re-suspended in MSC media at 1 x 10^5 viable cells per ml and 1ml added to 4 well chamber slides. The next day positive controls were set up by incubating some wells for 1 hour in 3ml MSC media containing 75µM H_2O_2 or exposure to U.V irradiation (200,000J) using a Strata linker. The media in each well was discarded and the cells washed twice in PBS and allowed to recover over 1 hour in fresh MSC media. The immunofluorescence protocol used for the differentiation studies was the followed. Briefly, media was discarded and each well washed twice with 0.5ml of D-PBS (-Ca^{2+}, -Mg^{2+}). The cells were fixed by adding 0.5ml of 10% Formalin solution and incubating at RT for 10 minutes. Cell were then washed three times with 1ml 1% BSA D-PBS (-Ca^{2+}, -Mg^{2+}). The cells were permeabilized and blocked using 0.5 ml of 0.3% Triton-X 1% BSA 10% Donkey serum D-PBS (-Ca^{2+}, -Mg^{2+}) and incubating at RT for 45 minutes. 250µl of H2AX Ab (2µg per ml in 1% BSA 10% Donkey serum D-PBS (-Ca^{2+}, -Mg^{2+}) was then added to each well and incubated for 1 hour at RT. Cells were washed three times with 1ml 1% BSA D-PBS (-Ca^{2+}, -Mg^{2+}). 300µl of a 1:100 dilution of FITC-conjugated donkey anti-mouse secondary was added to each well and incubated in the dark for 1 hour. Cells were washed a further three times with 1ml 1% BSA D-PBS (-Ca^{2+}, -Mg^{2+}), mounted in DAPI and cover slipped before viewing.

2.3 Molecular Biology Methods

2.3.1 Cell Pellets for Storage

Harvested cells that were required for subsequent RNA extraction were washed twice in ice-cold PBS and spun at 200 x g for 10 minutes. The pellet was then air-dried and snap-frozen in liquid nitrogen. The pellet was stored at -70ºC until further use.

2.3.2 Extraction of RNA

Before extraction, surfaces and pipettes were wiped with RNaseZap to remove traces of RNase's. RNase free pipette tips were used and microcentrifuge tubes were pre-treated with DEPC water (Add 0.1% DEPC to dH_20. Bring the DEPC into solution and incubate at 37ºC for 12 hours, then autoclave the solution for 15 minutes to remove DEPC). Total RNA was extracted using the techniques described below.

2.3.2.1RNA isolation using TRIzol® reagent

In a fume hood, TRIzol® reagent was allowed to warm to RT and 1ml added to a snap frozen cell pellet which was then homogenised by repetitive pipetting. The sample was incubated for 5 minutes and transferred to a 1.5ml micro-centrifuge tube. 200µl of chloroform was added and the tube shaken by hand for 15 seconds. Incubate for a further 2-3 minutes and then centrifuge at 4°C 12000 x g for 15 minutes. Remove the upper aqueous layer into a new tube, add 500µl isopropylalcohol and incubate for 10 minutes. The interface contains proteins and the lower layer genomic DNA. Centrifuge the tube at 4°C 12000 x g for 10 minutes and remove the supernatant without disturbing the pellet. Add 1.2ml 70% ethanol and mix by vortex. Centrifuge 4°C 7500 x g for 5 minutes. Discard the ethanol and allow the pellet to air dry. The RNA is dissolved in RNase-free water and heated to 55°C to aid solubilisation. The sample is divided into multiple aliquots and stored at -70ºC.

2.3.2.2 RNA Extraction by Nucleospin RNA II kit

Total RNA was isolated from snap frozen cell pellets as per the manufacturer's instructions (Macherey-Nagel). Approximately 1 x 10^6 cells were lysed by addition of 350µl of buffer RA1 and 3.5µl ß-mercaptoethanol and vortexing. The lysate was homogenised by passing through a 21 gauge needle 5 to 6 times and then applied to a NucleoSpin filter which contains the silica membrane. Contaminating genomic DNA, which is also bound to the silica membrane, was removed by treatment with DNase-1 solution for 15 minutes at RT. Salts, metabolites and macromolecular cellular components were removed in subsequent wash steps and pure RNA eluted under low ionic strength conditions with RNase-free water. The sample is divided into multiple aliquots and stored at -70ºC.

2.3.3 Assessment of RNA quality

RNA quality was assessed using the following three techniques:

2.3.3.1Genequant DNA/RNA calculator

The instrument was first calibrated with a blank and samples transferred to quartz capillary tubes for measurement. Optical density measurements were taken at 260nm. An OD measurement of 1 at 260 (A_{260}=1) corresponds to a concentration of approximately 50µg per ml double stranded DNA or 40µg per ml RNA. The ratio between the readings at 260nm and 280nm ($OD_{260:280}$) provides a measure of the sample purity. Samples of RNA with an $OD_{260:280}$ of 2.0 to 2.2 were of sufficient quality to be used for the techniques described in this research.

2.3.3.2Agilent 2100 Bio-analyser

The integrity of the RNA was observed on an Agilent 2100 Bioanalyser using the RNA 6000 LabChip™ kit. The LabChip™ contains multiple micro-channels etched into glass, and the channels are filled with a sieving polymer containing a fluorescent dye and molecular weight marker. The RNA is separated electrophoretically using strategically located electrodes. 1µl of RNA sample per

well is required for analysis and up to twelve samples can be analysed at once with results generated within thirty minutes. The RNA components are detected by fluorescence and translated into virtual gel images, sized and quantified in relation to internal standards. In addition, the software will analyse the electropherogram and generate an RNA integrity (RIN) number that can provide a numerical assessment of RNA integrity. RNA samples used for this study displayed two discrete ribosomal peaks, RNA ratio of between 2.0 and 2.2 and RIN values close or equal to 10. The samples and chips were prepared according to the manufacturer's instructions.

2.3.3.3NanoDrop ND-1000 Spectrophotometer

The Nanodrop ND-1000 spectrophotometer will measure RNA concentrations over a range of 2-3000ng per µl with a typical coefficient of variation of 2%. The instrument automatically calculates the high concentration and utilises the 0.2mm path length to calculate the absorbance. RNA was analysed following the manufacturer's protocol. Briefly, within the ND-1000 software Nucleic Acid application module, sample type was set to RNA-40. The instrument was calibrated with a blank and 1.5µl of RNA sample measured on the pedestals as a fluid column. Pedestals were wiped with a paper towel between samples to prevent carry over. Spectral measurement for each sample is rapid (less than ten seconds) and absorbance spectrum, $OD_{260:280}$ ratio and RNA concentrations are displayed as a printable report. An $OD_{260:280}$ of between 2.0 and 2.2 were used as a measure of sufficiently good quality RNA to be used for the techniques described in this research.

2.3.4 cDNA Synthesis

cDNA was prepared using the High Capacity cDNA Reverse Transcription kit (Applied Biosystems) as per the manufacturer's instructions. Stored, high quality RNA was adjusted to 1µg in 10µl RNase-free H_2O. Low concentration RNA samples were scaled up. Reactions were prepared in a PCR workstation (Labcaire) using RNase-free tubes and tips which were UV cross-linked prior to use. The RT master mix was made up on ice and contained 2µl 10X RT buffer, 0.8µl 25X dNTP Mix (100mM), 2µl 10X RT Random Primers, 1µl MultiScribe™ Reverse Transcriptase and 4.2µl RNase-free H_2O per reaction. To the 10µl of

master mix, 10µl of RNA sample was added and mixed by gentle pipetting. The tubes were sealed and briefly centrifuged. For each sample a no RT control mix, no template RT and no template no RT sample were also prepared. Samples were loaded onto a thermal cycler with the following conditions: 25ºC for 10 minutes, 37ºC for 120 minutes, 85ºC for 5 secs then 4ºC forever. 1µl of cDNA was subsequently used in a GAPDH-specific PCR for all RT-PCR reaction products and analysed on a 1% agarose gel containing ethidium bromide. This was done to determine the generation of cDNA and absence of genomic DNA contamination in the RNA sample and kit reagents (including the reverse transcriptase).

2.3.5 Gel Electrophoresis and UV Documentation

2.3.5.1Agarose Gel Electrophoresis

DNA produced by PCR was analysed using non-denaturing agarose gel electrophoresis which separates nucleic acids according to size. Electrophoresis grade agarose was added to 0.5X TBE buffer and heated in a microwave oven to dissolve the agarose to a final concentration of between 1 and 3% (w/v). The molten gel was allowed to cool to approximately 60ºC then poured into a casting tray and left to set. The gel was run in 0.5X TBE buffer at 100-200V. For loading, the samples were mixed with 1/5 the volume of gel loading buffer. DNA molecular weight standards were run alongside the samples. To visualise the nucleic acids, ethidium bromide (0.5µg per ml) was added to the molten gel and after electrophoresis the gel was visualised using UV transillumination.

2.3.5.2Polyacrylamide Gel Electrophoresis (PAGE)

During SAGE, the PCR products and ditags were isolated by 12% PAGE and the ligated concatamers were separated by 8% PAGE. 12% PAGE contained 14ml of 40% polyacrylamide (19:1 acrylamide:bis) and 31.3ml dH_2O. 8% PAGE contained 9.3ml of 40% polyacrylamide (37.5:1 acrylamide:bis) and 36ml dH_2O. To either mix, 930µl of 50X Tris Acetate Buffer, 470µl 10% APS and 30µl TEMED were added. The mixture was poured into a vertical gel apparatus and left to polymerise for 30 minutes. The gel was run in 1X TAE buffer at 130-160V for 2-3hr, as described in the text. After electrophoresis, the gel was stained for 30

minutes in 0.5X TBE containing ethidium bromide then visualised using UV transillumination.

2.3.5.3UV Gel Transillumination and Documentation

Analysis and photography of ethidium bromide agarose and polyacrylamide gels was performed using the Syngene Gene Genius Bio Imaging System with GeneSnap version 6.03 software. The gel image was printed and saved to file.

2.3.6 Serial Analysis of Gene Expression Protocol

The I-SAGE Long Kit (Invitrogen) for generating Long SAGE libraries was used following the manufacturers protocol as described below.

2.3.6.1 Preparing Adapter Linked cDNA

Oligo (dT) beads were re-suspended by vortex and 100µl transferred to an RNase-free siliconized 1.5ml microcentrifuge tube. The tube was placed on a magnetic stand for 2 minutes, the supernatant removed and beads washed with 500µl of Lysis/Binding buffer (37ºC). The tube was placed on a magnetic stand for 2 minutes.

To bind the mRNA, 10-50µg total RNA was made up to 1ml in Lysis/Binding Buffer, the supernatant removed from the beads and the entire 1ml of RNA sample added. The tube was placed on a rocking platform for 30 minutes at RT to ensure mixing of the beads and RNA. Place the tube on a magnetic stand for 2 minutes and discard the supernatant. Beads were washed twice with 1ml of Wash Buffer A and once with 1 ml of Wash Buffer B. The beads were washed a further four times with 1X First Strand Buffer.

The following reagents were mixed on ice for first-strand synthesis: 18µl 5X First Strand Buffer, 1µl RNaseOUT, 54.5µl DEPC Water, 9µl 0.1 M DTT and 4.5µl dNTP Mix (10mM). Supernatant was discarded and the beads re-suspended in first-strand mix (87.0µl) by slow vortex. The tube was incubated for 2 minutes at 37ºC and 3µl SuperScript II Reverse Transcriptase added. The tube was then incubated at 42ºC for 1 hour with mixing by slow vortex every 15 minutes.

The tube was chilled on wet ice for 2 minutes and the following added in order for second strand DNA synthesis: 465µl DEPC Water, 150µl 5X Second Strand Buffer, 15µl dNTP Mix (10mM), 5µl *E.Coli* DNA Ligase, 20µl *E.Coli* DNA Polymerase and 5µl *E.Coli* RNase H. Mix by vortex and pulse centrifuge to gather the beads. The tube was incubated at 16ºC for 2 hours with mixing by slow vortex every 15 minutes. The reaction tube was placed on ice and 45µl 0.5M EDTA added to stop the reaction. The tube was placed on a magnetic stand for 2 minutes and the supernatant removed. The beads were washed with 750µl of warm Wash Buffer C (75ºC) and the sample heated to 75ºC for 12 minutes to inactivate the polymerase. The beads were washed again with 750µl Wash Buffer C and then three times in Wash Buffer D. The beads were re-suspended in Wash Buffer D and a small sample (5µl) removed and stored at 4ºC for verification of cDNA synthesis in a separate PCR reaction. The tube was placed back on a magnetic stand and the supernatant discarded. The beads were re-suspended in 200µl of 1X Buffer 4 and transferred to a new tube. The old tube was washed once with 200µl of 1X Buffer 4 which was then transferred to a new tube. The tube was placed on a magnetic stand for 2 minutes and the supernatant discarded. The beads were washed once more in 200µl of 1X Buffer 4 and the tube placed on a magnetic stand.

To digest the cDNA with *Nla* III, the supernatant was discarded and the beads re-suspended in the following mix: 172µl LoTE, 2µl 100X BSA, 20µl 10X Buffer 4 and 6µl *Nla* III. The reaction was incubated at 37ºC for 1 hour and mixed by occasional slow vortex. The *Nla* III was then inactivated by washing twice with 750µl warm Wash Buffer C (37ºC). The beads were then washed three times with 750µl of Wash Buffer D and re-suspended in 750µl Wash Buffer D. 5µl of the sample was removed and stored at 4ºC to determine the efficiency of *Nla* III digestion in separate PCR reaction. Store the tube at 4ºC overnight and continue the protocol the following day.

2.3.6.2 Preparing Ditags

To ligate the LS adapters to the cDNA, the sample tube was placed on a magnetic stand for 2 minutes and the supernatant removed. The beads were washed twice with 150µl 1X Ligase Buffer, re-suspended in 100µl of 1X Ligase Buffer and divided into two fresh tubes (labelled A and B – 50µl in each). Both

tubes were washed once with 50µl 1X Ligase buffer, placed on a magnetic stand for 2 minutes and the supernatant discarded. The tubes were placed on ice and 14µl LoTE and 2µl 10X Ligase Buffer added. 1.5µl LS Adapter A (40ng per µl) was added to tube A and 1.5µl LS Adapter B (40ng per µl) to tube B. The beads were re-suspended and heated to 50ºC for 2 minutes, cooled at RT for 15 minutes and then placed on wet ice. 2.5µl of T4 DNA Ligase was added to each tube and incubated at 16ºC for 2 hours. Both tubes were washed three times with 500µl of Wash Buffer D and the beads re-suspended in 500µl of Wash Buffer D. A 5µl sample was removed and stored at 4ºC for use in a separate PCR reaction to confirm ligation of the adapters.

To releases the adapter and a short tag of cDNA from the beads, the ligation products were digested with *Mme* I. A solution of 10X SAM (400µM) was prepared by adding 1µl 32mM SAM to 79µl DEPC H_2O. A solution of 1X Buffer 4/1X SAM was prepared by adding 1µl 32mM SAM and 799µl 1X Buffer 4. Tubes A and B were placed on a magnetic stand for 2 minutes and the supernatant discarded. Each tube was washed twice with 200µl of 1X Buffer 4/1X SAM, the supernatant discarded and the tubes placed on wet ice. The following reagents were added to each tube: 70µl LoTE, 10µl 10X Buffer 4, 10µl 1X SAM (400µM) and 10µl *Mme* I. The tubes were incubated at 37ºC for 2.5 hours and occasionally mixed. The tubes were placed on a magnetic stand for 2 minutes and the supernatant (100µl) removed and transferred to two new microcentrifuge tubes. Do not discard the supernatant at this stage because it contains the tags.

The tags were pooled by combining supernatants into tube B and washing tube A once with 100µl LoTE (final volume tube B is 300µl) and then ethanol precipitated. 300µl Phenol/Chloroform (P/C) was added and mixed well by vortex. The tube was centrifuged at 13200rpm for 5 minutes at RT. The upper aqueous phase (300µl) was transferred to a new tube and 200µl removed to a new tube to be used as the template. 100µl DEPC H_2O was added to the other 100µl and used as a negative control. To each tube was added: 133µl ammonium acetate (7.5M), 3µl mussel glycogen and 1ml 100% ethanol. Tubes were vortexed, placed on dry ice for 20 minutes and centrifuged at 15400rpm for 30 minutes at 4ºC. Supernatants were discarded and the pellets washed twice with 1ml ice cold 70% ethanol. The ethanol was discarded and the pellets allowed to air dry at RT for 10 minutes. The sample and control pellets were re-suspended

in 4µl and 2µl LoTE respectively, and dissolved by incubation at 37ºC for 15 minutes.

Tags were ligated to form ditags by setting up the following reactions on ice:

1. **2X Ditag reaction:** 1.5µl 3mM Tris-HCl (pH 7.5), 0.9µl 10X ligase buffer, 0.9µl DEPC H_2O and 1.2µl T4 DNA ligase.

2. **2X Negative control:** 2.25µl 3mM Tris-HCl (pH 7.5), 0.75µl 10X ligase buffer and 0.75µl DEPC H_2O.

4µl of the 2X Ditag reaction mix was added to the tags re-suspended in 4µl LoTE (template) and 2µl of 2X Negative control mix added to the negative control (no ligase). Tubes were incubated at 16ºC overnight.

2.3.6.3 Amplifying Ditags

After the overnight incubation, 6µl LoTE was added to the sample and 10µl LoTE to the negative control (no ligase). To optimise the Ditag PCR and avoid cross-contamination, the negative control and sample were transferred to separate PCR workstations and the following diluted in sterile H_2O:

1. Negative control (no ligase) to 1/20 at Location 1.

2. Template (ligated product) to 1/20, 1/40, and 1/80 at Location 2.

3. LS Control Template (supplied at 10pg/µl) to 1/10 at Location 1.

Six tubes were set up on ice containing either 1µl of the negative control (no ligase), diluted templates, LS control template (positive control) or H_2O (negative control, no template) and 49µl of a PCR master mix containing: 5µl 10X BV Buffer, 3µl DMSO, 7.5µl dNTP mix (10mM), 2µl LS DTP-1, 2µl LS DTP-2, 29µl DEPC H_2O and 0.5µl Platinum® *Taq* DNA polymerase. The tubes were mixed, pulse centrifuged and amplified on a thermal cycler using the following cycling parameters: 95ºC 2 minutes (1 cycle); 95ºC 30 seconds, 55ºC 1 minutes and 70ºC 1min (25-35 cycles) and 70ºC for 5 minutes (1 cycle). PCR products were analysed on a 3% agarose gel and visualized under UV transillumination. A strong

ditag band (130bp) and a faint smaller band (100bp) containing adapter sequences without any transcript sequence should be seen and the negative controls free of contamination.

After optimisation, the ditags were scaled up in 600 reactions. A PCR master mix was made up on ice in a 25ml Universal container with the following reagents: 3ml 10X BV Buffer, 1.8ml DMSO, 1.2ml LS DTP-1,1.2ml LS DTP-2, 18ml DEPC H_2O and 300µl Platinum® *Taq* DNA polymerase. 50µl of the PCR mix was added to wells 1A and 12H of a 96 well PCR plate and 1µl of the 1:10 LS Control template (positive control) added to 1A and 1µl DEPC H_2O added to 12H. All the diluted and undiluted ditag templates were then added to the PCR master mix, mixed well and 50µl added to the remaining wells and another five 96 well PCR plates. The plates were sealed with adhesive PCR film, briefly centrifuged and amplified on a thermal cycler using the following parameters: 95ºC 2 minutes (1 cycle); 95ºC 30 seconds, 55ºC 1 minutes and 70ºC 1minute (27 cycles) and 70ºC for 5 minutes (1 cycle). 5µl of the PCR products from 5 random wells and the controls were combined with 1ul PCR dye and analysed on a 3% agarose gel. The 96 well plates were stored at -20ºC overnight.

2.3.6.4 Isolating the 130bp Ditags

The ditags were pooled by thawing the six 96-well plates on ice and combining the PCR products into two 50ml tubes (discard the control templates!). 12.5ml of P/C was added to each tube which was then vortexed and centrifuged at 2000rpm for 10 minutes at RT. The upper aqueous phase (~12.5ml) from each tube was transferred to two clean 50ml tubes and the following reagents added: 3.2ml ammonium acetate (7.5M), 48µl mussel glycogen and 34ml 100% ethanol. The tubes were vortexed, placed on dry ice for 20 minutes and centrifuged at 4000rpm for 30 minutes at 4ºC. The supernatant was discarded and the pellets washed twice with 25ml ice cold 70% ethanol by vortex and centrifuged at 4000rpm for 5 minutes at 4ºC. The ethanol was discarded and the pellets air dried for 30 minutes. The ditags were dissolved by vortex and incubation at 37ºC in LoTE (300µl) for 15 minutes.

The ditags were purified by combining the entire ditag sample (300µl) with 60µl PCR dye and loading multiple wells of a large format 12% polyacrylamide gel.

The gel was electrophoresed until the bromophenol blue dye front ran off the gel and the xylene cyanol dye front was 2cm from the bottom of the gel. The gel was removed and stained in buffer containing ethidium bromide.

To elute the DNA from the gel, the 130bp bands were excised from the gel using a scalpel in a dark room under U.V light. The gel was divided into small pieces and added to 0.5ml microcentrifuge tubes with holes in the bottom (made using a green needle) and placed within a 1.5ml microcentrifuge tube. To break up the gel, the tubes were centrifuged at 13200rpm RT for 3 minutes and the gel collected in the lower tube. 150ul of 5:1 LoTE: ammonium acetate (7.5M) mix was added and the tubes vortexed. To elute the DNA the tubes were incubated at 65ºC in a water bath for 2 hours. The contents of two tubes were combined into a S.N.A.P™ column fitted to a collection tube and centrifuged at 13200rpm for 2 minutes. All eluates were combined and 300µl aliquots put into new 1.5 ml tubes.

To precipitate the DNA, the following reagents were added to each 300µl aliquot: 133µl ammonium acetate (7.5M), 3µl mussel glycogen and 1ml 100% ethanol. The tubes were vortexed, placed on dry ice for 20 minutes and centrifuged at 15400rpm for 30 minutes at 4ºC. The supernatant was discarded and the pellets washed twice with 500µl of ice cold 70% ethanol. The ethanol was discarded and the pellets allow to air dry over 30 minutes. 14µl of LoTE was added to each pellet and the pooled into one tube (~126µl). The tube was stored at –20ºC overnight.

2.3.6.5 Isolating the 34-bp Ditags

34bp tags were produced by *Nla* III digestion of the 130 bp product. 126µl of 130bp ditags from the previous day were mixed with the following reagents: 45µl 10X buffer 4, 6µl 100X BSA, 36µl *Nla* III and 237µl DEPC H_2O. The tube was incubated at 37ºC for 2 hours. 150µl aliquots were transferred to 3 sterile tubes and 50µl LoTE added to each. A 5µl sample from 1 tube was analysed on a 3% agarose gel to assess *Nla* III digestion efficiency and we carried on to ethanol precipitation if more than 80% of the 130bp ditags were digested to 34bp ditags.

200µl of P/C was added to each tube and the tubes centrifuged at 13200rpm for 5 minutes RT. The upper aqueous phase (200µl) was transferred to three new tubes and the following added: 90µl ammonium acetate (7.5M), 3µl mussel glycogen and 850µl 100% ethanol. The tubes were place on dry ice for 20 minutes and centrifuged at 154000rpm for 30 minutes at 4ºC. Pellets were washed twice with 1ml ice cold 70% ethanol and allowed to air-dry at RT for 30 minutes. The pellets were dissolved in 10.8µl LoTE and combined into one tube (total volume 32µl).

The 34bp ditags were purified by combining with 8µl PCR dye and loading 6 wells of a 12% polyacrylamide gel (1mm cassette) containing molecular weight ladders. Electrophoresis was performed in 1X TBE buffer at 200V for 1 hour. The gel was removed from the cassette and stained in buffer containing ethidium bromide on a rocking platform for 15 minutes.

In a dark room and under U.V light, the 34bp region was excised from the gel using a scalpel. Small gel pieces were placed in 0.5ml tubes with holes in the bottom (made by a green needle) within a 1.5ml tube and centrifuged at 13200rpm for 2 minutes to break up the gel. To each tube was added 150µl of a 5:1 LoTE: ammonium acetate (7.5M) mix (125µl: 25µl) mix and mixed by vortex. The tubes were incubated at 37ºC in a water bath for 2 hours to elute the DNA from the gel.

The eluates were combined into S.N.A.P™ columns fitted to a collection tubes and centrifuged at 13200rpm for 2 minutes. The eluate (up to 900µl) was combined and 200µl aliquots added to fresh 1.5ml microcentrifuge tubes.

To precipitate the DNA, to each 200µl was added: 90µl ammonium acetate (7.5M), 3µl mussel glycogen and 850µl 100% ethanol. The tubes were vortexed, placed on dry ice for 20 minutes and centrifuged at 15400rpm for 30 minutes at 4ºC. The supernatant was discarded and the pellets washed twice with 1ml of ice cold 70% ethanol. Discard the ethanol and air-dry the pellets for 20 minutes on ice. The pellets were pooled, re-suspended in 7.75µl of LoTE and 1µl of 10X Ligase buffer and immediately used in the ligation reaction.

2.3.6.6 Forming Concatamers

1.25µl T4 DNA Ligase was added to 8.75µl of the 34bp DNA on ice. The tube was incubated at 16ºC for 3 hours on a thermal cycler. 2.4µl of PCR Dye was added to the mix and heated to 65ºC for 10 minutes on a thermal cycler. The reaction mix was pulse centrifuged and the entire sample loaded in one well of an 8% polyacrylamide gel (1mm cassette) along with molecular weight markers. Electrophoresis was performed in 1X TBE Buffer for ~ 1hour at 200V. The gel was removed from the cassette and stained in buffer containing ethidium bromide (1µg/ml) on a rocking platform for 15 minutes.

In the dark room and under U.V light, the concatamer 'smear' was excised and divided approximately into the following three regions:

1. 300 – 500bp
2. 500 – 800bp
3. 800 – 1kb

Each region was divided into two pieces and placed in a 0.5ml tube with a hole in the bottom (made using a green needle) within a labelled 1.5ml tube to identify the gel region. The gel was broken up by centrifuging at 13200rpm for 5 minutes at RT. 200µl of a 5:1 LoTE: ammonium acetate (7.5M) mix was added to each tube and mixed by vortex. To elute the DNA the tubes were incubated at 65ºC in a water bath for 2 hours. The contents of each tube were transferred to three S.N.A.P™ columns fitted to collecting tubes and centrifuged at 13200rpm for 2 minutes at RT. The eluate (200µl) from each tube was transferred to three fresh, labelled 1.5ml microcentrifuge tubes.

To ethanol precipitate the DNA, 200µl of P/C was added to each tube and mixed by vortex. The tubes were centrifuged at 13200rpm for 5 minutes at RT and the upper aqueous layer (200µl) transferred to new labelled 1.5 ml tubes. The following reagents were added to each tube: 133µl ammonium acetate (7.5M), 3µl mussel glycogen and 1ml 100% ethanol. The tubes were mixed by vortex, placed on dry ice for 20 minutes and centrifuged at 15400rpm for 30 minutes at

4ºC. The pellets were washed twice with 1ml ice cold 70% ethanol and air-dried for 20 minutes. Each pellet was re-suspended in 6µl of LoTE and stored at -20ºC.

2.3.6.7Cloning Concatamers into pZERO®-1

The pZERO®-1 vector was linearised by *Sph* I as recommended in the protocol. A tube containing the following reagents was set up on ice: 2µl pZERO®-1 (1µg/ml), 2.5µl 10X buffer 2, 1.4µl *Sph* I and 19.1µl sterile H_2O. The tube was incubated at 37ºC for exactly 30 minutes. 175µl LoTE was added to the digestion mix and 200µl P/C and mixed by vortex. The tube was centrifuged at 13200rpm for 3 minutes at RT. The aqueous upper layer (200µl) was transferred to a new tube and the following added: 65µl ammonium acetate (7.5M), 1.5µl mussel glycogen and 600µl 100% ethanol. The tube was mixed by vortex, placed on dry ice for 10 minutes and centrifuged at 15400rpm for 30 minutes at 4ºC. The supernatant was discarded, the pellet washed twice in ice cold 70% ethanol and allowed to air-dry for 10 minutes. The pellet was re-suspended in 60µl of LoTE and 10µl aliquots stored at –20ºC. To check the efficiency of *Sph* I digestion, 2µl of the digestion mixture and undigested pZERO-1 were analysed on a 1% agarose gel.

To ligate the concatamer into pZERO®-1, 6µl of each concatamer was added on ice to separate tubes and the following reagents: 1µl digested pZERO®-1, 1µl 10X ligase buffer and 2µl T4 DNA ligase. A no DNA and no ligase reaction were also set up replacing each reagent with an equivalent volume of H_2O. The tubes were incubated at 16ºC for 3 hours on a thermal cycler. 190µl of LoTE and 200µl of P/C was added to each tube, mixed by vortex and the tubes centrifuged at 13200rpm 5 minutes at RT. The upper aqueous layer was transferred to a clean tube and the following added: 133µl ammonium acetate (7.5M), 3µl mussel glycogen and 1ml 100% ethanol. The tubes were mixed by vortex, placed on dry ice for 10 minutes and centrifuged at 15400rpm for 30 minutes at 4ºC. The supernatant was discarded and the pellets washed four times with ice cold 70% ethanol. The pellets were air dried for 20 minutes, each one re-suspended in 12µl LoTE and stored at –20ºC.

2.3.6.8Making Low Salt LB Plates with Zeocin

For 1 litre of low salt LB agar, 10g of tryptone, 5 g yeast extract, and 5g sodium chloride were dissolved in 950ml dH_2O. The pH of the solution was adjusted to 7.5 with sodium hydroxide (5M). 15g agar was added and the volume made up to 1litre. The broth was divided into two 500ml glass bottles and autoclaved on a liquid cycle. The agar was cooled by placing the bottles in a waterbath at 55ºC. Zeocin™ stock solution (100mg/ml) was thawed on ice in the dark and 500µl added to the agar (final concentration 50µg/ml). The agar was mixed and poured into 10cm petri dishes and allowed to set at RT. Once set, the plates were inverted and stored at 4ºC in the dark until use.

2.3.6.9Transformation Reaction

SOC medium and the low salt LB plates containing Zeocin™ were brought to RT. Vials of One Shot Top10 Electrocomp *E.Coli* were thawed on ice and 1-2µl of the ligation reactions added to separate vials containing 40µl electrocompetent *E.Coli*. The cells were mixed gently, transferred to a chilled 0.1cm cuvette and shocked at 1400V using an electroporator (Cell Shock, Hybaid). The cells were recovered in 250µl SOC medium and incubated at 37ºC 300rpm for 1 hour using a heated shaker. A further 750µl SOC medium was added to each tube and mixed. 200µl of the No DNA and No Ligase transformation reactions and 100µl of the concatamer transformation reactions were plated on low salt LB plates containing Zeocin™. All the concatamer transformation reaction was plated out. Plates were inverted and incubated at 37ºC overnight. An efficient ligation reaction produced 100-150 colonies per plate, while the controls had less than 10 colonies per plate.

2.3.6.10 Screening and Sequencing Clones

In a PCR workstation, random colonies were picked using a pipette tip and placed in a 0.5ml tube containing the following PCR mix: 2.5µl 10X BV buffer, 1.25µl DMSO, 1.25µl dNTP mix (10mM), 1µl M13 Forward primer (5µM), 1µl M13 Reverse primere (5µM), 18µl DEPC H_2O and 0.2µl Platinum Taq DNA polymerase. The tubes containing the tips were kept on an ice block and put on a rotating platform at 150rpm for 30 minutes. The tips were ejected and removed and the

tubes amplified on a thermal cycler using the following parameters: 94ºC 2 minutes (1 cycle), 94ºC 30 seconds, 55ºC 1 minute, 70ºC 1 minute (24 cycles) and 70º 5 minutes (1 cycle).

4µl of the PCR products were analysed on a 2% agarose gel to determine the size and the percent of inserts in the SAGE library. For large scale PCR, the remaining colonies were picked into 96 well plates containing the same PCR mix and amplified in a thermal cycler using the above conditions. 1% agarose stacking gels were used to analyse two 96 well plates at once and inserts > 300bp in size put forward for PCR clean up.

2.3.7 PCR Clean Up

PCR clean up was performed using the Using ExcelaPure 96-well UF PCR Purification Kit and following the manufacturers protocol. A QIAvac multi-well vacuum manifold (Qiagen) and pressure regulator was connected to a pump and one ExcelaPure 96-well UF Plate positioned on top of the manifold. The PCR products were made up to 100µl with dH_2O and transferred to the centre of the membranes using a multi-channel pipette. A vacuum of -700mbar was applied for 10 minutes to dry the wells. The wash step was repeated to ensure optimal purity of the PCR products for downstream sequencing. DNA was recovered in 30µl dH_2O by placing on a plate shaker for 10 minutes or repetitive pipetting (20 times). Purified PCR products were transferred to a 96-well V-bottomed plate, sealed with an adhesive cover and stored at –20ºC until sequenced.

2.3.8 Sequencing of SAGE concatamer inserts

Cleaned up PCR products of 300 – 1200bp in size were kindly sequenced by the staff of the Molecular Services Unit, Beatson Laboratories. The PCR products were sequenced using the BigDye Kit and M13 Forward primer with one-tenth of the purified PCR product per sequencing reaction.

2.3.9 SAGE bioinformatics

Within a concatamer, linked ditags of approximately 34bp length are separated by a CATG sequence (the recognition site of *Nla* III). SAGE 2000 software uses the CATG sequence to identify and extract the ditags which are then halved into

individual tags. The software quantifies the number of times the tag occurs within a given population of clone inserts to generate a report for the abundance of an individual tag. The report can be exported as a text file and linked to gene databases for identification of the gene(s) corresponding to the tags or may be used to compare the abundance of tags in different SAGE libraries.

Within the SAGE 2000 software, a new project was created with the anchoring enzyme set as *Nla* III and the tag length set to 36bp. Before allowing the software to analyse all the sequence files, a few sequences were checked by eye to ensure they gave the expected intermittent CATG pattern. The sequence data of clones containing concatenated SAGE ditags was then entered. The SAGE 2000 software extracted tag data from the sequence files and added them to the opened project. After checking for duplicate ditags, individual tags were assigned a tag number and recorded. Tags derived from oligonucleotide linkers were excluded from further analysis.

The SAGE report was saved as both a text file and Microsoft® Access database file, which allowed more complex analysis of the data. Potential matching transcripts were identified by linking the report to the SAGEmap reference sequence database (downloaded by anonymous file transfer protocol (FTP) from ftp://ftp.ncbi.nlm.nih.gov/pub/sage/mappings/). The zip file selected was for Homo sapiens and the Nla III recognition site (SAGEmap_Hs_NlaIII_full.gz) and the file was up to date as of the 26th September 2007.

2.3.9.1Comparison of SAGE libraries

The SAGE 2000 software was unable to compare libraries using the 17bp tag so two published methods (SAGEstat and SAGEGenie) were used with different statistical methods. Previous work has shown that similar results are obtained when comparing two SAGE libraries of equivalent size regardless of the statistical technique used.

Differential expression of tags (genes) has been defined in previous SAGE studies by various criteria, including: two-fold, five-fold or ten-fold differences in tag ratio; p-values below 0.05, 0.01 and 0.001; and combinations thereof. For validation purposes, genes differentially expressed more than two-fold difference and p-value of less than 0.01 were selected and discussed further in

chapter 5. For interest, the MSC SAGE libraries were analysed online by pair-wise comparison with normal tissue, cancer tissue and stem cell SAGE libraries available at the SAGE genie website using selected criteria and discussed further in chapter 4.

2.3.10 Quantitative RT-PCR using Taqman Low Density Arrays

The expressions of candidate genes were measured using Taqman® Low Density Array (TLDA) cards (Applied Biosystems). TLDA cards are micro-fluidic cards that allow 384 reactions to run simultaneously. Each well contains custom-made lyophilised primers and probes and supplied by 8 ports in total, with each port delivering 100µl of a cDNA/PCR master mix to 48 wells (final volume 2µl/well). The plate can be custom designed with multiple formats e.g. 12 genes in quadruplicate across 8 samples, 96 genes in duplicate across 2 samples or 384 genes for one sample without replicates. Either 18S or GAPDH are provided as the endogenous control gene, although other candidate housekeeping genes can be added to the card so that relative quantification can be performed with reference to multiple housekeeping genes. The genes of interest for this project were chosen, ordered and preloaded from a database of ~47,000 optimised human, mouse and rat assays (http://www.appliedbiosystems.com). The customised TLDA card ordered had 96 genes enabling analysis of two individual cDNA samples in duplicate and 20 cards were supplied. The cDNA required for Taqman was synthesized from 1µg of RNA. 400ng was made up to 200µl in dH_2O and added to an equal volume of Taqman universal master mix (Applied Biosystems, Warrington, UK). 100µl was added to each port equating to 100ng of RNA. The plate was centrifuged twice at 1200rpm for 1 min, sealed and analysed using an ABI PRISM 7900HT Fast Real-Time PCR system.

2.3.11 TeloTAGGG Telomere Length Assay

Genomic DNA was extracted from frozen cell pellets using the DNEasy Blood and Tissue Kit (Qiagen) following the manufacturer's protocol. Extracted DNA was used in the TeloTAGGG Telomere Length Assay (Roche) following the manufacturer's protocol with minor modifications and is briefly described below.

2.3.11.1 Sample Preparation and Digestion

All samples were prepared and analysed simultaneously with handling and pipetting of solutions performed on ice. 1ul of enzyme mix was used per sample (1µl *HinfI* and 1µl *RsaI* is enough for two samples) and controls were included. Dilute 10µl each control DNA (1µg) with 7ul nuclease free water and dilute sample DNA (1µg) with dH_2O and to each add 1µl enzyme mix and 2µl 10x digestion buffer. Incubate at 37ºC for 2 hours and stop the reaction by adding 4ul 5x gel electrophoresis loading buffer. At this stage samples can be stored at 4ºC.

2.3.11.2 Gel Electrophoresis

Prepare a 0.8% Agarose gel (15cm in length) in 1xTAE buffer. Mix 4µl DIG molecular weight marker, 12µl dH_2O and 4µl loading buffer. Load the 24ul samples, and add 4ul 5x gel electrophoresis loading buffer to 10ul of DIG molecular weight marker mix & load either side of the sample lanes. Run the gel at 5V per cm in 1x TAE buffer until the bromophenol blue dye has travelled 10 cm from the wells (2-4 hours).

2.3.11.3 Blotting

Submerge the gel in HCl solution for 5-10 minutes until the bromophenol blue turns yellow with gentle agitation. Rinse the gel twice in water and submerge in denaturation solution twice for 15 minutes at RT. Rinse the gel twice in water and submerge in neutralisation buffer twice for 15 minutes at RT. Blot the gel onto a nylon membrane overnight by capillary transfer using 20X SSC as a transfer buffer. After transfer fix the DNA to the membrane by U.V crosslinking and then wash the membrane in 2X SSC.

2.3.11.4 Hybridisation

Pre-warm 50ml DIG Easy-Hyb solution to 42ºC and submerge the blot in 35ml of this solution and incubate at 42ºC for 30-60 minutes with gentle agitation. Prepare telomere hybridisation solution by adding 3ul telomere probe to 15mls Easy Hyb solution. Discard the pre-hybridisation solution and immediately add

the telomere hybridisation solution to the membrane and incubate at 42ºC for 3 hours (or overnight). Discard the hybridisation solution and wash the membrane twice with stringent wash buffer I for 5 minutes at RT with gentle agitation. Wash the membrane twice with stringent wash buffer II for 15-20 minutes at 50ºC with gentle agitation.

2.3.11.5 Chemoluminescence Detection

Rinse the membrane in 200ml 1X washing buffer for 1-5 minutes at RT with gentle agitation. Incubate the membrane in 200mls freshly prepared 1X blocking solution for 30 minutes at RT with gentle agitation. Prepare the anti-DIG-AP working solution immediately before use containing 10mls 10X blocking solution, 90mls dH_2O and 10µl anti-DIG-AP. Incubate the membrane in 100mls anti-DIG-AP working solution for 30 minutes at RT with gentle agitation. Wash the membrane twice in 200mls 1X washing buffer for 15 minutes. Incubate the membrane in 200mls 1X detection buffer for 2-5 minutes at RT with gentle agitation. Discard 1X detection buffer and blot the membrane DNA side up on a sheet of blotting paper (do not let the membrane dry). Place the membrane on saran wrap and apply 40 drops (~ 3mls) of substrate solution then wrap the membrane and incubate for 5 minutes at RT. Squeeze out the excess liquid and seal the edges. Expose the membrane to x-ray film for 5-20 minutes at RT.

2.3.11.6 Stripping

Warm 500mls stripping buffer to 37ºC and add 250mls to the membrane and wash for 15 minutes with agitation. Discard the stripping buffer and replace with the remaining 250mls and wash for a further 15 minutes with agitation. Discard the used stripping buffer and rinse the membrane with 2XSSC then blot dry with filter paper and wrap in cling film (store the membrane at RT).

2.3.11.7 Re-Probing

Continue from hybridisation section as described above.

2.3.11.8 Densitometry

Switch on the densitometer and wait for the lights to stop flashing before switching on the computer. Click on *Staff* and double click on *Quantity One*. From *Volumes Quick Guide*, click on *Select Scanner*. Select *GS-800* from pop-up and place autorad on scan plate. Select *X-ray film* and *Blue film*. Click on *Preview scan* and draw a box around the required area of the blot and click on *Acquire*. Save as a named file then close the scanner window. Click on *View* and *Rotate/Flip* until autorad is in the correct orientation. Save again and from drop down menu select *Lane, Frame Lanes* and enter the number of lanes on the gel. Stretch the frame to fit the gel and place anchors, if necessary, to bend the frame to fit the lanes. Select *Bands, Detect bands/Create bands* to detect bands in the standards lanes. Remove all bands except the ones in the molecular weight marker lanes. Zoom in to ensure all 21 bands on the markers have been identified in the correct places. Insert extra bands where needed and remove any excess. From the *Band analysis quick guide* select *Standards* to apply standards values to the marker lanes. Select *Edit* then *Gel layout* and add gel description and labels to each lane. Select *Bands* then *Detect bands*, *Contour* and *Create contours* and highlight smear on the autorad. Select band to contour and repeat for all smears. Save all lanes as a report and export table to an external memory stick/drive.

3 Characterisation of Mesenchymal Stem Cells from Ischaemic Heart Disease Patients

3.1 Introduction

The ease of isolation, expansion and differentiation capacity of MSC's make them ideal candidate cells for myocardial repair. Loss of cardiomyocytes following myocardial infarction induces contractile dysfunction of the heart and the muscle is gradually replaced with fibroblasts that contribute to scar tissue. Animal models have confirmed that the beneficial effects seen after intramyocardial or intravascular injection of MSC's occur via paracrine mechanisms that promote angiogenesis and minimise scarring. Only a small number of administered cells engraft and differentiate into endothelial cells or cardiomyocytes. The findings have encouraged researchers to use MSC's after MI in humans and early clinical trials have confirmed small benefits in myocardial contractility and perfusion (10;148).

Although these findings have demonstrated the feasibility of this approach, characterisation of administered cells was limited and did not meet the minimal criteria agreed by lead researchers in the field (33). MSC's were isolated from BM using standard methods and the surface marker profiles were typical of MSC's. However, differentiation studies were not carried out and therefore the stem cell characteristics of administered cells remain unknown. Somewhat surprisingly, in the study by Chen *et al* MSC's proliferated ten times greater than that typically seen by other researchers using similar volumes of BM and culture protocols. The results are in contrast to findings from studies using MSC's from aged donors that demonstrated cells proliferated poorly and appeared senescent almost immediately from isolation (11).

The lack of rigorous characterisation and perceived limitations of MSC's from this patient group has encouraged researchers to derive MSC's from healthy young donors in advance and store the cells as an 'off the shelf' allogeneic therapy. This approach has also been encouraged by the unique immunosuppressive properties of MSC's demonstrated *in vitro* (149;150) although recent *in vivo* studies demonstrated that allogeneic cells were rejected

suggesting this strategy may be inherently flawed (151;152). The results could explain the low levels of engraftment seen after cell administration in animal models and also suggest clinical trials using allogeneic cells are likely to under report potential benefits of this therapy.

Another concern that arises is that medical conditions impact on the absolute numbers and function of endogenous stem cell populations and in these patients typical MSC properties are lost. Endothelial progenitor cells (EPC's) obtained from patients with IHD have reduced frequency and impaired functional capacity when compared to those obtained from healthy age-matched donors (153;154). Telomere shortening of peripheral blood MNC's has been shown to predict the development of IHD in healthy subjects suggesting stem cell ageing may be linked to the development of the disease (155). Whether this is a cause or a consequence of IHD and other age-related conditions remains unknown and further research in this area is required to explain these findings.

Together these results question the suitability of autologous MSC's from aged patients with IHD for clinical application and to address this basic research in this area is required. Therefore, studying autologous MSC's from patients with IHD is essential to not only establish the characteristics of the cells themselves but also inform on suitability for clinical use. *In vitro* models of MSC ageing could also enhance understanding of the molecular mechanisms that regulate this process *in vitro* and also improve our ability to use autologous cells in cell-based therapies. The results in this chapter describe the most comprehensive characterisation of MSC's derived from patients with severe IHD undergoing coronary artery bypass grafting (CABG).

3.2 Results

3.2.1 Donor Characteristics and Isolation of MSC's

MSC's were isolated from thirty patients undergoing CABG and nine were used for the work described in this thesis (donors 12 and 23-30). The characteristics of the individual donors are shown in Table 1. Mean age of the donors was 59.9 ± 9.4 years and all were male except donor 29. Past medical history included smoking, diabetes and hyperlipidaemia which are common risk factors associated with IHD. Donor medications included anti-platelet, anti-anginal, anti-hypertensive and lipid lowering therapies which are used for symptom relief and secondary prevention. On average, 13.6 ± 1.2 ml of bone marrow was aspirated from three sites of the sternum and yielded a mean of 12.9 ± 13.5 x 10^7 MNC's after density centrifugation. Two days after plating the MNC fraction, adherent spindle-shape cells with fibroblastic morphology were indentified as colonies that expanded to confluence when the non-adherent fraction was removed (Figure 3-1 A-C). MSC cultures were heterogeneous in morphology as some cells appeared spread out and others were small and round with high nuclear-cytoplasm ratio (Figure 3-1 D).

The incidence of true MSC's in the bone marrow samples was calculated by evaluating the ability of the donor MNC samples to form fibroblastic colonies using the CFU-F assay. For each sample, MNC's were plated at three different concentrations and Giemsa stained colonies counted (Figure 3-2 A+B). MNC's from donor 24 contained the most colonies and donor 26 the lowest. The mean number of colonies in the eight samples was 10.1 ± 2.5 per 1 x 10^6 MNC's giving a frequency of 'true' MSC's of 1 in 105,905 MNC's (range 1 in 75,397 to 1 in 150,794).

MSC's from each donor were cultured to passage two and evaluated for their ability to form fibroblastic colonies when plated at low density using the CFE-F assay. For each sample, MSC's were plated at 10 cells per cm^2 in triplicate and Giemsa stained colonies counted (Figure 3-3 A+B). MSC's from donor 30 contained the most colonies and donor 28 the lowest. The mean percentage of MSC's at passage two that formed colonies was 28.7 ± 6.5 %.

Donor	Age	Sex	Operation	Past Medical History	Medications
12	49	M	CABG	Myocardial infarction, smoker	Aspirin, atenolol, clopidogrel, simvastatin
23	59	M	CABG	Myocardial infarction, hyperlipidaemia	Aspirin, atenolol, lisinopril, simvastatin
24	70	M	CABG	Paroxysmal atrial fibrillation, stroke, ulcerative colitis	Aspirin, atenolol, nicorandil, perindopril, simvastatin
25	54	M	CABG	Myocardial infarction, stroke, smoker	Aspirin, amlodipine, atenolol, atorvastatin, clopidogrel
26	65	M	CABG	Non-insulin dependent diabetes	Aspirin, atenolol, bendrofluazide, diltiazem, metformin, nicorandil, simvastatin
27	49	M	CABG	Myocardial infarction	Aspirin, atenolol, ramipril, simvastatin
28	68	M	CABG	Chronic obstructive pulmonary disease, hyperlipidaemia, myocardial infarction	Aspirin, beclomethasone, bisoprolol, clopidogrel, nicorette, salbutamol, simvastatin
29	52	F	CABG	Chronic obstructive pulmonary disease, hypertension, peptic ulcer disease	Aspirin, atorvastatin, beclomethasone, isosorbide mononitrate, nicorandil, omeprazole
30	73	M	CABG	Chronic renal failure	Alfacalcidol, amlodipine, allopurinol, aspirin, atenolol, calcium, lactulose

Table 1 Donor characteristics

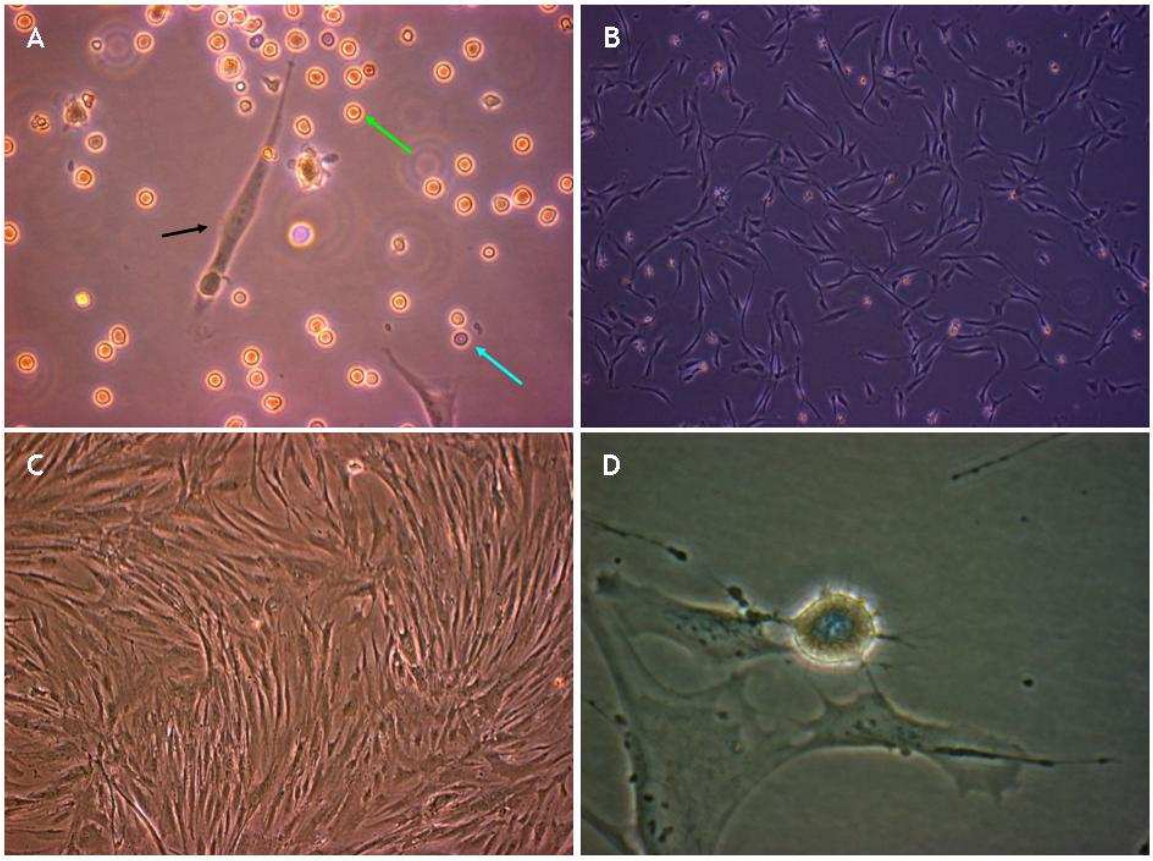

Figure 3-1 MSC's display characteristic morphology

Within 48 hours of plating the BM-MNC fraction, rare spindle shaped cells were identified (black arrow) that were characteristic of MSC's while most nucleated cells were non-adherent (green arrow) and red blood cells infrequent (blue arrow) (A) (20x). MSC's rapidly expanded from single colonies after the first media change (B) and achieved confluence in approximately seven days (C) (10x). At high magnification, MSC cultures contained cells heterogenous in size and shape (D) (40x).

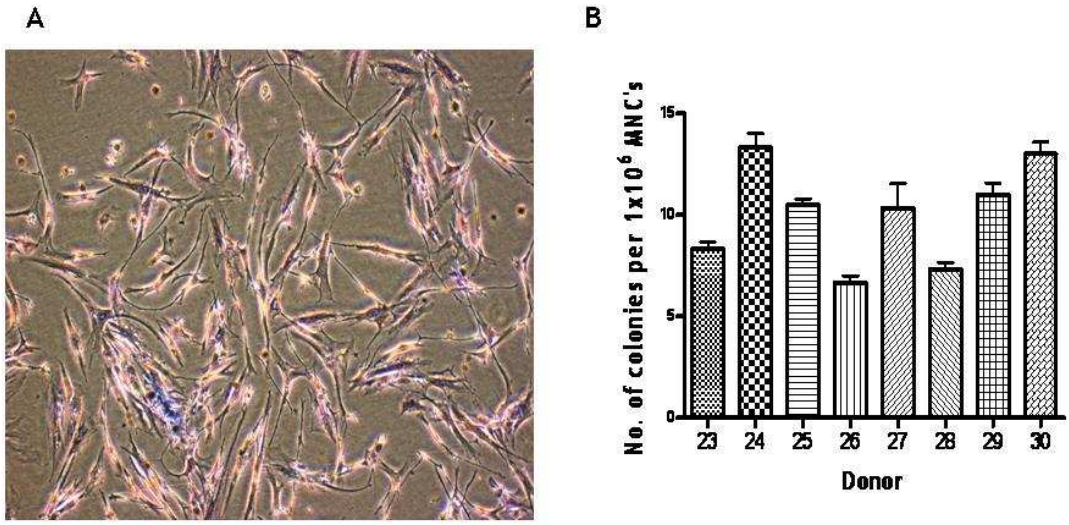

Figure 3-2 MSC's occur at low frequency in the sternal bone marrow using colony forming unit-fibroblast (CFU-F) assay

The BM-MNC fraction from each donor was plated once in a dilution series at three concentrations and cultured for two weeks. Cells were stained using Giemsa and colonies containing at least 20 cells were counted (A) (10x). Bars represent the mean number of colonies per million MNC's plated derived from the three dilutions. Error bars show the standard deviation (B).

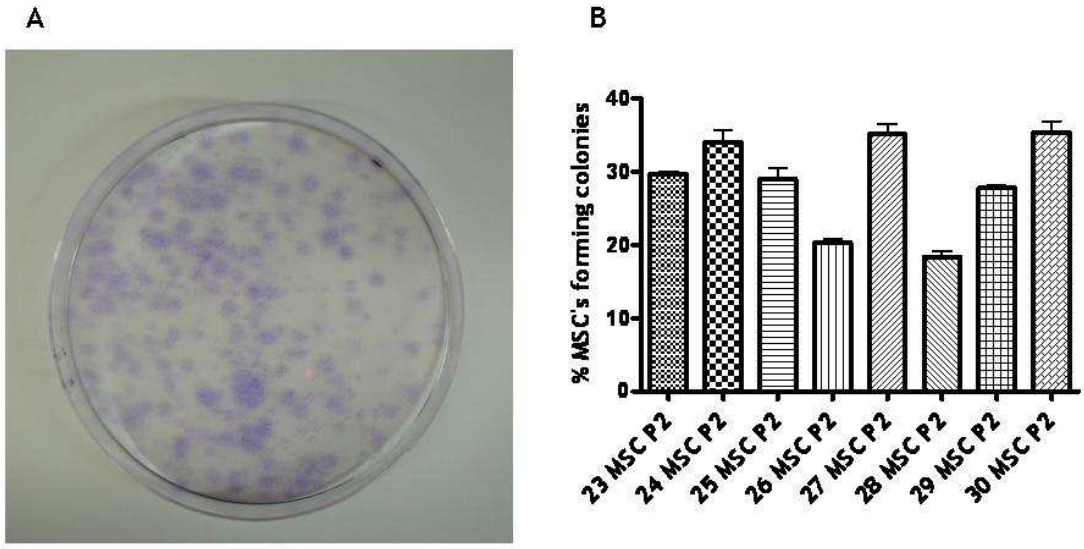

Figure 3-3 Progenitor potential of MSC's at passage two was determined using the colony forming efficiency-fibroblast (CFE-F) assay

MSC's at passage two were serially diluted and plated in triplicate at low density (10 cells per cm^2) in 100mm culture dishes. Giemsa stained colonies were counted to determine the percentage cells forming colonies (A). Bars represent the mean percentage of cells forming colonies from the three plates for each donor. Error bars show the standard deviation (B).

3.2.2 Surface Marker Profiles of Early Passage MSC's

Two-colour flow cytometry was used to determine that MSC's displayed a non-haematopoietic, non-endothelial surface marker profile. MSC cultures were analysed at passage two and representative plots are shown in Figure 3-4, Figure 3-5, Figure 3-6 and Figure 3-7. The percentage expression of each surface marker for the donors and the overall mean are shown in Table 2. The gated MSC population was heterogeneous in size and granularity as demonstrated by forward and side scatter properties (Figure 3-4A). The mean percentage of gated cells was 90.5 ± 2.1% and the geometric mean of the forward and side scatter was 511.4 ± 49.9 and 429.9 ± 59.1 respectively.

More than 90% of cells in the culture expressed the surface markers CD13, 29, 44, 49e, 73, 90, 105, 166 and HLA Class I. Two discrete populations of MSC's that lacked expression of CD105 and co-expression of CD29 and 44 were identified as shown in Figure 3-5 and Figure 3-6 respectively. The absence of significant haematopoietic or endothelial cell contamination was confirmed in that less than 1% of cells expressed the surface markers CD14, 31, 34, 45 and 133. Surface markers expressed on a small number (3-32%) of MSC's included CD49d, 71, 106, HLA Class II and the stem cell marker Stro-1.

To determine differences in the surface marker prolife at passage one and two, the results from five donors (18, 20 and 22-24) were compared using a paired student's t-test (Table 3). A significantly greater percentage of MSC's expressed the surface markers CD14, 31, 34 and 45 at passage one when compared to passage two. Dot plots revealed a discrete sub-population of cells expressing these markers which are likely to represent contamination with endothelial and haematopoietic cells (Figure 3-8).

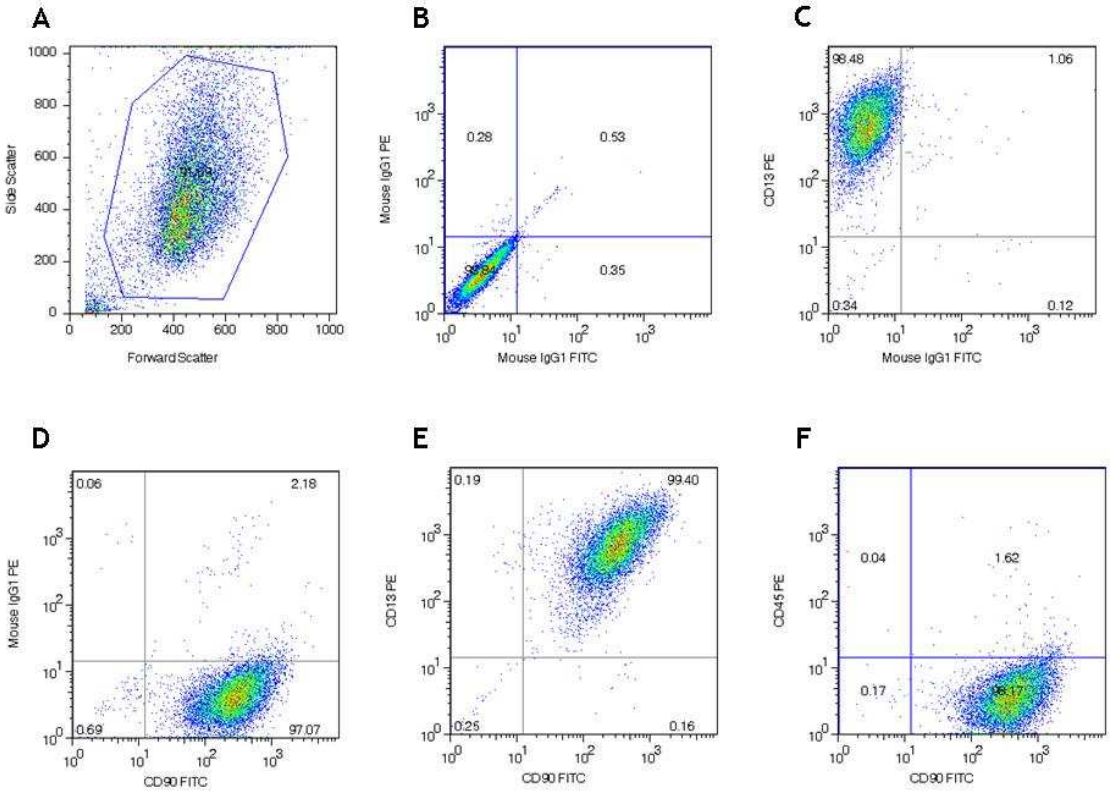

Figure 3-4 MSC's at passage two displayed characteristic surface marker profiles

Passage two cells were analysed using two colour flow cytometry after staining with phycoerythrin (PE) or fluorescein isothiocyanate (FITC) conjugated monoclonal antibodies. The plots were obtained by collecting 10,000 events and representative of the eight MSC cultures analysed. Within each quadrant of the grid the percentage of total cells analysed is shown. The gated MSC population demonstrated variability in forward and side scatter properties (A). Compensation was performed using isotype controls (B) and CD13 and 90 that are expressed on almost all MSC's *in vitro* (C, D and E). The majority of MSC's did not express CD45, a marker of committed haematopoietic cells (F).

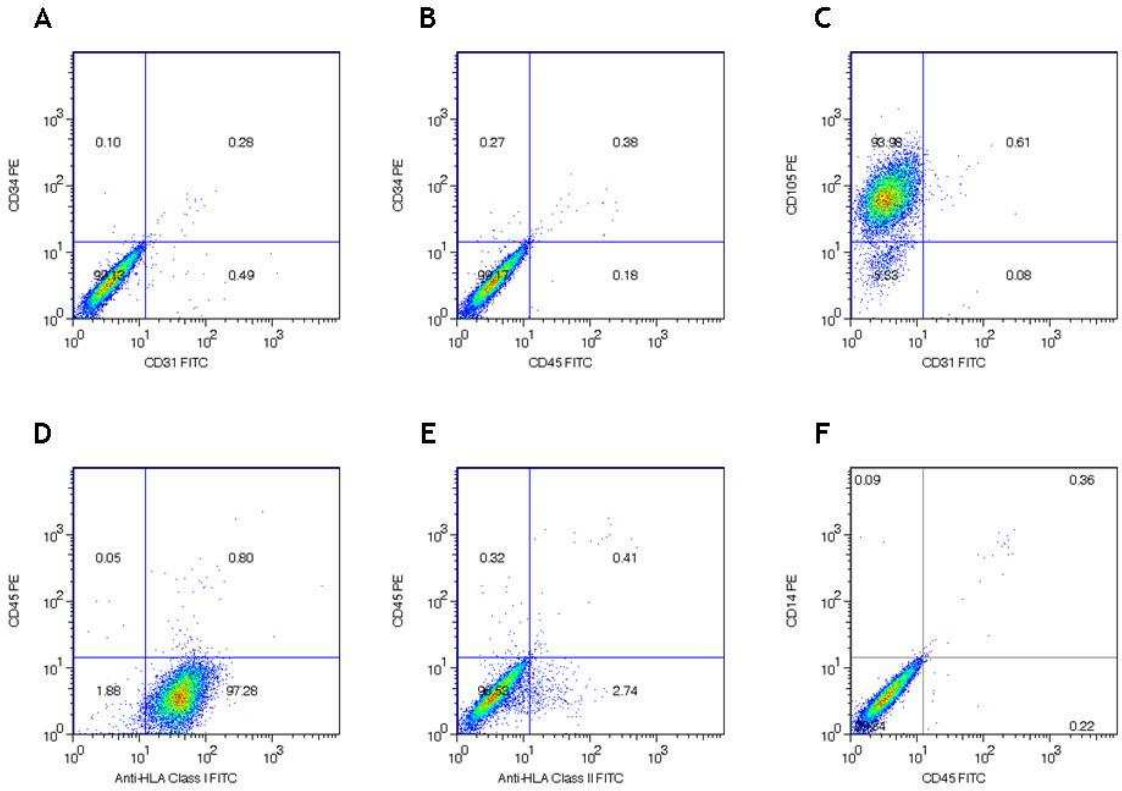

Figure 3-5 MSC's at passage two displayed characteristic surface marker profiles

The majority of MSC's did not express the surface markers CD31, 34 and 45 which confirmed the absence of significant endothelial or haematopoietic cell contamination (A, B and F). CD105 was expressed on most MSC's although a discrete CD105 negative population was identified of uncertain significance (C). HLA Class I antigens were expressed on the majority of cells (D) and although only a minority expressed Class II antigens (E).

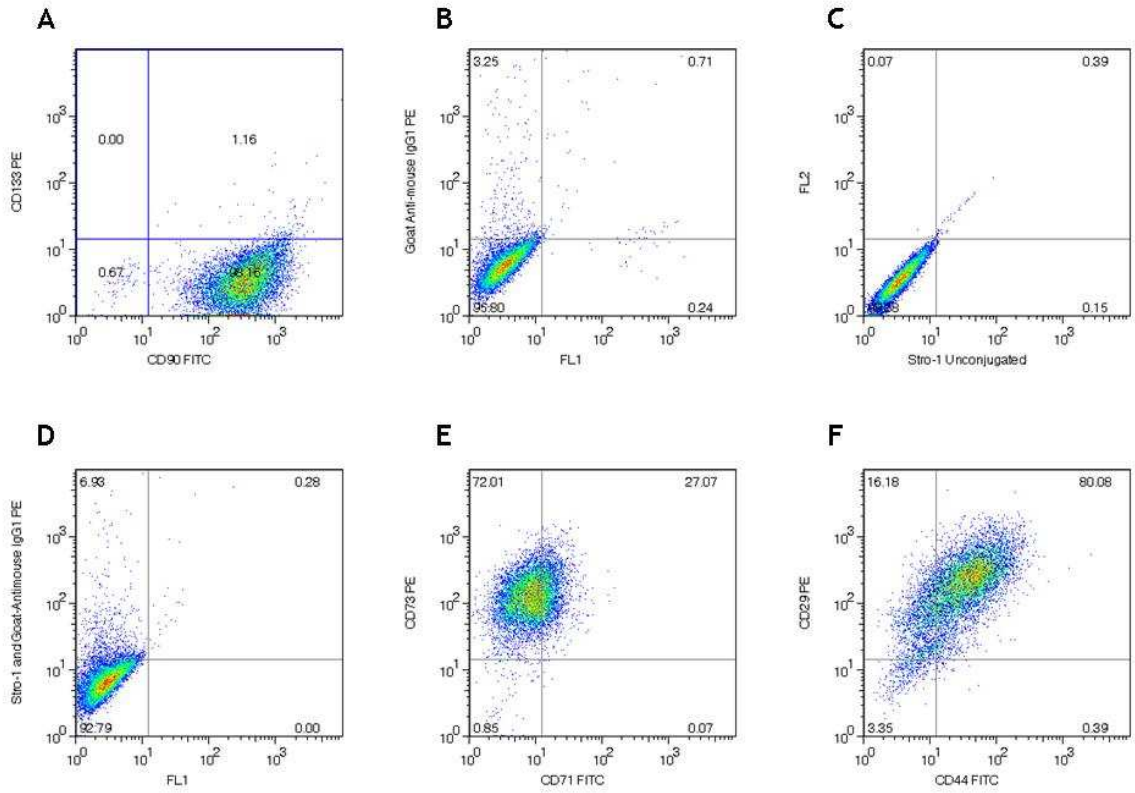

Figure 3-6 MSC's at passage two displayed characteristic surface marker profiles

The majority of MSC's did not express the stem cell marker CD133 (A) although Stro-1, which selects for a highly proliferative subset was confirmed on a small percentage of cells using secondary detection methods (B-D). Most MSC's expressed CD73 although CD71, an indicator of proliferation was found on less than a one third of cells assayed at near confluence (E). The markers CD29 (integrin ß1) and CD44 (hyaluronic acid receptor) were expressed on the majority of cells although a discrete population lacking these markers was identified (F).

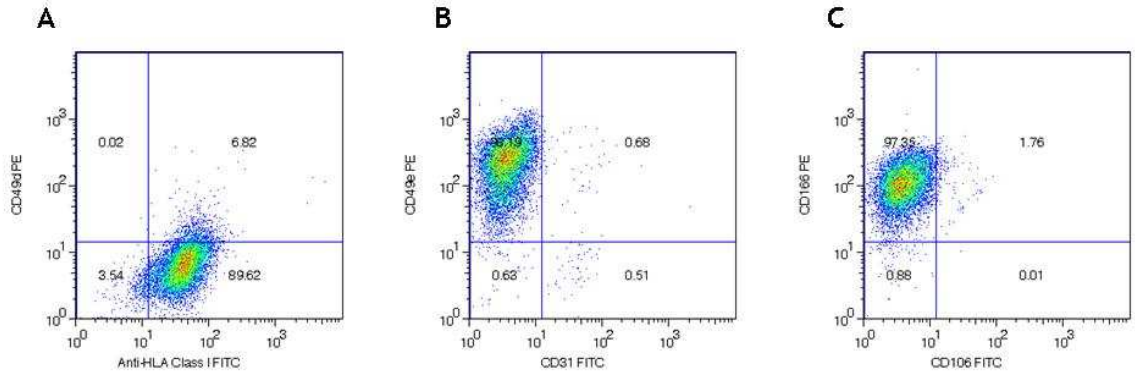

Figure 3-7 MSC's at passage two displayed characteristic surface marker profiles

The majority of MSC's were negative for the marker CD49d (integrin α4) (A) in contrast to CD49e (integrinα5) that was detected on virtually all cells (B). Similarly, CD166 (ALCAM) was detected on the majority ofcells whilst CD106 (VCAM-1) was found on a small percentage of MSC's in culture (C).

Surface Marker %	12 MSC P2	23 MSC P2	24 MSC P2	25 MSC P2	26 MSC P2	27 MSC P2	28 MSC P2	29 MSC P2	30 MSC P2	Mean %	Std Dev
CD13	99.1	97.3	99.5	98.5	99.1	99.9	99.4	98.8	99.2	99.0	± 0.8
CD14	1.3	0.5	0.5	0.1	0.2	0.4	0.3	0.2	0.4	0.4	± 0.3
CD29	N/A	98.4	96.3	97.3	98.5	98.6	97.2	99.6	99.7	98.2	± 1.2
CD31	0.7	1.0	0.7	0.6	0.3	0.2	0.4	0.7	0.7	0.7	± 0.3
CD34	0.8	0.4	0.4	0.4	0.3	0.3	0.4	0.1	0.3	0.4	± 0.2
CD44	N/A	83.3	80.5	89.4	92.5	98.3	92.6	96.3	98.5	91.4	± 6.7
CD45	0.3	1.0	0.6	0.2	0.2	0.2	0.5	0.3	0.4	0.4	± 0.3
CD49d	N/A	3.7	6.8	7.6	25.4	42.0	5.6	13.3	35.1	17.5	± 14.8
CD49e	N/A	98.8	98.9	99.4	99.4	99.4	99.5	98.9	99.5	99.2	± 0.3
CD71	57.1	22.4	27.1	30.9	49.9	30.5	2.3	23.7	43.6	31.9	± 16.4
CD73	99.0	99.2	99.1	97.7	99.4	99.5	99.5	99.3	99.3	99.1	± 0.5
CD90	98.7	99.4	99.3	99.7	97.7	98.7	98.8	99.7	99.6	99.1	± 0.6
CD105	93.5	94.3	94.6	95.4	96.8	97.6	94.6	94.7	98.5	95.5	± 1.7
CD106	N/A	3.0	1.8	7.2	11.3	11.5	0.2	8.6	8.7	6.5	± 4.3
CD133	0.8	1.1	1.2	2.8	0.2	0.2	0.5	0.4	1.0	0.9	± 0.8
CD166	N/A	57.5	99.1	98.5	96.1	97.2	98.7	97.5	99.3	93.0	± 14.4
HLA Class I	95.0	97.3	98.1	96.8	98.6	98.6	98.4	98.1	99.4	97.8	± 1.3
HLA Class II	3.9	23.6	3.2	0.8	5.6	1.9	6.3	25.3	29.9	11.2	± 11.6
Stro-1	0.1	0	3.3	2.7	1.2	7.6	10.4	1.5	0.7	3.0	± 3.7

Table 2 Surface marker profiles of MSC's at passage two by flow cytometry

The percentage of MSC's expressing each surface marker for the individual donors and overall mean including standard deviation are shown (N/A – result not available).

Surface Marker	Mean Expression MSC P1 % (n=5)	S.D	Mean Expression MSC P2 % (n=5)	S.D.	P value
CD13	96.68	2.74	98.83	1.05	n.s
CD14	3.85	2.22	0.46	0.03	0.01
CD29	96.83	3.06	97.63	1.28	n.s
CD31	5.40	3.48	0.67	0.37	0.02
CD34	3.25	1.35	0.42	0.10	0.00
CD44	55.43	24.84	70.60	12.43	n.s
CD45	6.17	3.54	1.61	1.03	0.02
CD49d	19.48	5.78	8.58	4.14	n.s
CD49e	96.71	3.00	98.96	0.24	n.s
CD71	42.16	28.61	26.57	16.11	n.s
CD73	93.40	5.20	98.09	2.23	n.s
CD90	93.03	6.74	95.69	6.02	n.s
CD105	93.57	6.13	93.05	3.23	n.s
CD106	4.33	1.24	1.45	1.19	n.s
CD133	2.28	1.93	1.38	1.18	n.s
CD166	91.42	7.85	85.60	19.27	n.s
HLA Class I	97.50	2.29	96.47	3.76	n.s
HLA Class II	28.96	18.98	15.68	12.51	n.s
Stro-1	2.74	2.56	1.05	1.41	n.s

Table 3 Comparison of surface marker profiles of MSC's at passage one and two by flow cytometry

The overall mean percentage surface marker expression and the standard deviation at passage one and two from five donor MSC cultures are shown. Comparisons were made using a paired student's t-test and p values are shown (n.s – not significant).

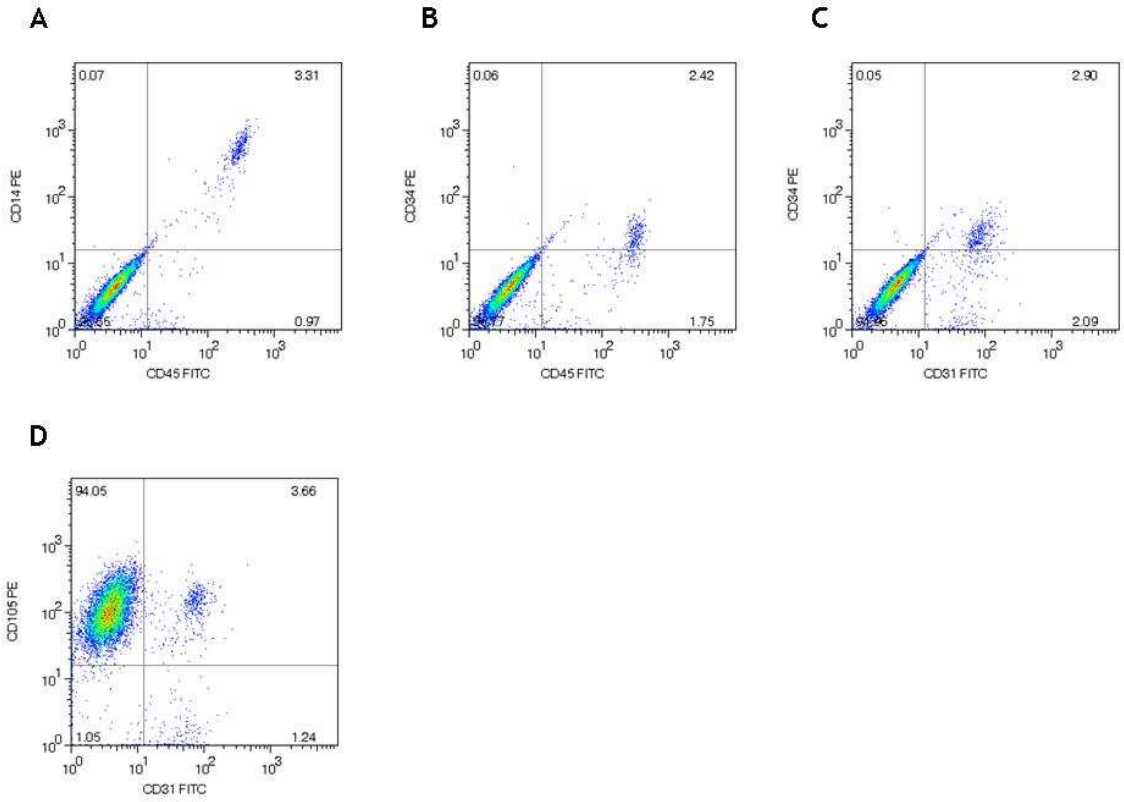

Figure 3-8 Contaminating cell populations were present in MSC's at passage one

Passage two cells were analysed using two colour flow cytometry after staining with phycoerythrin (PE) or fluorescein isothiocyanate (FITC) conjugated monoclonal antibodies. The plots shown were obtained after collecting 10,000 events and representative of the five MSC cultures analysed. Discrete populations of cells expressing macrophage (A), haematopoietic progenitor (B) and endothelial progenitor cell markers were identified at passage one but not passage two.

3.2.3 Differentiation of Early Passage MSC's

The differentiation potential of MSC's at passage two was determined by culturing in either adipogenic, osteogenic or chondrogenic medium for 21 days. Adipogenic differentiation was confirmed by the accumulation of large cytoplasmic lipid vacuoles that stained red using Oil Red O (Figure 3-9 E-H and M-P). MSC's cultured in control media did not stain (Figure 3-9 A-D and I-L). Immunofluorescence demonstrated that the adipogenic specific gene, fatty acid binding protein-4 (FABP-4) was highly expressed around the periphery of the lipid vacuoles (Figure 3-10). Osteogenic differentiation was confirmed by the accumulation of cell aggregates and calcium deposits that stained red with Alizarin Red S (Figure 3-11 E-H and M-P). MSC's cultured in control media did not stain (Figure 3-11 A-D and I-L). Immunofluorescence with the osteogenic specific gene, osteocalcin was problematic due to high background staining that could not be resolved using the antibody provided with the kit (images are not shown).

MSC's pellets in chondrogenic differentiation medium were larger than controls due to increased deposition of proteogylcans that stained with Alcian blue (Figure 3-12 A-D and I-L). Vacuoles were identified in differentiated pellets but not the controls. Control pellets were fragile because of their smaller size and only three out of eight remained intact after fixation and processing (images are not shown). The processing, staining and sectioning was performed by Histology Services, Beatson Institute, Glasgow. Immunofluorescence using the chondrogenic specific gene, aggrecan showed increased staining in the differentiated cells compared to the controls (Figure 3-13).

3.2.4 Growth Kinetics of MSC's

Under the culture conditions defined in this research, the growth kinetics of MSC's from eight donors were analysed from isolation until the ninth passage (Figure 3-14 A-C). From the time of plating the MNC fraction, MSC's reached passage one and two after 11.0 ± 1.3 days and 18.5 ± 3.4 days respectively. MSC's at passage two were counted on a daily basis in order to establish growth profiles from plating to near confluence (Figure 3-14 C).

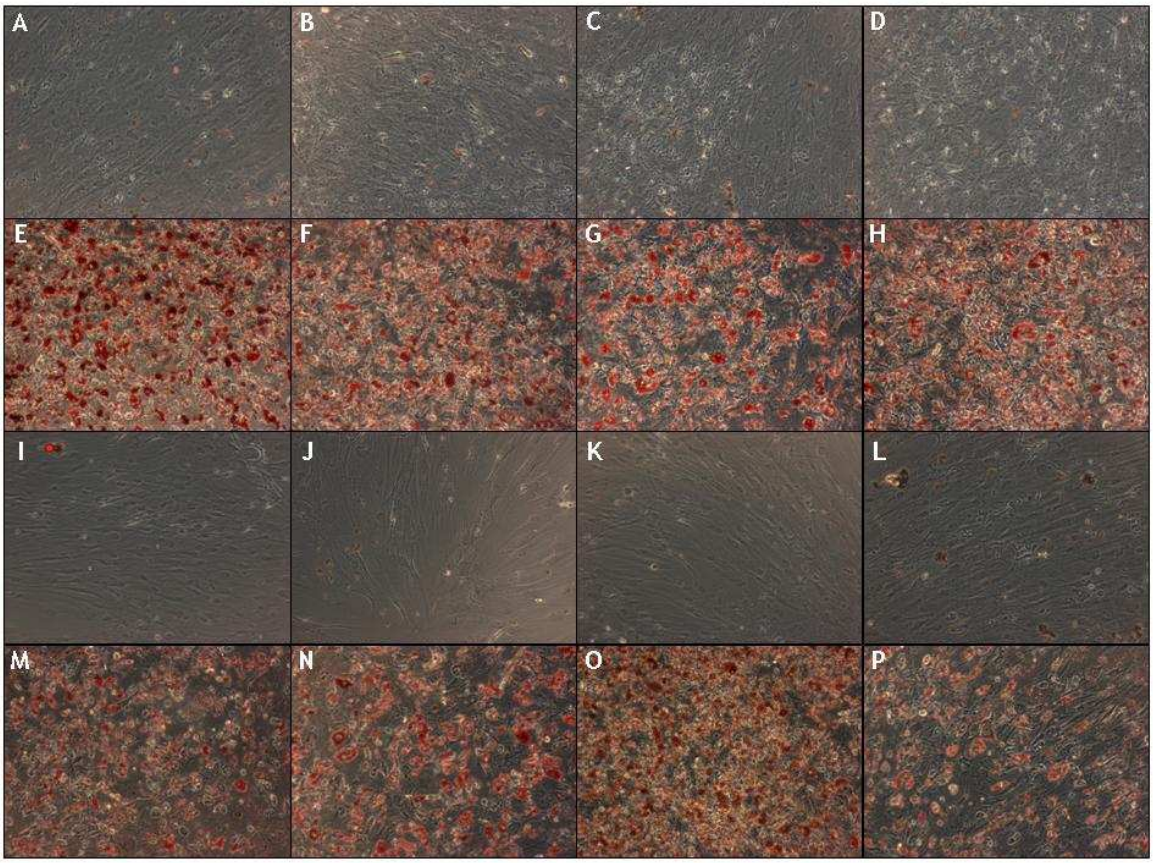

Figure 3-9 MSC's samples undergo adipogenic differentiation in defined conditions

Eight MSC cultures (Donors 23-30) at passage two were grown to 100% confluence before culturing for three weeks in control or adipogenic culture medium containing hydrocortisone, isobutylmethylxanthine and indomethacin. Control MSC's (A-D, I-L) did not stain with lipid soluble Oil Red O while those in adipogenic media (E-H, M-P) stained red confirming differentiation to this lineage (4x magnification).

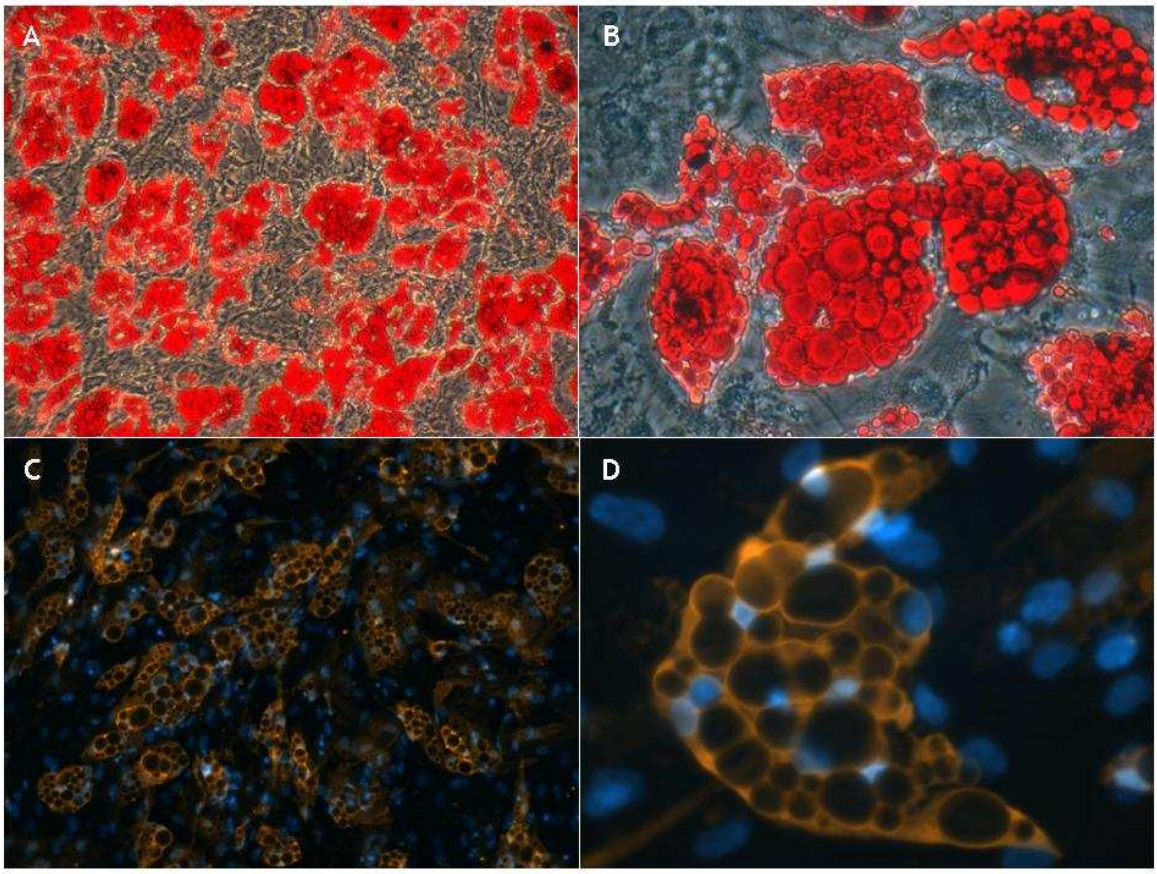

Figure 3-10 MSC's express fatty acid binding protein 4 (FABP-4) after adipogenic differentiation

MSC's stained red with Oil Red O after adipogenic differentiation (A) (10x magnification). At high magnification the stain was shown to accumulate within lipid droplets in the cell cytoplasm (B) (40x magnification). FABP-4, found expressed on adipocytes was demonstrated in MSC's using polyclonal goat anti-mouse FABP-4 labelled with a tetramethylrhodamine isothiocyanate (TRITC) conjugated donkey anti-goat secondary (C) (10x magnification). The expression of FABP-4 was most intense around the periphery of lipid droplets (D) (100x magnification). Nuclei were stained using 4', 6-diamidino-2-phenylindole (DAPI) and appear blue. Immunofluorescence images were taken with fixed exposure times.

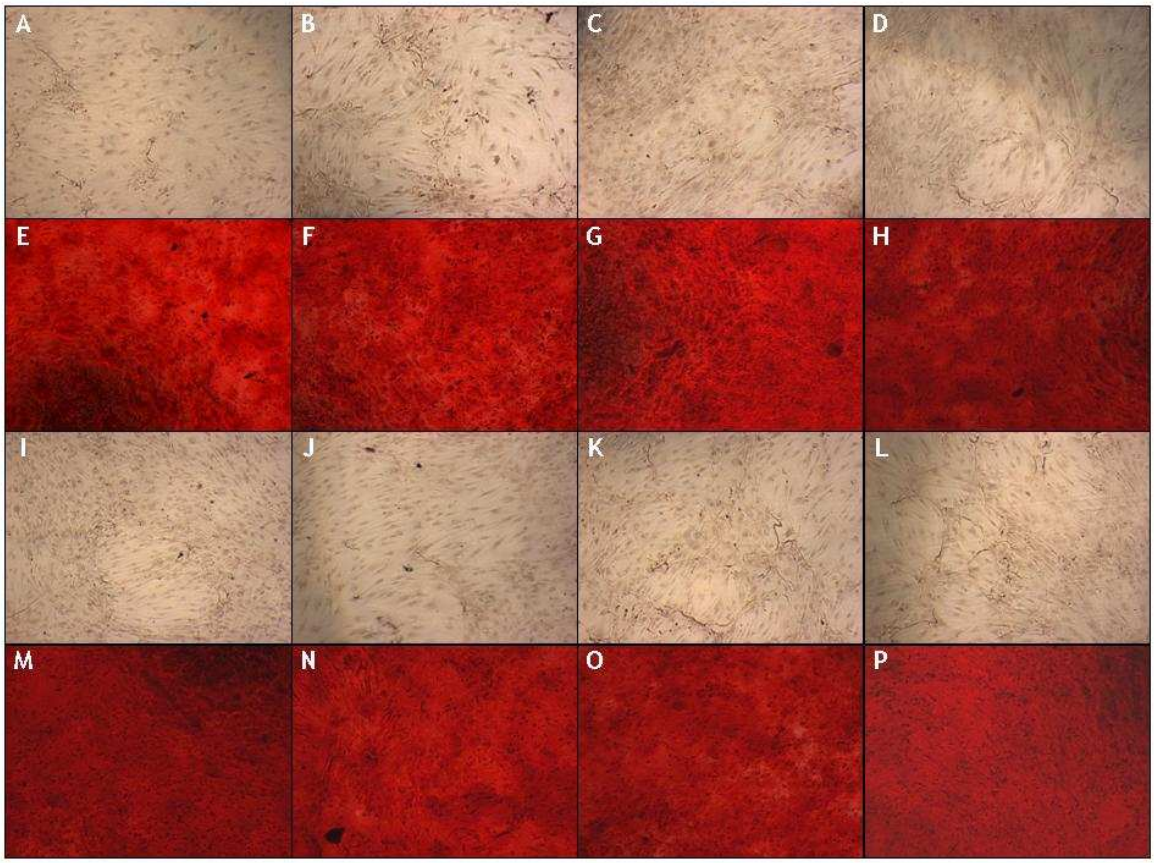

Figure 3-11 MSC samples undergo osteogenic differentiation in defined conditions

Eight MSC cultures (Donors 23-30) at passage two were grown to 70% confluence before culturing for three weeks in control or osteogenic culture medium containing dexamethasone, ascorbate phosphate and ß-glycerol phosphate. Control MSC's (A-D, I-L) did not stain with the calcium stain, Alizarin Red S while those in osteogenic media (E-H, M-P) were bright red confirming osteogenic differentiation and mineralisation (4x magnification).

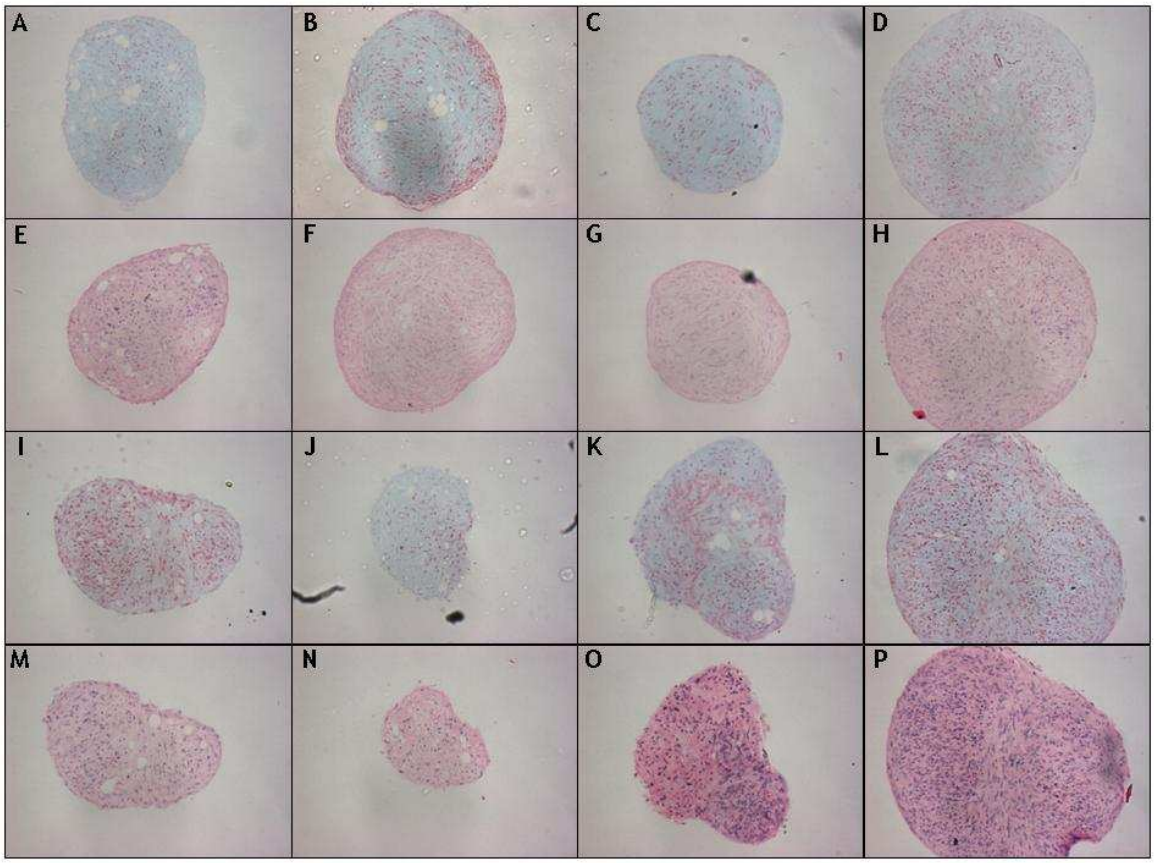

Figure 3-12 MSC samples undergo chondrogenic differentiation in defined conditions

Eight MSC cultures (Donors 23-30) at passage two were centrifuged into pellets before culturing for three weeks in chondrogenic culture medium containing dexamethasone and transforming growth factor ß3 (TGF-ß3). The differentiated pellets were formalin-fixed, paraffin-embedded pellets and cut into 2µM sections. Proteoglycans found in cartilage, such as chondroitin sulphate were detected in the pellets using Alcian blue (A-D, I-L). A baseline stain with Haematoxylin and Eosin (H+E) (E-H, M-P) was performed that demonstrates basophilic structures purple (nuclei) and eosinophilic structures pink (intra and extracellular proteins) (4x magnification).

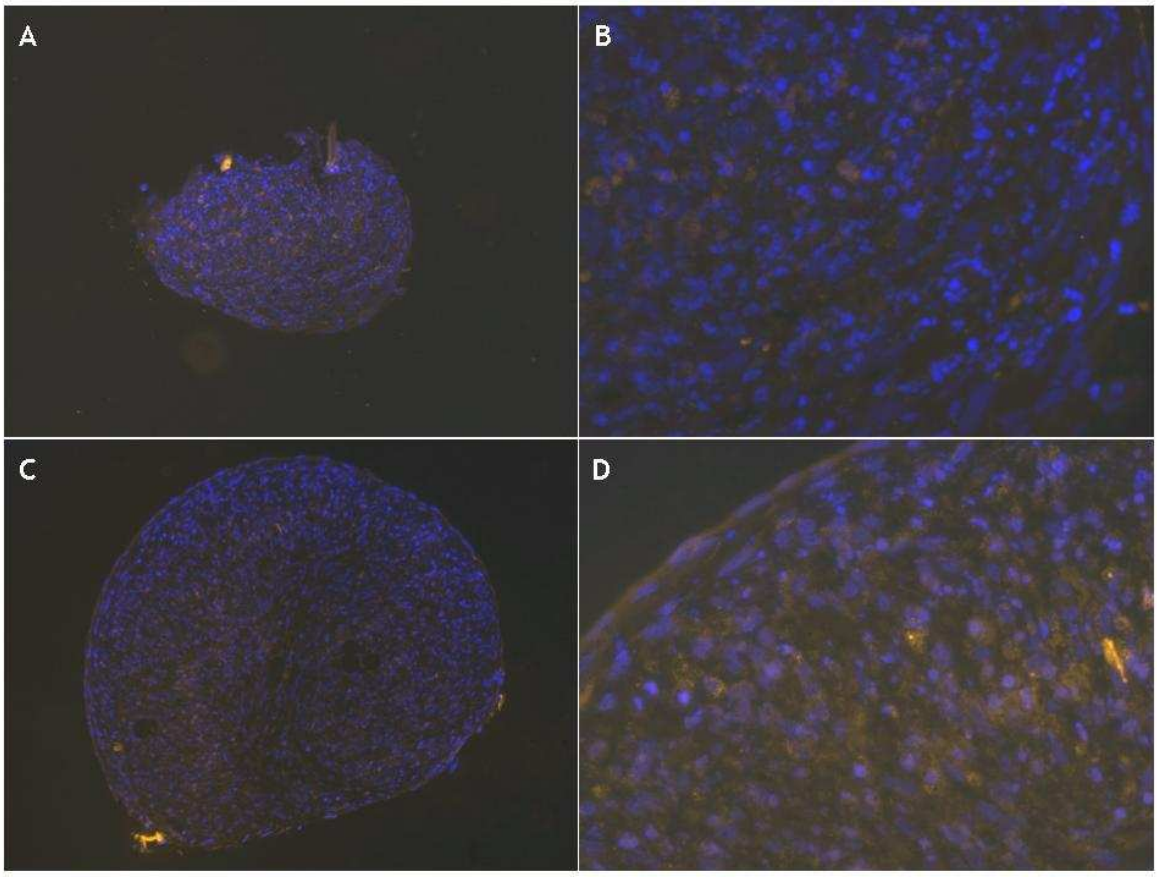

Figure 3-13 Expression of aggrecan increased in MSC pellets undergoing chondrogenic differentiation

MSC pellets treated for 21 days in chondrogenic culture medium (C) were larger in comparison to the controls (A) (10x magnification). Increased deposition of aggrecan, an extracellular matrix protein abundant in cartilage was seen in the differentiated pellets (D) in comparison to controls (B) (40x magnification). Expression was detected using goat anti-human aggrecan labelled with a TRITC conjugated donkey anti-goat secondary (B and D). Nuclei are stained blue (DAPI). Images were taken with fixed exposure times.

A

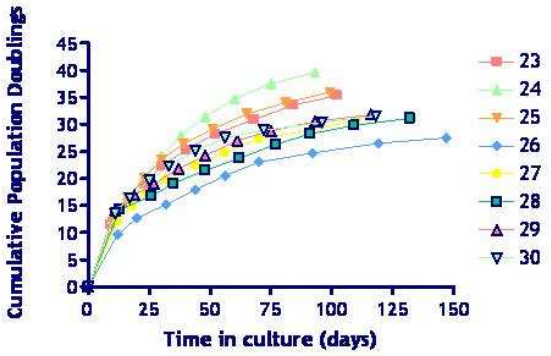

B

	Passage number	Mean (n=8)	S.D
Time in culture (days)	1	11.0	± 1.3
	2	18.5	± 3.4
	5	46.4	± 8.6
	9	114.6	± 18.0
Cumulative population doublings	1	12.4	± 1.6
	2	15.8	± 1.4
	5	24.5	± 2.3
	9	32.9	± 3.8
Population doubling time (hrs)	1	21.5	± 3.6
	2	58.3	± 27.6
	5	92.2	± 23.5
	9	366.1	± 152.8
% of proliferative capacity to P9 (No. P.D's/Total P.D's at P9)	1	38.1	± 5.4
	2	48.1	± 4.3
	5	74.4	± 2.7
	9	100	± 0

C

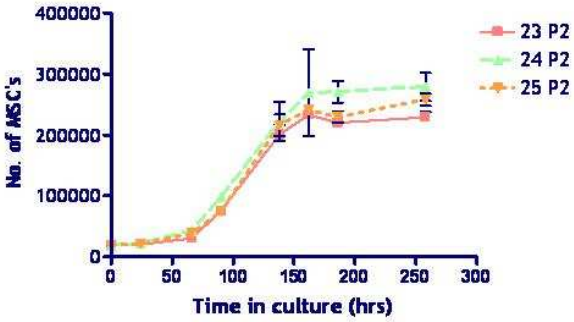

Figure 3-14 Growth kinetics of MSC's during expansion *in vitro*

The cumulative number of population doublings until passage nine was plotted against time in culture for eight cultures (A). Population doublings were determined from viable cell counts using the formula: PD = (log $_{\text{(no. MSC's harvested)}}$ − log $_{\text{(no. MSC's plated)}}$) / log 2. The overall mean and standard deviation derived from the eight samples are shown in the table (B). At passage two, three samples (donors 23, 24 and 25) were counted on a daily basis in duplicate wells to determine the growth profile of MSC's from initial plating to confluence (C).

MSC's displayed a characteristic lag phase for two days followed by logarithmic growth until day six when proliferation decreased and the cells reached confluence. With prolonged culture the interval between passages increased and showed greater variation between MSC's from different donors. Mean population doubling time increased from 58.6 ± 27.3 to 92.2 ± 23.5 hours to 366.1 ± 152.8 hours at passages two, five and nine respectively.

By determining the frequency of true MSC's by CFU-F and the number of MNC's plated, the number of population doublings from isolation to the first passage was estimated. MSC's underwent 12.4 ± 1.6 population doublings by passage one, equivalent to 38.1 ± 5.4 % of the total culture period. The rapid early growth of MSC's occurred in only 11 ± 1.3 days, equivalent to 9.7 ± 0.9 % of the total culture period.

3.2.5 Surface Marker Profile of Late Passage MSC's

The percentage expression of a limited number of surface markers was analysed at passage nine in cells from four donors (23-25 and 27) and compared to those at passage two using a paired student's t-test (Figure 3-15). Late passage MSC's showed decreased viability as shown by the accumulation of cells in the bottom left of the forward and side scatter dot plot (Figure 3-15A). The percentage of MSC's gated for analysis was significantly decreased in comparison to cell at passage two (69.9% ± 8.5 % versus 90.2 ± 1.4%, p 0.003). There was no difference in the forward scatter properties of gated late passage MSC's (geometric mean of 490.7 ± 51.5 versus 478.6 ± 40.9, n.s) although there was significant reduction in side scatter properties (geometric mean 363.2 ± 43.9 versus 449.4 ± 48.7, p 0.04) in comparison to cells at passage two. A smaller percentage of MSC's at passage nine expressed the surface markers CD29, 44, 105 and HLA Class I (Figure 3-15E).

3.2.6 Differentiation of Late Passage MSC's

The differentiation potential of MSC's at passage nine was determined by culturing the cells in either adipogenic or osteogenic differentiation medium for 21 days. MSC's cultured in adipogenic differentiation media accumulated less cytoplasmic lipid vacuoles that stained with Oil Red O when compared to cells

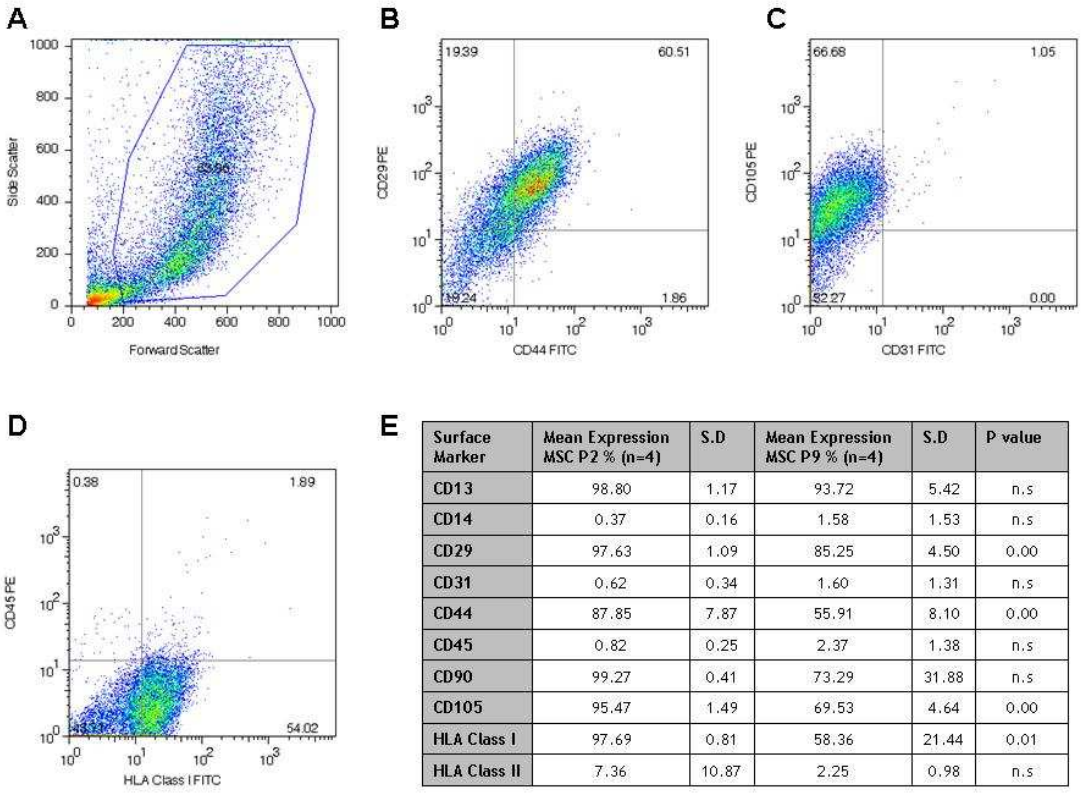

E

Surface Marker	Mean Expression MSC P2 % (n=4)	S.D	Mean Expression MSC P9 % (n=4)	S.D	P value
CD13	98.80	1.17	93.72	5.42	n.s
CD14	0.37	0.16	1.58	1.53	n.s
CD29	97.63	1.09	85.25	4.50	0.00
CD31	0.62	0.34	1.60	1.31	n.s
CD44	87.85	7.87	55.91	8.10	0.00
CD45	0.82	0.25	2.37	1.38	n.s
CD90	99.27	0.41	73.29	31.88	n.s
CD105	95.47	1.49	69.53	4.64	0.00
HLA Class I	97.69	0.81	58.36	21.44	0.01
HLA Class II	7.36	10.87	2.25	0.98	n.s

Figure 3-15 Late passage MSC's show alterations in surface marker expression

Four MSC cultures at passage nine were analysed using a restricted set of surface markers and representative plots shown. The gated MSC population demonstrated greater variability in forward and side scatter properties and cell viability was decreased (A). A significant percentage of MSC's lost expression of the surface markers CD29, 44, 105 and HLA Class I in comparison to those at passage two and representative plots shown (B-D). The mean percentage expression and standard deviation from the four cultures are shown in the table (E). Comparisons were made using a paired student's t-test and p values are shown (n.s – not significant).

at passage two (Figure 3-16). MSC's cultured in osteogenic differentiation media developed aggregates and calcium deposits that stained red with Alizarin Red S (Figure 3-17). The aggregates were smaller and the extent of the staining reduced in comparison to cells at passage two. Chondrogenic differentiation was not performed because cell numbers were limited and required for other assays at passage nine.

3.2.7 Telomere Lengths of Early and Late Passage MSC's

Genomic DNA was extracted from eight cultures at passage two and nine and used in the TeloTAGGG telomere length assay (Roche Diagnostics Ltd). Telomere lengths were determined from southern blot by densitometry (Figure 3-18). The protocol and results were produced by Sharon Burns, research assistant within the group of Professor W.N Keith.

The mean telomere length of MSC's at passage two was 7.3 ± 0.8 kB and donor 23 displayed the longest and donor 27 the shortest telomeres (8.3 and 6.2 kB, respectively). At passage nine, MSC's displayed telomere losses apart from donors 25 and 30 that showed gains of 0.08 and 4.7 kB respectively. The overall mean telomere length of MSC's at passage nine was 7.0 ± 2.3 kB (6.2 ± 0.7 kB excluding donor 30) and the mean telomere loss in comparison to passage two was 0.3 ± 2.2 kB (1.0 ± 0.9 kB excluding donor 30). MSC's from donor 23 showed the greatest telomere loss between passages two and nine equivalent to 2kB of telomeric DNA. Overall, eight cultures underwent a mean of 17.2 ± 3.2 population doublings between passages two and nine equivalent to a mean telomere loss per population doubling of 17.5 ± 141.7 bp (64.4 ± 53.6 bp excluding donor 30).

To determine telomerase expression, three MSC samples (donors 23, 24 and 25) were analysed using the Telomeric Repeat Amplification Protocol (TRAP). The technique was performed by Stacey Hoare, research assistant within the group of Professor W.N Keith. Telomerase expression was not detected in any of the samples (results are not shown).

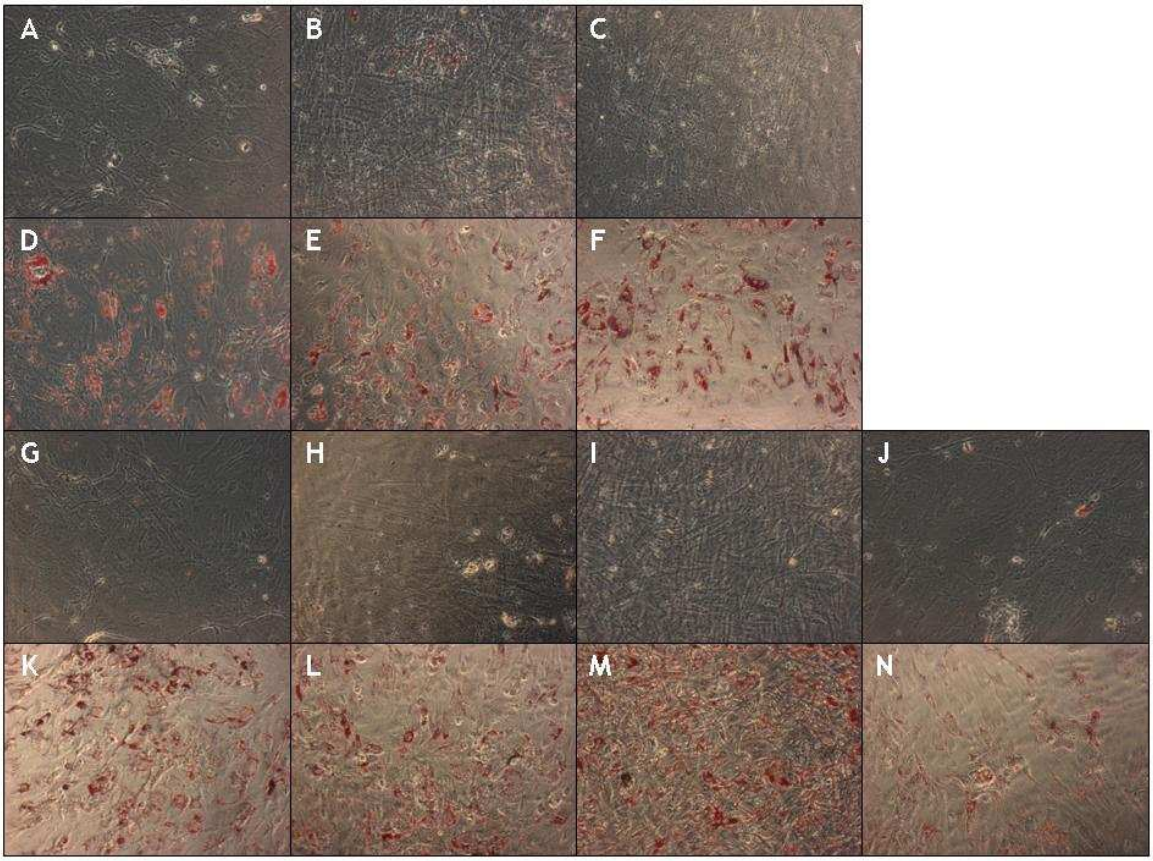

Figure 3-16 Late passage MSC's had decreased adipogenic differentiation capacity

Eight MSC cultures (Donors 23-30) at passage nine were plated at 100% confluence before culturing for three weeks in control or adipogenic culture medium containing hydrocortisone, isobutylmethylxanthine and indomethacin. In control MSC's (A-C, G-J), a few cells accumulated Oil Red O suggesting spontaneous differentiation had occurred. MSC's grown in adipogenic media (D-F, K-N) retained the capacity for adipogenic differentiation although to a lesser extent than cells at passage two (4x magnification). Cells from donor 26 were destroyed as a result of contamination and images are not shown.

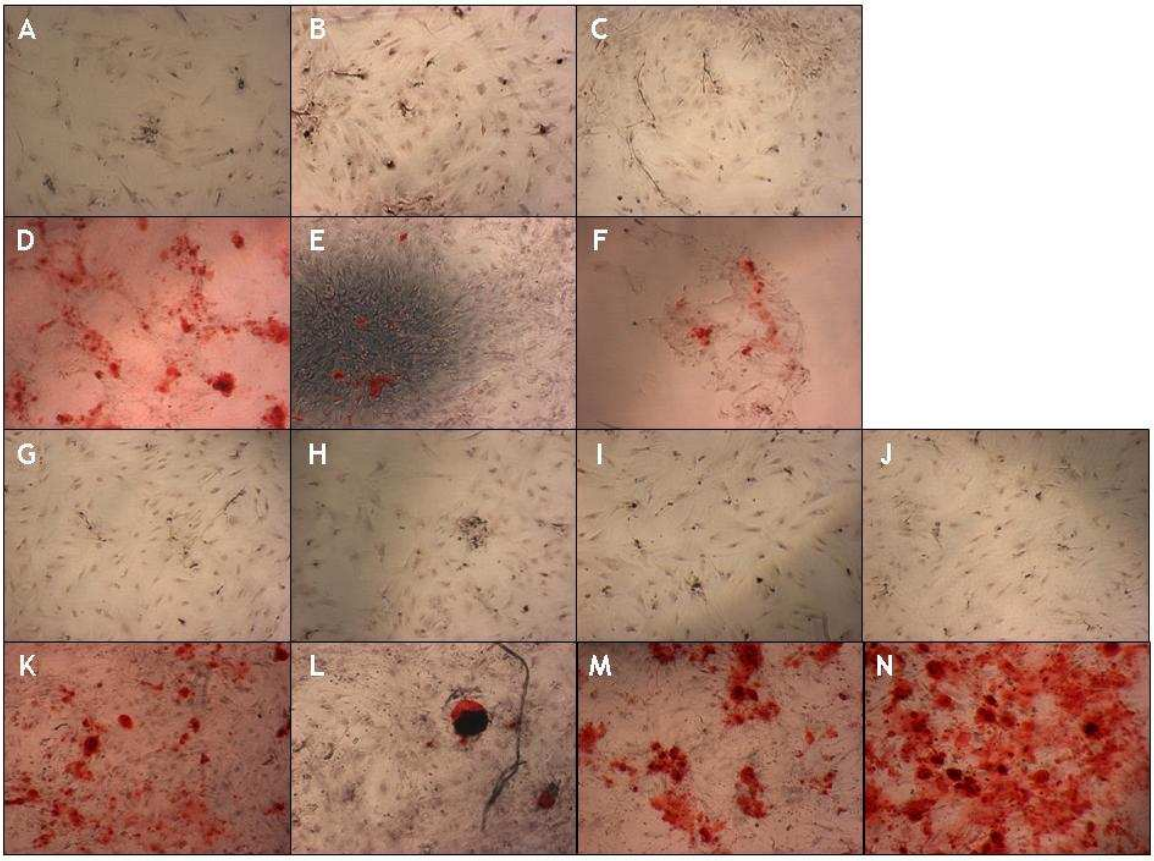

Figure 3-17 Late passage MSC's show decreased osteogenic differentiation capacity

Eight MSC cultures (Donors 23-30) at passage nine were grown to 70% confluence before culturing for three weeks in control or osteogenic culture medium containing dexamethasone, ascorbate phosphate and ß-glycerol phosphate. Control MSC's (A-C, G-J) did not stain for calcium using Alizarin Red S while those in osteogenic media (D-F, K-N) showed variable staining confirming that the osteogenic differentiation capacity of MSC's significantly decreased at late passage (4x magnification). Cells from donor 26 were destroyed as a result of contamination and images are not shown.

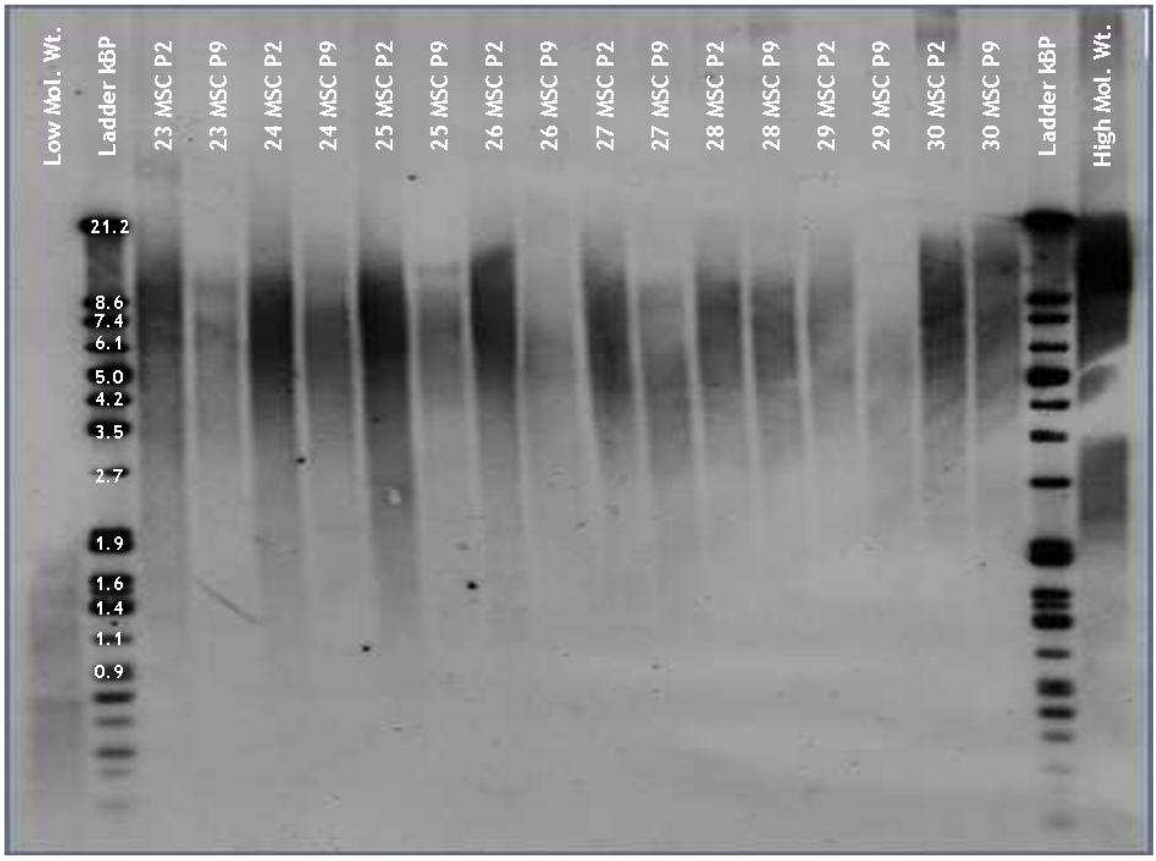

Figure 3-18 Telomere shortening was observed in most MSC cultures after prolonged expansion

The telomere lengths of eight MSC's cultures at passage two and nine were determined using the TeloTAGGG telomere length assay and displayed on a single southern blot. Telomere lengths were calculated from the blot by densitometry following the manufacturer's protocol. Undigested low and high molecular weight DNA and ladders are shown.

3.2.8 Expression of Senescence Associated β-Galactosidase in MSC's

The activity of the enzyme SA ß-Gal was assessed at pH 6 using the Senescent Cells Staining Kit (Sigma) and calculating the percentage of MSC's staining blue from eight donors (Figure 3-19). The mean percentage of SA ß-Gal positive cells at passage two was 1.5 ± 3.3 % although this reached 10% in cells from donor 28. In contrast, 47.2 ± 12.1 % MSC's stained positive for SA ß-Gal at passage nine and cells displayed a senescent morphology. SA ß-Gal staining was most intense in the peri-nuclear region of MSC's viewed at high magnification (Figure 3-19D).

3.3 Discussion

The ease with which MSC's can be isolated and expanded *in vitro* has enhanced the clinical application of these cells for the treatment MI (9;10). However, MSC's used in these studies have not been extensively characterised and the characteristics of cells from patients with IHD is poorly understood. In our donor population the frequency of MSC's was approximately 1 in 1 x 10^5 MNC's and similar to the findings of previous studies (1 in 3.4 x 10^4 to 1 in 3 x 10^5)(11;17;91;156;157). The effect of ageing on the frequency of MSC's in the BM is not clear because Baxter *et al* reported a decrease in MSC's with increasing age and Stenderup *et al* could not demonstrate a difference. MSC's in our study displayed a fibroblast-like morphology and were heterogeneous in size and shape. Colter *et al* have described that MSC's cultures are composed of rare small round cells, spindle shaped cells and large flat cells and that each population has different proliferative and differentiation potential (32). Our study identified similar small rapidly self-renewing (RS) cells although these were rare and not the focus of further experiments. These cells are recognised as MSC progenitors and enriched when cultures are plated low density (<3 cells per cm^2) (59).

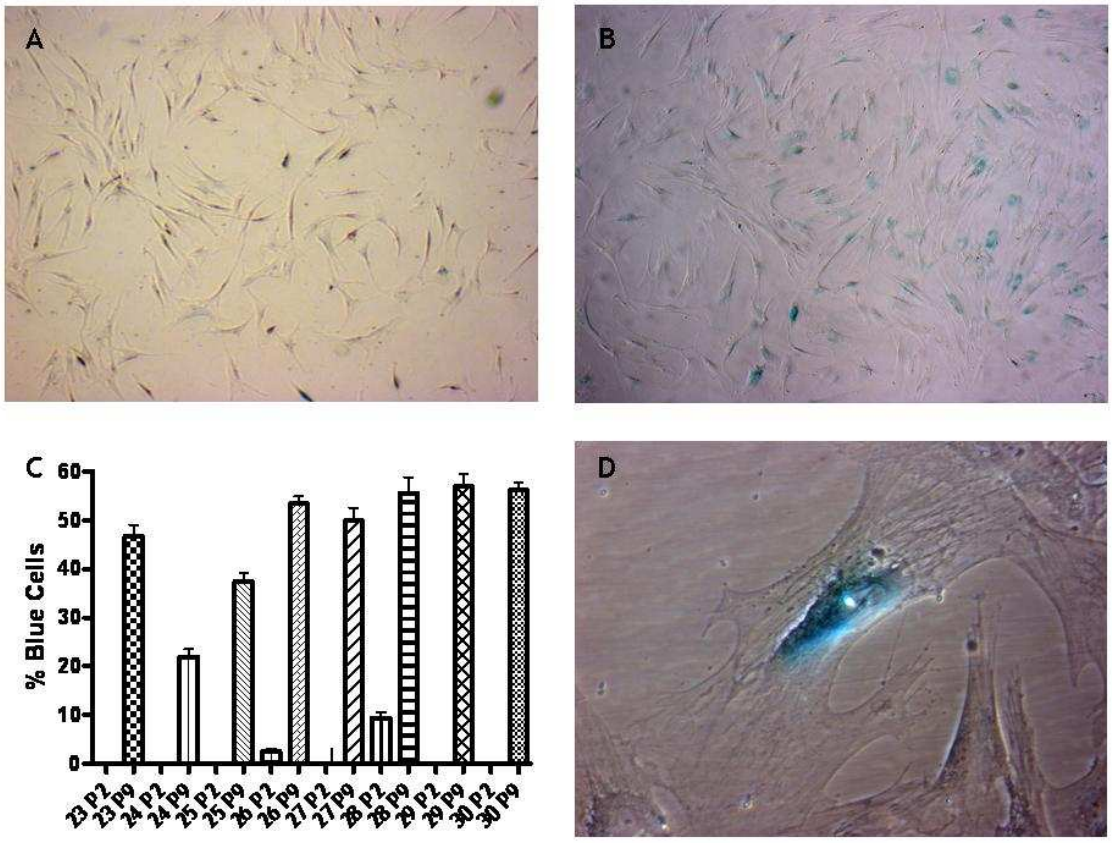

Figure 3-19 Senescence Associated β-Galactosidase (SA β-Gal) staining increased in late passage MSC's

The activity of the enzyme SA ß-Gal was assessed at pH 6 using the Senescent Cells Staining Kit (Sigma). Representative photographs of MSC's at passage two (A) and nine are shown (B) (4x magnification). At least 300 cells were counted in random fields to determine the percentage of SA ß-Gal (blue) cells (C). Bars represent the mean and error bars the standard deviation. MSC's displayed a senescent morphology and intense peri-nuclear staining with SA ß-Gal (40x magnification).

When viewed under a microscope, early passage MSC's contained mostly spindle shaped cells and less frequently, large flat cells. In contrast, the study by Baxter *et al* demonstrated that MSC's from aged donors contained predominantly large flat cells that proliferated poorly (11). The difference in comparison to our results may be explained by differences in culture methods used and the characteristics of the donors. Our study used more serum (20% compared to 10%), a lower plating density and low glucose media containing Glutamax and all have been shown to enhance the proliferation of MSC's (58).

The surface marker profiles of MSC's have been extensively investigated by different groups and a minimal criteria for characterisation has been agreed (33). In our study the majority of MSC's (>90%) expressed the surface markers CD13, CD29, CD44, CD49e, CD73, CD90, CD105, CD166 and MHC Class I. This profile is remarkably similar to that described in the original study by Pittenger *et al* (17). Many of these proteins have diverse roles although their exact functions in MSC's remain poorly understood. CD73 (ecto-5'-nucleotidase) is important for cell-cell integrity as defects in vascular permeability have been demonstrated in CD73 knockout mice (158). Distinct epitopes on CD73 are recognised by the monoclonal antibodies, SH3 and SH4 that were initially thought to be specific markers of MSC's but later shown to be widely expressed (159). CD90 (Thy1) has been recognised on other stem cell populations and somatic cells including fibroblasts so cannot prospectively identify MSC's. Similarly, the monoclonal antibody SH2 which was developed for the identification of MSC's in fact recognises an epitope of CD105 (endoglin) and is expressed in other cell types (160).

The surface markers CD49d, 71, 106 and MHC Class II were found expressed on a moderate number (5-90%) of MSC's in our culture conditions. CD106 (vascular cell adhesion molecule 1, VCAM-1) expression can vary with the source of MSC's used. MSC's derived from cord blood do not express CD106 (161), a small percentage of BM MSC's express this marker (162) and significantly higher levels are seen in MSC's derived from adipose tissue (163). Furthermore, Gronthos *et al* have described a method to isolate almost all of the CFU-F population from the BM MNC using magnetic selection and the combination of markers CD106 and Stro-1 (34). We identified a higher percentage of MSC's expressing MHC Class II (mean 11.2%) in comparison to earlier studies although the antibody we used

detected all class II subtypes (HLA-DR, DP and DQ) and HLA-DR expression is typically described. In fact, it has been suggested that HLA-DR expression should be less than 2% in MSC's cultured in standard conditions (33). HLA-DR expression can be induced in MSC's in response to cytokines such as interferon-γ (164) and also growth factors such as basic fibroblast growth factor (b-FGF) (165). A further study to determine HLA-DR expression alone in our MSC's is required to ensure the immune profile is similar to that reported in earlier studies.

In our study a small percentage of MSC's at passage two (<3%) expressed the markers CD14, CD31, CD34, CD45, CD133 and Stro-1. Cultures at passage one contained small populations of endothelial and haematopoietic cells and is a recognised problem when using the plastic adherence technique for isolation of MSC's. Tondreau *et al* have described immunodepletion (Rosette step) and magnetic-activated cell sorting (MACS) using the stem cell marker CD133 as a method to purify MSC's from the MNC fraction (166). Both methods produce homogenous cultures from initial isolation although at later passages the cultures are similar to those isolated by plastic adherence so the benefits, particularly for clinical application remain uncertain. The surface marker Stro-1 was present on 3% of MSC's at passage two and it is recognised that Stro-1 can isolate a subset of MSC progenitors with enhanced proliferative and osteogenic differentiation capacity (167). As discussed earlier, together with CD106 this combination has shown the most promise in identifying the most primitive MSC's to date. However, with long-term culture the expression of these markers is not sustained and further research is required to identify culture conditions that maintain the self-renewal of this population.

MSC's derived from our donors achieved almost thirty population doublings before the onset of growth arrest. The results are similar to other studies that have derived MSC's from aged donors (11;12;91). SA β-Gal was detected in almost 50% of MSC's at passage nine and two studies have reported similar levels of expression (12;68) . In contrast, Wagner *et al* reported that 80% of MSC's expressed SA β-Gal at passage ten and differences in the culture protocols used and interpretation of the assays may explain these differences (40). Similar to the studies by Heo and Wagner *et al*, we did not detect SA β-Gal activity in early

passage MSC's confirming that expression is a late event and questioning the utility of this marker in identifying senescence of MSC's during expansion.

The telomere length of MSC's used in our study was determined as an additional marker of cell ageing and senescence. The mean telomere length of MSC's at passage two was 7.3kB and almost 2-3kB shorter than reported by earlier studies (11;12). The rate of telomere shortening was 64bp per PD (excluding donor 30) which is similar to that reported in these studies (mean 88 and 100bp per PD respectively) and suggests telomere shortening is a characteristic feature of MSC's during expansion. Baxter *et al* also showed that the rate of telomere loss *in vitro* was independent of donor age and estimated that MSC's lost 17bp of telomeric DNA per year *in vivo* (11). The telomere lengths in MSC's at early and late passage are variable and inconsistent amongst some of these studies although donor characteristics, culture protocols and interpretation of the assays may be contributing factors. Telomere dysfunction can also initiate a senescence response and in other cell types, oxidative stress has been shown to significantly increase telomere loss (168). In mesothelial cells, oxidative stress can initiate senescence by damaging non-telomeric DNA and therefore telomere shortening is not a pre-requisite for the intiation of senescence (169). A recent study has confirmed that late passage MSC's show high levels of oxidative stress during expansion and senescence *in vitro* and therefore it appears likely that telomere shortening and dysfunction together contribute to the senescence of MSC's cultured in standard conditions (40;68).

Similar to other reports, we did not detect telomerase activity in MSC's which is required for telomere maintenance during cell division (72;76;81). However, recent evidence has suggested that MSC's may regulate telomerase expression in a cell cycle dependent manner and at levels below the sensitivity of the TRAP assay (78). This could explain our own results and those from earlier studies. Collaborative research from our group has demonstrated that telomerase is actively repressed in MSC's at the chromatin level and can be detected using the TRAP assay if MSC's are exposed to de-methylation agents or histone deacetylase inhibitors (79;80). The role of telomerase in MSC's is of interest because hTERT over expression has been shown to extend the proliferative and differentiation capacity of MSC's (81). In addition to its critical role in senescence and ageing of MSC's, active repression of telomerase may function as a tumour suppressor

and barrier to transformation. MSC's transduced with hTERT show genetic instability and transformation after extended culture periods and generated sarcoma-like tumours in immunodeficient animals (83).

Lastly, we determined the effects of prolonged culture on the typical characteristics of MSC's. In comparison to MSC's at passage two, late passage cells displayed a significant reduction in adipogenic and osteogenic differentiation capacity. In particular, two of the cultures lost the capacity for osteogenic differentiation altogether. There is conflicting results in the literature regarding the effects of prolonged culture on the differentiation ability of MSC's. MSC's derived from young donors appear to maintain osteogenic differentiation (19;37;38) or have increased osteogenic differentiaion capacity at late passage in comparison to early passage cells (40). The study by Muraglia *et al* supports these findings because it was shown that at the clonal level MSC's with adipogenic differentiation capacity were lost earliest during expansion (38). Furthermore, it was shown that MSC's from aged donors contained fewer multi-potent clones suggesting a critical role of donor age on the frequency and properties of MSC's.

Similar to our own results, MSC's from aged donors show a similar decline in adipogenic and osteogenic differentiation capacity at late passage (12;91) while in another study osteogenic differentiation decreased to a much greater extent (71). Therefore, prolonged culture and senescence of MSC's is associated with a reduced capacity for differentiation although the exact restriction in lineage fate appears strongly influenced by the characteristics of the donor. During ageing, the bone marrow is gradually replaced with fat and the capacity for bone formation is reduced. It would be interesting to speculate that MSC's contribute to these pathological changes and research in this area may lead to the development of new treatments for patients with age-related conditions such as osteoporosis.

3.4 Conclusion

The results confirm that MSC's derived from CABG patients meet the minimal criteria proposed by the International Society for Cellular Therapy in 2006 (33). MSC's could be expanded for almost thirty population doublings and achieved

levels of expansion similar to that previously reported. Late passage MSC's showed evidence of cell ageing and displayed a senescent morphology, increased expression of SA ß-Gal and a reduction in telomere length. Furthermore, late passage MSC's showed a decline in adipogenic and osteogenic differentiation capacity confirming loss of their normal stem cell characteristics. Our results support the findings of previous studies which gave us confidence that the transcriptional profiles generated by SAGE could identify genes associated with MSC ageing and senescence *in vitro*.

4 Serial Analysis of Gene Expression Profiles of Mesenchymal Stem Cells

4.1 Introduction

Serial analysis of gene expression (SAGE) is based on three main principles:

1. A short sequence tag (10-27bp) obtained from a defined position within the cDNA is sufficiently unique to identify a transcript.

2. Tags can be formed into long DNA fragments (concatamers), which can be cloned and sequenced to improve efficiency of the transcriptome analysis.

3. The expression level of each transcript is quantified by the number of times a tag is observed within a SAGE library.

We used the long SAGE technique for this research in which the tag length generated is approximately 17bp long, each representing a single mRNA (110). This short nucleotide sequence should, in theory, contain sufficient information to identify the transcript uniquely, providing the tag is from a defined position within the transcript. For example, a 17bp tag should be able to distinguish 17,179,869,184 (4^{17} = 4 possible nucleotides in 17 possible positions) transcripts, assuming that the distribution of nucleotides at the tag site is random. When these tags are concatenated and cloned, each clone insert should contain up to 35 tags joined serially, although in practice the inserts were usually shorter. The boundaries between each tag are recognised by a 4bp nucleotide sequence (CATG) corresponding to the recognition site of the *Nla*III restriction enzyme used during SAGE. The mRNA transcript corresponding to the long SAGE tag is identified using publicly available databases and analysed using described methods (108;109).

Figure 4-1 provides a schematic of how SAGE is put into practice. Double stranded cDNA is synthesized from mRNA captured using magnetic oligo (dT) beads. The cDNA is then cleaved using the anchoring enzyme *Nla*III, which is a restriction endonuclease with a 4bp recognition and cleavage site (CATG). On average, *Nla*III would be expected to cleave every 256bp (4^4 = 4 possible

nucleotides at 4 possible positions). Most mRNA transcripts are considerably longer than this and are therefore cleaved at least once. This process creates a unique site on each mRNA transcript that corresponds to the *Nla*III restriction site which is the most 3' and located closest to the polyA tail.

The cleaved cDNA is then divided in half and ligated via the anchoring restriction site to one of two oligonucleotide adapters containing a recognition site for the tagging enzyme *Mme*I, a type IIS restriction enzyme. The oligonucleotide adapters are designed so that cleavage of the ligation products with *Mme*I releases the adapter plus a short piece of the original cDNA, which is the SAGE tag from the oligo (dT) beads. The two adapter-tag pools are ligated to each other and amplified by PCR using adapter specific primers. As well as amplifying the tag sequences, this process allows orientation of the tag sequences as two tags (ditags) that are linked tail to tail (3' end to 3' end) and flanked by CATG, the recognition site for *Nla*III. It also enables repeated ditags, potentially produced by PCR bias to be identified after sequencing and excluded from the final analysis.

Cleavage of the PCR product with *Nla*III releases the 34bp ditags which are then isolated and concatenated (linked) by ligation. The concatamers are cloned and sequenced and individual sequences analysed using SAGE 2000 software. Interesting tags can be further investigated using bio-informatics software available online. The laboratory work, characteristics of the SAGE libraries generated and the results are now discussed.

4.2 SAGE Method and Data Analysis

4.2.1 SAGE Protocol

Within our research group their was considerable experience of the SAGE technique (123). Since first described, refinement to the protocol and the development of a kit to generate either short or long SAGE libraries has simplified the process. Reagents and buffers are quality controlled and provided ready to use.

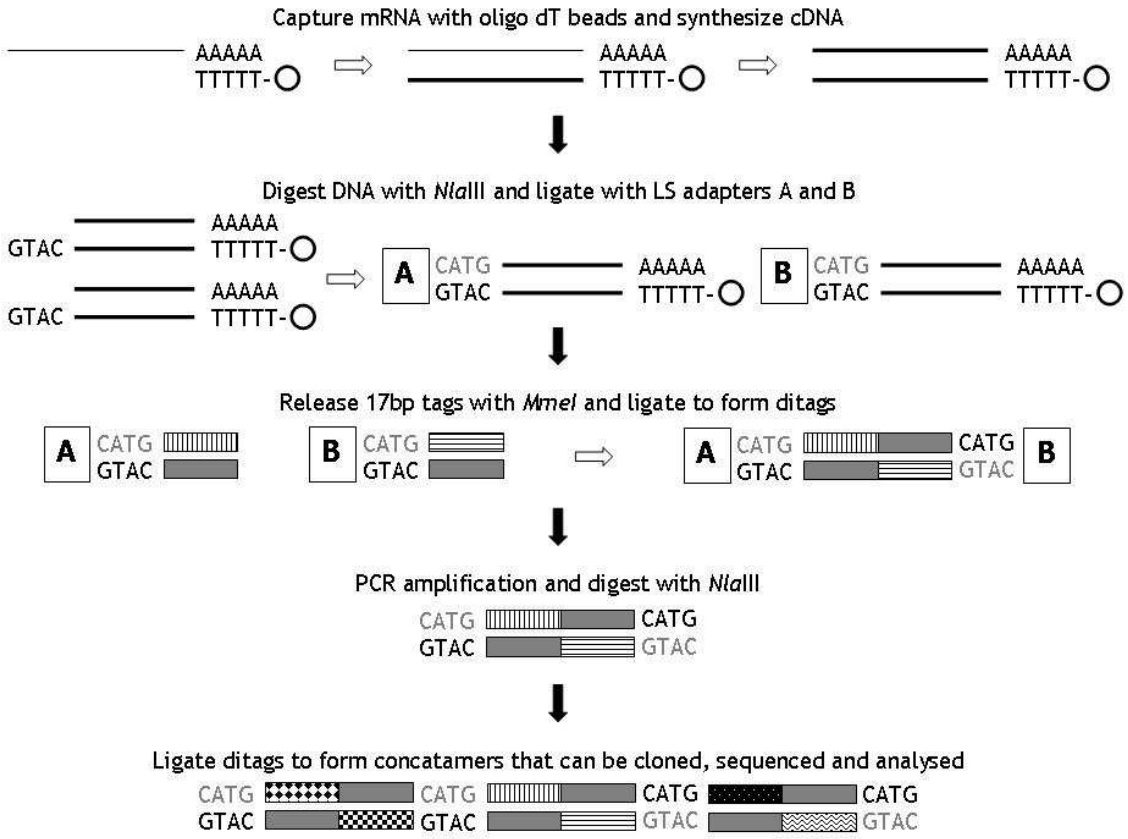

Figure 4-1 Schematic diagram of serial analysis of gene expression (SAGE)

This diagram provides a simplified explanation of the SAGE method.

We were able to generate SAGE libraries (from mRNA to concatamer formation) in ten days with colony PCR and clean up prior to sequencing requiring two weeks. The SAGE libraries were fully sequenced within four months. All sequencing was provided by the Molecular Services Unit, Beatson Institute, Glasgow.

The SAGE method requires sufficient amounts of high quality RNA. We extracted RNA from snap frozen MSC's using TRIzol® reagent as recommended by the manufacturer. For each SAGE library, the amount of total RNA used was 10µg. Within the protocol, a number of steps are recommended to ensure the reaction processes have occurred efficiently. Demonstrating robust cDNA formation, cDNA digestion and linkage of the adapter's usually guaranteed successful generation of the 130bp ditags (Figure 4-2 and Figure 4-3). It was important to use silicon tubes and careful pipette technique in order to prevent loss of the magnetic beads that are the template for subsequent reactions.

The amount of LS adapters A and B recommended by the protocol was sufficient for the generation of the 130bp ditags. Stronger 130bp bands (ditags) than 100bp bands (adapter dimers) were found when analysed by gel electrophoresis (Figure 4-3). If using RNA in amounts out with the recommended range (5-50µg), further optimisation would be required.

It is essential avoid PCR cross contamination of the template with positive and negative controls. PCR reactions were always performed in two hoods in two different locations using fresh reagents, disposable PCR tips and specific pipettes. The PCR optimisation step was always carried out with serial dilution of the template as recommended by the protocol in order to confirm the reactions worked. During scale up PCR, the master mix was calculated based on 600 PCR reactions using the entire template in order to generate large amounts of 130bp ditags. The entire PCR was performed using 28 cycles. During gel purification, smearing of the 130bp ditags and 100bp bands resulted from overloading the wells with DNA (Figure 4-4). In retrospect, it would have been better to use multiple large-format gels to avoid this.

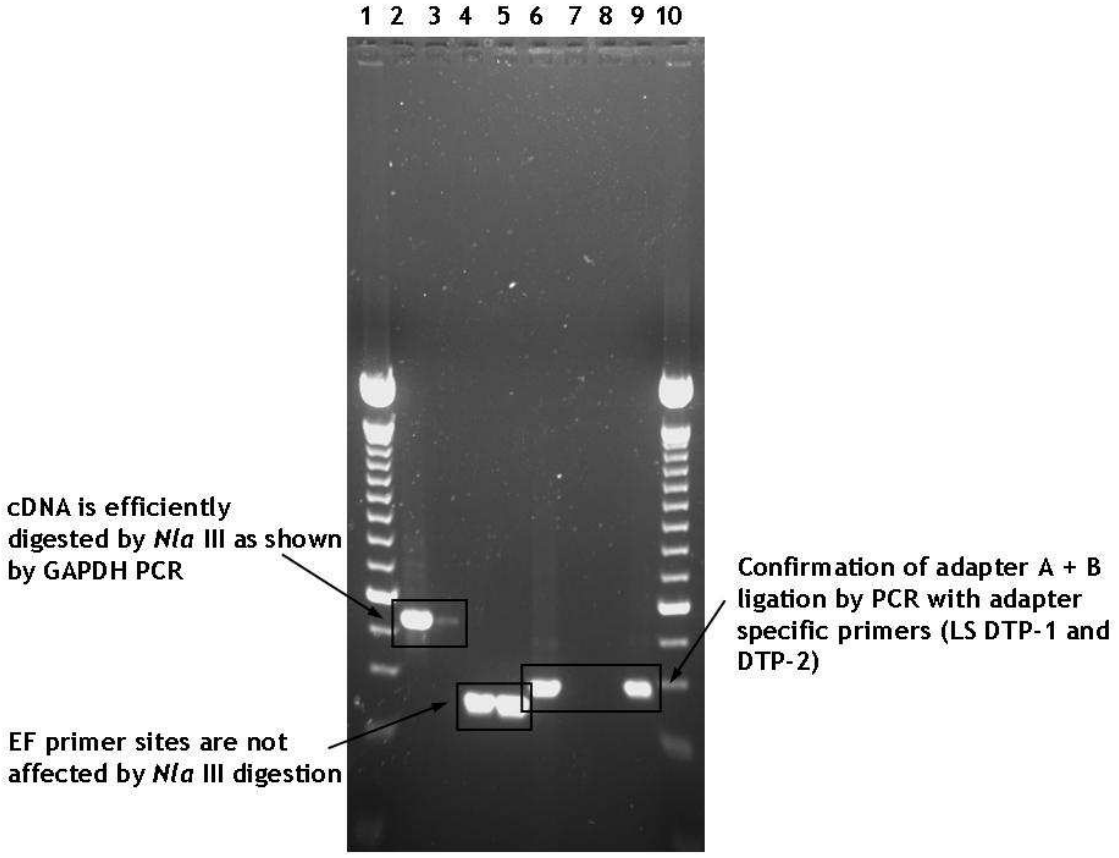

Figure 4-2 Gel electrophoresis of PCR-based verification steps in the SAGE protocol

The long-SAGE™ kit recommends a number of PCR-based verification steps to validate the initial stages in the protocol. cDNA synthesis and efficient digestion by *Nla*III was confirmed by PCR using GAPDH primers (Lanes 2 + 3). Despite *Nla*III digestion, the EF primer sites are maintained (Lanes 4 + 5). Ligation of adapters (A + B) are confirmed by PCR using adapter specific primers (Lanes 6 + 9) and no product is produced using the opposite adapter (lane 7 + 8). 100bp DNA ladders were loaded at the ends of the gel (Lanes 1 + 10).

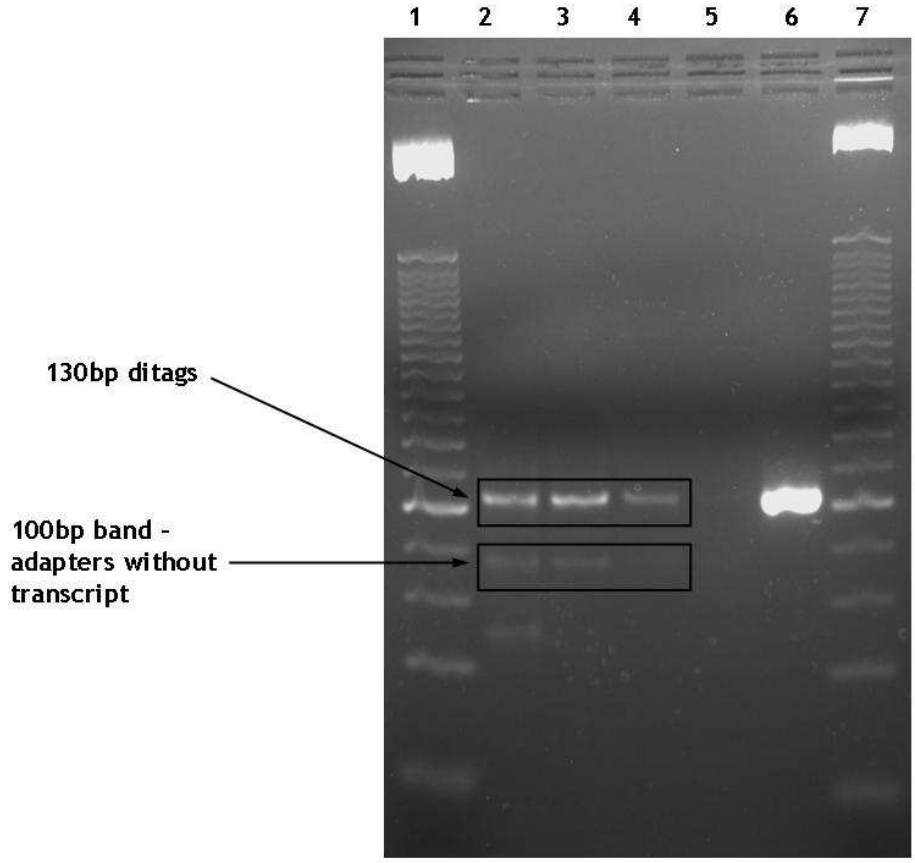

Figure 4-3 Gel electrophoresis of optimisation PCR for generation of 130bp ditags

A serial dilution of the ditag template (1/20, 1/40 and 1/80) for use in an optimisation PCR reaction confirms the presence 130bp ditags and a lower 100bp band of ligated adapters without transcripts (Lanes 2 – 4). Absence of contamination of the PCR reagents and a strong band with the LS control template provided in the kit aid in optimisation of PCR conditions (Lanes 5 + 6). 25bp DNA ladders were loaded at either end of the gel (Lanes 1 + 7).

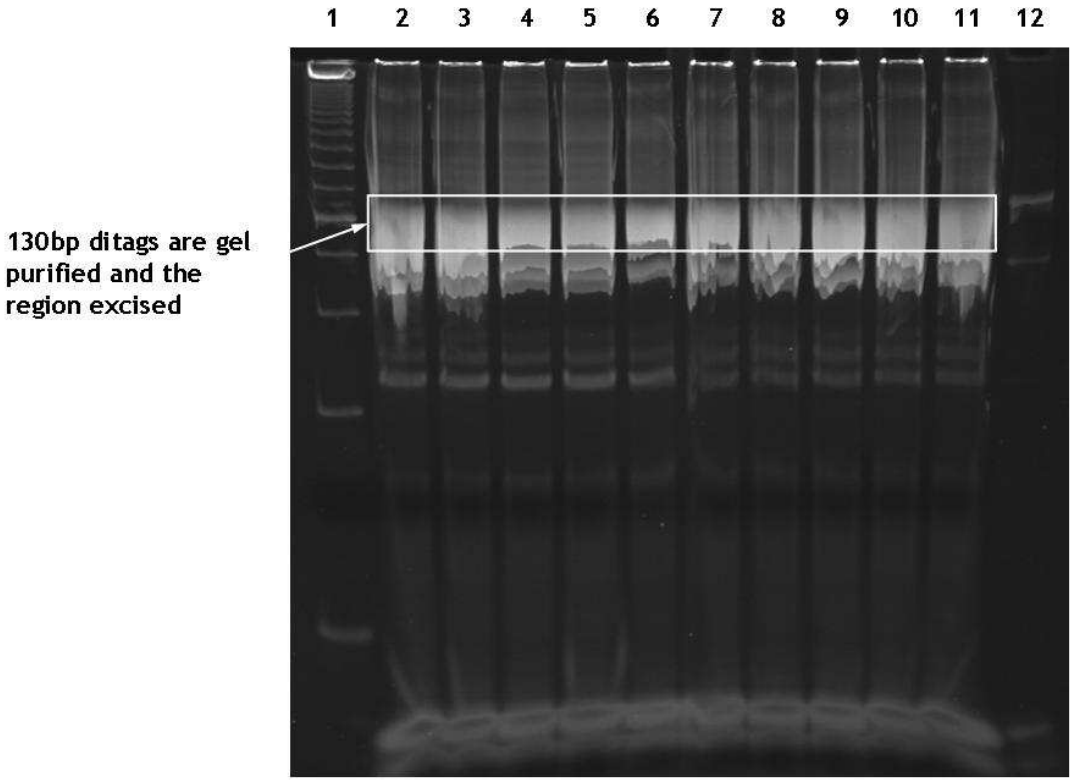

Figure 4-4 Gel purification of 130bp ditags

The 130bp ditags from 600 scale-up PCR reactions were purified by electrophoresis of the precipitated DNA on a large format 12% polyacrylamide gel (Lanes 2-12). The large amount of DNA loaded in each well resulted in poor separation of the 130bp (ditags) and 100bp (adapters without transcript) bands. The 130bp region was excised as shown, the DNA recovered from the gel and used for the remaining SAGE protocol. Lower molecular weight species including primers can be seen further down the gel. A 25bp DNA ladder is shown (Lane 1).

In fact, cutting out the approximate 130bp region from the gel did not appear to cause any problems in downstream reactions. The 130bp ditags were shown to be efficiently digested using *Nla*III releasing the 34bp ditags (Figure 4-5). It was important to the 34bp ditags on ice because they can degrade at higher temperatures. The 34bp ditags were isolated and the incomplete digestion products and excess adapters removed by further gel purification (Figure 4-6).

For the generation of concatamers, the ligation reaction was performed for 3 hours. After gel separation, the 300bp to 1.2kB region was excised using the molecular markers as guides and the region divided roughly into three before elution of the DNA (Figure 4-7). The pZERO®-1 vector was linearised by a 30 minute digestion with *Sph*I before ligation with each concatamer region. It is important not to over digest the vector as this could disrupt the LacZα-ccdB lethal gene and result in a large number of transformants that do not contain inserts. Large concatamers (>900bp) were found to clone less efficiently than shorter ones (400-600bp) and a good example of gel electrophoresis of colony PCR's is shown in Figure 4-8. Altering the concatamer: vector ratio or alternatively, a brief digestion of the concatamer with *Nla*III has been shown to improve cloning efficiency (170).

4.2.2 SAGE Data Analysis

After sequencing, the concatamer sequence files were analysed using SAGE 2000 software, version 4.5. A project file is generated and the following parameters specified: anchoring enzyme is *Nla*III, with its CATG recognition site; the tag length is set to 17bp; and the maximum ditag length, over which any ditags are excluded from the analysis, is set to 36bp. The SAGE software then builds a database of all possible tags (4^{17}) in order to perform the analysis of each individual sequence (Figure 4-9). Thereafter, the sequence files are added and used to form a SAGE report: this includes number of sequences loaded; number of duplicate ditags which are usually excluded from any further analysis; and the list of tags and their absolute count. The report can then be analysed by comparison with a downloadable reference sequence database such as SAGE map or on-line using SAGE Genie.

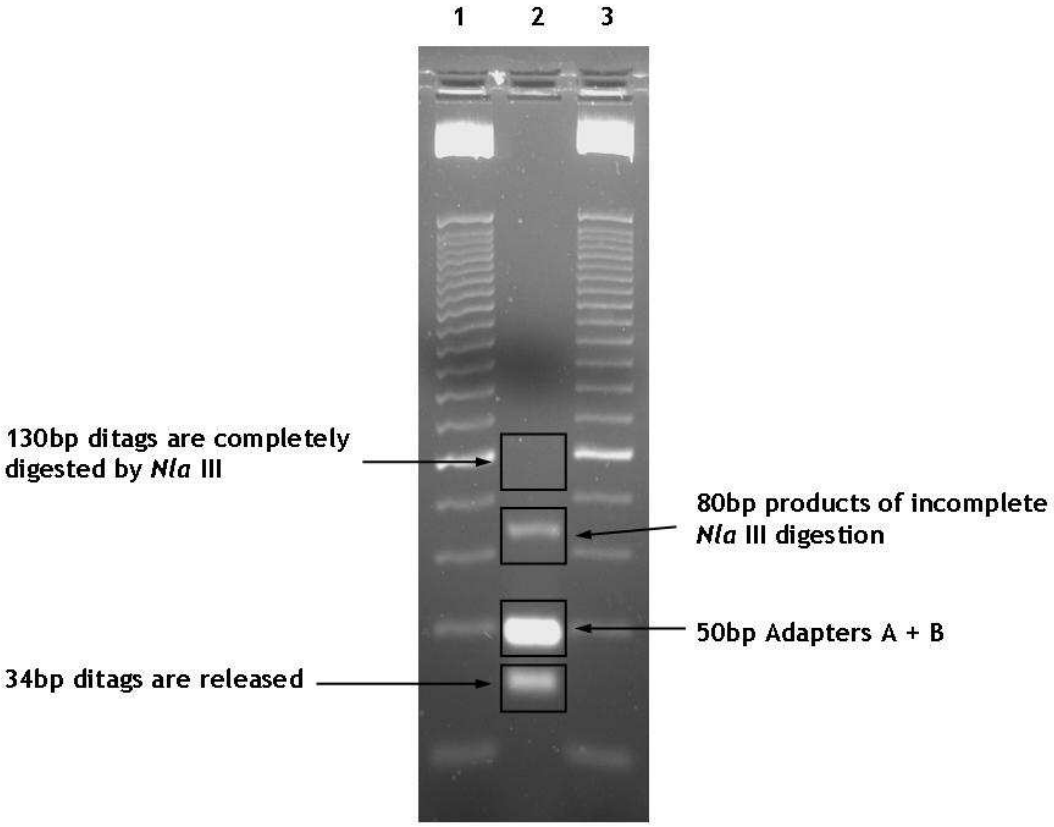

Figure 4-5 Gel electrophoresis confirmed efficient digestion of the 130bp ditags

The complete absence of a 130bp ditag band and generation of 34bp ditags confirmed efficient digestion by the anchoring enzyme *Nla*III (Lane 2). The large 50bp band of released adapters occurred as a result of poor gel purification of the 130bp ditag as shown in the previous image. 25bp DNA ladders are shown either side (Lanes 1+3).

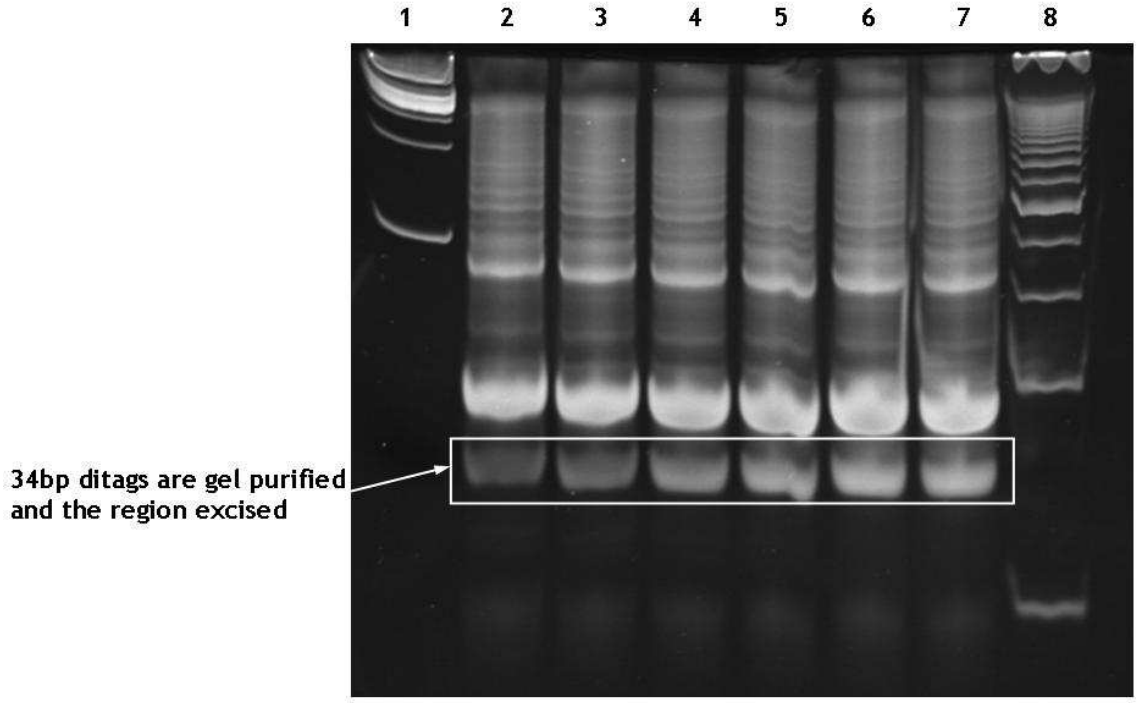

Figure 4-6 Gel purification of the 34bp ditags

The 34bp ditags released by *Nla*III were purified on an 8% polyacrylamide gel and the bands excised to recover the DNA. The adapters and partially and completely undigested larger species are shown in the upper region of the gel. 100bp and 25bp DNA ladders are shown at either end of the gel (Lanes 1+8).

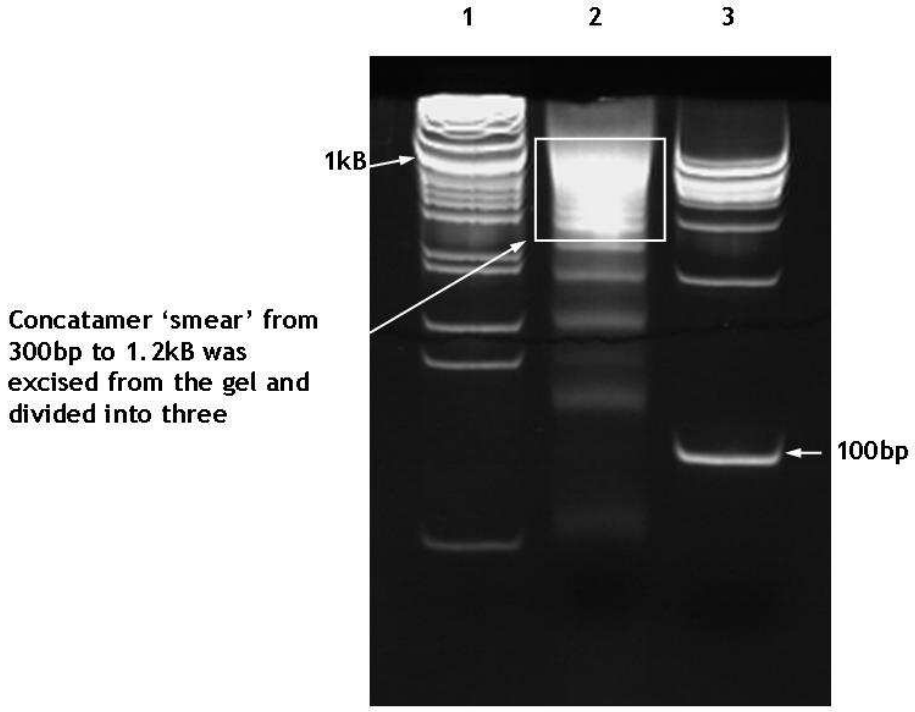

Figure 4-7 Gel electrophoresis confirmed generation of concatamers

The 34bp ditags are ligated to produce long concatamers that are then separated using an 8% polyacrylamide gel (Lane 2). 1kb and 100bp DNA ladders were used to visualise the 300bp to 1.2kB region which was excised and purified for subsequent cloning (Lanes 1+3).

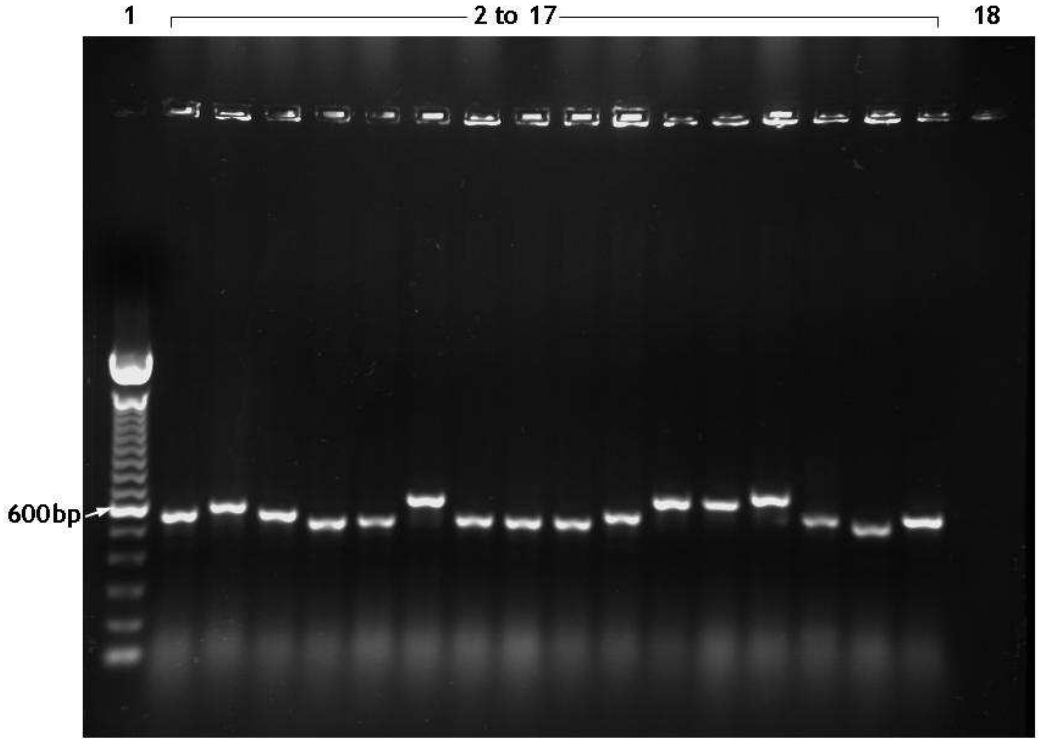

Figure 4-8 Gel electrophoresis of colony PCR from cloned concatamers

Single bacterial colonies containing the cloned concatamers are picked and subjected to PCR amplification with primers specific to the vector on either side of the polylinker. The products were separated by electrophoresis on a 1% agarose gel as shown (Lanes 2 -17). The aim was to achieve PCR products of >500bp as these should contain at least 16-17 tags (around 200bp flanking vector plus 17bp per tag). Although not displayed on this gel, some colonies lacked inserts or contained short concatamers which were not purified for sequencing. A 100bp DNA ladder and negative control (no template) are shown (Lanes 1+18).

NNCCTCTAGATG**CATG**TTCATACACCTATCCCCAATACTTATAAAGTACN 50
NNNNNCGGCTGGCCAAGACTTAATACTGCCAGTCA**CATG**CCTCAGGATAC 100
TCCTCAAGAACTCAGCTCCTTA**CATG**GAAAAATGGTTGATGGATACCCAG 150
ATTTGATAA**CATG**TATTGAAATACATATTGGGGTTTATGCCCAATC**CATG** 200
TTTCCAATCTCTCTCTCCTTTATTTAATCCTCCC**CATG**CCTATTTACTGG 250
AAACCTGGAGAACATAAAGGGC**CATG**GATTGCTGGAGGTCTTTTATACAG 300
TCTTTGAAC**CATG**GGTGGCACTCAGTCTCTCAAAAAGGCCAAATCC**CATG** 350
GGCTTTGATTTTTTTCACTTTTGGTTTTTGGT**CATG**ATGGCGCCTCCTGC 400
CCGGTACTTTATTGATGGTA**CATG**CTCACCTAAGCCACAGGGCCTCTGTC 450
CTGGCTT**CATG**GCCCGCAGGGTCAAGGGGTTTTAGGGACGTTAAC**CATG**G 500
AAGCAGGACCAGTAAGGGGATAGGTGTATGAA**CATG**GTGTGTTTGTAATA 550
ATAAAAGTAGCTAATACTCA**CATG**GGGCTGGGGTCCTCCTGTGGCTCTCT 600
CCCTGGGA**CATG**ATCCGTGCCCTTGCTTCTGGGAGGGGGGTTGAG**CATG**G 650
GCTTTACCCTTCCCTGCGATGGACGTGTTCCT**CATG**TTANNNNCNGTCTC 700
TCANATCTAGTTTAGAAAA**CATG**CTCGAGCGGCCGCCAGTGTGATGGATA 750
TCTGCAGAATTCCAGCACACTGGCGGCCGNTACTAGTGGATCCGAGCTCG 800
GTACCAAGCTTGATGCATAGCTTGAGTATTCTATAGTGTCACCTAAATAG 850
CTTN 854

Figure 4-9 Sequence of cloned concatamer containing ditags separated by CATG's

This is an example of sequencing of the insert sequence. The insert is delineated by the first and last CATG sites. When this sequence is put into the SAGE program, the ditags are identified, extracted and split into tags (simply by dividing the ditags down the middle). A catalogue of all tags is then assembled.

During this research, the SAGE map reference database underwent a prolonged up-date which was not completed until the end of September 2007. Therefore, SAGE Genie, developed by the Cancer Genome Anatomy Project (CGAP) was used instead (109). The SAGE data is uploaded as a tab de-limited text file and the analysis performed online using the Digital Gene Expression Display (DGED). One advantage of this method is that the reference databases include single nucleotide polymorphism (SNP's) associated alternative tags (171).

4.2.3 Assessment of SAGE Library Quality

By calculating the number of tags generated per clone and the number of clones per µl of ligation reaction, the total number of tags for each SAGE library can be estimated if all the ligation reaction were transformed. The estimated total library sizes were more than 100,000 tags which was the recommended minimum in the protocol. Most SAGE users generate libraries of over 40,000 tags with each sequenced clone producing between 25 and 30 tags. We could never achieve this degree of efficiency and between 12 and 19 tags were generated per concatamer and each library required the sequencing of more than 2400 clones (Table 4). Rather than attempt optimisation of the whole process in order to improve efficiency we chose to perform additional colony PCR.

The number of duplicate ditags that occurred (<5%) in the three SAGE libraries was similar to the findings of large scale SAGE datasets (172). Duplicate ditags were originally thought to arise from PCR artefact and as a result it was common practice to exclude them from analysis (173;174). However, a recent analysis of 298 SAGE libraries by Kahttra *et al* demonstrated that duplicate ditags occur more frequently in long SAGE libraries that contain a small number of high abundance tags (172). Other researchers have shown that removal of duplicate ditags can introduce error so it has been suggested to analyse the duplicate ditag population (174;175). For the purposes of this research the duplicate ditags were excluded from further analysis.

	12 MSC P2	25 MSC P2	25 MSC P9
Total Tag Count	40736	40580	42674
No. of sequenced concatamers	3419	3242	2304
Tags per sequence	11.9	12.5	18.5
Number of Unique Tags	20828	23059	21581
Duplicate Ditags (%)	1190 (2.9%)	724 (1.8%)	1917 (4.5%)

Table 4 Characteristics of the three SAGE libraries

4.2.4 Problems with Tag to Gene Assignment

Investigation of individual SAGE tags is relatively straight forward where a tag matches a single gene but is much more difficult if multiple or no matches exist. It has been demonstrated that up to two thirds of unique SAGE tags do not match the reference databases, limiting the information obtained by SAGE (118). Of the unmatched tags up to two thirds are estimated to be truly novel and the remaining third occur as a result of either alternative splicing, alternative polyadenylation, SNP's and sequence error.

Alternative splicing increases the complexity of the human transcriptome and may occur in up to two thirds of human transcripts (176). Investigation of unmatched tags can be addressed by RT-PCR using the SAGE tag as a primer in order to generate longer 3' cDNA fragments that can be sequenced and analysed on-line (177). Alternatively, software tools such as SAGE2Splice have been shown to map up to 6% of unmatched SAGE tags to potential splice junctions within the genome (178).

The use of alternative polyadenylation cleavage sites downstream of a polyadenylation signal may lead to more than one SAGE tag from what is in essence a single mRNA species. One study calculated that this may affect 2.8% of human transcripts (179). SNP's create similar difficulties with tag to gene assignment as they can affect up to 9% of known human transcripts. To enhance tag to gene assignment, databases such as SAGE Genie incorporate SNP prediction algorithms in order to improve tag mapping (171). Sequence error is usually estimated to be in the range of 0.2-1.0% per base and therefore up to 17% of tags in long SAGE libraries could have arisen due to error. Erroneous tags have also been shown to occur more frequently with modifications of the SAGE technique that incorporate additional PCR steps (114). The use of Phred scores or discarding ambiguous sequences using specific software tools can remove much of this error prior to data analysis (180-182). In fact, Chen *et al* demonstrated that tags that arise due to sequence error are in fact less frequent than one would expect and account for less that 2% of the total tags in a SAGE library. Most of the errors are single base substitutions with two or more base substitutions being extremely rare (118).

Tags match sequences derived from mRNA much more reliably than those from EST's due to the nature of the SAGE technique. In order to check the tag to gene matches using either SAGE map or SAGE Genie, we manually checked a number of original mRNA/cDNA sequences for a specific gene, usually via the UniGene or SAGE Genie database. The last (3' most) CATG tetranucleotide was identified and the immediately adjacent, downstream, SAGE tag was confirmed. To ensure the CATG site is truly the most 3' requires the mRNA/cDNA sequence contains a polyadenylation site (AAU/TAAA) downstream. The UniGene or SAGE Genie databases contain a wealth of other information on each gene, such as mRNA expression, chromosomal location and so on.

4.2.5 Statistical Methods for Comparing SAGE Libraries

Over the years, a number of computational tools and statistical methods have been developed to correctly perform the analysis of SAGE experiments. Because SAGE determines absolute expression levels, comparisons between individual libraries are relatively easy to perform. Five commonly used statistical methods for the analysis of SAGE data include the Madden test, Audic and Claverie test, SAGE300, Z-test and Fisher's Exact test (102;183-186). A direct comparison of these methods in the evaluation of SAGE data has been published (187). The authors have shown the Madden test can only be used reliably on libraries of equal size and tends to be more conservative due to the measure of variance in the statistical method. The other methods give essentially the same result for libraries of equal or different sizes and the Z-test has the advantage that it can be used for the analysis of more than two libraries.

SAGE Genie performs comparisons of SAGE data using the Fishers Exact test. As an alternative, I used SAGE Stat software that uses the Z-test for comparison and is available for download upon request (185). When comparing the SAGE libraries of donor 25 at passage two and nine using either method the number of differentially expressed tags was 332 and 317 tags respectively (with p value set to <0.05). Tags not present in one library are assigned an arbitrary value of 1 rather than 0 using SAGE Stat, which would account for the observed difference in number of differentially expressed tags. SAGE Stat is useful not only for the testing of SAGE data but also in experimental design of SAGE experiments. Statistical inferences can be calculated based on fold differences for a given tag,

effects of p value, power of a test as well as estimation of subsequent SAGE library size. The two examples generated from my own data are shown. Figure 4-10A demonstrates that low abundance tags require large differences in expression to reach significance if the SAGE libraries are of similar size. Secondly, if the abundance of a specific tag is known in one library the size of the subsequent SAGE library generated (for a set p value and power) can be calculated if one was looking to detect a specific enrichment of that tag (Figure 4-10B).

4.3 SAGE Profiles of Mesenchymal Stem Cells

Having described how the SAGE method was performed and methods to analyse the data, the large-scale mRNA profiles of MSC's in short-term (passage 2 – P2) and long-term culture (Passage 9 – P9) are now discussed.

4.3.1 Generation of MSC Long SAGE Libraries

Three SAGE libraries were created from two patients – donor 12 and 25. The first SAGE library generated was from donor 12 MSC's at passage 2 (12 MSC P2) – the time point was chosen as most researchers characterise MSC's at this culture point. The original plan was to generate a further library at late passage and even during differentiation to a specific lineage. However, due to loss of patient material when a cryostorage unit failed further MSC's cultures had to be generated.

Donor 25 demonstrated normal proliferative characteristics and was used to generate SAGE libraries at passage two and nine (25 MSC P2 and P9). Due to time constraints it was not possible to generate a further SAGE library on differentiated MSC's as initially planned. After excluding the tags from duplicate ditags and the adapter sequences, a total of 123,990 tags were derived from 38,126 unique tags. The libraries from 12 MSC P2, 25 MSC P2 and 25 MSC P9 contained 40,736, 40,580 and 42,674 tags respectively (Table 4).

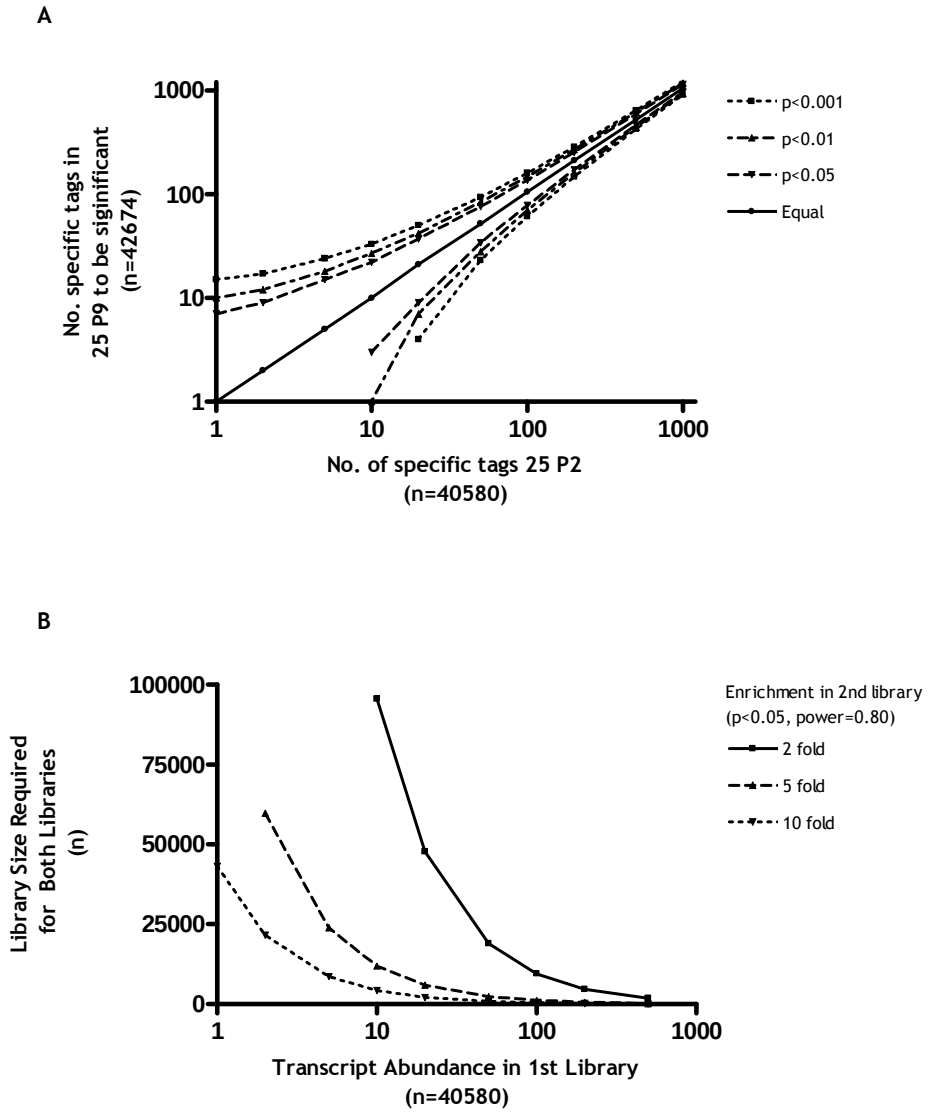

Figure 4-10 Statistical inferences from SAGE data

Using SAGE Stat software, a matrix of critical values can be generated based on the size of the SAGE libraries (A). This demonstrates the difference in tag counts required to reach significance depending on the relative abundance of a specific tag. SAGE can detect small differences in high abundance tags and large differences in low abundance tags based on set statistical thresholds. If the abundance of a specific tag in a SAGE library is known the required size of a subsequent library to detect a specific fold difference in expression (for given power and p-value) can be calculated (B).

4.3.2 Analysis of MSC SAGE Libraries

The distribution of the unique tags and their abundance for each of the SAGE libraries is shown in Figure 4-11. In the three SAGE libraries, an average of 16,997 (78%) unique tags occurred only once and 18 (0.08%) tags occurred more than 100 times in each library. Of the unique tags, 30% reliably matched a specific gene (UniGene), 7% a single deposited sequence (accession number) and the remainder were unmatched.

2,960 unique tags were identified in the three SAGE libraries that accounted for 57,003 of the total tags. Of these, 77% matched a specific gene which confirms that high abundance tags are usually matched to known genes. The twenty most abundant tags with their respective counts and abundance are shown in Table 5. The most abundant tag, TTCATACACCTATCCCC, occurred 866 times (0.7%) in all three libraries and was shown to be significantly increased in MSC's after long-term culture. An online search using SAGE Genie anatomic viewer revealed that this tag occurs frequently (4,161,709 times in all online long SAGE libraries) and is highly expressed in a variety of normal and cancer tissues. This tag can be matched to a single deposited sequence generated from human mitochondrial DNA. The data was part of a larger study investigating the diversity of the human mitochondrial genome (188). The tags TGATTTCACTTCCACTC and CACCTAATTGGAAGCGC were also differentially expressed and matched other sequences deposited in the same mitochondrial database. Tags that matched known genes were found to be highly expressed in other profiling studies on MSC's and will be discussed later.

4.3.3 Comparison of MSC's and Online SAGE Libraries

The SAGE library of donor 25 MSC P2 was compared digitally to all publicly available long SAGE libraries using SAGE Genie (110 libraries containing a total of 177,118,916 tags were available for comparison and were derived from a variety of cell lines, normal tissues and tumour samples). For this comparison, a difference in tag ratio (Z) of five fold and a p-value of 0.001 or less was used. 144 tags that were found to be over-expressed in MSC's, included genes such as transgelin (TAGLN), fibronectin 1 (FN1) and myosin light polypeptide 9 (MYL9).

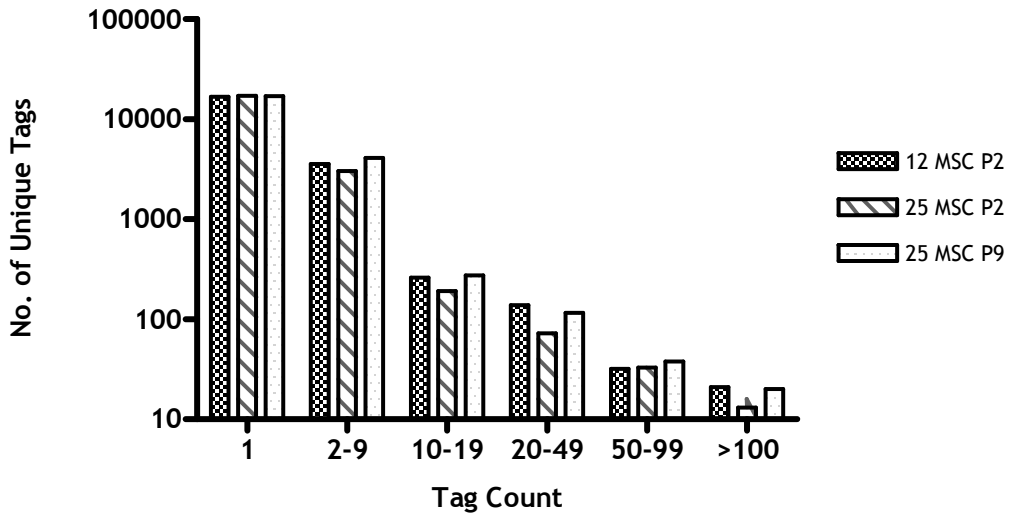

Figure 4-11 Distribution of unique tags and tag frequency in the three SAGE Libraries

Bars represent the number of unique tags in each MSC SAGE library.

Long Tag	UniGene ID	Symbol	Description	Chromosome Location	Tags in 25P2	Tags in 25P9	Tags in 12P2	Total Tags	Abundance (%)
TTCATACACCTATCCCC			Predicted to be a mitochondrial gene		218	500	148	866	0.70
ACCAAAAACCAAAAGTG	Hs.645250	COL1A1	Collagen, type I, alpha 1	17q21.33	289	177	138	604	0.49
ACAGGCTACGGACGACC	Hs.632099	TAGLN	Transgelin	11q23.2	160	159	224	543	0.44
TGTGTTGAGAGCTTCTC	Hs.644639	EEF1A1	Eukaryotic translation elongation factor 1 alpha 1	6q14.1	145	157	241	543	0.44
GCCCCCAATAAAGGCAG	Hs.445351	LGALS1	Lectin, galactoside-binding, soluble, 1 (galectin 1)	22q13.1	166	199	177	542	0.44
GAAGCAGGACCAGTAAG	Hs.170622	CFL1	Cofilin 1 (non-muscle)	11q13	137	188	129	454	0.37
TGATTTCACTTCCACTC			Predicted to be a mitochondrial gene		74	240	120	434	0.35
CTAGCCTCACGAAACTG	Hs.514581	ACTG1	Actin, gamma 1	17q25	100	150	164	414	0.33
TACCATCAATAAAGTAC	Hs.544577	GAPDH	Glyceraldehyde-3-phosphate dehydrogenase	12p13	125	207	76	408	0.33
GCTTTATTTGTTTTTTT	Hs.520640	ACTB	Actin, beta	7p15-p12	189	179	13	381	0.31
TTGGTCCTCTGCCCTGG	Hs.632703	RPL41	Ribosomal protein L41	12q13	114	107	158	379	0.31
ATGTGAAGAGTTTCACA	Hs.111779	SPARC	Secreted protein, acidic, cysteine-rich (osteonectin)	5q31.3-q32	226	76	72	374	0.30
TCCAAATCGATGTGGAT	Hs.642813	VIM	Vimentin	10p13	73	166	131	370	0.30
GGGGAAATCGCCAGCTT	Hs.446574	TMSB10	Thymosin, beta 10	2p11.2	72	106	183	361	0.29
TTGGGGTTTCCTTTACC	Hs.524910	FTH1	Ferritin, heavy polypeptide 1	11q13	103	147	110	360	0.29
TTTGCACCTTTCTAGTT	Hs.591346	CTGF	Connective tissue growth factor	6q23.1	141	89	101	331	0.27
GGAGTGTGCTCAGGAGT	Hs.504687	MYL9	Myosin, light polypeptide 9, regulatory	20q11.23	118	104	108	330	0.27
CACCTAATTGGAAGCGC			Predicted to be mitochondrial gene		79	124	121	324	0.26
CTTCCAGCTAACAGGTC	Hs.511605	ANXA2	Annexin A2	15q21-q22	61	137	123	321	0.26
GTGCTGAATGGCTGAGG	Hs.632717	MYL6	Myosin, light polypeptide 6, alkali, smooth muscle and non-muscle	12q13.2	78	88	138	304	0.25

Table 5 Twenty most abundant tags identified in the three MSC SAGE libraries

These genes were highly expressed in all three SAGE libraries. Five tags (GGCCGCACCATAATGAG, CACAAGGCTCACATCTC, ACCCAAAAACCAAAAGT, TTAAAATAGCACCTTTA and ATGTGAANAGTTTCACA) were identified that were only present in MSC's.

A separate comparison was performed using the same statistical thresholds against SAGE libraries derived from haematopoietic stem cells (1), embryonic stem cells (11), monocyte depleted mono-nuclear cells (2), rhabdomyosarcoma (1) and breast tissue stroma (1). The numbers of differentially expressed tags were 466, 317, 326, 260 and 226 respectively demonstrating that MSC's share more transcriptional similarity to tissues of mesenchymal origin.

4.3.4 Comparison of Early and Late Passage MSC SAGE Libraries

The effect of alteration of p-value (P) on the number of differentially expressed tags between our SAGE libraries when a difference in level of expression of a tag (Z) is more or less than one is shown in Figure 4-12A. The biggest difference in the number of differentially expressed tags was in the comparison of 12 MSC P2 and 25 MSC P2. Figure 4-12B demonstrates that the numbers of differentially expressed tags were similar to other publicly available SAGE comparisons. As with our data, the number of differentially expressed tags is greatest when comparing tissues of different origins rather than a cell line under different experimental conditions.

The direct comparison of 25 MSC P2 and P9 was the focus of most of our results in order to minimise donor and experimental differences. When Z is more or less than 1 and the p-value set to 0.05, 0.01 and 0.001 the numbers of differentially expressed tags were 332, 132 and 64 respectively. Of the 332 differentially expressed tags, 234 (70%) tags matched a specific UniGene, 43 (13%) tags matched a single accession number only and 23 (7%) tags were unknown. 218 (66%) differentially expressed tags were over-expressed at passage nine and the remaining 114 (34%) tags under-expressed. The known chromosomal locations of 258 tags were identified and shown in Figure 4-13. Chromosomes two, one, eleven and nineteen contained the most differentially expressed tags respectively.

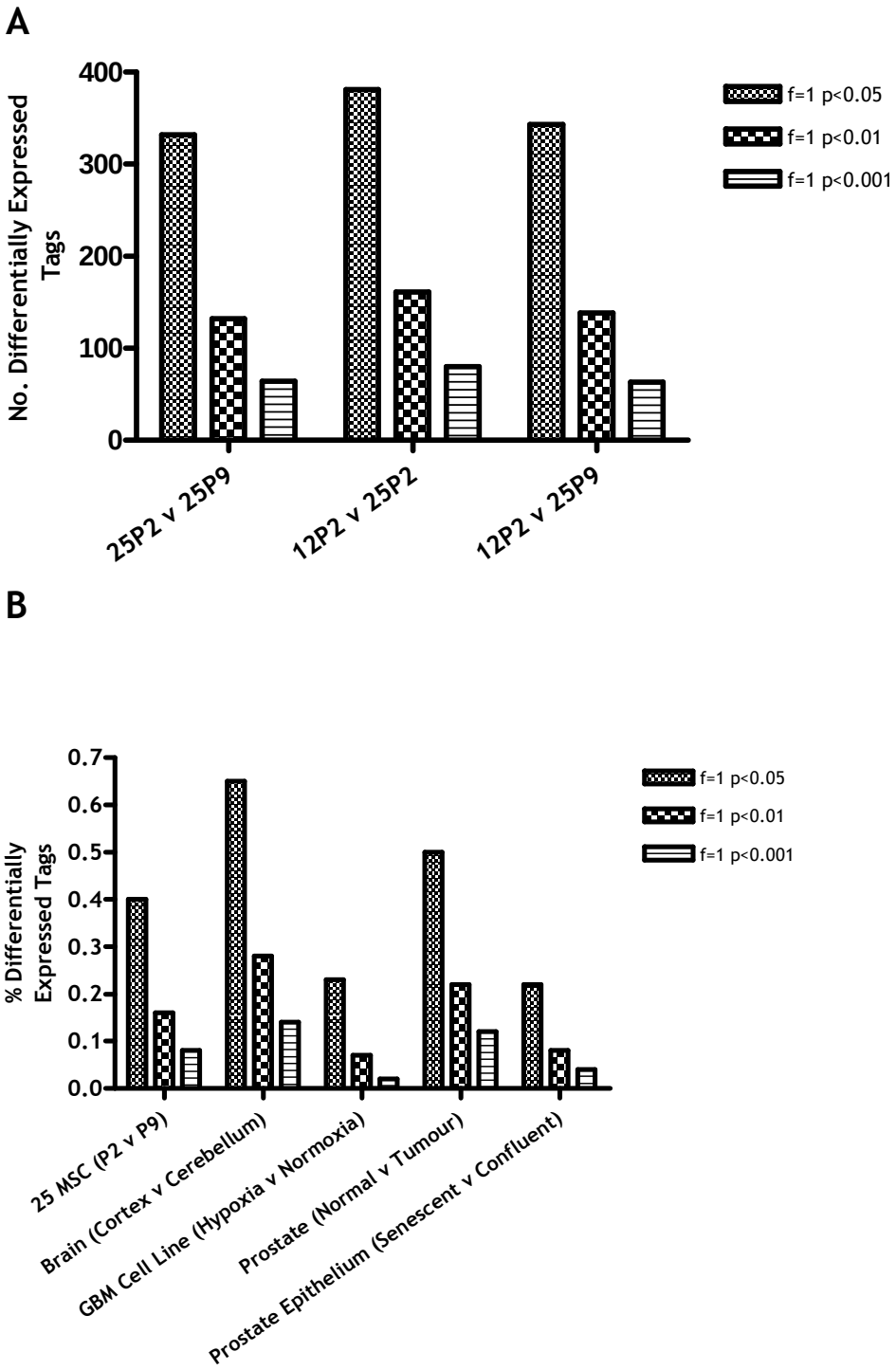

Figure 4-12 Pattern of differentially expressed tags in the MSC SAGE libraries matched online SAGE comparisons

The numbers of differentially expressed tags in the three comparisons were determined using SAGE Genie for different p values (A). The overall percentage of differentially expressed tags was determined from published comparisons available via the SAGE Genie website (B).

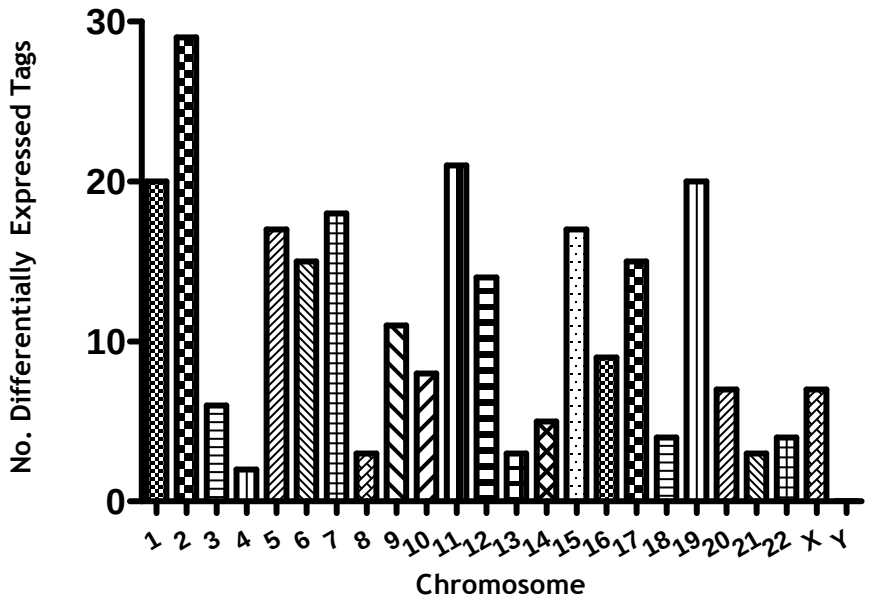

Figure 4-13 Chromosomal location of differentially expressed tags in MSC's at late passage

The known chromosomal locations of 243 differentially expressed tags in the comparison of 25 MSC P2 and P9 are shown. Bars represent the number of tags that matched an individual chromosome.

Fifteen genes were identified that matched forty seven differentially expressed tags demonstrating that within SAGE, multiple tags exist for some transcripts. Most of these tags matched genes that encode for cytoskeletal proteins that were highly abundant in the three MSC libraries. For example, collagen type I, alpha 1 (COL1A1) matched seven differentially expressed tags (ACCAAAAACCAAAAGTG, GACCAGCAGACTGGCAA, TGGAAATGACCCAAACA, CCGGGGGAGCCACCAGC, GACTTTGGAAAATATTT, GGCCCCCCTGGATTGGC and GGAGGAGAGCGTGTGCG).

In the comparison of 12 MSC P2 and 25 MSC P9, 111 (33%) differentially expressed tags were identified that were also found in the comparison of 25 MSC P2 and P9. 100 (90%) of the tags showed changes in expression in the same direction. In the comparison of 12 MSC P2 and 25 MSC P2, 82 (25%) differentially expressed tags were identified that were found in the comparison of 25 MSC P2 and P9. All of these tags showed changes in expression in the same direction. The significance of these findings is that in addition to identifying genes altered with prolonged expansion of MSC's, it would appear that differences are detectable between donor cultures as early as the second passage.

4.3.5 Investigation of Differentially Expressed SAGE Tags

Differentially expressed tags (Z more or less than 5 and $p<0.001$) in the comparison of 25 MSC P2 and 25 MSC P9 were analysed and twenty of the most over and under expressed tags shown in Table 6 and Table 7. The genes marked in italics were those found in the comparison of 12 MSC P2 and 25 MSC P9. Most of the over-expressed tags at passage nine had very low counts at passage two and matched known genes. These included transcription factors, genes involved in oxido-reductase activity and proteolysis. Conversely, the under-expressed tags were either unknown or matched genes highly abundant in the three libraries.

4.3.6 Analysis of Differentially Expressed Tags using MetaCore™

The differentially expressed tags from the comparison of 25 MSC P2 and P9 ($Z <> 1$ and $p < 0.05$) were analysed digitally using MetaCore™ systems biology software.

Long Tag	UniGene ID	Symbol	Description	Tags in 25 P2	Tags in 25 P9	Fold change	P value
ATTGGAGATGTCCTTTG			*Unknown*	1	18	18.56	0
ATTTGTCCCAGCCTGGG	Hs.518805	HMGA1	*High mobility group AT-hook 1*	2	33	17.01	0
AAAAAGCAGATGACTTG	Hs.443914	SOD1	Superoxide dismutase 1	1	16	16.50	0
GGTTATTTTGGAGTGTA	Hs.414795	SERPINE1	*Serpin peptidase inhibitor, clade E*	3	44	15.12	0
TACTTTATAAGTATTGG	Hs.643357	ADAMTS1	*ADAM metallopeptidase with thrombospondin type 1 motif, 1*	2	28	14.44	0
AGGTCTGCCAGAAGGCC	Hs.567256	AKR1C2	*Aldo-keto reductase family1, member C2*	1	14	14.44	0
AACAAAGATATATTTTC	Hs.459088	KIAA1199	*KIAA1199 (transmembrane protein 2-like)*	1	14	14.44	0
CAAATGCTGTATTCTTC	Hs.655132	STAT1	Signal transducer and activator 1	1	14	14.44	0
GCCCGCAGGGTCAAGGG	Hs.74375	DVL1	*Dishevelled 1*	1	13	13.40	0
GGCCATCTCTTCCTCAG	Hs.74405	YWHAQ	Tyrosine 3-monooxygenase/tryptophan 5-monooxygenase activation protein, theta polypeptide	1	13	13.40	0
GCCGTGGAGAGCACCGG	Hs.632177	MVP	Major vault protein	1	12	12.37	0
CAAAACTGTTTGTTGGC	Hs.481720	MYO10	*Myosin X*	1	11	11.34	0
AATAGGGTCAAAGGGGA	Hs.370247	APLP2	*Amyloid like precursor protein 2*	2	18	9.28	0
GATCCCAACATTGTTGG	Hs.406510	ATP5B	*ATP synthase, H+ transporting, mitochondrial F1 complex, beta polypeptide*	3	27	9.28	0
GGGTTTTTATTATTTTT	Hs.473583	YBX1	Y box binding protein 1	2	16	8.25	0
ACCCTTGGCCATAATAT	Hs.631495	Hs.631495	*Transcribed locus, strongly similar to NADH dehydrogenase subunit 1*	4	32	8.25	0
TCTGCAAATTAGGAGGG	Hs.193491	TUBB6	Tubulin, beta 6	3	24	8.25	0
TTCTTATTTTAGGAGAG	Hs.25338	PRSS23	*Protease, serine, 23*	4	30	7.73	0
ACTAACACCCTTAATTC		CF454031	*Predicted to be a mitochondrial gene*	7	52	7.66	0
GCGCTGGAGTGAGATGG	Hs.110695	SF3B5	*Splicing factor 3b, subunit 5, 10kDa*	3	21	7.22	0

Table 6 Twenty most over-expressed tags in MSC's at late passage

Long Tag	UniGene ID	Symbol	Description	Tags in 25 P2	Tags in 25 P9	Fold Change	P value
TCTTTGCCTTCAAAGAG		BQ292225	Unknown	20	1	-19.40	0
TTCCAGACTGTTGACCT	Hs.632099	TAGLN	Transgelin	19	1	-18.43	0
GTTCCACAGAAGCTTTG	Hs.489142	COL1A2	*Collagen, type 1, alpha 2*	17	1	-16.49	0
GGCCCCATTCCAGGACA	Hs.203717	FN1	Fibronectin 1	16	1	-15.52	0
AAATGATGTACTCAGAA			Unknown	16	1	-15.52	0
CCTCCAGCCCCCAGCT	Hs.210283	COL5A1	*Collagen, type 5, alpha 1*	13	1	-12.61	0
GAGCATTGCACCACCCG	Hs.111779	SPARC	*Secreted protein, acidic, cysteine-rich (osteonectin)*	12	1	-11.64	0
GCTTAAGGTTTGTGGTT			Unknown	11	1	-10.67	0
TAAAATACGGCTGGTTC		AA219270	Unknown	11	1	-10.67	0
CTTTGGAGGCCAGCGGG	Hs.203717	FN1	Fibronectin 1	11	1	-10.67	0
GAAGAAGATGAAAATGA		AA599895	Unknown	17	1	-16.49	0
GGAGGAGAGCGTGTGCG	Hs.172928	COL1A1	*Collagen, type 1, alpha 1*	14	1	-13.58	0
CCGTGACTTGAGACTCA	Hs.489142	COL1A2	Collagen, type 1, alpha 2	14	1	-13.58	0
TTAAAAGATTTAGACAC			Unknown	14	1	-13.58	0
AGAGCACACCTCTTAGA	Hs.203717	FN1	Fibronectin 1	13	1	-12.61	0
CCACAGGGGATTCTCCT	Hs.443625	COL3A1	*Collagen, type 3, alpha 1*	47	4	-11.40	0
GCCCTTTCTCTGTAGTT	Hs.7835	MRC2	Mannose receptor, C type 2	51	5	-9.89	0
TTTGGTTTTCCAAAAAA	Hs.489142	COL1A2	*Collagen, type 1, alpha 2*	27	3	-8.73	0
TTATGTTTAATAAGCTA	Hs.406475	LUM	Lumican	17	2	-8.24	0
CTTTATTCCAGCAATCA		AI342124	*Unknown*	17	2	-8.24	0

Table 7 Twenty most under-expressed tags in MSC's at late passage

Less stringent statistical criteria were used to establish biological patterns that may be lost if the threshold were set too high. 243 UniGene identifiers were uploaded, and 234 (96%) matched genes within the MetaCore™ database. The twenty most common canonical maps that matched the differentially expressed genes are shown in Figure 4-14. These maps included chemokine, cell adhesion, cytoskeletal re-modelling, glycolysis and MAPK signalling pathways. The genes were assigned gene ontological descriptions using standard methods (GO processes) and the software's own version (GeneGO processes) as shown in Figure 4-15 and Figure 4-16. The gene list was matched to known metabolic pathways which demonstrated alteration in membrane lipid and glucose metabolism (Figure 4-17).

The network building algorithm was used to build a network of direct gene/protein interactions around the up-loaded gene list. Genes with direct interactions clustered around the transcription factor, activator protein 1 (AP-1) (Figure 4-18). AP-1 is a heterodimeric protein that can initiate a multitude of cellular processes in response to varying cellular stimuli. When a network was built by auto-expansion (interactions are predicted with genes not included in the analysed list) a cluster developed around the transcription factor, hepatocyte nuclear factor 4 alpha (HNF4A) (not shown). The nuclear protein encoded by this gene is known to regulate the expression of genes involved in glucose transport and metabolism.

4.4 Discussion

SAGE is an excellent method of large-scale mRNA expression profiling which produces comprehensive, quantitative and reproducible gene expression profiles. We did not experience any technical difficulties in performing SAGE although the technique is labour intensive if performed individually. Although some research groups have generated large numbers of SAGE libraries using automated devices, microarray technology has evolved rapidly and is now favoured by most researchers. The rapid generation of results and analysis; the large coverage of known genes; and the versatility of the equipment that enables comparative genomic hybridization (CGH), SNP and microRNA (miRNA) profiles to be determined using the same platforms has further enhanced its application.

Figure 4-14 Twenty most significant canonical maps associated with differentially expressed genes in late passage MSC's

234 differentially expressed tags in the comparison of 25 MSC P2 and P9 that matched a Unigene identifier were analysed using Metacore™ systems biology software. The statistical algorithm uses a z-score equation to assign genes to specific sub-networks and the significance can be determined by the network size (p value 0.05).

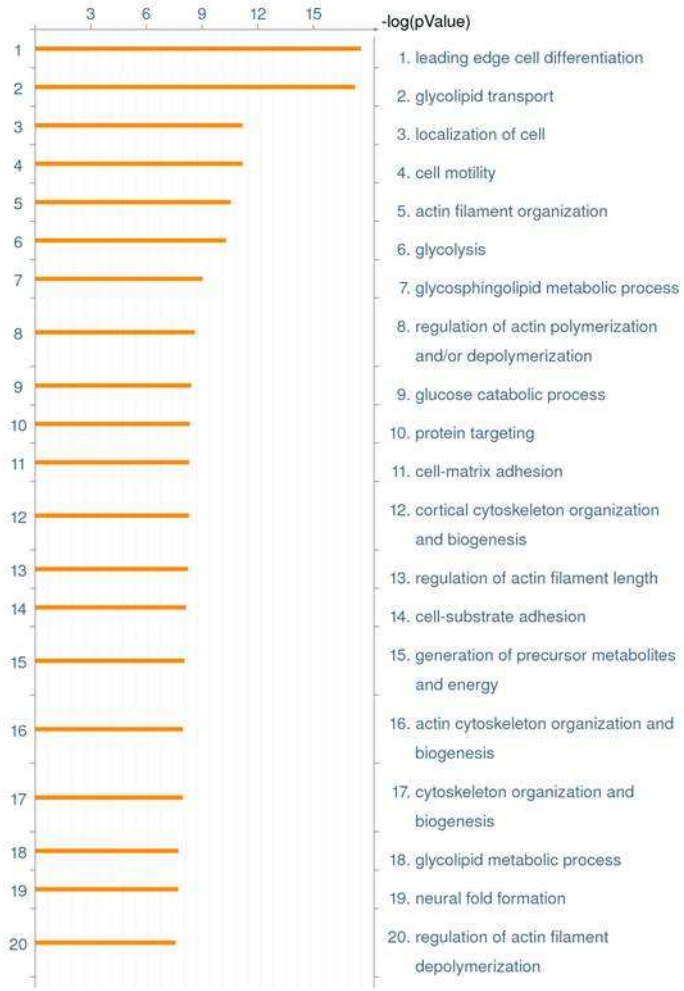

Figure 4-15 Twenty most significant gene ontology (GO) processes associated with differentially expressed genes in late passage MSC's

234 differentially expressed tags in the comparison of 25 MSC P2 and P9 that matched a Unigene identifier were analysed using Metacore™ systems biology software. The statistical algorithm uses a z-score equation to assign genes to specific sub-networks and the significance can be determined by the network size (p value 0.05).

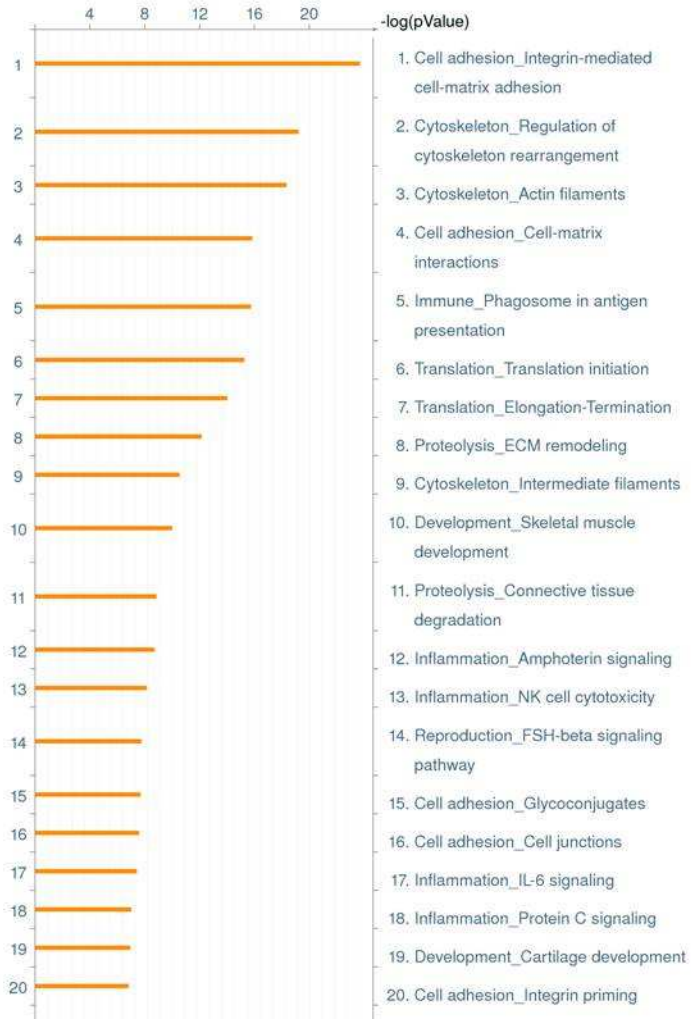

Figure 4-16 Twenty most significant GeneGO processes associated with differentially expressed genes in late passage MSC's

234 differentially expressed tags in the comparison of 25 MSC P2 and P9 that matched a Unigene identifier were analysed using Metacore™ systems biology software. The statistical algorithm uses a z-score equation to assign genes to specific sub-networks and the significance can be determined by the network size (p value 0.05).

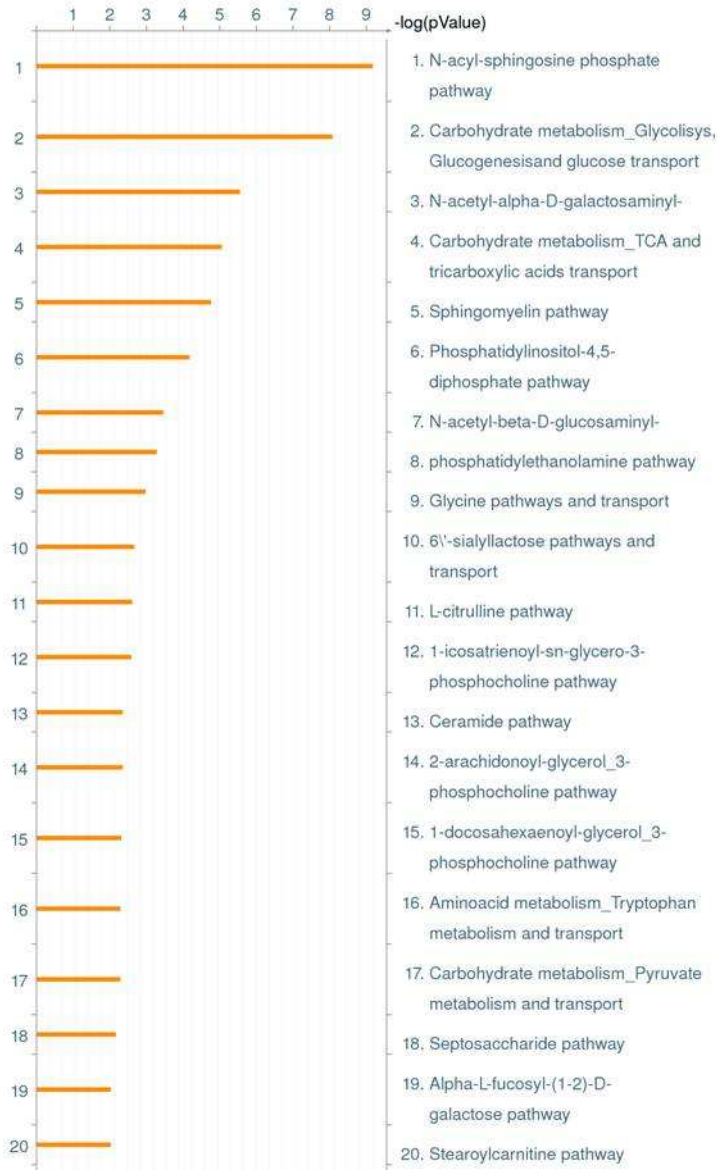

Figure 4-17 Twenty most significant metabolic maps associated with differentially expressed genes in late passage MSC's

234 differentially expressed tags in the comparison of 25 MSC P2 and P9 that matched a Unigene identifier were analysed using Metacore™ systems biology software. The statistical algorithm uses a z-score equation to assign genes to specific sub-networks and the significance can be determined by the network size (p value 0.05).

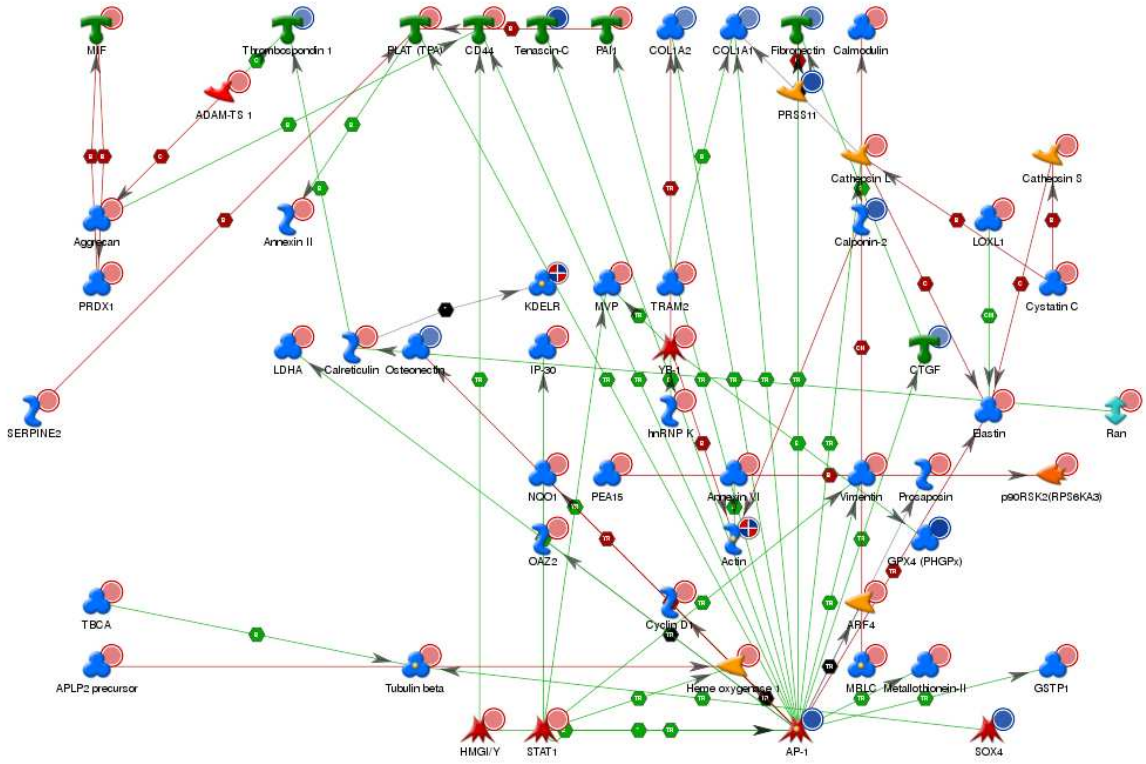

Figure 4-18 A network of direct interactions built around the differentially expressed gene list showed a cluster around the transcription factor AP-1

234 differentially expressed tags in the comparison of 25 MSC P2 and P9 that matched a Unigene identifier were analysed using Metacore™ systems biology software. Network analysis was performed using the direct interactions network building algorithm within the software. Green arrows represent positive, red negative and grey unspecified interactions on the network. Red and blue circles represent the SAGE expression data. Red: significantly overexpressed in MSC's passage nine. Blue: significantly underexpressed in MSC's passage nine (p value 0.05).

The investigation of unmatched tags in order to identify novel genes is one of the most attractive aspects of the SAGE technique although we did not have the opportunity to perform this. The use of RT-PCR, using the SAGE tag as a primer and generating longer, more specific 3' cDNA sequences has already been described. In fact, our research group has used this method in the discovery of gastrokine 1, a potential tumour suppressor gene highly expressed in normal stomach and absent in gastric cancer (189). An additional advantage of SAGE is that repeat analysis of the data can be performed when the reference sequence databases are periodically up-dated and therefore novel genes may be identified at a later date from the original dataset.

Each of the SAGE libraries generated contained approximately 40,000 tags matching approximately 20,000 genes (Table 4). From the three libraries, 18 (0.08%) tags had counts of more than one hundred in each and 16,997 (78%) tags occurred only once. The majority of tags in each library did not match known genes whilst 30% were reliably assigned a UniGene identity. This pattern of tag distribution and gene assignment is in agreement with earlier SAGE publications (123;124).

The most abundant genes found in all three MSC's SAGE libraries were similar to other published expression profiles of MSC's (45;105;141;142). Silva *et al* and Panepucci *et al* produced short SAGE libraries on MSC's derived from human BM and cord blood respectively. Although the donors and culture protocols were different, seven of the twenty most abundant genes in our libraries were identified in these studies. The genes included: cytoskeletal proteins such as collagen, type I, alpha 1 (COL1A1), transgelin (TAGLN), cofilin-1 (CFL1) and vimentin (VIM); eukaryotic translation elongation factor 1 alpha 1 (EEF1A1) which functions in the delivery of aminoacyl t-RNA's to the ribosome; and extra-cellular matrix proteins lectin, galactoside-binding, soluble, 1 (LGALS1) and secreted protein, acidic, cysteine-rich (SPARC). These genes are considered the molecular foundation of MSC's although are widely expressed in other tissues and cell types.

We found three unmatched tags (TTCATACACCTATCCCC, TGATTTCACTTCCACTC and CACCTAATTGGAAGCGC) that were present in the SAGE libraries and significantly increased at late passage. A search of SAGE Genie revealed that

these tags matched publicly available sequences derived from mitochondrial DNA. The results suggest transcriptional alterations occur in the mitochondria during prolonged culture and ageing of MSC's. It is widely accepted that mitochondrial dysfunction and increased production of reactive oxygen species (ROS) can lead to DNA damage and initiate the onset of senescence. In support of our findings, a recent study has shown that the senescence of MSC's is stress induced and high levels of ROS are found in late passage cells (68).

We identified a five unknown tags unique to MSC's in the comparison of SAGE library 25 MSC P2 to 110 publicly available long SAGE libraries. The tags were of low abundance in MSC's (counts <10) and included GGCCGCACCATAATGAG, CACAAGGCTCACATCTC, ACCCAAAAACCAAAAGT, TTAAAATAGCACCTTTA and ATGTGAANAGTTTCACA. Using SAGE Genie, GGCCGCACCATAATGAG was identified as an internal tag in an expressed sequence transcript (EST) similar to transforming growth factor beta-induced protein ig-h3 precursor (accession number: AK094055). ACCCAAAAACCAAAAGT was identified as an internal tag in an unidentified EST (accession number: BE814198) and the remaining tags were unmatched.

These tags are of interest because they could represent novel markers of MSC's. Furthermore, one tag matched the gene for CD248, also known as endosialin. CD248 is found expressed on stromal fibroblasts and pericytes (190). It has been suggested that MSC's reside in a perivascular niche (20) and a recently adipose derived MSC's and pericytes were shown to have a remarkably similar surface marker profile *in vitro* and express the markers Stro-1, CD146 and 3G5. In addition, cells displaying these markers have been identified in the vicinity of blood vessel walls *in vivo* (191). A further study of CD248 expression in our MSC's would be of great interest.

We uncovered a gene expression signature using SAGE that can distinguish between MSC's at early and late passage. 332 tags matched 243 known genes and 100 of these genes were found in the comparison with early passage cells from a different donor. This overlap would confirm that these transcripts could identify molecular changes of ageing in MSC's. Metacore™ analysis of the direct interactions within the gene signature highlighted a signalling network involved in repression of AP-1 in late passage cells. AP-1 is a heterodimer composed of

DNA binding proteins that include Jun, FOS and ATF subgroups of transcription factors. AP-1 can regulate gene expression in response to a variety of stimuli as well as control key cellular processes such as proliferation, apoptosis and differentiation (Reviewed by (192)). Late passage MSC's showed significantly decreased expression of both c-Fos and Jun which would explain the reduction in proliferation seen in the cells. In studies using fibroblasts, short term exposure to oxidants increased AP-1 expression but sustained activation eventually resulted in decreased expression (193). The results would infer that oxidative stress may contribute to the senescence of MSC's and indeed, Heo *et al* have recently demonstrated that MSC's display high levels of ROS levels during prolonged expansion (68).

Metacore™ analysis also revealed that late passage MSC's display significant alterations in genes associated with cytoskeletal remodelling, inflammation, extra-cellular matrix re-modelling and glycolysis. The results are remarkably similar to that seen in microarray studies of replicative senescence in fibroblasts (92;194). It is well recognised that the senescent phenotype has the potential to cause detrimental effects on tissue function due to enhanced tissue re-modelling and impaired wound healing. This would be an undesirable feature of cells used in cell therapy approaches and would emphasise the need to characterise cultures at the molecular level prior to clinical use.

The significance of altered glycolysis in late passage MSC's is uncertain and requires further investigation. Most normal cells generate ATP through mitochondrial oxidative phosphorylation although in cancer cells it has been recognised that aerobic glycolysis predominates (Warburg effect). Although an inefficient method of energy production, it is thought to sustain the high levels of proliferation seen in cancer cells and enhance resistance to oxidative stress. In late passage MSC's this would be a useful property in the face of ongoing culture stress or may simply be a consequence of mitochondrial dysfunction in the cell and a method of sustained ATP production. Further studies of glucose uptake in the cells would be of interest, particularly as the media concentration can alter the proliferative ability of MSC's with reduced proliferation seen with higher concentrations ofglucose (58).

Lastly, we found that differentially expressed genes in late passage MSC's were more commonly associated with chromosome two which has been shown in a previous study to contain senescence-initiating genes (195). Tanaka *et al* performed chromosomal transfer experiments in human cervical carcinoma cells and showed that chromosome two could induce growth arrest and a senescent phenotype. In addition, the cells still expressed telomerase suggesting the mechanism may be telomere independent. The findings are in contrast to a recent study that demonstrated an over-representation of genes on chromosome 4 in MSC's undergoing replicative senescence using microarray (40). It remains unknown if these differences arise from the technique of gene expression profiling used or that MSC's initiate senescence via entirely different molecular mechanisms in our own and this study.

4.5 Conclusion

We have identified a gene expression signature using SAGE capable of distinguishing MSC's at early and late passage. This signature contains a regulatory signalling network centred on AP-1 down regulation that determines the molecular phenotype of aged MSC's. We identified genes associated with senescence, cell cycle regulation, oxidative stress and apoptosis. Importantly, late passage MSC's display enhanced inflammatory and extra-cellular matrix re-modelling properties which may be detrimental on tissue function if used for cell-based therapies. The results provide us with candidate genes that may represent transcriptional markers of MSC ageing and senescence. The validation studies and the individual genes that were identified in late passage MSC's are discussed further in the next chapter.

5 Validation of SAGE Using Taqman® Low Density Arrays

5.1 Introduction

Because SAGE is labour-intensive and hence limited to a small number of experiments, the resulting candidate genes require validation in multiple samples (102;106). Validation of RNA expression was traditionally performed by Northern blotting or conventional reverse-transcription polymerase chain reaction (RT-PCR), although this has largely been superseded by fluorescence based, real-time RT-PCR. The technique is easy to use, accurate and highly reproducible and the results require minimal post-processing. Although this method was originally a single gene approach, developments in micro-fluidics mean it is now possible to perform real-time RT-PCR on three hundred and eighty four genes simultaneously using Taqman® low density arrays (TLDA's) (Applied Biosystems). In addition, TLDA's are available in a choice of formats that allow the number of genes, replicates and samples to be determined by the researcher.

The most critical aspect of real-time RT-PCR is the selection of a suitable control gene for normalisation of the results. Commonly used controls in real-time PCR include 'housekeeping' genes such as glyceraldehyde 3-phosphate dehydrogenase (GAPDH), ß-actin (ACTB) and the ribosomal RNA's (rRNA) such as 18S. Often these genes are chosen on the assumption that they are expressed at constant levels across samples although it has been recognised that suitable control genes should be determined for individual experiments (196). To address this, TLDA's have been developed to assay potential control genes and approaches on selecting suitable candidates have been published (197).

The results of SAGE had identified candidate genes differentially expressed in late passage MSC's and many were assigned to a signalling network that clustered around the transcription factor, AP-1. Using ninety six gene TLDA's our aim was to validate the SAGE results in multiple donor samples and also identify genes that represent novel markers of MSC ageing and senescence during expansion *in vitro*.

5.2 Results

5.2.1 Selection of Control Genes for Normalisation Using TLDA's

Comparison of the SAGE libraries had identified differential expression of tags that matched the housekeeping genes, ACTB and GAPDH. Therefore, to identify the best candidate gene to use as a control for normalisation in our experiments, we used the TLDA endogenous control assay (Applied Biosystems). The array contains sixteen pre-determined control genes that are measured in triplicate in eight samples simultaneously. Before using the TLDA, a small volume of cDNA reaction was used in a GAPDH PCR to confirm generation of cDNA and absence of genomic DNA. This was performed whenever cDNA was created and a representative gel is shown in Figure 5-1.

The average cycle thresholds (C_T) of the sixteen control genes determined from seven samples are shown in Figure 5-2. The results of the eighth, donor 12 MSC's at passage one was excluded because of greater variability in the average C_T. This was thought to have arisen from haematopoietic and endothelial cell contamination in passage one cultures as described in chapter 3. The results demonstrate that 18S is expressed at high levels, and tyrosine 3-monooxygenase/tryptophan 5-monooxygenase activation protein, zeta polypeptide (YWHAZ) at low levels in MSC's. The standard deviation of the C_T was calculated and the results shown in Figure 5-3. The results demonstrate that the genes with the lowest standard deviation, and therefore the lowest variation across samples were 18S (0.06), UBC (0.33), RPLP0 (0.41) and ACTB (0.43). Although 18S had the lowest variability, it was noticed that some wells on the array had unusually low C_T values and if included the overall results would have demonstrated that 18S had the greatest variability. Therefore, ubiquitin C (UBC) was selected as the best control gene and as alternatives ribosomal protein, large, P0 (RPLP0), polymerase (RNA) II (DNA directed) polypeptide A (POLR2A), ACTB and GAPDH were also added to the array.

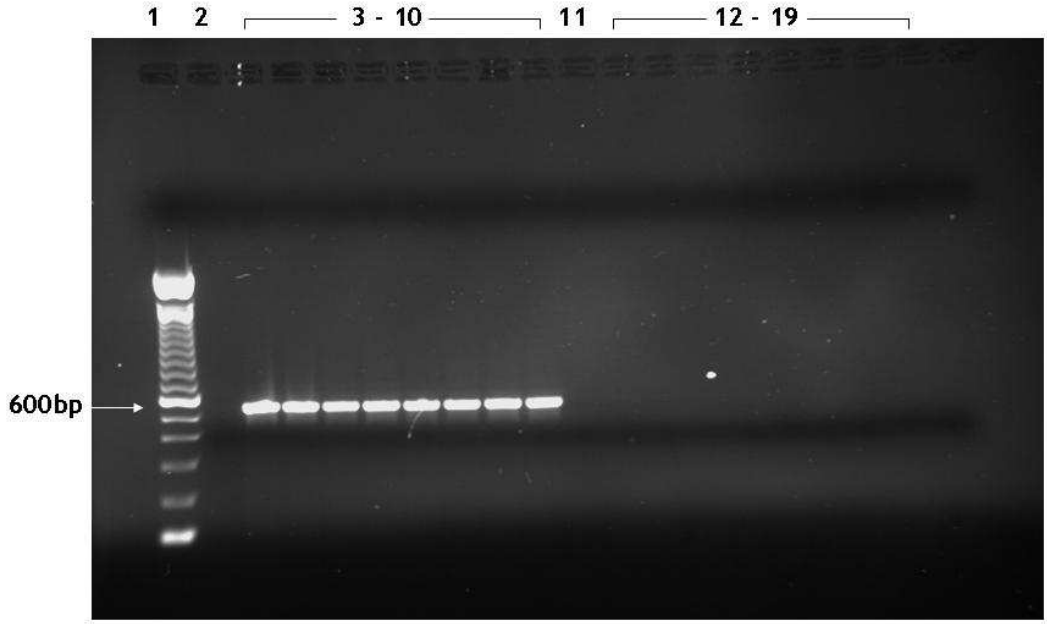

Figure 5-1 GAPDH PCR confirms cDNA synthesis and absence of genomic DNA contamination

cDNA was generated from eight RNA samples using the High Capacity cDNA Archive Kit (Applied Biosystems). 1µl of each cDNA reaction was then used as a template for a GAPDH PCR and the reaction products analysed on a 1% agarose gel. Strong DNA bands of similar intensity confirmed the production of cDNA from the RNA samples (lanes 3 – 10). No template (Lane 2), no template no RT (Lane 11) and no RT controls (Lanes 12 – 19) demonstrated the absence of genomic DNA contamination in reagents and samples. A 100bp molecular ladder is shown (Lane 1).

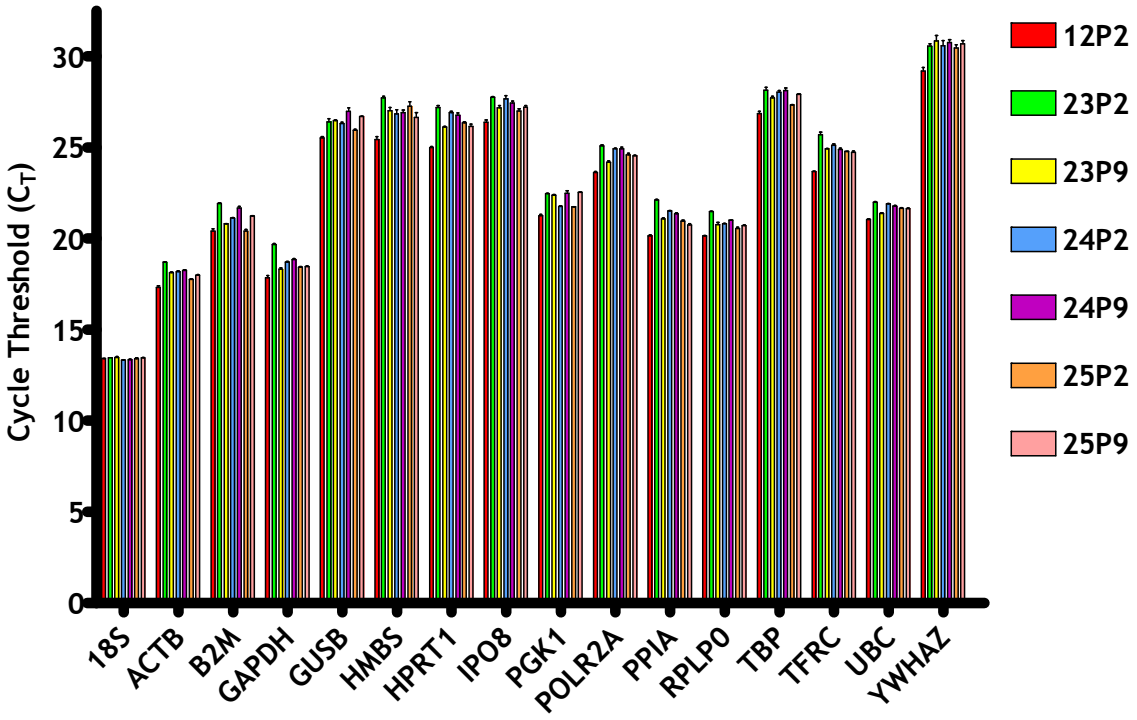

Figure 5-2 Variable abundance of potential control genes for normalisation was demonstrated in MSC's

The expression of sixteen endogenous control genes was analysed in seven MSC samples at passage two and nine using the TLDA endogenous control panel (Applied Biosystems). Each bar represents the average C_T of each gene measured in triplicate; error bars show the standard deviation.

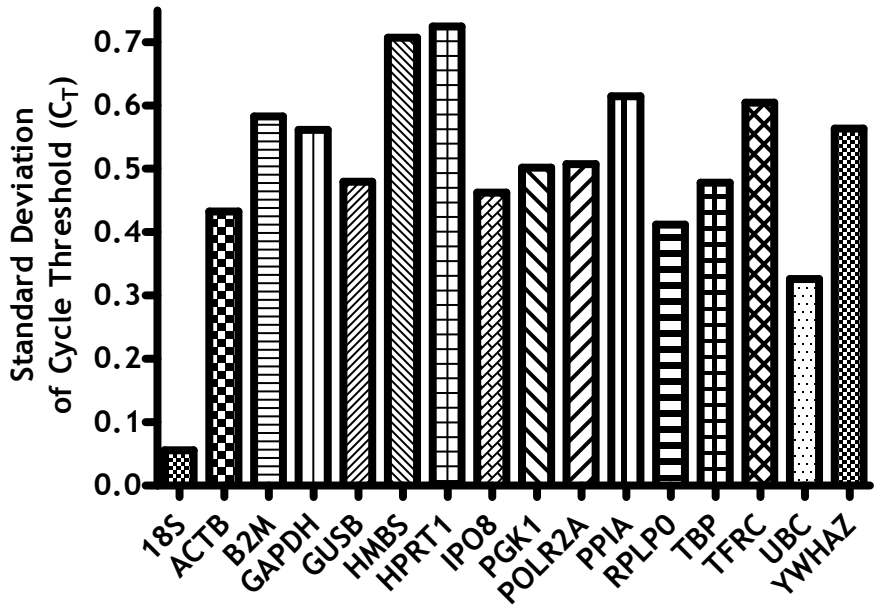

Figure 5-3 Suitable controls for normalisation were identified that showed the least variation in expression in MSC's

The standard deviation of the average C_T was determined for each gene from the seven samples. Gene expression was measured in triplicate for each sample.

5.2.2 Selection of Candidate Genes for the Custom-Made TLDA's

TLDA format 96b was chosen to enable analysis of ninety six genes in duplicate in two samples simultaneously. The process of selecting genes for the custom-made TLDA in order to validate the SAGE results is shown in Figure 5-4. Genes were selected to include: those most significantly different between MSC's at passage two and nine; those on AP-1 regulatory network; endogenous controls; non significant genes of variable abundance by SAGE; cell cycle genes; and genes associated with the p38 pathway. Further information on each gene and its function can be found in the appendix (Table 8). With the exception of heat shock 70kDa protein 8 (HSPA8), assays were selected to include probes that spanned exon junctions and therefore minimise the chance of amplification from genomic DNA. The differentially expressed SAGE tags were manually identified in the original sequences from which the assays were developed to ensure a match. The abundance and differential expression of tags in the three SAGE libraries that matched genes on the TLDA are found in the appendix (Table 9).

Seventy six genes on the array were chosen to match tags differentially expressed more that two fold in the comparison of SAGE libraries 25 MSC P2 and P9. Of these, fifty six genes were identified that had more than two fold change in tag odds ratio and $p < 0.01$ and were the focus of the validation studies. The other nineteen genes were of lower significance ($p<0.05$) but included to validate the regulatory network involving the transcription factor, AP-1. Of note, forty two differentially expressed tags in the comparison of SAGE libraries 12 MSC P2 and 25 MSC P9, and thirty three in the comparison of libraries 25 MSC P2 and 12 MSC P2 matched genes included on the array.

5.2.3 Confirmation of the Reproducibility of TLDA's

In this study, the number of TLDA's provided with the order was limited and it was not possible to perform a dilution series and ensure consistent amplification when the amount of template varied. For the experiments described here cDNA equivalent to 100ng RNA was loaded onto each lane of the array as recommended by the manufacturer's protocol.

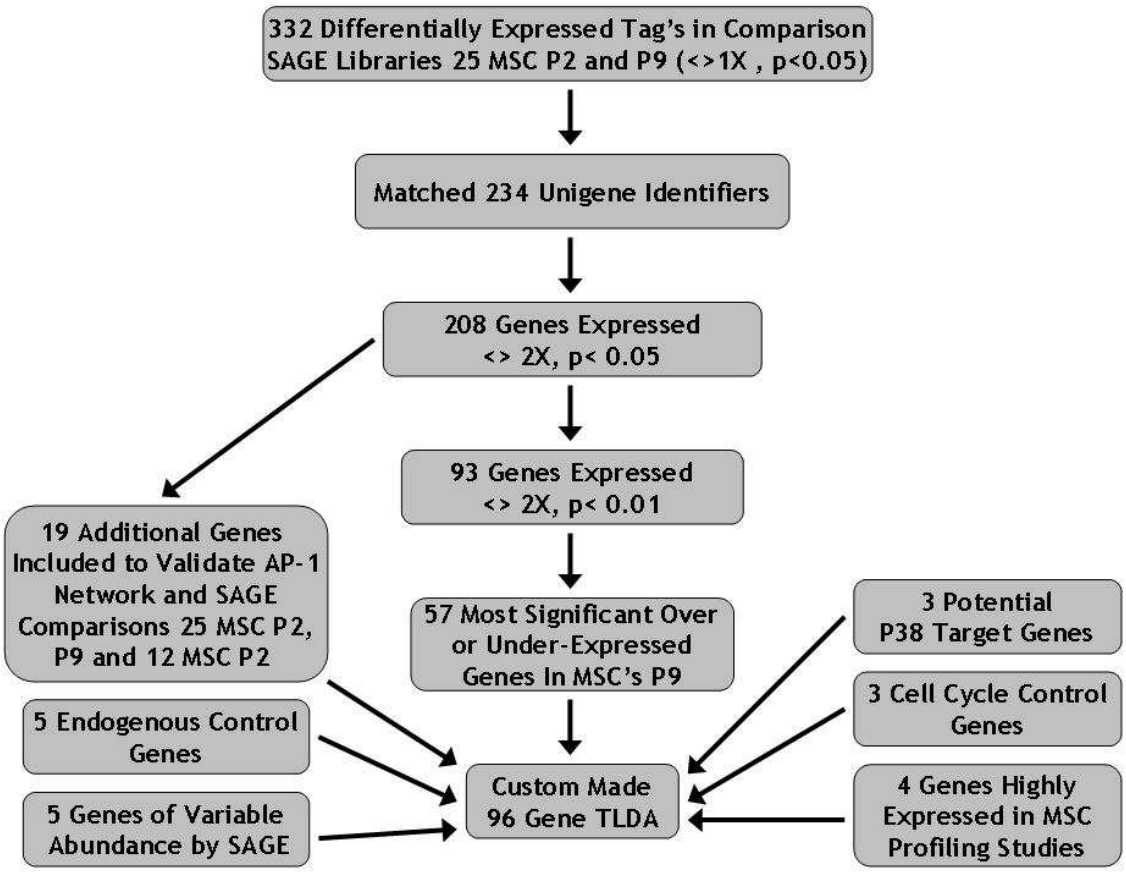

Figure 5-4 Process of selection of genes for validation using custom-made TLDA

cDNA from donor 30 cells at passage nine was analysed on two separate occasions on different arrays to determine variablility in amplification between arrays. From both studies, the mean relative quantities (RQ) for each gene were calculated using the $2^{-\Delta\Delta C}{}_T$ method where $\Delta\Delta C_T = ((C_{T,\ Target} - C_{T,\ Control})_{\ Time\ y} - (C_{T,\ Target} - C_{T.\ Control})_{\ Time\ x})$. The standard error of the C_T was used to calculate 95% confidence intervals, called the minimum RQ (RQ Min) and maximum RQ (RQ Max). UBC was the control gene, time x defined as MSC's at passage two and time y defined as MSC's at passage five or nine, where stated. Mean RQ values were plotted against each other and a line of best fit drawn using linear regression as shown in Figure 5-5. The r^2 value of 0.98 confirmed a strong correlation and therefore the arrays appeared reproducible when using the same cDNA sample. The assay for cytochrome c oxidase subunit Vb (COX5B) did not amplify and was excluded from the analysis.

5.2.4 Validation of the SAGE Results Using TLDA's

In order to determine that the tag counts in SAGE library 25 MSC P2 were representative of mRNA abundance by RT-PCR, the techniques were compared. The relative abundance was determined for the genes collagen, type I, alpha 1 (COL1A1), connective tissue growth factor (CTGF), insulin-like growth factor binding protein 4 (IGFBP4), RPLP0 and interleukin 6 signal transducer (IL6ST) by comparison with the gene forkhead box O3A (FOXO3A) which was expressed at low levels in MSC's. The abundance was calculated as $((C_T\ FOXO3A - C_T\ Gene)^2)$ for RT-PCR and (Tag count gene/Tag count FOXO3A) for SAGE, and the results are shown in Figure 5-6. The two techniques were comparable although the higher abundance of COL1A1 in SAGE may be an artefact of the tag based approach and may have become less obvious if the SAGE library size was increased.

In order to validate differentially expressed tags in the comparison of SAGE libraries 25 MSC P2 and P9, the expression of seventy six matching genes were determined in the same samples using the arrays. Mean RQ values were determined by $2^{-\Delta\Delta C}{}_T$ method and a comparison made between donor 25 MSC's at passage two and nine. Genes were identified as differentially expressed if the mean RQ, including RQ Min and RQ Max did not overlap. The results from this comparison can also be found in the appendix (Table 10).

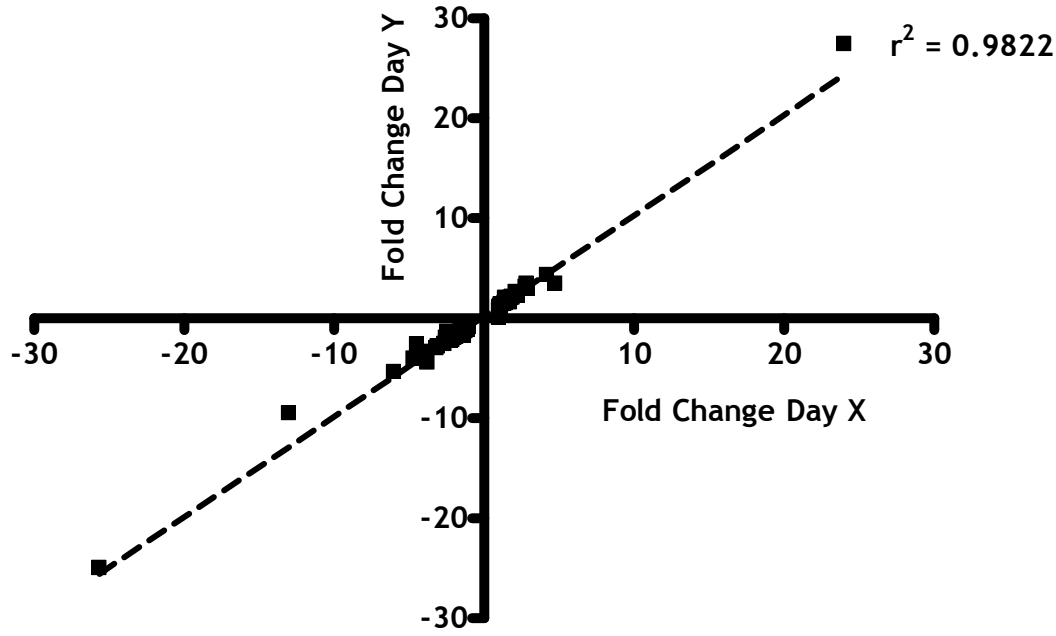

Figure 5-5 TaqMan® low density arrays displayed excellent reproducibility

cDNA from donor 30 MSC's at passage nine was analysed on two occasions (day X and Y) and the relative quantity (RQ) of genes on the array calculated using the $2^{-\Delta\Delta C}{}_T$ method. Baseline expression was determined in cells at passage two and normalised to the control, UBC. RQ values for each gene were plotted, and those less than 1 displayed as 1/RQ in order to determine a line of best fit by linear regression.

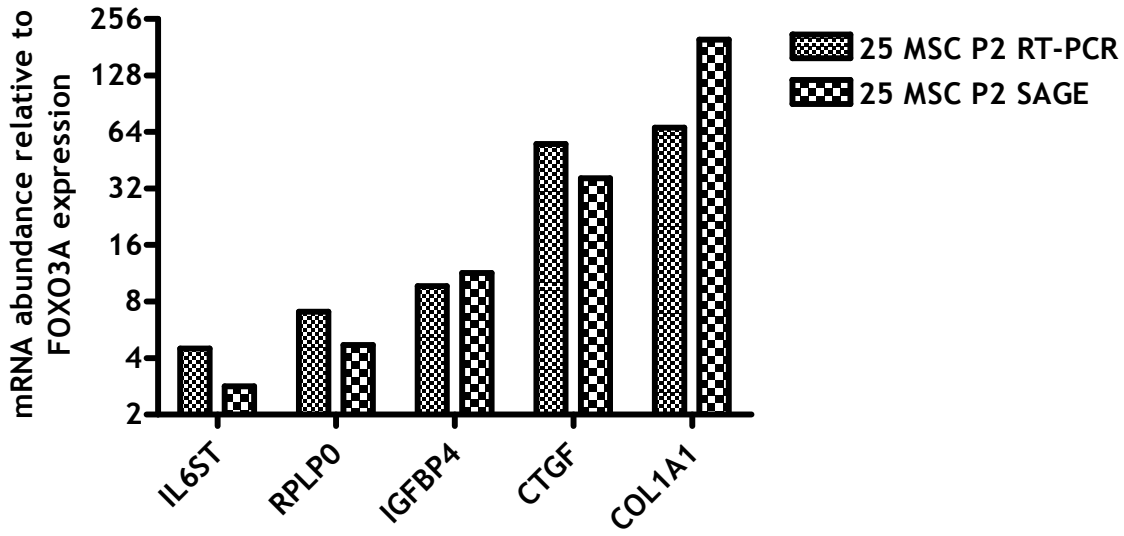

Figure 5-6 mRNA abundance detected by SAGE was comparable to that found by RT PCR

Bars represent mRNA abundance relative to FOXO3A as determined by RT-PCR ($(C_T$ FOXO3A- C_T GENE$)^2$) or SAGE (Tag count gene/Tag count FOXO3A) in donor 25 MSC's at passage two. C_T for each gene was measured in duplicate. The Y axis scale is set to $\log_2$ to aid visualisation of the results.

Forty one genes (54%) were confirmed as differentially expressed at passage nine and only the expression of cathepsin S (CTSS) was in the opposite direction to SAGE. High mobility group AT-hook 1 (HMGA1) showed increased expression that was not significant because of the large standard error in C_T but it was decided not to exclude this gene from further analysis. Eight genes were identified in MSC's from donor 25 at passage five that were significantly different to MSC's at passage two but not passage nine. However, the mean RQ values were similar at both time points and these genes were considered for further analysis.

To refine the gene list further, we identified thirty four genes (45% total validated) that were differentially expressed more than two fold i.e. mean RQ greater than two and less than half. This was the fold difference chosen in the selection of SAGE tags for validation. The expression of twenty one genes increased (Figure 5-7) in donor 25 MSC's at passage nine and thirteen decreased (Figure 5-8). The levels of expression by SAGE appeared greater than that by RT-PCR, particular for genes whose expression increased in MSC's at late passage. It was noted that twenty two genes from the list of thirty four were also significantly different in MSC's at passage five from the same donor.

The results from the same TLDA's were used to validate the differential expression of genes identified on the network clustered on AP-1. Sixteen genes (50% of those validated on the network) were found to be differentially expressed between donor 25 MSC's at passage two and nine (Figure 5-9). The expression of the gene FOS showed a trend of decreased expression with increasing passage number although this was not significant (mean RQ of 0.85 and 0.68 at passage five and nine respectively).

5.2.5 Determining Transcriptional Markers of Late Passage MSC's

To determine if the transcriptional changes were a consistent feature of late passage cells, TLDA's were used to analyse gene expression in seven other MSC cultures at passage two, five and nine. All the results, including those from donor 25 were then used to determine the mean RQ for all genes on the array and comparisons made between groups using a paired student's t-test. The results can be found in the appendix (Table 11).

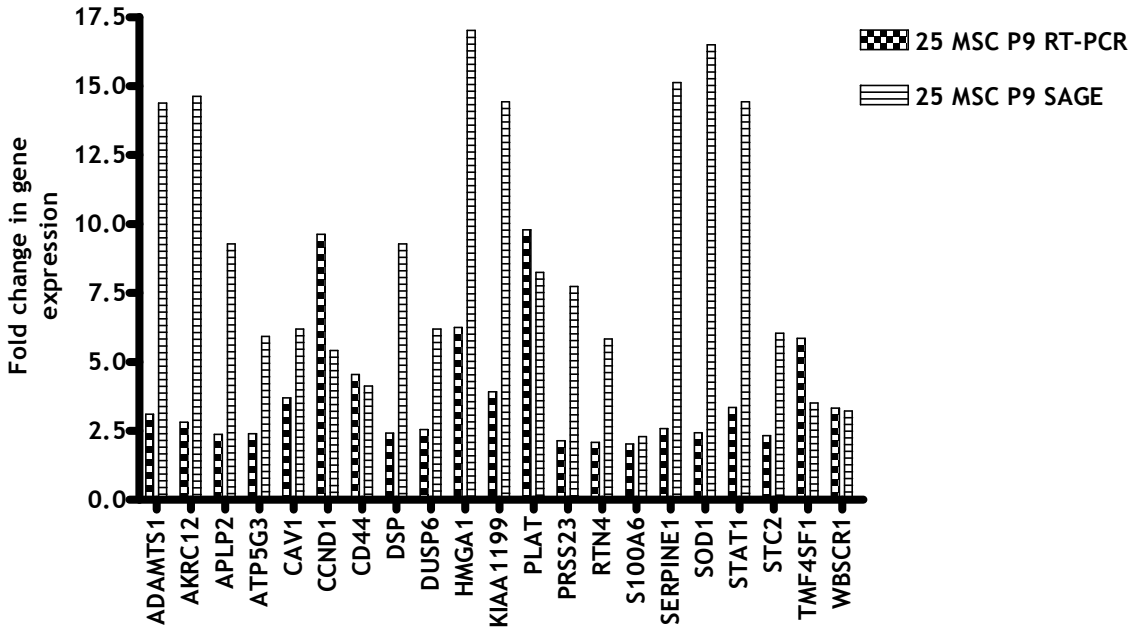

Figure 5-7 Genes that matched tags significantly increased by SAGE were confirmed by RT-PCR

RQ values were calculated in donor 25 MSC's at passage nine using the $2^{-\Delta\Delta C}{}_T$ method with baseline expression determined in cells at passage two and normalised to the control, UBC. Bars represent the mean RQ value for each gene measured in duplicate and the odds ratio for the same gene identified in the SAGE comparison 25 MSC P9:P2.

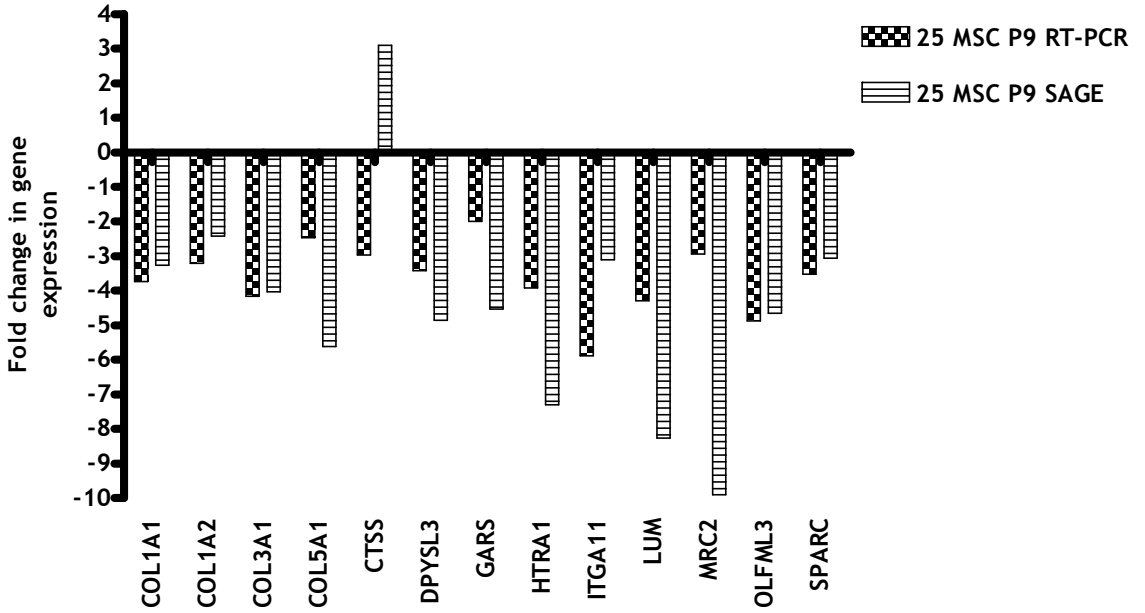

Figure 5-8 Genes that matched tags significantly decreased by SAGE were confirmed by RT-PCR

RQ values were calculated in donor 25 MSC's at passage nine using the $2^{-\Delta\Delta C}{}_T$ method with baseline expression determined in cells at passage two and normalised to the control, UBC. Bars represent fold change in expression, equivalent to 1/mean RQ value for each gene measured in duplicate and the 1/odds ratio for the same gene identified in the SAGE comparison 25 MSC P9:P2.

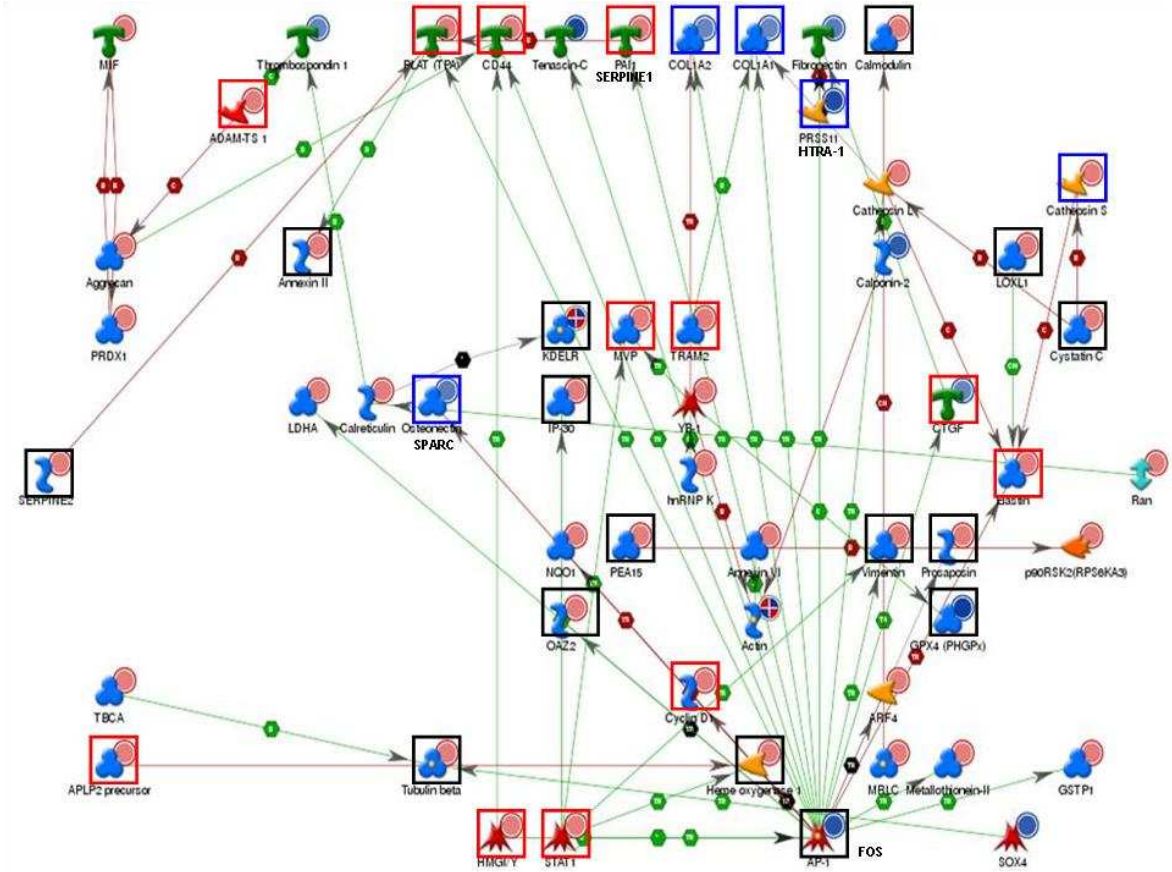

Figure 5-9 Validation studies supported the existence of a signalling network identified from differentially expressed SAGE tags

Thirty two genes on the network of direct interactions built using Metacore™ were validated by RT-PCR in cells from donor 25 at passage two and nine. Mean RQ values were calculated using the $2^{-\Delta\Delta C}{}_T$ method with baseline expression determined in MSC's at passage two and normalised to the control, UBC. Genes were considered significantly different if the 95% confidence intervals of the mean RQ did not overlap. Green arrows represent positive, red negative and grey unspecified interactions on the network. Red and blue circles represent the SAGE expression data and squares represent the expression of genes validated by RT-PCR. Red: significantly up in MSC's at passage nine. Blue: significantly down in MSC's at passage nine. Black: not significant. Gene aliases are shown in black text.

Twenty four (71%) genes from the reduced list of thirty four were confirmed as differentially expressed in all cultures at passage nine and eighteen genes showed changes in expression of more than two fold. From this list, sixteen genes showed increased expression (Figure 5-10 and Figure 5-11), and only two decreased in late passage MSC's (Figure 5-12). As shown in the figures, the genes CAV1, CCND1, PLAT and OLFML3 were differentially expressed in MSC's at passage five and nine suggesting they could discriminate between cultures of different proliferative age *in vitro*.

The overall results from the TLDA's were used to validate the differential expression of genes identified on the network clustered on AP-1. Eighteen (56%) genes validated on the network were found to be differentially expressed between eight donors MSC's at passage two and nine (Figure 5-13). Only eight were expressed at levels more than two fold as highlighted in the figure. In contrast to the findings in donor 25, the mean expression of the gene FOS was significantly decreased in the eight donor samples.

5.2.6 Determining the Expression of Cell Cycle Control Genes in Late Passage MSC's

Several important pathways control cell proliferation including the $p16^{INK4a}$ – Rb pathway, the p53 – $21^{CIP1/WAF1}$ pathway and PTEN – $p27^{Kip1}$. The cyclin dependent kinase inhibitors (CDKN's) 1A, 1B and 2A encode the proteins p21, 27 and 16 respectively and were included on the array to assess activity of these pathways in MSC's. It was noted that SAGE had not identified differential expression of these genes in MSC's from donor 25 at early and late passage. The mean RQ values were determined for these genes as well as the gene FOS in eight MSC cultures at passage two, five and nine and the results are shown in Figure 5-14. The increased expression of CDKN1A and 2A would infer activation of both p53 and Rb pathways, while CDKN1B was decreased and would suggest a decline in activity of the PTEN pathway during expansion of MSC's *in vitro*.

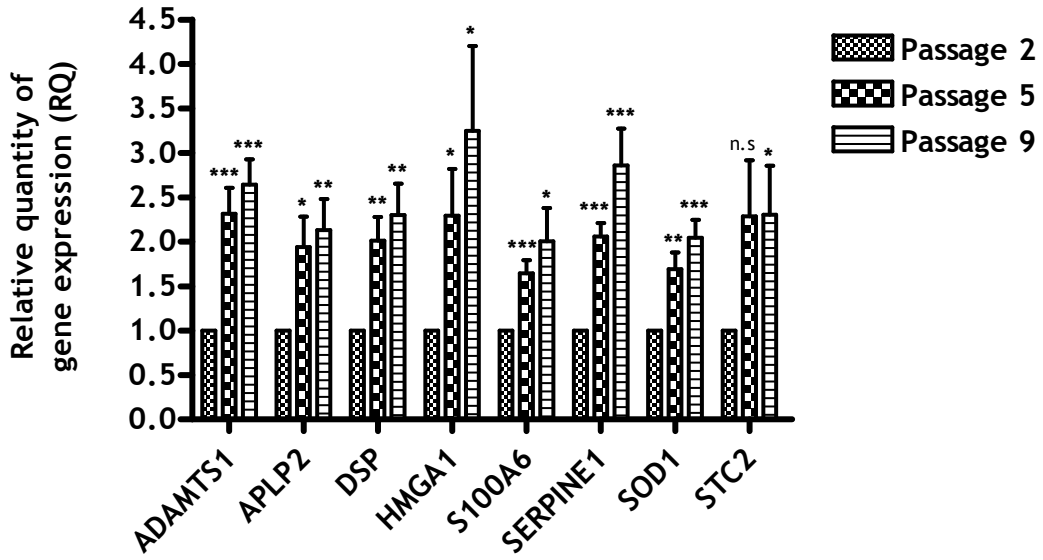

Figure 5-10 Genes with significantly increased expression in all MSC cultures during expansion

RQ values were calculated using the $2^{-\Delta\Delta C}{}_T$ method with baseline expression determined in MSC's at passage two and normalised to the control, UBC. Comparisons were made using a paired student's t-test, p value ≤ 0.05 *, 0.01 ** and 0.001 ***. Bars represent the mean RQ value from eight cultures; each gene was measured in duplicate. Error bars represent the standard deviation.

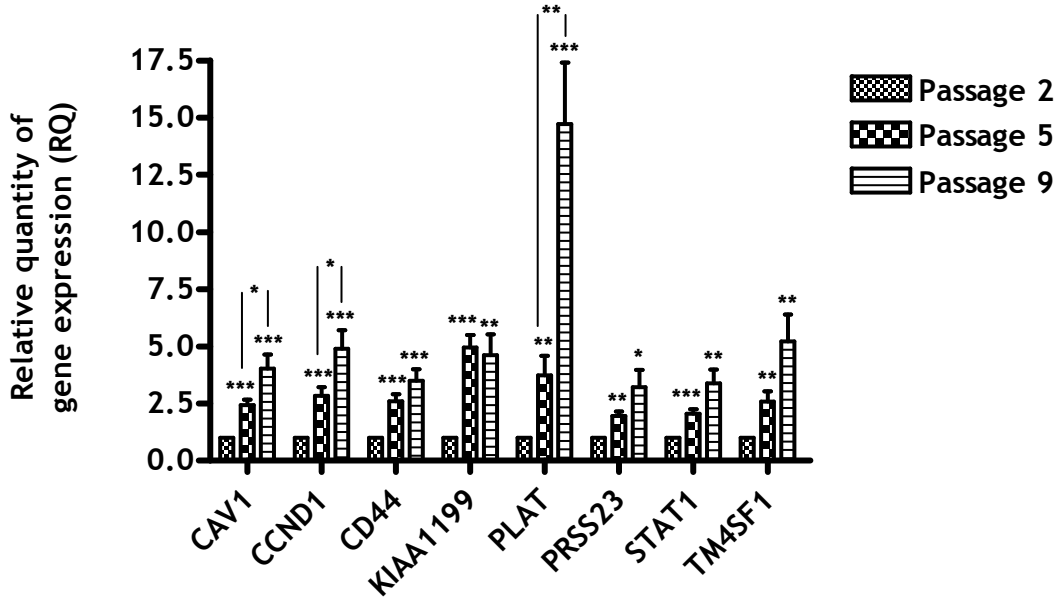

Figure 5-11 Genes with significantly increased expression in all MSC cultures during expansion

RQ values were calculated using the $2^{-\Delta\Delta C}{}_T$ method with baseline expression determined in MSC's at passage two and normalised to the control, UBC. Comparisons were made using a paired student's t-test, p value ≤ 0.05 *, 0.01 ** and 0.001 ***. Bars represent the mean RQ value from eight cultures; each gene was measured in duplicate. Error bars represent the standard deviation. RQ values significantly different at passage five and nine are highlighted.

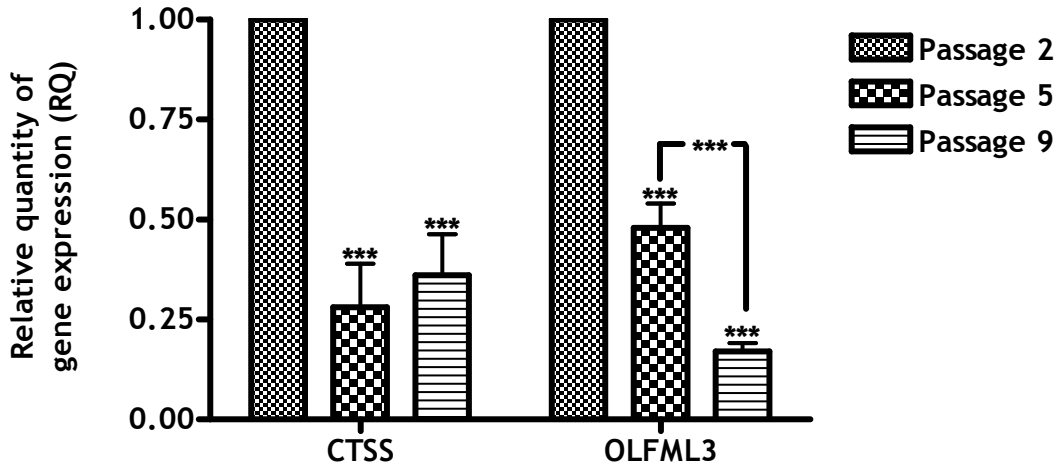

Figure 5-12 Genes with significantly decreased expression in all MSC cultures during expansion

RQ values were calculated using the $2^{-\Delta\Delta C}{}_T$ method with baseline expression determined in MSC's at passage two and normalised to the control, UBC. Comparisons were made using a paired student's t-test, p value ≤ 0.001 ***. Bars represent the mean RQ value from eight cultures; each gene was measured in duplicate. Error bars represent the standard deviation. RQ values significantly different at passage five and nine are highlighted.

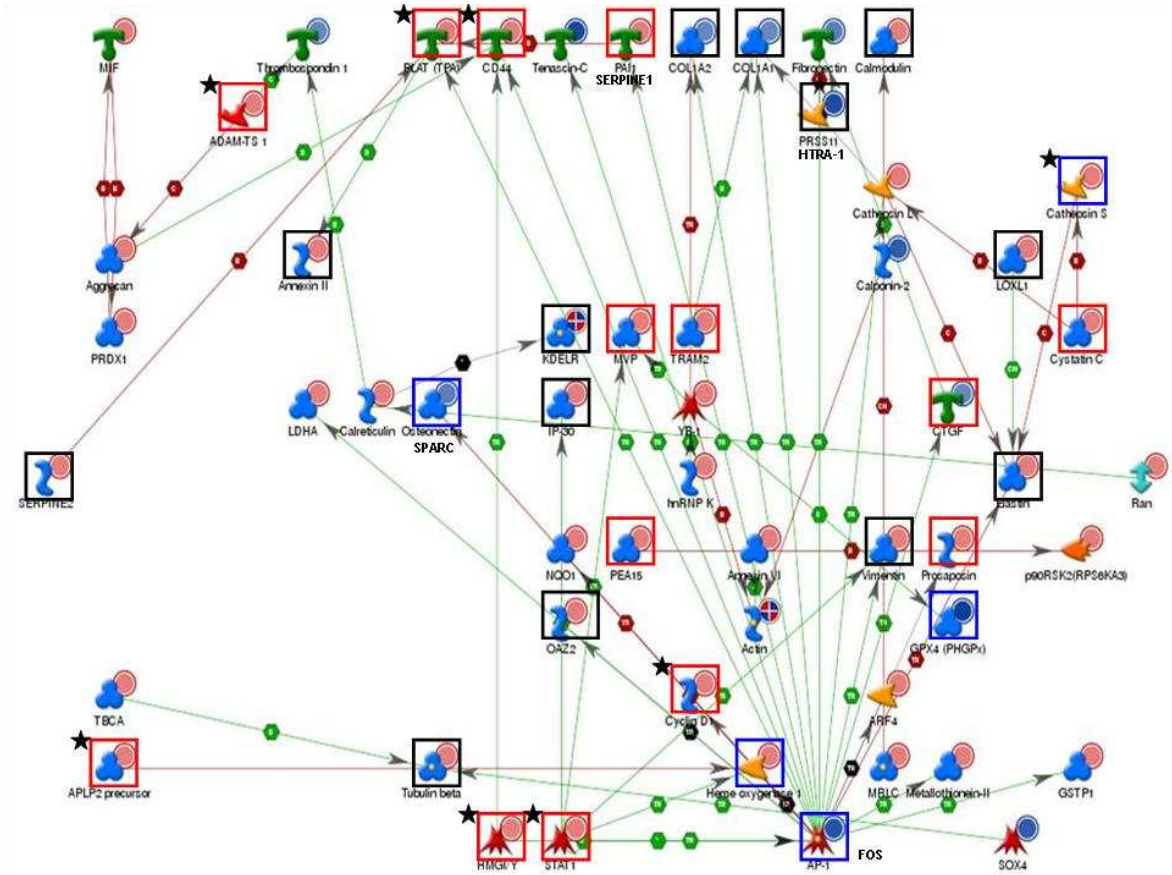

Figure 5-13 Altered expression of genes on the regulatory network were detected in eight MSC cultures at late passage

Thirty two genes on the network of direct interactions built using Metacore™ were validated by RT-PCR in eight MSC cultures. Green arrow's represent positive, red negative and grey unspecified interactions on the network. Red and blue circles represent the SAGE expression data while squares represent the expression of genes validated by RT-PCR. Red: significantly up in MSC's at passage nine. Blue: significantly down in MSC's at passage nine. Black: not significant. Gene aliases are shown in black text. Black stars: genes with altered expression more than two fold in comparison to MSC's at passage two. Comparison of RQ values at passage two and nine performed using a paired student's t-test and p value ≤ 0.05.

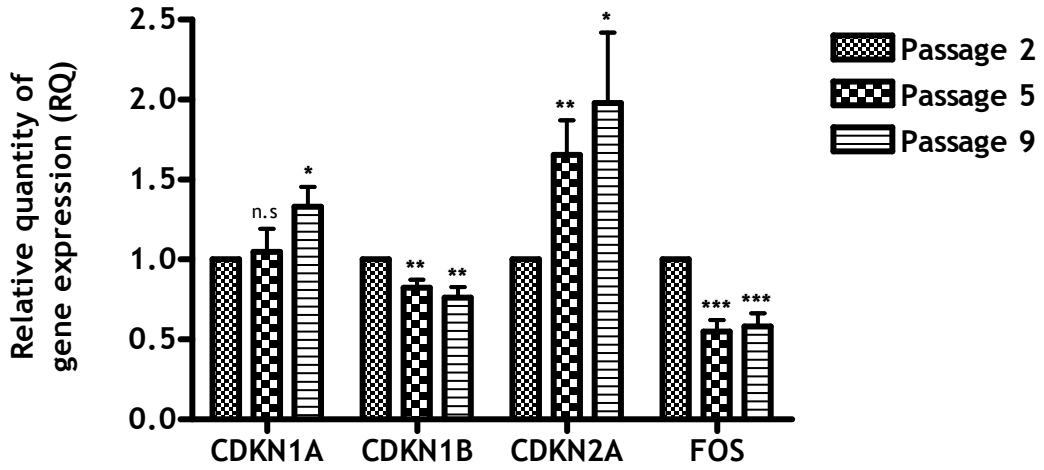

Figure 5-14 MSC's show altered expression of cell cycle control genes during expansion

The RQ values were calculated using the $2^{-\Delta\Delta C}{}_T$ method with baseline expression determined in MSC's at passage two and normalised to the control, UBC. Comparisons were made using a paired student's t-test, p value ≤ 0.05 *, 0.01 ** and 0.001 ***. Bars represent the mean RQ value from eight cultures; each gene was measured in duplicate. Error bars represent the standard deviation.

5.2.7 Subjective Scoring of MSC Culture Age

Four genes (CAV1, CCND1, PLAT and OLFML3) were found differentially expressed at passage five and nine and could potentially be used to discriminate the culture age of different MSC samples. It was decided to retrospectively score all the cultures in order to highlight differences between donor cells. Therefore, the mean RQ value for each gene was reviewed in individual cultures at passage five and nine and a value of one assigned to the culture with the least expression and eight to the culture with the highest expression. Total scores were calculated for each culture and the results shown in Figure 5-15. MSC's from donor 26 displayed the highest score at passage five and donor 23, the highest score at passage nine. MSC's from donor 24 had the lowest scores at passages five and nine. The scores did correlate with proliferative ability because MSC's from donor 26 proliferated slowly and together with cells from donor 23 could not be expanded beyond nine passages. In contrast, MSC's from donors 24 and 27 were able to proliferate until passage twelve before growth arrest. Although the results are subjective, it would be of interest to determine if the expression of these genes can predict the proliferative potential of individual MSC cultures from initial isolation or first passage and a prospective study would be required to address this.

5.3 Discussion

One concern that arose from SAGE was that late passage MSC's had altered expression of housekeeping genes commonly used for normalisation of RT-PCR. The importance of determining the best gene for a control has been highlighted by other studies and we used a similar approach (196;197). The gene UBC was identified as a suitable candidate in the initial study although on review of all the results, GAPDH, POLR2A and RPLP0 performed equally well. Our results suggest ACTB is not suitable as a control because mean expression decreased in late passage MSC's from the eight donors used in this study. Therefore, our results provide insight for other researchers on the selection of appropriate control genes suitable for expression profiling experiments using MSC's.

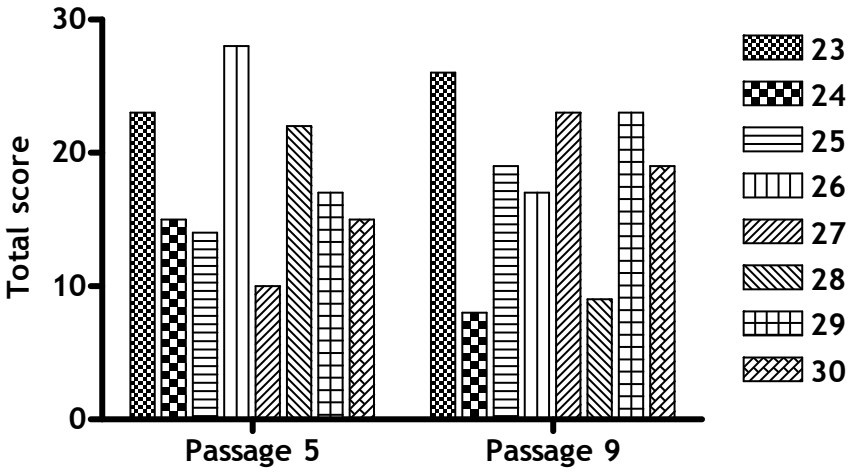

Figure 5-15 Retrospective analysis identified differences in ageing of MSC cultures from different donors

The mean RQ values of the genes CAV1, CCND1, PLAT and OLFML3 were used to identify differences in cultures by assigning a value of one to the culture with least expression of a gene to eight for the culture with the highest expression. The bars represent the total scores of the four genes in each sample measured at passage five and nine.

The validation studies have confirmed the validity of the SAGE results. By determining tag counts in the SAGE libraries for selected genes and the relative abundance by RT-PCR we have shown that both techniques correlate relatively well. Therefore, we were confident that the SAGE libraries were representative of mRNA expression in MSC's. Furthermore, genes abundant in MSC's, such as COL1A1, CTGF, TGFBI and VIM were confirmed by RT-PCR and have been demonstrated in other studies of the MSC transcriptome (45;105;141;142). To determine the differential expression of genes identified by SAGE, seventy six genes were validated by RT-PCR using custom-made TLDA's. The results on cDNA derived from the same RNA confirmed that forty one (54%) genes were differentially expressed and thirty four (45%) showed changes greater than two fold by RT-PCR. The differences in mRNA expression by SAGE were generally greater than those detected by RT-PCR and may be due to differences between the techniques. Reassuringly, the success of our SAGE validation was not dissimilar to that reported by earlier SAGE studies (102;123;198).

In our study, we identified eighteen genes (23%) in passage nine cells with expression more than two fold different to those at passage two. Of these, sixteen were increased and only two decreased. Interestingly, the genes CAV1, CCND1, PLAT and OLFML3 were differentially expressed between passage five and nine and could potentially discriminate MSC's of different culture age. The results would suggest that the transcriptional alterations are part of a common molecular program that occurs beyond passage two and lends support to the findings of a recent study in which the expression of senescence-associated genes was shown to increase with each subsequent passage (40).

We identified genes that explain the decline in proliferation seen in late passage MSC's. Late passage cells showed increased expression of cyclin D1 (CCND1), a key regulator of G1/S transition in the cell cycle and increased levels have been found in fibroblasts undergoing replicative or stress-induced senescence (199-201). In addition, the cyclin dependent kinase inhibitors 1A and 2A (CDKN1A and CDKN2A) were increased at passage nine and imply the activation of both the p53 and p16-pRB pathways. In support, increased expression of SERPINE1 and HMGA1 was also demonstrated in late passage MSC's and both have been identified as downstream targets of these pathways (202;203). HMGA1 proteins are critical components of senescence associated heterochromatin foci (SAHF's)

and function to maintain senescence by the silencing of genes critical for cell growth and proliferation (204). These findings provide further evidence of an increased senescence response during the expansion of MSC's *in vitro*.

Our study identified genes that could enable late passage MSC's to resist apoptosis and tolerate increased levels of oxidative stress. The stanniocalcin, STC2 showed increased expression in late passage cells and is important for normal phosphate and calcium metabolism (205). The expression of STC2 is increased in cells exposed to xenotoxins and reducing agents and knockdown studies reveal increased cell death upon exposure to the same agents (206). Similarly, caveolin proteins such as CAV1 can be induced in cells exposed to oxidising agents and knockdown studies also report an increase cell death (207). In addition, the overexpression of CAV1 can initiate senescence in fibroblasts (208) and increased expression has been demonstrated previously in senescent MSC's (96). In this study, forced over-expression of CAV1 in MSC's resulted in a loss of adipogenic differentiation capacity and the results are similar to that identified in this study when cells underwent prolonged culture. Therefore, CAV1 plays an important role in both the senescence of MSC's and in determining the restriction of lineage fate seen during prolonged expansion.

The increased expression of superoxide dismutase 1 (SOD1) in MSC's was also confirmed at late passage. The protein encoded by this gene is critical for the removal of reactive oxygen species (ROS) and knockout mice display premature ageing and susceptibility to cancer formation due to increased level of ROS (209). It has been demonstrated that MSC's have a low tolerance of oxidative stress (210) and this is supported by a recent study showing that MSC's culture in low oxygen conditions have enhanced proliferative and differentiation capacity (62). These findings would suggest ROS levels are important in the initiation of senescence in MSC's and that increased SOD1 expression may allow late passage cells to tolerate high levels of oxidative stress. Providing further support, knockdown of SOD1 induces premature senescence of fibroblasts confirming a crucial role in reducing intra-cellular ROS and preventing DNA damage that contributes to the initiation of a senescence response (211).

Our study identified genes that would suggest late passage MSC's have inflammatory properties and enhanced ability to remodel the extracellular

matrix. The expression of signal transducer and activator of transcription 1 (STAT1) increased, similar to the findings recently described by Wagner *et al* in a study of MSC's undergoing replicative senescence (40). STAT1 expression increases in response to interferon's and sustained signalling has been demonstrated to initiate senescence in fibroblasts by the activation of p53 (212). High expression of STAT1 in synovial fibroblasts is thought to enhance tissue destruction in patients with active rheumatoid arthritis suggesting that such alterations of MSC properties could have detrimental effects on tissue homeostasis and repair (213). In addition, late passage MSC's were enriched for genes involved in proteolysis and turnover of the extra-cellular matrix. ADAM metallopeptidase with thrombospondin type 1 (ADAMTS1) and tissue plasminogen activator (PLAT) exhibit such properties and have been found at increased levels in patients with neurodegenerative disorders (214) as well as in senescent fibroblasts (215). The role of serine protease 23 (PRSS23), also found at increased levels in late passage MSC's is poorly understood although a proteomic study of ovarian function suggests a critical role in the breakdown of the extra-cellular matrix during normal follicular development (216). In contrast to the pattern of expression by SAGE, the protease cathepsin S (CTSS) was found at significantly decreased levels by RT-PCR. CTSS is important for the remodelling of the vasculature (217) and also the digestion of proteins required for intact MHC Class II immune responses (218). Interestingly, CTSS deficient mice display decreased immune responsiveness and further studies would be required to establish if late passage MSC's have similar changes in their immune characteristics. This could be a mechanism by which senescent MSC's evade immune detection and clearance that could enhance prolonged survival *in vivo*.

Our results have identified other genes whose functions are not completely understood. KIAA1199 was first identified in chromosome transfer experiments that induced senescence in renal cell carcinoma cell lines (219). Further research demonstrated high expression in normal fibroblasts and low levels in the transformed counterparts and cancer cell lines implying this gene may function as a tumour suppressor (220). The results of this study were in contrast to our findings because KIAA1199 expression did not differ in cells of different proliferative history. We detected high levels of expression after passage two while the fibroblast cultures described by Michishita *et al* were assayed beyond thirty eight population doublings. Interestingly, expression was not significantly

different between MSC's at passage five and nine suggesting that this gene may be a marker of cell mortality as implied by the study. Decreased expression of olfactomedin like three (OLFML3) was found in late passage MSC's and this was interesting because this family of secreted proteins are poorly understood. They are typically found enriched in mucus linings, hence their name and are required to maintain the normal properties of the extra-cellular matrix (221). Interestingly, mutations of myocilin which contains an olfactomedin domain results in the accumulation of intracellular proteins that have been implicated in the pathogenesis of age-related glaucoma (222). More recently, it has been suggested that olfactomedins may function as oncogenes because the family member OLFML4 was found highly expressed in pancreatic cancer cell lines. In support, knockdown studies using siRNA were shown to initiate the onset of a senescent phenotype confirming a role of olfactomedins in cell proliferation (223). The results of these studies suggest that decreased expression of OLFML3 in late passage MSC's may fundamentally alter the properties of the cells and maintain growth arrest.

Finally, our results indicate that during the expansion of MSC's a highly consistent pattern of gene expression emerges that can be detected in all cultures and before the onset of growth arrest. The transcriptional alterations follow a common molecular program that would appear to be regulated by the decline in activity of the transcription factor AP-1. Although we only validated one component of this transcription factor (the gene FOS), SAGE identified decreased expression of JUN and would support our findings. AP-1 activity has been shown to increase in fibroblasts in response to physiological stimuli such as oxidative stress although sustained activation eventually results in a decline in activity (193). As some evidence suggests that oxidative stress is a major component of routine MSC culture that can be overcome using media supplemented with selenium (210) or low oxygen conditions (62) it seems plausible that these factors have important effects on the regulation of AP-1 activity. Only recently, Heo *et al* demonstrated that late passage MSC's exposed to oxidants displayed a similar phenotype to those undergoing proliferative stress providing further evidence that ROS and oxidative stress are important factors in the onset of senescence in MSC's during routine culure (68). Therefore, we would speculate that the alterations in gene expression we detected represent a response to culture stress and together with telomere

erosion leads to a decline in the functional properties of MSC's and the onset of senescence.

5.4 Conclusion

Our study has identified a regulatory pathway that controls the transcriptional changes observed during the expansion and senescence of MSC's *in vitro*. We have identified eighteen genes that could be used as markers of senescence or an enhanced senescence response seen during extended culture

Four genes were identified that discriminate the proliferative history of individual MSC cultures and further validation is required in a prospective study. The results enhance our understanding of the molecular mechanisms that regulate proliferation and senescence of MSC's and these markers could be used to ensure quality control of MSC's prior to use in clinical trials or laboratory research. In addition, these markers may be used to optimise existing culture protocols as well as in the development of novel culture techniques.

6 Investigating the Effects of p38 MAPK Mitogen-Activated Protein Kinase Inhibition in MSC's

6.1 Introduction

Pharmacological manipulation of stem cells using small molecules is an attractive approach to investigate the exact function of specific molecular pathways in these cells. In recent years, the Wingless (Wnt) and p38 MAPK mitogen-activated protein kinase (MAPK) pathways have been shown to be important in the regulation of self-renewal and senescence.

Wnt proteins are secreted lipid modified signalling molecules that regulate cell proliferation and cell fate during embryological development. The proliferative effects are largely mediated through the canonical pathway by the binding of extra-cellular Wnt proteins to their cognate receptors, Frizzled (Fzd). This causes inactivation of glycogen synthase kinase-3 (GSK3) which prevents phosphorylation and degradation of the transcription factor, ß-catenin. Subsequently, ß-catenin relocates to the nucleus and drives the expression of proliferative genes such as cyclin D1 or c-Myc. The small molecule (2′Z, 3′E)-6-Bromoindirubin-3′-oxime (BIO) has been identified as a specific inhibitor of GSK3 and shown to mimic Wnt signalling in Xenopus embryo's (224). In a recent study, BIO was used to maintain self-renewal and prevent spontaneous differentiation of mouse and human ESC's *in vitro* (132). In addition, BIO has been shown to enhance proliferation of human CSC's (26) and even rodent cardiomyocytes (225). At the time of this research, the effect of BIO on MSC's had not been reported although the Wnt signalling pathway has been defined in MSC's (226) and is recognised to influence MSC fate (227). Therefore, we wanted to investigate the effect of GSK3 inhibition in MSC's.

The p38 MAPK pathway plays an essential role in the cellular response to inflammatory cytokines and environmental stress. Like other MAPK pathways, the p38 MAPK signalling cascade involves sequential activation of MAPK kinase kinases (MAP3Ks) and MAPK kinases (MKKs). Numerous substrates of p38 MAPK have been identified including other protein kinases, transcription factors and key regulators of the cell cycle (228). A further role of p38 MAPK as a tumour

suppressor has been demonstrated recently. Mice deficient in the downstream gene, p38 MAPK-regulated/activated protein kinase (PRAK) show increased skin carcinogenesis in response to the mutagen, dimethlybezanthracene (DMBA) (229). It was demonstrated that PRAK is essential for the initiation of senescence by the activation of the tumour suppressor, p53. In support, other studies have demonstrated that p38 MAPK is activated in senescent cells *in vitro* in response to telomere shortening, oncogenes and oxidative stress (230). Therefore, it appears p38 MAPK activation is a common pathway to senescence regardless of the initiating mechanism.

The exact insults that result in the activation of p38 MAPK remain poorly understood although reactive oxygen species (ROS) appear increasingly important. HSC's from mice deficient in the ataxia-telangiectasia mutated (ATM) gene lose functional capacity with age and demonstrate high levels of intra-cellular ROS (231). It was shown that anti-oxidants or the small molecule inhibitor of p38 MAPK, 4-(4-Fluorophenyl)-2-(4-methylsulfinylphenyl)-5-(4-pyridyl) 1H-imidazole (SB203580) could prevent this and HSC's maintained the ability to reconstitute haematopoiesis *in vivo*. The contribution of p38 MAPK activation to the premature ageing of other cell types has been demonstrated. In fibroblasts from patients with Werner' syndrome (a premature ageing disease) it was shown that SB203580 could restore proliferation to levels seen in fibroblasts from healthy donors (232). Therefore, it would appear that ROS and the resulting DNA damage may contribute to ageing as a general phenomenon. The results of these studies led us to speculate that p38 MAPK activation could contribute to the decline in stem cell properties of MSC's.

Therefore, we set out to investigate the effects of both drugs on the proliferative capacity of MSC's during prolonged expansion *in vitro*. The results are discussed and contributions from colleagues are acknowledged where appropriate.

6.2 Results

For the experiments described in this chapter, cultures were established from cryopreserved MSC's at passage two recovered overnight and grown in medium containing drug or an equivalent volume of dimethyl sulfoxide (DMSO) as a

control. Medium was replaced twice a week and contained fresh drug or DMSO. The final concentration of DMSO was 0.005% and would not be expected to cause significant cell toxicity.

6.2.1 *Dose Titration of SB203580 and BIO in MSC's*

To obtain data on drug sensitivity, MSC's were treated with SB203580 or BIO in a dilution series and viable cell counts determined after seven days (Figure 6-1). MSC's cultured in SB203580 displayed a proliferative advantage at the concentrations tested although this was not significant in comparison to the controls. MSC's cultured in 1μM of SB203580 underwent more population doublings (PD) in comparison to the controls at seven days although this was not significant (4.36 versus 3.85 PD; p value 0.06). Viability of cultures was always greater than 95% suggesting the concentration of SB203580 used was not toxic to the cells.

A greater range of concentrations of BIO was tested based on the amounts described in previous studies (26;132;225). MSC's cultured in 3nM to 1μM BIO showed similar proliferation to the controls whereas 3μM and 10μM BIO significantly inhibited MSC proliferation (Figure 6-1B). At these concentrations, MSC's altered cell morphology with some cells long and tubular, and others large and flat. The appearances raised the possibility of differentiation or the onset of senescence although further studies were not performed.

Due to time constraints and the variable effect of BIO on MSC's it was decided to focus our research on the effect of SB203580 in detail. Five MSC cultures (donors 23, 25, 27, 28 and 29) with average proliferation were cultured continuously in either 1μm SB203580 or an equivalent volume of DMSO (control). The concentration was selected based on the manufacturers suggested IC_{50} (50nM to 600nM) as well as the slight proliferative advantage seen at this concentration. Research on Werner's syndrome fibroblasts and HSC's used much higher concentrations (10μM) of SB203580 although this increases the possibility of off target effects which have not been considered in these studies (207;231;232).

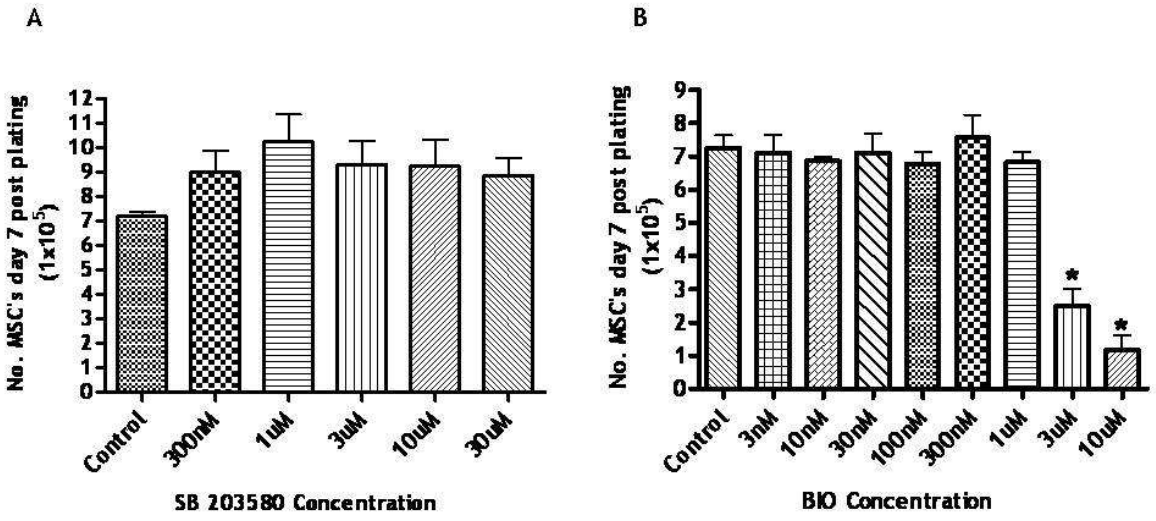

Figure 6-1 Dose titration of a p38 MAPK and GSK3 inhibitor in MSC's

MSC's at passage two were cultured in medium containing varying concentrations of SB203580 or BIO. Bars represent the mean viable cell counts obtained from three donor MSC cultures in either drug. Error bars represent the standard deviation. Comparisons were made to controls using a paired student's t-test; p value ≤ 0.05 *.

6.2.2 SB203580 Does Not Alter Cell Cycle Rate of MSC's

To determine if SB203580 altered the rate of cell division in MSC's we used the CellTrace™ CFSE Cell Proliferation Kit (Molecular Probes, Invitrogen). This was a gift from Heather Jorgensen, post doctorate within the research group of Professor T. Holyoake. Carboxy-fluorescein diacetate succinimidyl diester (CFSE) is a colourless dye that passively diffuses into cells and remains non-fluorescent until the acetate groups are removed by intracellular esterases. The resulting carboxyfluorescein succinimidyl ester is highly fluorescent and reacts with intracellular amines to form fluorescent conjugates that are retained by the cell. CFSE is partitioned equally between daughter cells during cell division and as a result high resolution tracking of cell division can be monitored by the reduction in fluorescence seen using flow cytometry.

Early passage MSC's were labelled with CFSE and cultured in MSC medium containing either SB203580 or DMSO for five days. In some flasks, mitomycin C was used to inhibit cell proliferation and determine the maximum level of fluorescence known as $CFSE_{max}$. The remaining flasks were analysed on day one, three and five and the results shown in Figure 6-2. There was increased uptake of CFSE in SB203580 treated cells compared to controls despite similar incubation times (Geometric mean $CFSE_{max}$ (FL1) 480.2 ± 195.7 and 284.5 ± 106.8 respectively; p value 0.09). Representative overlay histograms for the controls (Figure 6-2A) and SB203580 treated cells (Figure 6-2B) demonstrate this finding. It was noted that the fluorescence curves were spread out unlike the distinct peaks seen during cell division of HSC's. This was thought to reflect the heterogeneity in MSC size and granularity (FSC and SSC properties) as well as variation in the rate of dividing cells and the absolute number of cells that entered or exited the cell cycle.

The number of PD's was determined using the formula: $PD = (\log_{(\text{Geometric mean CFSE max - Geometric mean unstained cells})} - \log_{(\text{Geometric mean CFSE Day x - Geometric mean unstained cells})}) / \log 2$. The results showed that SB203580 treatment did not alter the cell cycle rate of MSC's (Figure 6-2C). In fact, the control cells had proliferated to a greater extent than drug treated cells at day three (3.5 ± 0.5 versus 2.7 ± 0.6; p value 0.06) although at day five the results were similar (5.0 ± 0.3 versus 4.8 ± 0.5; p value 0.40).

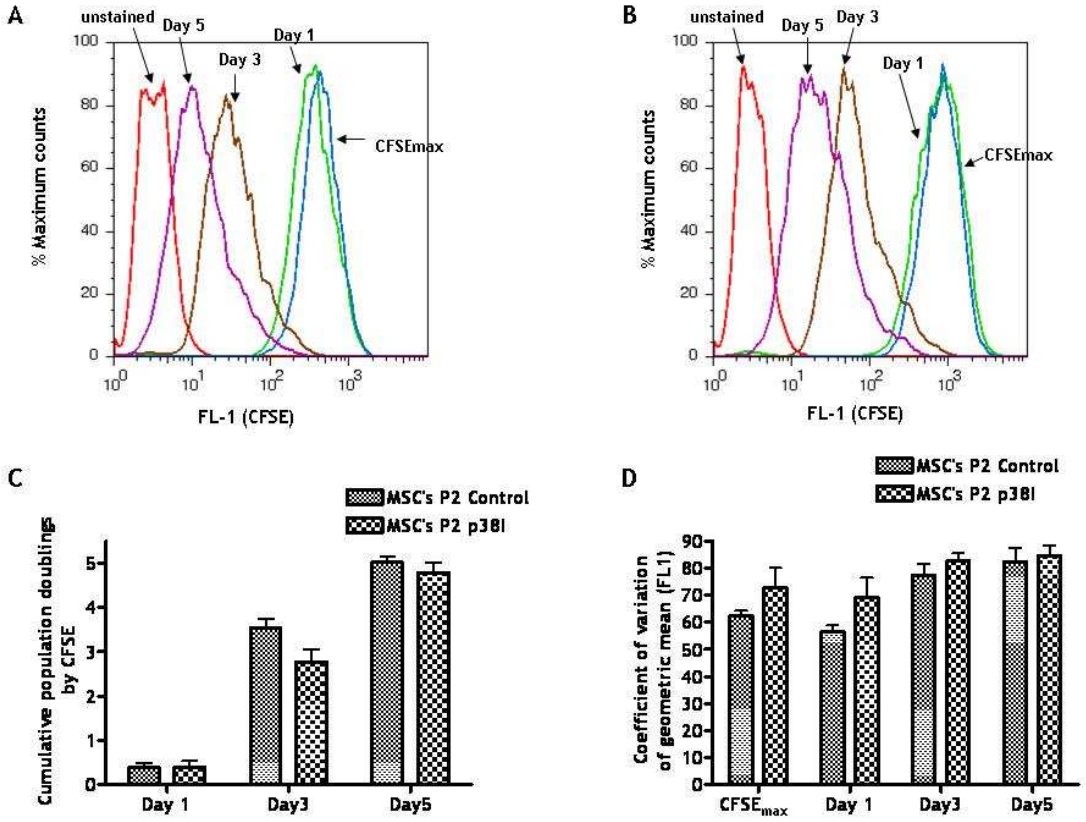

Figure 6-2 SB203580 does not alter cell cycle properties of early passage MSC's

The rate of cell division in MSC's was determined by flow cytometry using the CellTrace™ CFSE Cell Proliferation Kit (Molecular Probes, Invitrogen). Representative overlay histograms of control (A) and SB203580 treated (B) cells are shown. The mean population doublings were calculated at each time point using the formula PD = log (Geometric mean CFSE max - Geometric mean unstained cells) – log (Geometric mean CFSE Day x – Geometric mean unstained cells)) / log 2 (C). The coefficient of variation of fluorescence was calculated at each time point (D). Bars represent the overall mean from five donor MSC cultures. Error bars represent the standard deviation. Comparisons were made to controls using a paired student's t-test.

It was noted that by CFSE, MSC's achieved one additional PD compared to that calculated using viable cell counts (PD = ($\log_{\text{(no. MSC's harvested)}} - \log_{\text{(no. MSC's plated)}}$) / log 2). This would support the findings in chapter 3 where it was shown that by CFE-F less than 50% of MSC's retain progenitor potential and therefore only half the plated cells undergo further cell division.

To ensure that SB203580 did not alter the characteristics of the dividing population the coefficient of variation (CV) of the mean fluorescence was determined for drug treated cells and their respective controls (Figure 6-2D). There was no significant difference between drug treated MSC's or the controls which confirmed that SB203580 does not alter cell cycle properties or number of dividing MSC's during short-term exposure.

6.2.3 SB203580 Increases the Proliferative Capacity of MSC's

If p38 MAPK activation is important for senescence in MSC's, we predicted that MSC's cultured in SB203580 should proliferate to a greater extent than those in control media. MSC's from five donors underwent serial passage in the presence or absence of SB203580 until the control cells reached the ninth passage. In this experiment, it was not possible to expand MSC's from donor 23 beyond passage eight. Drug treated cells were expanded beyond nine passages to determine the onset of growth arrest which was defined as a failure to reach near confluence after thirty days. The growth curves for donors 23, 25, 27 and 28 (Figure 6-3 A-D) and donor 29 (Figure 6-4A) are shown separately to aid visualisation of the results. SB203580 increased the proliferation of all cultures in comparison to the controls although the drug was less effective in donor 27.

The overall mean results from the experiments are summarised in Figure 6-4 B + C. Between passage two and six, drug treated MSC's proliferated at a similar rate to the controls although at passage nine, drug treated cells maintained their proliferation. As a consequence, MSC's treated with the drug were cultured for a shorter period before reaching passage nine (56 ± 7 days versus 71 ± 14 days; p value 0.09) and underwent significantly more PD's (23.9 ± 2.3 versus 18.2 ± 3.5; p value 0.02).

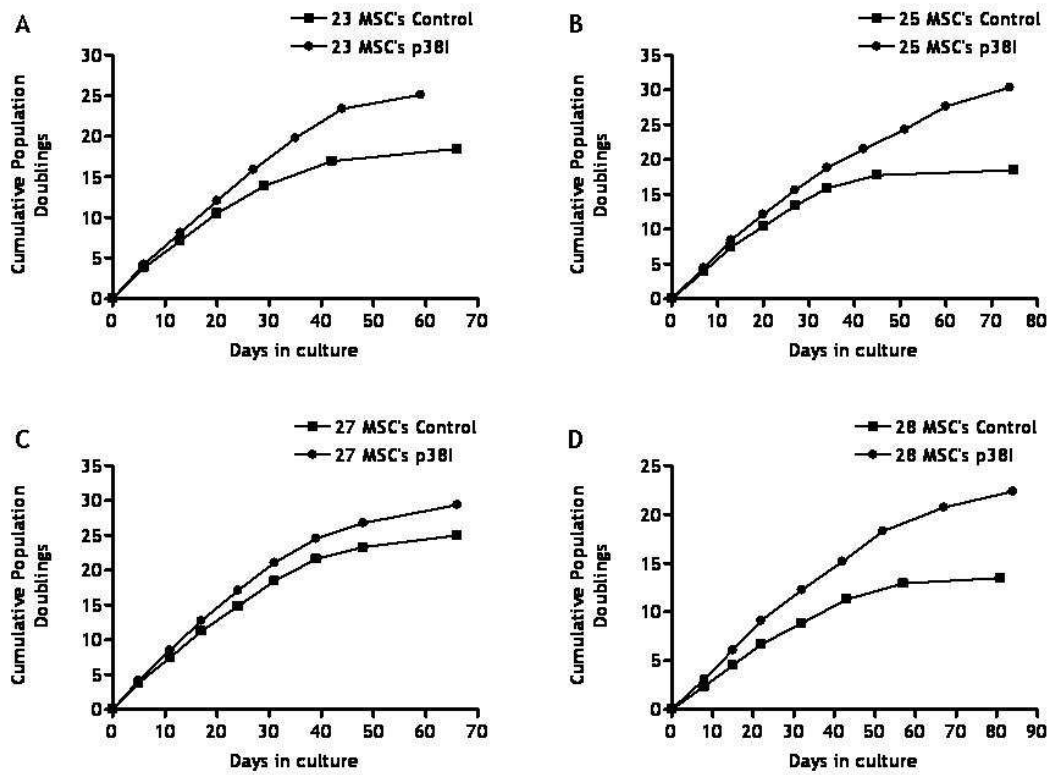

Figure 6-3 SB203580 enhances the long term proliferative capacity of MSC's

MSC's from donors 23 (A), 25 (B), 27 (C) and 28 (D) were cultured in medium containing either 1μM SB203580 or an equivalent volume of DMSO. Population doublings were determined from viable cell counts at each passage. PD = (log $_{\text{(no. MSC's harvested)}}$ − log $_{\text{(no. MSC's plated)}}$) / log 2.

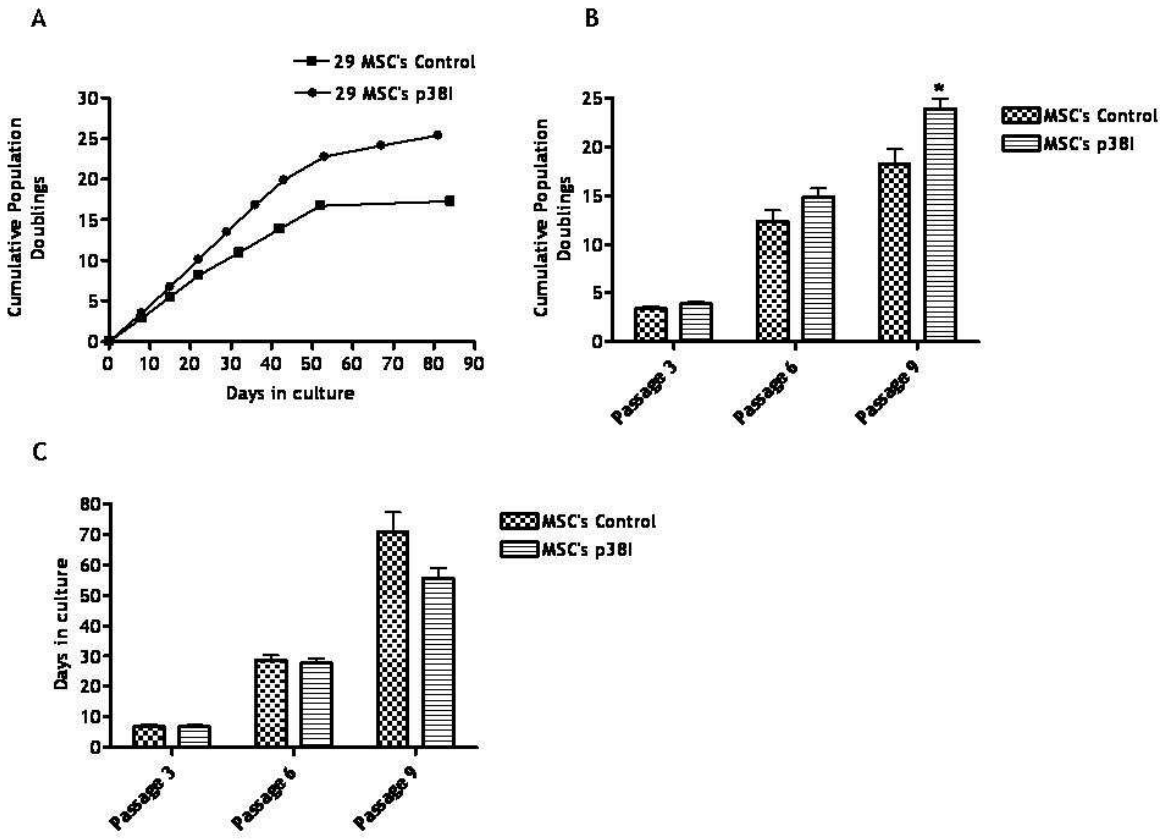

Figure 6-4 SB203580 enhances the proliferative capacity of MSC's

MSC's from donor 29 (A) were cultured in medium containing either 1μM SB203580 or an equivalent volume of DMSO. Population doublings were determined from viable cell counts at each passage. PD = (log $_{\text{(no. MSC's harvested)}}$ − log $_{\text{(no. MSC's plated)}}$) / log 2. Cumulative population doublings (B) and time in culture at different passages (C) are shown. Bars represent the overall mean from five donor MSC cultures. Error bars represent the standard deviation. Comparisons were made to the controls using a paired student's t-test; p value ≤ 0.05 *.

This was equivalent to a 32% increase in proliferation at passage nine and a 43% increase when drug treated cells were compared to controls at the onset of growth arrest (26.5 ± 3.3 versus 18.5 ± 4.2; p value 0.01). By our estimations, cultures treated with 1μM SB203580 from isolation could potentially achieve 50 PD's before growth arrest. The proliferative lifespan would therefore be similar to that described in studies on MSC's derived from from young donors (11;12)

6.2.4 SB203580 Preserves Progenitors and Osteogenic Differentiation in Late Passage MSC's

To investigate if SB203580 altered the number of MSC progenitors in long-term cultures, the CFE-F assay was performed at passages three, six and nine (Figure 6-5). At passage three, the mean percentage of cells forming colonies was similar between drug treated cells and the controls (36.9 ± 6.1 % versus 36.6 ± 6.2 %; p value 0.90). At passage six, significantly more colonies were observed in drug treated cells from two donors (23 and 25) although the overall results from the five cultures were similar to the controls (18.9 ± 3.0 % versus 16.7 ± 3.9 % respectively; p value 0.1). However, at passage nine drug treated cells from donors 23, 25, 28 and 29 contained significantly more colonies and the overall results were significantly different to the controls (7.1 ± 3.5 % versus 3.7 ± 3.0 % respectively; p value 0.01). The results demonstrate that SB203580 maintains MSC progenitors with colony-forming potential during expansion.

In chapter three, it was demonstrated that MSC's display a reduction in differentiation capacity at late passage. Therefore, late passage MSC's cultured in the presence or absence of SB203580 were tested for their ability to undergo adipogenic and osteogenic differentiation. During differentiation, the drug was not added to the medium and after three weeks cells were stained using either Oil Red O or Alizarin Red S. Representative images from the adipogenic differentiation experiment are shown in Figure 6-6. Drug treated cells from donors 25 and 29 maintained the ability to undergo adipogenic differentiation compared to their respective controls (Figure 6-6 F+B, I+J)). However, this effect was not observed in the other donor cultures which lost adipogenic differentiation ability to a similar extent than the controls.

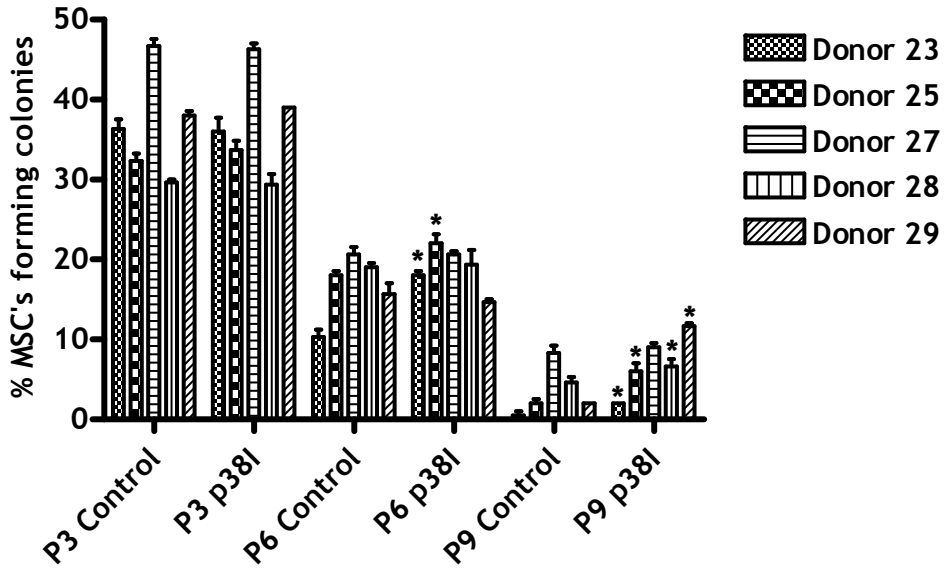

Figure 6-5 SB203580 preserves the progenitor potential of MSC cultures during expansion

MSC's were cultured in medium containing either SB203580 or an equivalent volume of DMSO. The CFE-F assay was performed in triplicate on MSC's at passage three, six and nine. Colonies were stained with Giemsa and those containing at least twenty cells counted. Bars represent the mean percentage MSC's forming colonies. Error bars represent the standard deviation. Comparisons were made to the controls at each passage using a paired student's t-test; p value ≤ 0.05 *.

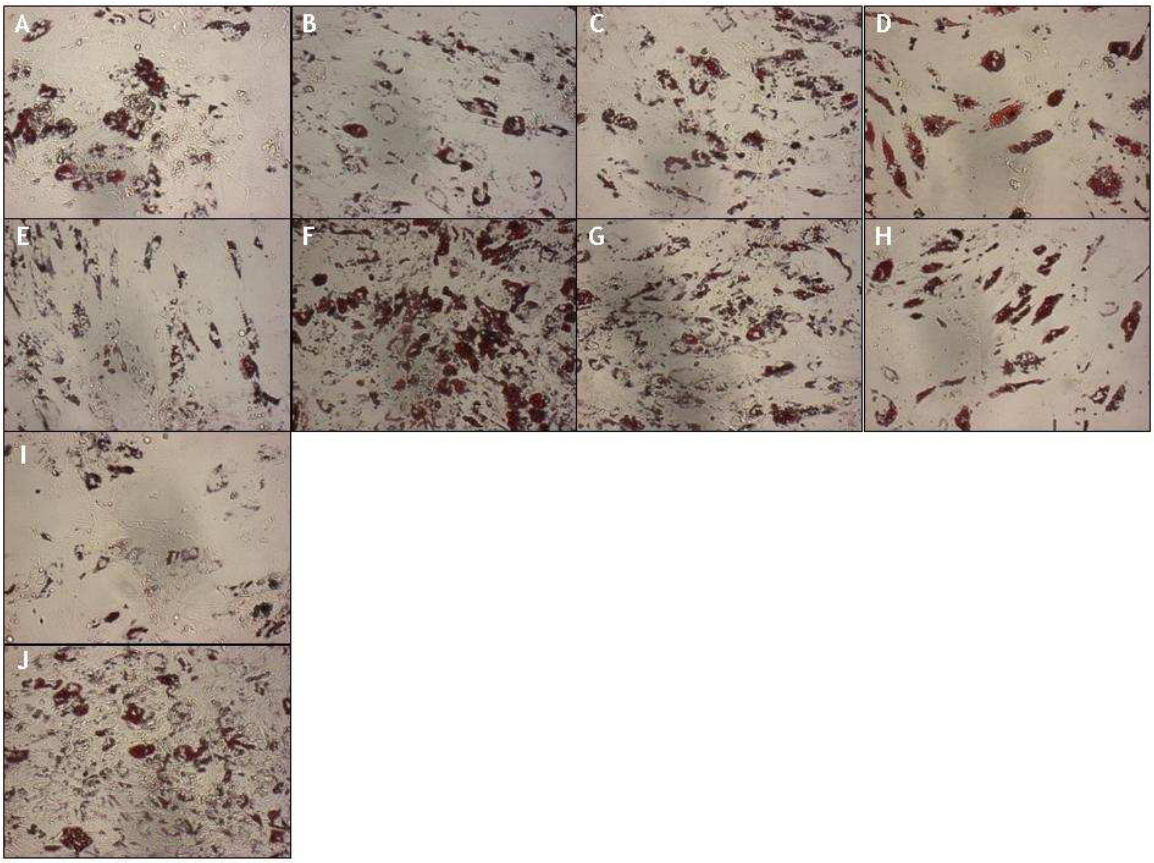

Figure 6-6 SB203580 had variable effects on the adipogenic differentiation capacity of MSC's at late passage

MSC's were cultured in medium containing either SB203580 or an equivalent volume of DMSO until late passage. Cells were then re-plated at 100% confluence and cultured for three weeks in adipogenic differentiation medium without the drug. Representative images are shown of MSC's from donors 23, 25, 27, 28 and 29 treated with DMSO (A-D, I) or SB203580 (E-H, J). Lipid is stained red using Oil Red O (4x magnification).

In contrast, four of the SB203580 treated cultures showed increased amounts of staining with Alizarin Red S in comparison to the controls and confirmed that osteogenic differentiation capacity was maintained during expansion (Figure 6-7). The best examples were MSC's from donors 25 and 29 (Figure 6-7 F+J) and similar to the previous experiment, SB203580 appeared ineffective on cells from donor 27. Together with the CFE-F assay, the results suggest that SB203580 could potentially preserve an osteogenic progenitor population during expansion and a modified version of the CFU-F could be used to investigate this further (167).

6.2.5 SB203580 Does Not Prevent Telomere Erosion but Decreases the Expression of SA β-Gal at Late Passage

In chapter three it was demonstrated that telomere erosion and the expression of senescence associated ß-galactosidase (SA ß-Gal) was a characteristic feature of late passage MSC's. Therefore, both methods were used to investigate the effects of SB203580 during prolonged expansion of MSC's. Genomic DNA was extracted from late passage cells and used in the mTRF length assay. Telomere lengths were determined from a single Southern blot by densitometry (Figure 6-8). There was insufficient material from the control cells of donor 25 and therefore excluded from further analysis. The method and results were produced by Sharon Burns, research assistant within the group of Professor W.N Keith.

First, we compared the telomere lengths of the controls to their counterparts not subject to a freeze-thaw cycle as described in chapter three. The results were almost identical which confirmed our MSC's undergo growth arrest at a critical telomere length (6.2 ± 1.2 kB versus 6.0 ± 0.8 kB; p value 0.82).

Furthermore, drug treated cells at late passage had similar mean telomere lengths to controls providing further evidence that 6kB is the critical telomere length of MSC's used in our study (5.9 ± 1.1 versus 6.2 ± 1.2 kB; p value 0.73). To account for differences in the proliferative history of SB203580 treated and control MSC's, the rate of telomere loss was calculated for each group and the results were similar (70.5 ± 67.8 bp/PD versus 73.3 ± 73.2 bp/PD; p value 0.96).

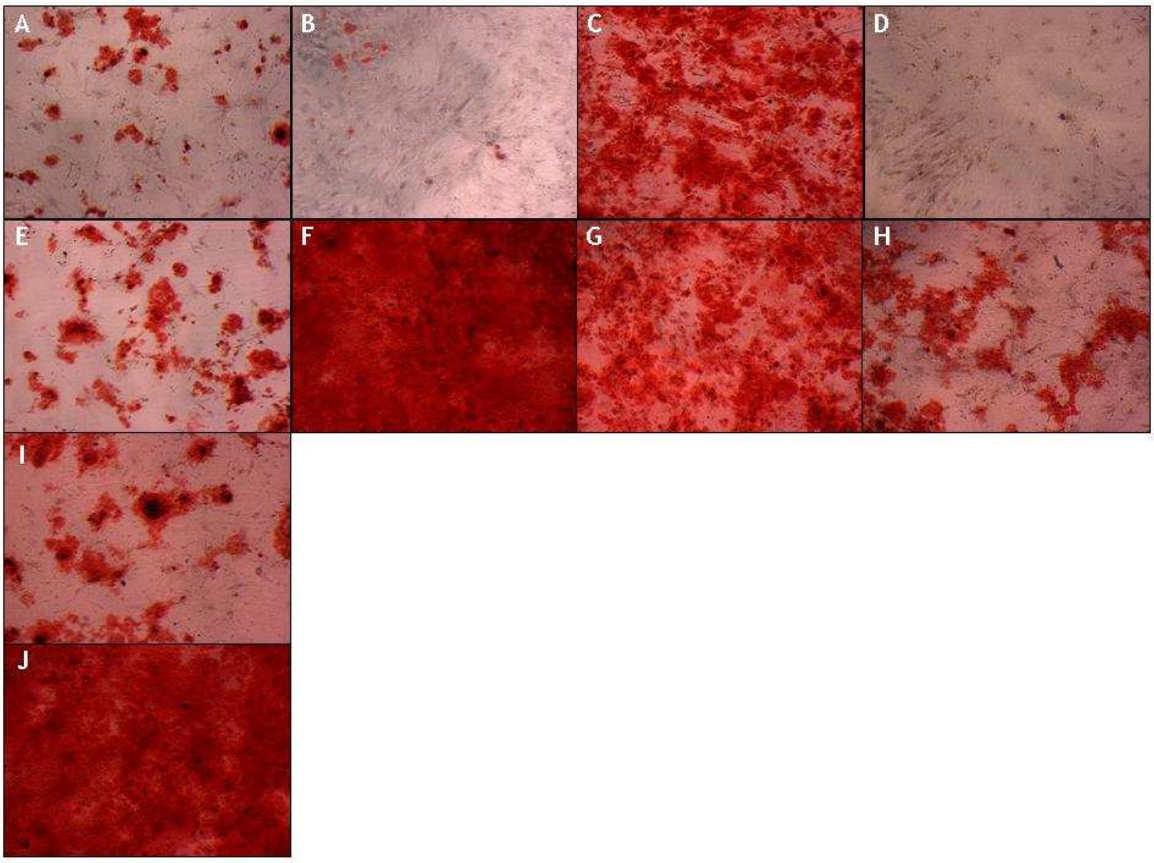

Figure 6-7 SB203580 maintained the osteogenic differentiation capacity of MSC's at late passage

MSC's were cultured in medium containing either SB203580 or an equivalent volume of DMSO until late passage. Cells were then re-plated at 70% confluence and cultured for three weeks in osteogenic differentiation medium without the drug. Representative images are shown of MSC's from donors 23, 25, 27, 28 and 29 treated with DMSO (A-D, I) or SB203580 (E-H, J). Calcium is stained red using Alizarin Red S (4x magnification).

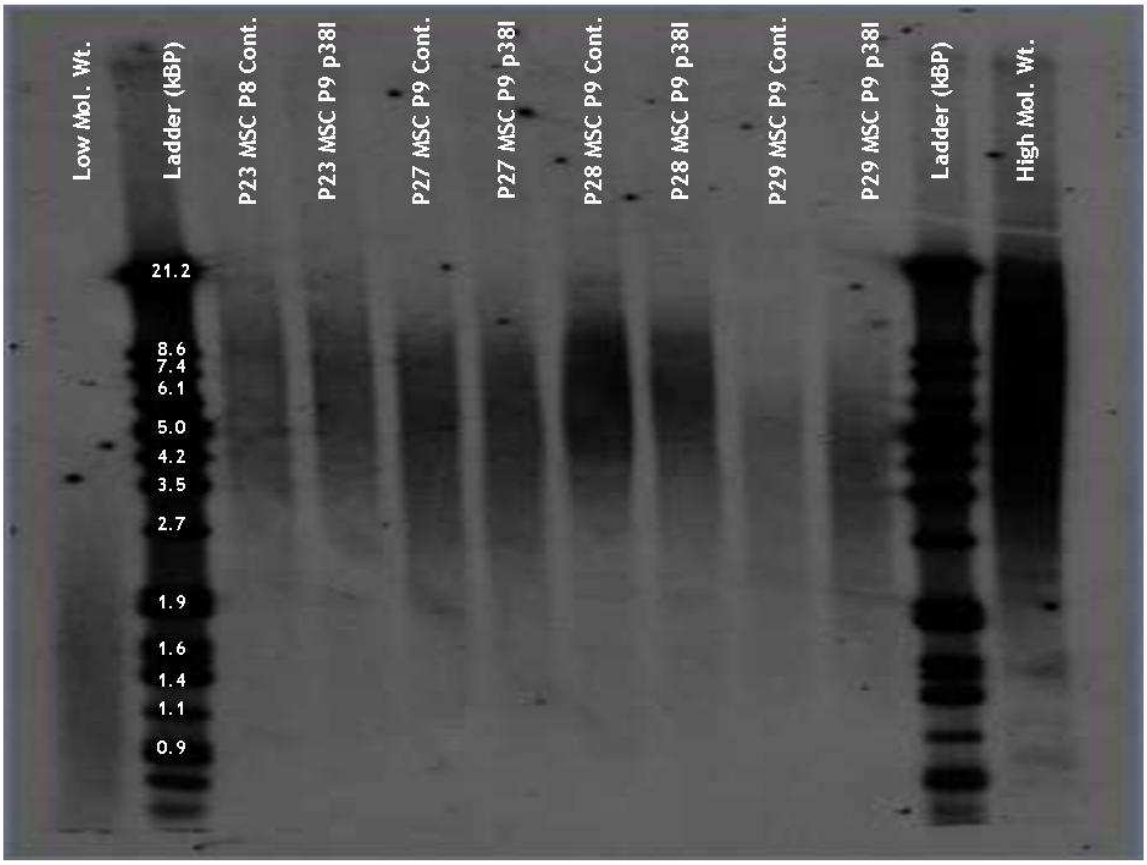

Figure 6-8 SB203580 does not prevent telomere erosion in MSC's during expansion

Genomic DNA was extracted from late passage MSC's cultured in medium containing either SB203580 or an equivalent volume of DMSO and telomere lengths determined using the TeloTAGGG telomere length assay (Roche Diagnostics Ltd) and displayed on a single blot. Telomere lengths were calculated from the blot by densitometry following the manufacturer's protocol. Undigested high and low molecular weight DNA and molecular ladders are shown.

The large standard deviation can be explained by heterogeneity in the rate of telomere loss between different donor MSC's. Donor 27 displayed the lowest and donor 29 the highest rate of telomere shortening in this study (mean 12.7 ± 12.8 and 161.9 ± 4.0 bp/PD respectively).

MSC's at late passage were stained for SA ß-Gal expression at pH 6.0 using the Senescent Cells Staining Kit (Sigma) and the percentage of cells determined using the same methods described in chapter three (Figure 6-9). MSC's treated with SB203580 showed significantly decreased expression of SA ß-Gal at late passage in comparison to the controls (19.4 ± 11.9 % versus 54.2 ± 13.4 %; p value <0.001).

6.2.6 Assessment of DNA Damage in MSC's

Histone H2AX is phosphorylated rapidly and extensively to form γ-H2AX in response to agents that cause DNA double strand breaks (233). In addition, the detection of γ-H2AX in the nuclei of senescent human fibroblasts has confirmed that telomere shortening or dysfunction can initiate a DNA damage response (DDR) (234). MSC's displayed significant telomere losses during expansion and it was decided to determine the expression of γ-H2AX as a surrogate marker of DNA damage.

In the first study, the expression of γ-H2AX was determined by flow cytometry using the H2A.X Phosphorylation Assay Kit (Upstate, Millipore). Drug treated cells from donor 25 were treated with mitomycin C and hydrogen peroxide to generate positive controls. In addition, the human promyelocytic leukemia cell line (HL-60) was used as a positive control because it was known to display high rates of apoptosis and therefore, γ-H2AX. The cell line was a gift from the research group of Professor T. Holyoake. Representative histograms of the results are shown for control and SB203580 treated MSC's (Figure 6-10 A+B). The signal from the nuclear expression of γ-H2AX was low as demonstrated by the small shift in mean fluorescence between isotype and γ-H2AX stained cells. Therefore, we determined the mean cell fluorescence using the formula: geometric mean γ-H2AX stained cells - geometric mean isotype stained cells.

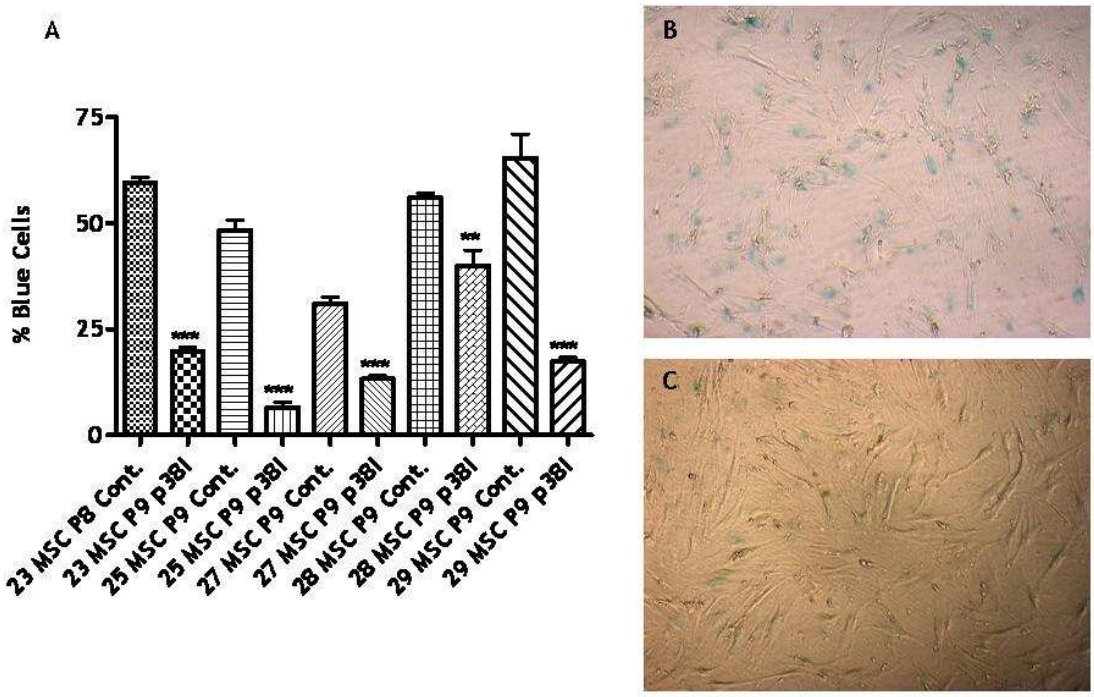

Figure 6-9 SB203580 decreased expression of SA β-Gal in late passage MSC's

MSC's were cultured in medium containing either SB203580 or an equivalent volume of DMSO until late passage. The activity of the enzyme SA β-Gal was assessed at pH 6 using the Senescent Cells Staining Kit (Sigma). At least 300 cells were counted in random fields in order to determine the mean percentage of SA β-Gal (blue) positive cells (A). Error bars represent the standard deviation. Comparisons were made to the controls using a paired student's t-test; p value ≤ 0.001 ***. Representative images from control (B) and SB203580 treated (C) cultures are shown (4x magnification).

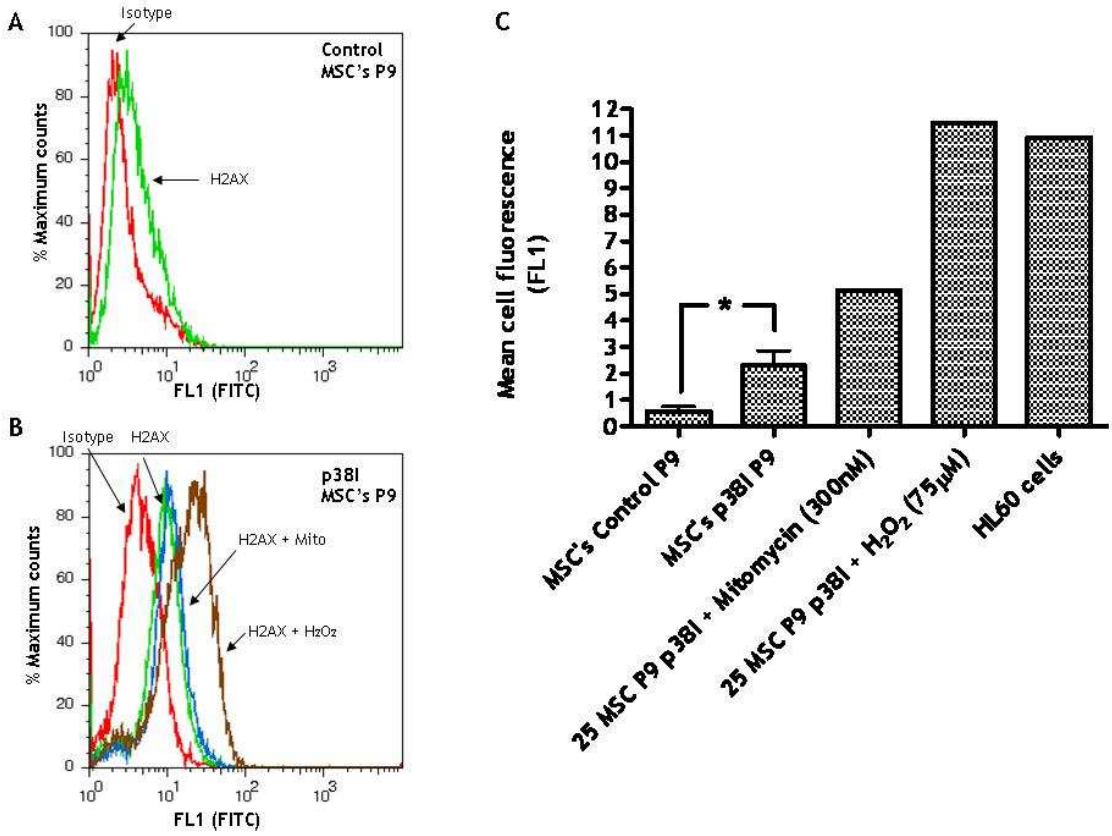

Figure 6-10 SB203580 treated MSC's show increased DNA damage using the marker γ-H2AX

MSC's were cultured in medium containing either SB203580 or an equivalent volume of DMSO until late passage. Expression of γ-H2AX was determined by flow cytometry using the H2AX Phosphorylation Assay Kit (Upstate, Millipore). Representative overlay histograms are shown of control (A) and SB203580 treated MSC's including those treated with mitomycin C and hydrogen peroxide (B). The expression of γ-H2AX is represented as the change in mean fluorescence (geometric mean γ-H2AX stained cells - geometric mean isotype stained cells) (C). Bars represent the mean of five control and drug treated MSC cultures. Positive controls and the HL-60 cell line were obtained from a single experiment. Error bars represent the standard deviation. Comparisons were made between drug treated and control MSC's using a paired student's t-test (p value ≤ 0.05 *)

This method was previously described in a study to detect intra-nuclear hTERT by flow cytometry where the returning fluorescence signal was noted to be weak (235). The results are summarised in Figure 6-10 C. SB203580 treated MSC's expressed significantly more γ-H2AX compared to controls cells (mean cell fluorescence 2.31 ± 1.24 versus 0.57 ± 0.40; p value 0.02). Much higher levels of γ-H2AX were detected in MSC's exposed to DNA damaging agents and in the HL-60 cell line. The results suggest that SB203580 treated MSC's exhibit higher levels of DNA damage during expansion than the controls.

Because this method appeared to have a low sensitivity the expression of γ-H2AX was also determined using immunofluorescence. This experiment had to be performed using cryopreserved cells because it was performed when the long-term cultures had finished and time constraints meant it was impossible to repeat the whole experiment. Early passage cells were used as negative controls and positive controls were obtained by inducing DNA damage with hydrogen peroxide or ultra-violet (U.V) irradiation. In this experiment, to improve detection we used an unconjugated γ-H2AX monoclonal antibody detected with a FITC-conjugated secondary (Figure 6-11). γ-H2AX was detected in the nuclei of 4.7 ± 1.4 % MSC's at passage two and 15.1 ± 5.8 % and 13.8 ± 5.0 % of at late passage cultured with or without SB203580, respectively. The results were not significantly different and did not support the findings by flow cytometry although this experiment has obvious limitations.

It was noted that most nuclei contained only one or two γ-H2AX foci which would account for the low signal detected by flow cytometry. In contrast, MSC's exposed to either hydrogen peroxide or U.V irradiation had multiple γ-H2AX foci and some cells appeared to have initiated DNA fragmentation and apoptosis. Together, the results demonstrate that MSC's show increased levels of DNA damage during their expansion compared to early passage cultures. The flow cytometry experiment revealed that SB230580 allowed the accumulation of DNA damage and inhibited normal DNA damage responses allowing the cultures to proliferate to a much greater extent than the controls.

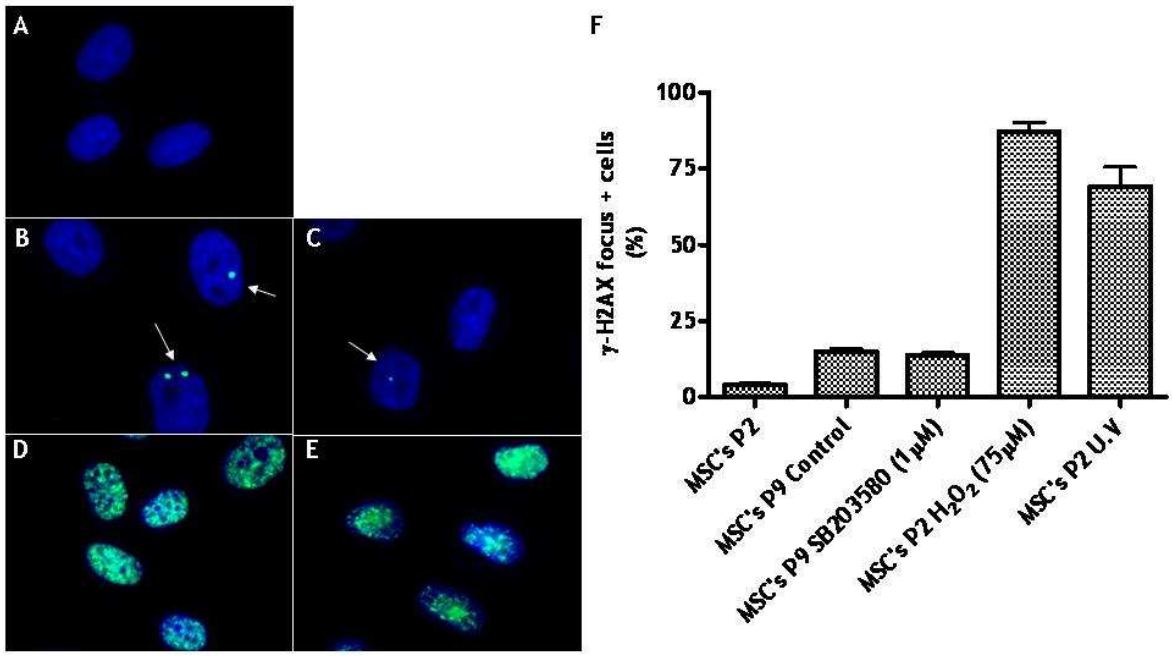

Figure 6-11 γ-H2AX was expressed as discrete nuclear foci in MSC's

The expression of γ-H2AX was determined by immunofluorescence in MSC's at: early passage (A); late passage controls (B); late passage treated with SB203580 (C); passage two exposed to ultra-violet irradiation (D); and passage two exposed to hydrogen peroxide (E). On average, more than 200 cells were counted in random fields to determine the mean percentage of γ-H2AX positive cells (F). Bars represent the mean results from five donor cultures. The results for MSC's at passage two were obtained from a single experiment. Error bars represent the standard deviation. Comparisons were made between drug treated and control MSC's using a paired student's t-test (not significant). White arrows show discrete γ-H2AX foci stained green (FITC) and nuclei are blue (DAPI) (100x magnification).

6.2.7 SB203580 Treatment Does Not Alter the Expression of Genes Associated with MSC Ageing

The gene expression profile of late passage MSC's cultured with or without SB203580 were determined using the same TLDA's as described in chapter five. The results can be found in the appendix (Table 12). The standard deviation of the cycle thresholds of ACTB, GAPDH, POLR2A, RPLP0 and UBC were calculated (1.2, 1.1, 0.6, 0.7 and 0.6, respectively) from all samples to ensure UBC remained a suitable control. The RQ of gene expression was calculated using the formula $2^{-\Delta\Delta C}{}_T$ with baseline expression determined in MSC's at passage two.

To determine if cryopreservation altered the expression profile of late passage MSC's the TLDA results were compared to cells from the same donors cultured from initial isolation and not subjected to a freeze-thaw cycle (data not shown). Using a paired student's t-test, only GAPDH showed a significant decrease in expression in cultures established from cryopreserved cells (mean RQ 0.5 ± 0.3 versus 1.0 ± 0.4; p value 0.05). By linear regression, the r^2 value was 0.7 (95% confidence intervals) which gave us confidence that MSC's in this experiment displayed similar transcriptional alterations to those identified in chapter five

The genes identified in chapter five as differentially expressed in late passage MSC's were compared in SB203580 treated cells and their respective controls. The levels of expression were not significantly different and the sixteen genes with increased expression at late passage are shown in Figure 6-12 and Figure 6-13 and the two that decreased expression shown in Figure 6-14. There was a non-significant increase in expression of HMGA1 (RQ 10.4 ± 9.3 versus 4.6 ± 5.4), KIAA1199 (RQ 12.2 ± 11.0 versus 7.8 ± 6.6) and desmoplakin (DSP) (RQ 7.9 ± 4.7 versus 4.5 ± 2.9) in drug treated MSC's. There was a non-significant decrease in expression of PLAT (RQ 17.0 ± 10.7 versus 27.0 ± 31.4), CAV1 (RQ 3.6 ± 1.1 versus 5.6 ± 5.1), PRSS23 (RQ 2.4 ± 1.2 versus 3.7 ± 1.7) and STAT1 (RQ 3.6 ± 1.9 versus 6.3 ± 5.2).

Previous studies have identified both CAV1 (207) and STAT1 (236) as transcriptional targets of p38 MAPK and the slight reduction of expression in drug treated MSC's suggested some inhibition of this pathway.

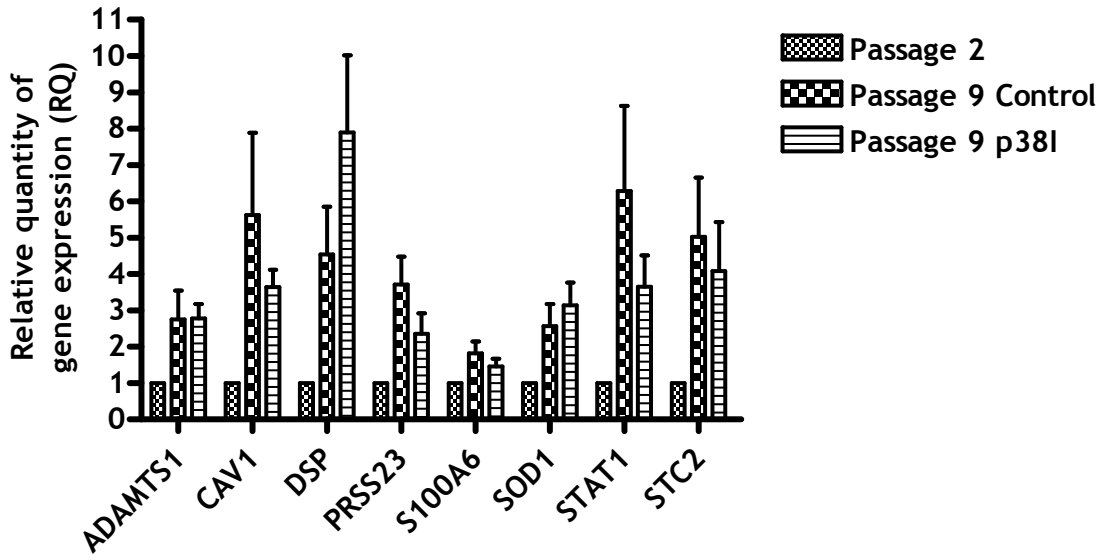

Figure 6-12 SB203580 does not alter the expression of genes associated with MSC ageing

RQ values were calculated using the $2^{-\Delta\Delta C}{}_T$ method with baseline expression determined in MSC's at passage two and normalised to the control, UBC. Comparisons were made between SB203580 treated and control cells using a paired student's t-test (not significant). Bars represent the mean RQ value from five donor cultures; each gene was measured in duplicate. Error bars represent the standard deviation.

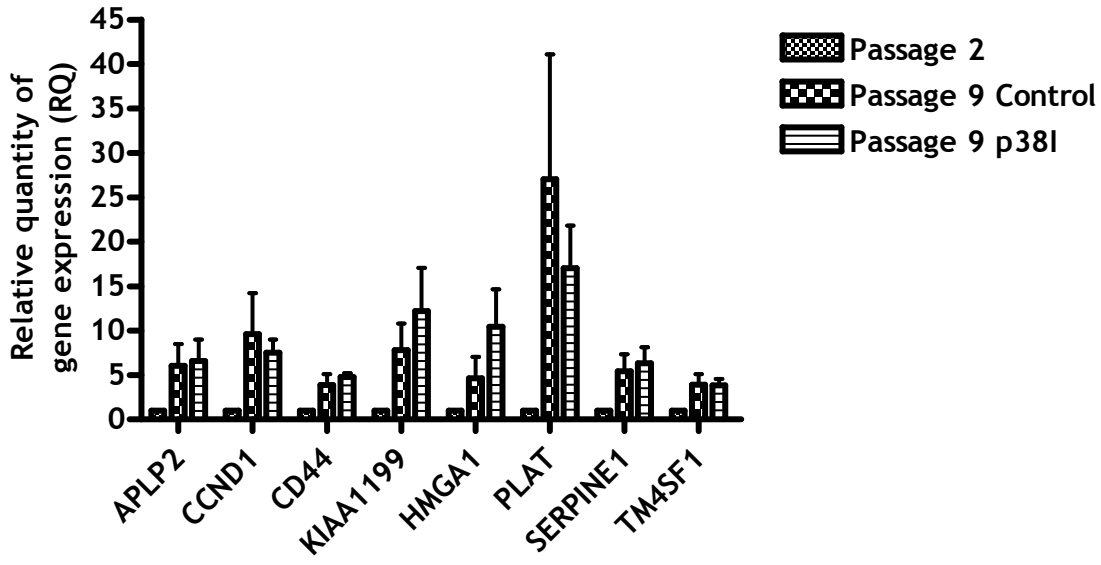

Figure 6-13 SB203580 does not alter the expression of genes associated with MSC ageing

RQ values were calculated using the $2^{-\Delta\Delta C}{}_T$ method with baseline expression determined in MSC's at passage two and normalised to the control, UBC. Comparisons were made between SB203580 treated and control cells using a paired student's t-test (not significant). Bars represent the mean RQ value from five donor cultures; each gene was measured in duplicate. Error bars represent the standard deviation.

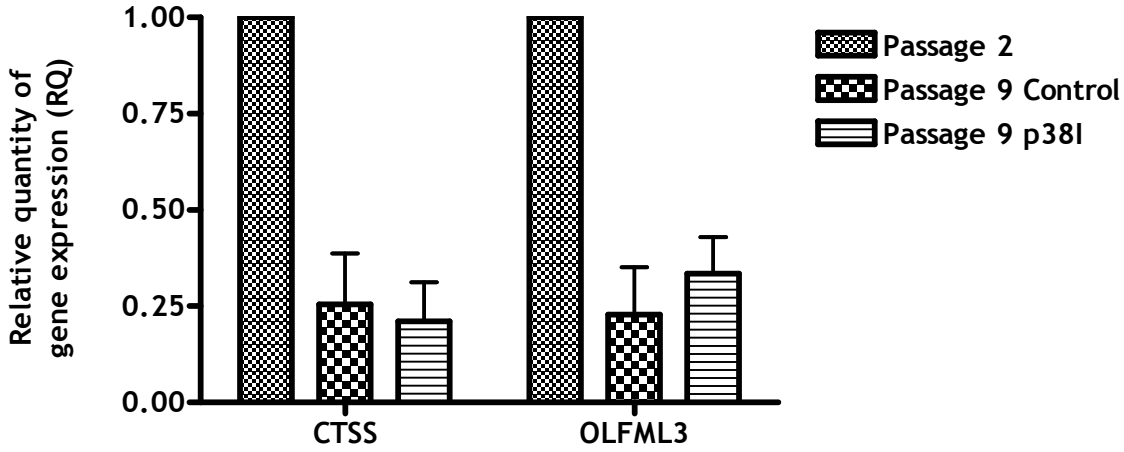

Figure 6-14 SB203580 does not alter the expression of genes associated with MSC ageing

RQ values were calculated using the $2^{-\Delta\Delta C}{}_T$ method with baseline expression determined in MSC's at passage two and normalised to the control, UBC. Comparisons were made between SB203580 treated and control cells using a paired student's t-test (not significant). Bars represent the mean RQ value from five donor cultures; each gene was measured in duplicate. Error bars represent the standard deviation.

On the TLDA were genes described as targets of p38 MAPK from earlier studies including connective tissue growth factor (CTGF), heat shock 70kDa protein 8 (HSPA8), interleukin 6 signal transducer (IL6ST), prostaglandin-endoperoxide synthase 2 (PTGS2) and transglutaminase-2 (TGM2) (237-239). It was disappointing that none were expressed at levels significantly different to the controls (Figure 6-15). TGM2 was expressed at increased levels in drug treated cells compared to the controls (5.0 ± 4.8 versus 2.4 ± 2.0), in contrast to the decreased expression seen in the study by Zer *et al* using rodent fibroblasts (237).

We also determined the expression of the cell cycle genes CDKN1A, CDKN1B, CDKN2A and FOS because the drug treated MSC's showed a proliferative advantage when compared to controls (Figure 6-16). The results were similar in both groups although CDKN2A was expressed at lower levels in the SB203580 treated MSC's. A similar effect of SB203580 was demonstrated in HSC's from ATM deficient mice suggesting that p38 MAPK can regulate the $p16^{INK4a}$ – Rb pathway although the exact mechanisms have not been determined (231).

To account for the fact that drug treated MSC's had proliferated to a much greater extent, the RQ of gene expression per population doubling was calculated and compared to that of the controls (data not shown). Only the expression of PRSS23 significantly decreased in SB203580 treated MSC's compared to the controls (mean RQ/PD 0.10 ± 0.09 versus 0.20 ± 0.05, p value 0.04). The results confirmed that SB203580 treated MSC's expressed a similar transcriptional signature to the controls at late passage and highlight the need to determine the exact transcriptional targets of SB203580 and the p38 MAPK pathway in MSC's.

Another issue is that our results are based on mRNA analysis and many of these proteins are known to be regulated by post-translational modifications so it remains entirely possible that the function of many of these proteins was dramatically altered by SB203580 treatment despite similar levels of mRNA expression. Therefore, further study of the protein levels of the genes we validated is essential to support or refute the results obtained by TLDA.

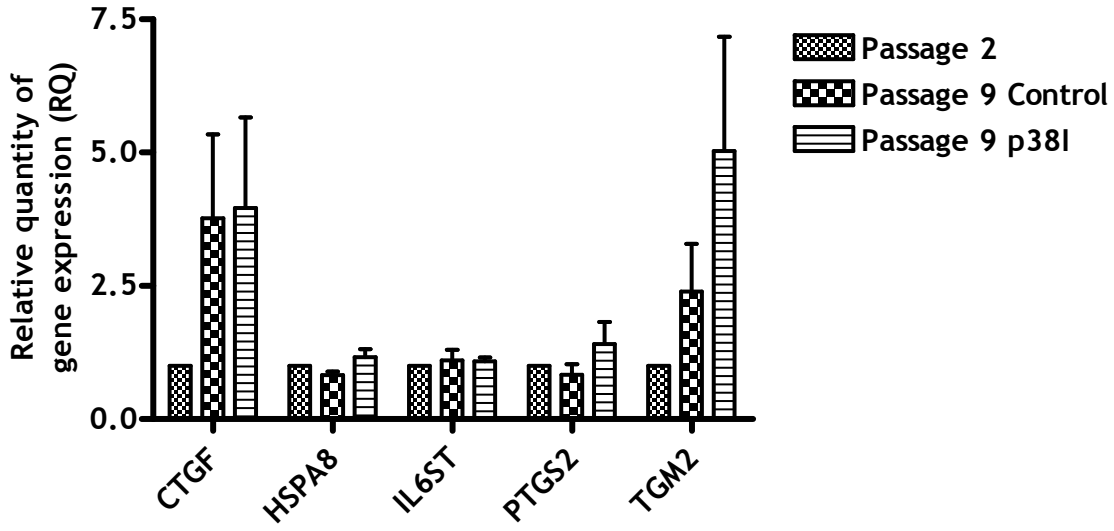

Figure 6-15 SB203580 does not alter the expression of putative p38 MAPK target genes in MSC's at late passage

RQ values were calculated using the $2^{-\Delta\Delta C}{}_T$ method with baseline expression determined in MSC's at passage two and normalised to the control, UBC. Comparisons were made between SB203580 treated and control cells using a paired student's t-test (not significant). Bars represent the mean RQ value from five donor cultures; each gene was measured in duplicate. Error bars represent the standard deviation.

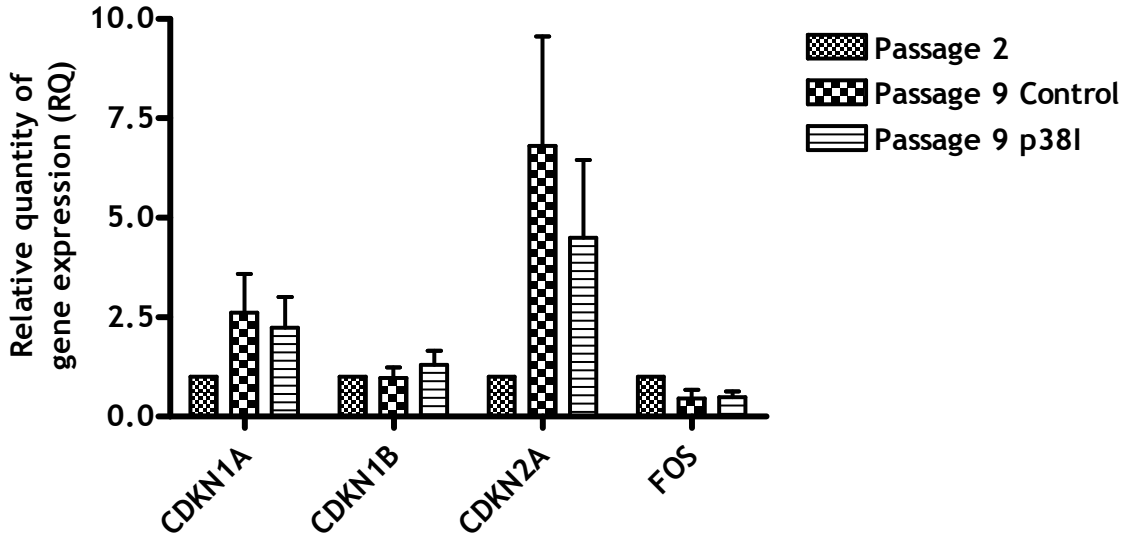

Figure 6-16 SB203580 does not alter the expression of cell cycle genes in MSC's at late passage

RQ values were calculated using the $2^{-\Delta\Delta C}{}_T$ method with baseline expression determined in MSC's at passage two and normalised to the control, UBC. Comparisons were made between SB203580 treated and control cells using a paired student's t-test (not significant). Bars represent the mean RQ value from five donor cultures; each gene was measured in duplicate. Error bars represent the standard deviation.

6.2.8 SB203580 Suppresses p38 Kinase Activity in Late Passage MSC's

The protein studies were kindly performed by Alan Bilsland, a post doctorate within the research group of Professor W.N. Keith as described in an earlier publication (240). To assess the status of the p38 MAPK pathway, protein was extracted from MSC's grown in the presence or absence of SB203580 and probed with antibodies specific for p38 MAPK and its activating phosphorylation (Figure 6-17). Interestingly, the levels of phosphorylated p38 MAPK were highest in SB203580 treated cells from donors 23 and 27 which would suggest that the drug concentration used was insufficient to prevent p38 MAPK activation or alternative activating pathways exist. This finding is in agreement with a study on fibroblasts derived from Werner's syndrome patients treated with the same drug (232). Much lower levels were detected in the controls although we have not analysed protein levels in early passage cells to confirm that p38 MAPK activation increases during prolonged expansion of MSC's. This is a major limitation to the interpretation of the results from this experiment.

The protein, v-akt murine thymoma viral oncogene homolog 1 (AKT) is a target of both the phosphoinositide 3-kinase (PI-3 kinase) and p38 MAPK pathway (241;242). As shown in Figure 6-17, the phosphorylation of AKT was suppressed by SB203580 in MSC's from donor 28. However, levels were similar to the controls in other cultures. The protein levels of macrophage stimulating 1 (MST1), which is known to be upstream of p38 MAPK were also determined as shown in the blot (243). The findings were similar in that phosphorylation of MST1 was suppressed in SB203580 treated cells from donors 23 and 29, but not those from donor 28.

Together, our results demonstrate that SB203580 can inhibit kinases upstream and down stream of p38 MAPK but does not prevent its activation. The variable targeting of the p38 MAPK appeared dependent on the donor cells themselves suggesting different susceptibility to the drug. Off target effects have also been considered and in MSC's from donor 28 we have identified that SB203580 can inhibit the c-Jun N-terminal kinase (JNK) pathway as well (data not shown). More detailed experiments are required to determine the exact effects of SB203580 on the MAPK pathways in MSC's.

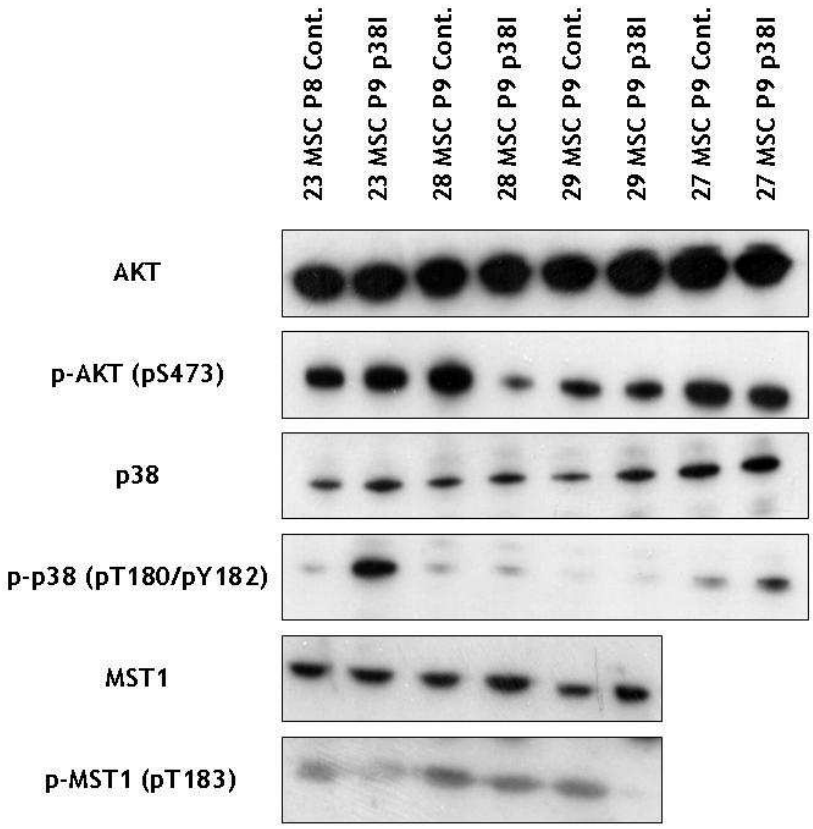

Figure 6-17 SB203580 has variable effects on the p38 MAPK pathway in MSC's

MSC's were cultured in medium containing either SB203580 or an equivalent volume of DMSO until late passage. Protein was extracted and western blotting performed using phospho-specific antibodies to detect AKT phosphorylation on Serine^{473} [(p-AKT (pS473)], p38 MAPK phosphorylation on Threonine^{180} and Tryosine^{182} [(p-p38 MAPK (pT180/pY182)] and MST1 phosphorylation on Threonine^{183} [p-MST1 (pT183)]. Blots for total protein are also shown (AKT, p38 MAPK and MST1). Each blot is representative of a single experiment.

6.2.9 SB203580 Treatment Causes Genomic Alterations in Late Passage MSC's

By inhibiting a normal senescence response, we speculated that SB203580 treatment may increase genomic instability in MSC's. Therefore, array comparative genomic hybridization (aCGH) was used to detect chromosomal deletions or duplications in the genome of MSC's. The technique was performed by Stacey Hoare, research assistant within the research group of Professor W.N. Keith. Genomic DNA was extracted from late passage cells cultured with or without the drug and labelled with cyanine using the Genomic DNA Enzymatic Labelling Kit (Agilent Technologies). 1µg of labelled DNA was then analysed using the Human Genome CGH Microarray Kit 244A (Agilent Technologies) following the manufacturer's protocol (www.agilent.com/chem/goCGH). In addition, reference DNA (Promega) was used as sex-matched controls. Each microarray contains over 236,000 biological probes sourced from UCSC hg 18 (NCBI Build 36) allowing a resolution of approximately 8.9 kB. The results were generated using CGH Analytics software (Agilent Technologies).

The samples for this study included cells from four donors (23, 27, 28 and 29) treated in the presence or absence of SB203580. When the control cells were compared to reference DNA, very few duplications or deletions were identified (Figure 6-18). This would suggest that MSC's retain a high degree of genomic stability during expansion in keeping with the results of a previous study that used aCGH and chromosomal analysis on late passage MSC's (85). However, on review of the sex chromosomes a loss of the Y chromosome in control cells from donor 28 was identified (data not shown). We were confident that this was not a mix up with cells from female donor 29 because a complete duplication of the X chromosome would have been observed when compared to sex-matched reference DNA.

In the comparison of SB203580 treated cells and the controls the results raised some concern (Figure 6-19). The drug treated cells displayed high levels of genomic instability with predominantly chromosomal duplications rather than deletions. The exact significance is uncertain because none of these cultures showed evidence of transformation when cultured for two weeks after growth arrest.

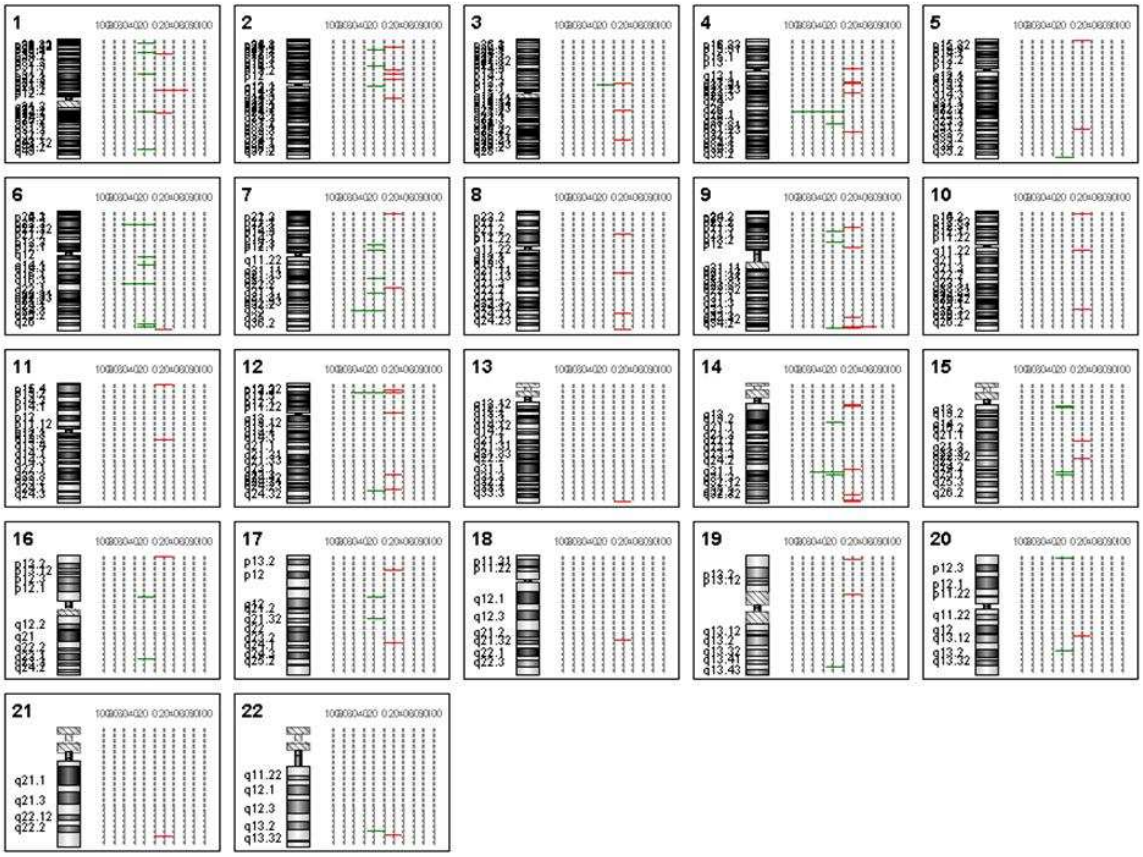

Figure 6-18 Control MSC's maintain genomic stability at late passage

Genomic DNA was extracted and labelled from control MSC's at late passage (donors 23, 27, 28 and 29). 1µg was analysed using the Human Genome CGH Microarray Kit 244A (Agilent Technologies). The results were compared to sex-matched reference DNA (Promega) using CGH Analytics software (Agilent Technologies). Chromosomal regions containing duplications (red) and deletions (green) are highlighted.

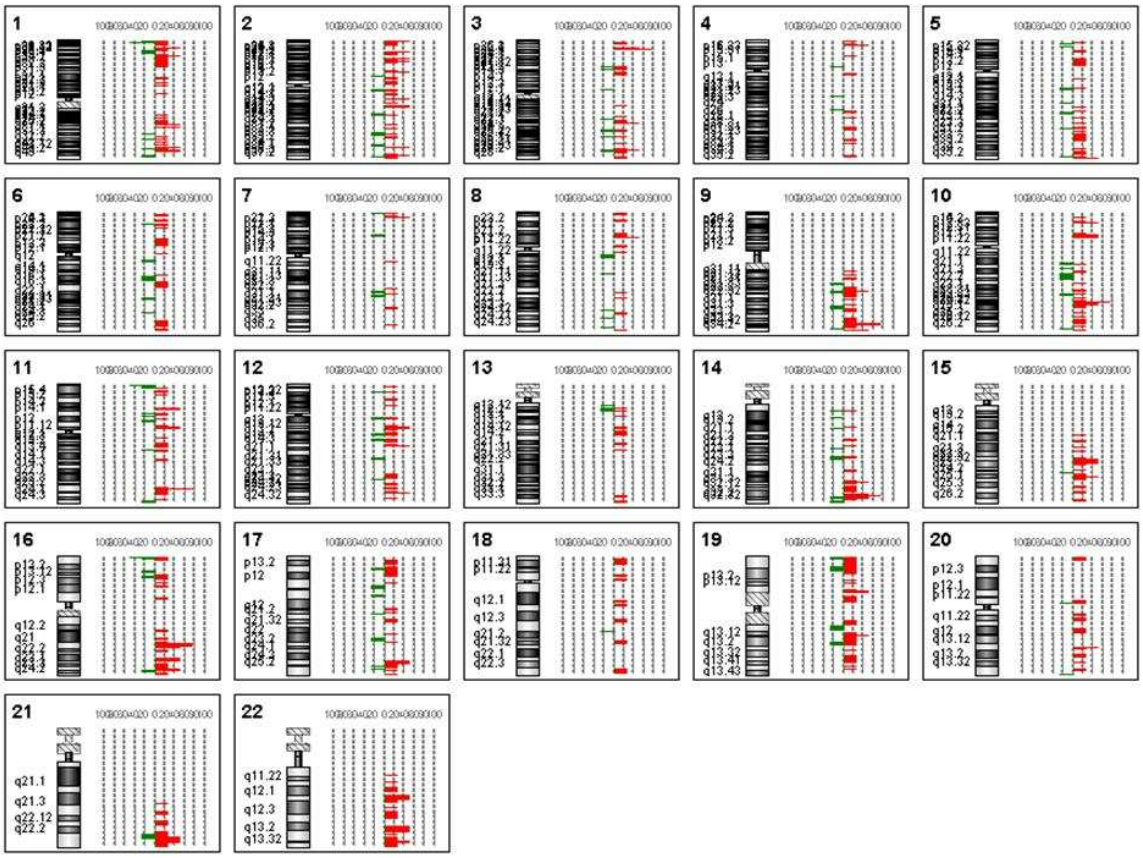

Figure 6-19 MSC's treated with SB203580 show increased genomic instability at late passage

Genomic DNA was extracted and labelled from SB203580 treated MSC's at late passage (donors 23, 27, 28 and 29). 1µg was analysed using the Human Genome CGH Microarray Kit 244A (Agilent Technologies). The results were compared to control MSC's using CGH Analytics software (Agilent Technologies). Chromosomal regions containing duplications (red) and deletions (green) are highlighted.

Unfortunately, it was not possible to to commit additional time to analyse these results in depth. It would be of interest to examine the chromosomal regions of tumour suppressor genes and also the genes identified as markers of aged MSC's. However, these genes were not differentially expressed when compared to the controls by TLDA which would make it unlikely that duplications or deletions occurred in their respective chromosomal regions.

6.3 Discussion

In contrast to results seen in other cell types BIO did not enhance the proliferation of MSC's cultured short term in the presence of the drug (26;132;225). Tateishi *et al* treated CSC's with 10nM BIO and demonstrated a 50% increase in the number of Ki67 positive cells when grown as cardio-spheres. CSC's in this study had similar surface marker and gene expression profile to that described for MSC's so it was surprising the drug did not produce a similar effect. In fact, BIO appeared toxic at high concentrations and significantly inhibited MSC proliferation and our results are similar to the effects recently described in adipose-derived MSC's (244). The morphological changes suggested BIO may have induced differentiation or senescence of MSC's and recent evidence confirms a role of Wnt proteins in the onset of senescence. The knockdown of Wnt2 by siRNA can induce SAHF formation and senescence of human fibroblasts (245) and MEF's grown in Wnt3a conditioned media have been shown to senesce prematurely (246). Therefore, the extent and duration of Wnt signals may be the most important factor in determining the effect of this pathway in different cell types.

The studies using SB203580 provide preliminary evidence that the p38 MAPK pathway can contribute to the decline in proliferation and differentiation capacity of MSC's during expansion *in vitro*. The growth rate and replicative lifespan of the cells were significantly increased when cultured in the presence of SB203580 and at levels seen in MSC's derived from young donors (11;12). In effect, SB203580 maintains the proliferative rates seen in early passage cells and the growth curves are shifted up. By CFSE, we determined that the proliferative advantage was not due to an increase in cell cycle rate. In the study by Davis *et al* using Werner's syndrome fibroblasts, SB203580 was shown to decrease the number of fibroblasts that exited the cell cycle during expansion measured by

the incorporation of bromodeoxyuridine as a marker of DNA synthesis (232). We suspect the drug has a similar effect on MSC's and performing an identical experiment is required to confirm this. In keeping with the results of the same study, SB203580 treated MSC's appeared smaller than their controls and fibroblast growth factor-2 (FGF-2) has been shown to have a similar effect on the morphology of MSC's (64;247). Therefore, the increase in proliferation seen in drug treated cells could be explained by an increase in cell density at confluence because of the smaller size or even loss of contact inhibition. The smaller size of drug treated cells would also explain the increased brightness seen when SB203580 treated MSC's were incubated for a similar time in CFSE as the controls. Alternatively, SB203580 may alter the properties of the cell membrane and therefore alter the penetration of the dye.

It was demonstrated that SB203580 treated cells retained progenitor potential at late passage and would suggest that p38 MAPK contributes to the loss of functional capacity of MSC's. The results are supported by studies on HSC's from ATM deficient mice and Werner's syndrome fibroblasts where SB203580 was shown to maintain both function and proliferative lifespan of these cell types (231;232). Earlier studies on MSC's have identified small rapidly self-renewing (RS) cells in culture that have the greatest proliferative potential which leads us to speculate that these cells are exhausted during expansion *in vitro* (32). The lack of specific markers to identify and isolate such cells is a major limitation in the field although the combination of Stro-1 and CD106, or the marker CD271 (LNGFR) have shown the most promise in studies to date (191;248). Using flow cytometry and cell sorting based on cell size or these surface markers could enable the effects of SB203580 to be determined on MSC subsets in an attempt to explain our findings in greater depth.

In addition to maintaining the number of colony forming cells at late passage, SB203580 treated MSC's maintained the ability to undergo osteogenic differentiation which typically decreased during expansion. If this effect resulted from the increase in progenitors in drug treated cultures, these cells appear similar to a subset of MSC's expressing the marker Stro-1 that display enhanced osteogenic differentiation capacity (167). Further experiments whereby a modified version of the CFU-F assay is used to assess adipogenic or osteogenic progenitors would enable us to determine the exact effects of

SB203580 on the pluripotency and maintenance of MSC progenitors during expansion. Another possibility is that SB203580 maintained MSC's in an undifferentiated state and prevented the lineage restriction that typically occurs during expansion. In support, genes associated with the p38 MAPK pathway are found enriched in differentiated MSC's when compared to their undifferentiated counterparts using microarray (144). Furthermore, another study has shown that the JNK inhibitor SP600125 can prevent osteogenic differentiation of MSC's when cultured in osteogenic media confirming that other MAPK pathways are important in regulating MSC differentiation (249). This is particularly relevant because we found some evidence that SB203580 had activity on this pathway despite the low concentrations used in our attempt to minimise off-target effects. The ability to preserve the osteogenic differentiation capacity of MSC's either through maintenance of the undifferentiated state or preservation of osteogenic progenitors has relevance in the application of MSC's for the treatment of bone diseases and would merit further research (3).

SB203580 treated cells showed similar rates of telomere shortening which was initially surprising given the increased proliferation of these cultures. The rate of telomere shortening in other cell types has been shown to vary depending on ambient oxygen levels, with the lowest rates observed in low oxygen conditions (168). One possibility is that SB203580 maintained the telomere length of a progenitor population within MSC cultures. This population may be so small that it is not possible to detect differences in telomere length using the TeloTAGG mean telomere length assay. Using flow cytometry and cell sorting based on specific surface markers or cell size as described earlier could enable telomere lengths to be determined in single cells using specialised techniques methods previously reported (250).

Of some concern was that drug treated cells continued to proliferate despite a similar critical telomere length as the controls. The results infer that SB230580 inhibited a normal telomere-initiated senescence response. We noted that in this experiment the controls had a mean telomere length of 6kB which was similar to our earlier studies. In a previous study, MSC's were shown to undergo senescence at a critical telomere length of approximately 10kB (11). This discrepancy is hard to explain although it does question the relevance of telomere length in determining the proliferative capacity of MSC's. It would

also suggest telomere dysfunction itself may be more important. Further support that SB203580 treatment may enable MSC's to inhibit a normal senescence response was provided by the gene expression studies. Using TLDA's, SB023580 did not prevent the characterisitic gene expression changes seen in late passage MSC's cultured without the drug. It is difficult to interpret the exact significance of this result as it would have been better to compare the expression profiles of drug treated cells and controls after an equivalent number of population doublings. This may have confirmed that SB203580 prevented the expression of ageing associated genes in MSC's and that the assay time point missed this difference. If a similar result was obtained from this experiment it would confirm that SB203580 does not prevent the onset of a senescence phenotype at the transcriptional level. A detailed analysis of global gene expression of MSC's treated with SB203580 compared to controls using SAGE or microarray is required to confirm the exact targets of this drug in MSC's. Although known p38 MAPK targets, CAV1 and STAT1 showed decreased expression this provides only indirect evidence that SB203580 was targeting this pathway (207;236). Given that our analysis was based on mRNA expression and many of these proteins are regulated by post-translational modifications, further experiments are required to determine protein levels of some of these genes in SB203580 treated MSC's.

The limited protein studies peformed did provide some evidence that SB203580 was targeting the p38 MAPK pathway in MSC's although the results were not clear cut. Depending on the donor cells used, SB203580 was shown to inhibit the upstream kinase MST1 and downstream substrate AKT. However, activation of p38 MAPK itself was not inhibited and actually increased in some cultures. A similar effect of SB203580 has been observed in Werner's syndrome fibroblasts although the effects on upstream kinases were not investigated in this study (232). The time point chosen to assay p38 MAPK activity also appears crucial because a study using fibroblasts treated with powerful oxidants showed that SB203580 prevented premature senescence by the inhibition of p38 MAPK phosphorylation when assayed 48 hours after exposure (207). Few studies have determined the effects of this drug in cells during continous exposure and expansion *in vitro*. Therefore, our results provide the basis for further studies to unravel MAPK signalling pathways and establish their exact role in the senescence of MSC's *in vitro*. Given the limitations of our results further

experiments are required to consolidate these findings. Firstly, it needs to be demonstrated by protein studies that p38 MAPK activation is a feature of long term culture of MSC's. The variable sensitivity of different MSC cultures to the drug suggests that studies to determine the IC_{50} for each different donor MSC's are also required. It seems likely that individual donor cells require specific concentrations of SB203580 to ensure a consistent effect. It would then be easier to determine the effects of SB203580 on proteins involved in the p38 and other MAPK pathways using moderate throughput techniques such as powerblots. Together with gene expression profiling studies and identifying transcriptional targets of SB203580 for validation it would be possible to confirm or refute our findings with greater confidence.

By flow cytometry we demonstrated that MSC's treated with SB203580 showed increased levels of DNA damage in comparison to the controls and therefore, p38 MAPK activation may be critical for normal DNA damage responses in MSC's. It was concerning that these cells were still proliferating in the context of increased accumulation of DNA damage and shortened telomeres. The results provide further evidence that p38 MAPK inhibition may prevent a normal senescence response and is supported by both *in vitro* (230) and *in vivo* studies (229). The flow cytometry method appeared to have poor sensitivity and it was unfortunate that the immunofluorescence studies were not performed at the same time. This would have provided additional confirmation of our results although another possibility is that protein studies could be performed retrospectively to detect γ-H2AX on archived cell pellets that were generated from SB203580 treated and control MSC's.

The array CGH study provided further evidence that intact p38 MAPK signalling is required to maintain genomic stability in MSC's. The controls showed minimal chromosomal alterations in comparison to the reference DNA and would support the findings of a previous study using aCGH and chromosomal analysis on late passage cells (85). The loss of chromosome Y in donor 28 was unexpected and we believed this may have arisen *in vitro* because a similar change was not seen in the drug treated counterparts. Interestingly, the loss of chromosome Y is a common finding in the bone marrow compartment with advanced age and in patients with myelodysplastic syndrome although the exact clinical significance remains unknown (251;252). In contrast, MSC's treated with SB203580 displayed

marked genomic instability with predominantly chromosomal duplications. We suspected that these changes may have arisen in a progenitor cell population and the potential risk would be that SB203580 could increase susceptibility to further genetic events that could result in cell transformation. It has been recognised that human (13;14) and mouse (253;254) MSC's can undergo transformation *in vitro*. Furthermore, MSC's transduced with hTERT have been shown to undergo transformation after prolonged culture due to both chromosomal losses and epigenetic events (83). Together with our results this highlights that the tight regulation of proliferation in MSC's and senescence is critical for the maintenance of genomic stability in conditions of cellular stress. Of note, p38 MAPK inhibitors are currently under development for the treatment of inflammatory conditions such as rheumatoid arthritis and we would speculate that such agents could in fact increase susceptibility to the development of cancer itself (255). The identification of side population cells in mesenchymal tumours such as sarcomas provide further evidence that these cancers may originate in MSC's and our results highlight the importance of p38 MAPK activation in the initiation of a senescence response *in vitro*. Comparison of publicly available aCGH data derived from mesenchymal tumours would be of interest to determine if a pattern of chromosomal changes can be identified with similarities to those seen in SB203580 treated MSC's.

6.4 Conclusion

We have identified that inhibition of p38 MAPK using the small molecule SB203580 can prevent the decline in proliferation and differentiation of MSC's during expansion. Confirming a potential tumour suppressor role of p38 MAPK treatment with SB203580 allowed the accumulation of genomic instability in MSC cultures possibly as a consequence of impaired DNA damage responses in a progenitor cell population. Our results provide some evidence that MSC's are aged prematurely in response to undefined cellular stress that activate the p38 MAPK pathway and identifying these insults should improve understanding of MSC ageing and enhance the ability to use MSC's in cell therapy approaches.

7 Summary and Conclusions

Mesenchymal stem cells (MSC's) are stroma-derived adult stem cells that have shown promise in animal models of tissue repair which has encouraged use in clinical trials. MSC's are rare and require significant expansion *in vitro* to generate sufficient cells for such approaches. The expansion process itself induces rapid ageing of MSC's as shown by a decline in proliferative and differentiation capacity (11;12). It has been recognised that there is a need for human models of adult stem cell ageing in addition to transgenic animal studies that have provided important insights into stem cell ageing to date (Reviewed in (95)). Therefore, understanding the molecular mechanisms that control MSC ageing *in vitro* should not only enhance our ability to use MSC's for cell therapy but also give insight into mechanisms of tissue and organ ageing.

First, we have established the isolation and characterisation of MSC's from the sternal BM of patients undergoing CABG and demonstrated that these cells meet the defining criteria set out by the International Society for Cellular Therapy (33). MSC's could be expanded for almost thirty population doublings and achieved levels of expansion similar to that previously reported (11;12). Late passage MSC's showed evidence of cell ageing with the development of a senescent morphology, expression of the marker SA ß-Gal and a reduction in telomere length. In addition, the cells showed a decline in adipogenic and osteogenic differentiation capacity confirming loss of their stem cell properties. The findings were confirmed in multiple cultures which gave us confidence that our model of MSC ageing *in vitro* was reproducible and not entirely influenced by the donor characteristics themselves. Our studies confirmed that sternal BM is a reliable source of MSC's and this approach for harvesting autologous cells may be suitable for clinical application.

The next part of our study used SAGE to determine the expression profile of MSC's during expansion. Three libraries, two at passage two and one at passage nine were generated containing 123,990 tags of which 38,126 were unique. Less than 1% of the tags were differentially expressed matching 243 known genes. This pattern of differential expression was similar to that reported by other SAGE studies. We confirmed genes abundant in our libraries matched those expressed in other expression profiling studies of MSC's. Analysis of known

direct interactions between genes revealed a regulatory signaling network centered on down-regulation of activator protein 1 (AP-1) in late passage MSC's. This network highlights the importance of global analysis of gene expression and also demonstrates that small changes in a combination of genes in a signalling pathway are responsible for defining a cell phenotype. By investigating signaling networks we can enhance understanding of the biology of senescence and its regulation in MSC's. Transcriptional changes in MSC's at passage nine included genes associated with inflammation, regulation of cell cycle, metabolism and extracellular matrix re-modelling. These characteristics are typical of other senescent cell types and thought to be detrimental on normal tissue function and homeostasis. The effect of using aged MSC cell preparations for cell therapy has not been addressed in animal studies to date and it remains unclear if these cells are beneficial or even detrimental when used for tissue repair. The results emphasise the need to characterise MSC's at the molecular level prior to clinical use and when comparing MSC preparations from different researchers.

TLDA's were used to perform a comprehensive evaluation of gene expression in multiple MSC cultures at different passages and confirmed the SAGE findings. The success of the validation was similar to other SAGE studies and good considering the nature of primary cell culture work. Eighteen genes were identified as differentially expressed in late passage MSC's and CAV1, CCND1, PLAT and OLFML3 were able to discriminate between cultures at different passage number. The results confirm that ageing and senescence of MSC's cultures is detectable much earlier than the onset of growth arrest. Our findings support the study by Wagner *et al* that demonstrated senescence of MSC's occurs immediately from isolation and increases during expansion (40). It remains to be determined if this reflects an accumulation of senescent cells in culture or an enhanced stress response. Further studies using the four gene signature may address this although the detection of CAV1 (207), CCND1 (199)and PLAT (215) in senescent fibroblasts would infer senescent MSC's do in fact accumulate during expansion. These markers are likely to outperform current methods of detection of senescence in MSC's such as SA ß-Gal expression, lipofuscin accumulation and telomere shortening although prospective studies are required to confirm this. The validation study confirmed that genes on the AP-1 regulatory network were differentially expressed in all cultures. This is a stress response transcription factor and a recent study has shown that MSC's senesce prematurely in response

to increased levels of oxidative stress (68). The regulatory network that defines the senescent phenotype remains a novel finding and has not been reported. Our results also provide molecular markers that could be used to ensure quality control of MSC's in clinical trials and enhance optimisation of existing culture protocols.

Lastly, we have provided further evidence that MSC's senesce prematurely in response to undefined stresses because inhibition of p38 MAPK signalling prevented the decline in proliferation and differentiation of MSC's during expansion. Interestingly, similar findings have been demonstrated in HSC's (231) and Werner's syndrome fibroblasts (232). However, these studies did not assess genomic integrity and in MSC's the use of SB230580 allowed the accumulation of genomic instability. Although the cultures could not be transformed there was evidence of impaired DNA damage responses. Therefore, intact p38 MAPK signalling appears to have a tumour suppressor role in MSC's as it does in other cell types.

Overall, the conclusions can be summarised:

- The sternal BM of patients undergoing CABG is a reliable source of MSC's that could be used for cell-based therapies. The expansion of MSC's is associated with a decline in stem cell properties and the onset of senescence. This may ultimately limit the applicability of autologous cells derived from IHD patients although further studies in animal models of tissue repair are required.

- MSC ageing is associated with an increased resistance to oxidative stress and apoptosis, enhanced extra-cellular matrix re-modelling and an inflammatory phenotype at the transcriptional level.

- The molecular phenotype appears to be regulated by decreased expression of the transcription factor, activator protein 1 (AP-1).

- Eighteen genes have been identified that represent markers of MSC ageing and senescence *in vitro* and the expression of CAV1, CCND1, PLAT and OLFML3 can be used to discriminate cultures of different proliferative history.

- Activation of p38 MAPK signalling pathway contributes to the loss of progenitors, decline in proliferation and loss of osteogenic differentiation capacity in late passage cultures. The p38 MAPK pathway appears critical for the maintenance of genomic stability in MSC's by regulating normal DNA damage responses.

Overall, this study has provided an excellent platform towards understanding the molecular mechanisms that regulate ageing and senescence of MSC's *in vitro*. This study also raises several important questions:

- Can CAV1, CCND1, PLAT and OLFML3 be used prospectively as molecular markers of MSC senescence?

- What stresses activate the p38 MAPK pathway in MSC's?

- What are the transcriptional targets of p38 MAPK signalling in MSC's?

- Can anti-oxidant treatments produce similar effects to SB203580 in MSC's without detrimental effects on genomic stability?

- Does genomic instability arise in a progenitor cell population within MSC cultures?

The ideal culture protocol for MSC's is yet to be defined but our results suggest that strategies to minimise oxidative stress by culturing cells in low ambient oxygen levels and in the presence of anti-oxidants are likely to have beneficial effects on preserving the stem cell properties of MSC's. Grayson et al recently reported that MSC's cultured in 2% oxygen had a thirty fold greater expansion than cells grown in standard conditions and maintained differentiation capacity (62). Furthermore, anti-oxidants have beneficial effects in other cell types although their effects in MSC's have not been extensively researched. Applying such strategies immediately upon isolation of the cells is likely to significantly increase the proliferative capacity of the cells and maintain their stem cell characteristics *in vitro*.

Therefore, autologous cells appear the way forward for clinical application to minimise immune responses and optimised culture protocols may overcome the

perceived limitations of this approach. This is a very exciting area of research for the future and there is no doubt that understanding stem cell ageing will inform on new treatments for age-related conditions including IHD and cancer.

8 Reference List

(1) Redfield MM. Heart failure--an epidemic of uncertain proportions. N Engl J Med 2002; 347(18):1442-1444.

(2) Stewart S, MacIntyre K, Capewell S, McMurray JJ. Heart failure and the aging population: an increasing burden in the 21st century? Heart 2003; 89(1):49-53.

(3) Horwitz EM, Prockop DJ, Fitzpatrick LA, Koo WW, Gordon PL, Neel M et al. Transplantability and therapeutic effects of bone marrow-derived mesenchymal cells in children with osteogenesis imperfecta. Nat Med 1999; 5(3):309-313.

(4) Koc ON, Day J, Nieder M, Gerson SL, Lazarus HM, Krivit W. Allogeneic mesenchymal stem cell infusion for treatment of metachromatic leukodystrophy (MLD) and Hurler syndrome (MPS-IH). Bone Marrow Transplant 2002; 30(4):215-222.

(5) Koc ON, Gerson SL, Cooper BW, Dyhouse SM, Haynesworth SE, Caplan AI et al. Rapid hematopoietic recovery after coinfusion of autologous-blood stem cells and culture-expanded marrow mesenchymal stem cells in advanced breast cancer patients receiving high-dose chemotherapy. J Clin Oncol 2000; 18(2):307-316.

(6) Lazarus HM, Koc ON, Devine SM, Curtin P, Maziarz RT, Holland HK et al. Cotransplantation of HLA-identical sibling culture-expanded mesenchymal stem cells and hematopoietic stem cells in hematologic malignancy patients. Biol Blood Marrow Transplant 2005; 11(5):389-398.

(7) Le Blanc K, Rasmusson I, Sundberg B, Gotherstrom C, Hassan M, Uzunel M et al. Treatment of severe acute graft-versus-host disease with third party haploidentical mesenchymal stem cells. Lancet 2004; 363(9419):1439-1441.

(8) Bang OY, Lee JS, Lee PH, Lee G. Autologous mesenchymal stem cell transplantation in stroke patients. Ann Neurol 2005; 57(6):874-882.

(9) Chen SL, Fang WW, Ye F, Liu YH, Qian J, Shan SJ et al. Effect on left ventricular function of intracoronary transplantation of autologous bone marrow mesenchymal stem cell in patients with acute myocardial infarction. Am J Cardiol 2004; 94(1):92-95.

(10) Katritsis DG, Sotiropoulou PA, Karvouni E, Karabinos I, Korovesis S, Perez SA et al. Transcoronary transplantation of autologous mesenchymal stem cells and endothelial progenitors into infarcted human myocardium. Catheter Cardiovasc Interv 2005; 65(3):321-329.

(11) Baxter MA, Wynn RF, Jowitt SN, Wraith JE, Fairbairn LJ, Bellantuono I. Study of telomere length reveals rapid aging of human marrow stromal cells following in vitro expansion. Stem Cells 2004; 22(5):675-682.

(12) Stenderup K, Justesen J, Clausen C, Kassem M. Aging is associated with decreased maximal life span and accelerated senescence of bone marrow stromal cells. Bone 2003; 33(6):919-926.

(13) Rubio D, Garcia-Castro J, Martin MC, de la FR, Cigudosa JC, Lloyd AC et al. Spontaneous human adult stem cell transformation. Cancer Res 2005; 65(8):3035-3039.

(14) Wang Y, Huso DL, Harrington J, Kellner J, Jeong DK, Turney J et al. Outgrowth of a transformed cell population derived from normal human BM mesenchymal stem cell culture. Cytotherapy 2005; 7(6):509-519.

(15) Owen M, Friedenstein AJ. Stromal stem cells: marrow-derived osteogenic precursors. Ciba Found Symp 1988; 136:42-60.

(16) Caplan AI. Mesenchymal stem cells. J Orthop Res 1991; 9(5):641-650.

(17) Pittenger MF, Mackay AM, Beck SC, Jaiswal RK, Douglas R, Mosca JD et al. Multilineage potential of adult human mesenchymal stem cells. Science 1999; 284(5411):143-147.

(18) Friedenstein AJ, Chailakhjan RK, Lalykina KS. The development of fibroblast colonies in monolayer cultures of guinea-pig bone marrow and spleen cells. Cell Tissue Kinet 1970; 3(4):393-403.

(19) Digirolamo CM, Stokes D, Colter D, Phinney DG, Class R, Prockop DJ. Propagation and senescence of human marrow stromal cells in culture: a simple colony-forming assay identifies samples with the greatest potential to propagate and differentiate. Br J Haematol 1999; 107(2):275-281.

(20) da Silva ML, Chagastelles PC, Nardi NB. Mesenchymal stem cells reside in virtually all post-natal organs and tissues. J Cell Sci 2006; 119(Pt 11):2204-2213.

(21) Fukumoto T, Sperling JW, Sanyal A, Fitzsimmons JS, Reinholz GG, Conover CA et al. Combined effects of insulin-like growth factor-1 and transforming growth factor-beta1 on periosteal mesenchymal cells during chondrogenesis in vitro. Osteoarthritis Cartilage 2003; 11(1):55-64.

(22) Sottile V, Halleux C, Bassilana F, Keller H, Seuwen K. Stem cell characteristics of human trabecular bone-derived cells. Bone 2002; 30(5):699-704.

(23) De Ugarte DA, Morizono K, Elbarbary A, Alfonso Z, Zuk PA, Zhu M et al. Comparison of multi-lineage cells from human adipose tissue and bone marrow. Cells Tissues Organs 2003; 174(3):101-109.

(24) De Bari C, Dell'Accio F, Tylzanowski P, Luyten FP. Multipotent mesenchymal stem cells from adult human synovial membrane. Arthritis Rheum 2001; 44(8):1928-1942.

(25) Jankowski RJ, Deasy BM, Huard J. Muscle-derived stem cells. Gene Ther 2002; 9(10):642-647.

(26) Tateishi K, Ashihara E, Honsho S, Takehara N, Nomura T, Takahashi T et al. Human cardiac stem cells exhibit mesenchymal features and are maintained through Akt/GSK-3beta signaling. Biochem Biophys Res Commun 2007; 352(3):635-641.

(27) Noort WA, Kruisselbrink AB, in't Anker PS, Kruger M, van Bezooijen RL, de Paus RA et al. Mesenchymal stem cells promote engraftment of human umbilical cord blood-derived CD34(+) cells in NOD/SCID mice. Exp Hematol 2002; 30(8):870-878.

(28) Miura M, Gronthos S, Zhao M, Lu B, Fisher LW, Robey PG et al. SHED: stem cells from human exfoliated deciduous teeth. Proc Natl Acad Sci U S A 2003; 100(10):5807-5812.

(29) In 't Anker PS, Scherjon SA, Kleijburg-van der Keur C, Groot-Swings GM, Claas FH, Fibbe WE et al. Isolation of mesenchymal stem cells of fetal or maternal origin from human placenta. Stem Cells 2004; 22(7):1338-1345.

(30) In 't Anker PS, Scherjon SA, Kleijburg-van der Keur C, Noort WA, Claas FH, Willemze R et al. Amniotic fluid as a novel source of mesenchymal stem cells for therapeutic transplantation. Blood 2003; 102(4):1548-1549.

(31) Erices AA, Allers CI, Conget PA, Rojas CV, Minguell JJ. Human cord blood-derived mesenchymal stem cells home and survive in the marrow of immunodeficient mice after systemic infusion. Cell Transplant 2003; 12(6):555-561.

(32) Colter DC, Sekiya I, Prockop DJ. Identification of a subpopulation of rapidly self-renewing and multipotential adult stem cells in colonies of human marrow stromal cells. Proc Natl Acad Sci U S A 2001; 98(14):7841-7845.

(33) Dominici M, Le Blanc K, Mueller I, Slaper-Cortenbach I, Marini F, Krause D et al. Minimal criteria for defining multipotent mesenchymal stromal cells. The International Society for Cellular Therapy position statement. Cytotherapy 2006; 8(4):315-317.

(34) Gronthos S, Zannettino AC, Hay SJ, Shi S, Graves SE, Kortesidis A et al. Molecular and cellular characterisation of highly purified stromal stem cells derived from human bone marrow. J Cell Sci 2003; 116(Pt 9):1827-1835.

(35) Tondreau T, Meuleman N, Delforge A, Dejeneffe M, Leroy R, Massy M et al. Mesenchymal stem cells derived from CD133-positive cells in mobilized peripheral blood and cord blood: proliferation, Oct4 expression, and plasticity. Stem Cells 2005; 23(8):1105-1112.

(36) Gang EJ, Bosnakovski D, Figueiredo CA, Visser JW, Perlingeiro RC. SSEA-4 identifies mesenchymal stem cells from bone marrow. Blood 2007; 109(4):1743-1751.

(37) Bruder SP, Jaiswal N, Haynesworth SE. Growth kinetics, self-renewal, and the osteogenic potential of purified human mesenchymal stem cells

during extensive subcultivation and following cryopreservation. J Cell Biochem 1997; 64(2):278-294.

(38) Muraglia A, Cancedda R, Quarto R. Clonal mesenchymal progenitors from human bone marrow differentiate in vitro according to a hierarchical model. J Cell Sci 2000; 113 (Pt 7):1161-1166.

(39) Barry F, Boynton RE, Liu B, Murphy JM. Chondrogenic differentiation of mesenchymal stem cells from bone marrow: differentiation-dependent gene expression of matrix components. Exp Cell Res 2001; 268(2):189-200.

(40) Wagner W, Horn P, Castoldi M, Diehlmann A, Bork S, Saffrich R et al. Replicative senescence of mesenchymal stem cells: a continuous and organized process. PLoS ONE 2008; 3(5):e2213.

(41) Shim WS, Jiang S, Wong P, Tan J, Chua YL, Tan YS et al. Ex vivo differentiation of human adult bone marrow stem cells into cardiomyocyte-like cells. Biochem Biophys Res Commun 2004; 324(2):481-488.

(42) Oswald J, Boxberger S, Jorgensen B, Feldmann S, Ehninger G, Bornhauser M et al. Mesenchymal stem cells can be differentiated into endothelial cells in vitro. Stem Cells 2004; 22(3):377-384.

(43) Gang EJ, Jeong JA, Han S, Yan Q, Jeon CJ, Kim H. In vitro endothelial potential of human UC blood-derived mesenchymal stem cells. Cytotherapy 2006; 8(3):215-227.

(44) Sanchez-Ramos J, Song S, Cardozo-Pelaez F, Hazzi C, Stedeford T, Willing A et al. Adult bone marrow stromal cells differentiate into neural cells in vitro. Exp Neurol 2000; 164(2):247-256.

(45) Tremain N, Korkko J, Ibberson D, Kopen GC, DiGirolamo C, Phinney DG. MicroSAGE analysis of 2,353 expressed genes in a single cell-derived colony of undifferentiated human mesenchymal stem cells reveals mRNAs of multiple cell lineages. Stem Cells 2001; 19(5):408-418.

(46) Seshi B, Kumar S, King D. Multilineage gene expression in human bone marrow stromal cells as evidenced by single-cell microarray analysis. Blood Cells Mol Dis 2003; 31(2):268-285.

(47) Tondreau T, Lagneaux L, Dejeneffe M, Massy M, Mortier C, Delforge A et al. Bone marrow-derived mesenchymal stem cells already express specific neural proteins before any differentiation. Differentiation 2004; 72(7):319-326.

(48) Rose RA, Jiang H, Wang X, Helke S, Tsoporis JN, Gong N et al. Bone marrow-derived mesenchymal stromal cells express cardiac-specific markers, retain the stromal phenotype, and do not become functional cardiomyocytes in vitro. Stem Cells 2008; 26(11):2884-2892.

(49) Kuznetsov SA, Krebsbach PH, Satomura K, Kerr J, Riminucci M, Benayahu D et al. Single-colony derived strains of human marrow stromal

fibroblasts form bone after transplantation in vivo. J Bone Miner Res 1997; 12(9):1335-1347.

(50) Gao J, Dennis JE, Muzic RF, Lundberg M, Caplan AI. The dynamic in vivo distribution of bone marrow-derived mesenchymal stem cells after infusion. Cells Tissues Organs 2001; 169(1):12-20.

(51) Shake JG, Gruber PJ, Baumgartner WA, Senechal G, Meyers J, Redmond JM et al. Mesenchymal stem cell implantation in a swine myocardial infarct model: engraftment and functional effects. Ann Thorac Surg 2002; 73(6):1919-1925.

(52) Yoon J, Min BG, Kim YH, Shim WJ, Ro YM, Lim DS. Differentiation, engraftment and functional effects of pre-treated mesenchymal stem cells in a rat myocardial infarct model. Acta Cardiol 2005; 60(3):277-284.

(53) Gnecchi M, He H, Liang OD, Melo LG, Morello F, Mu H et al. Paracrine action accounts for marked protection of ischemic heart by Akt-modified mesenchymal stem cells. Nat Med 2005; 11(4):367-368.

(54) Tang YL, Zhao Q, Qin X, Shen L, Cheng L, Ge J et al. Paracrine action enhances the effects of autologous mesenchymal stem cell transplantation on vascular regeneration in rat model of myocardial infarction. Ann Thorac Surg 2005; 80(1):229-236.

(55) Amado LC, Saliaris AP, Schuleri KH, St John M, Xie JS, Cattaneo S et al. Cardiac repair with intramyocardial injection of allogeneic mesenchymal stem cells after myocardial infarction. Proc Natl Acad Sci U S A 2005; 102(32):11474-11479.

(56) Yoon YS, Park JS, Tkebuchava T, Luedeman C, Losordo DW. Unexpected severe calcification after transplantation of bone marrow cells in acute myocardial infarction. Circulation 2004; 109(25):3154-3157.

(57) Breitbach M, Bostani T, Roell W, Xia Y, Dewald O, Nygren JM et al. Potential risks of bone marrow cell transplantation into infarcted hearts. Blood 2007; 110(4):1362-1369.

(58) Sotiropoulou PA, Perez SA, Salagianni M, Baxevanis CN, Papamichail M. Characterization of the optimal culture conditions for clinical scale production of human mesenchymal stem cells. Stem Cells 2006; 24(2):462-471.

(59) Sekiya I, Larson BL, Smith JR, Pochampally R, Cui JG, Prockop DJ. Expansion of human adult stem cells from bone marrow stroma: conditions that maximize the yields of early progenitors and evaluate their quality. Stem Cells 2002; 20(6):530-541.

(60) Pochampally RR, Smith JR, Ylostalo J, Prockop DJ. Serum deprivation of human marrow stromal cells (hMSCs) selects for a subpopulation of early progenitor cells with enhanced expression of OCT-4 and other embryonic genes. Blood 2004; 103(5):1647-1652.

(61) Stute N, Holtz K, Bubenheim M, Lange C, Blake F, Zander AR. Autologous serum for isolation and expansion of human mesenchymal stem cells for clinical use. Exp Hematol 2004; 32(12):1212-1225.

(62) Grayson WL, Zhao F, Bunnell B, Ma T. Hypoxia enhances proliferation and tissue formation of human mesenchymal stem cells. Biochem Biophys Res Commun 2007; 358(3):948-953.

(63) Bianchi G, Banfi A, Mastrogiacomo M, Notaro R, Luzzatto L, Cancedda R et al. Ex vivo enrichment of mesenchymal cell progenitors by fibroblast growth factor 2. Exp Cell Res 2003; 287(1):98-105.

(64) Ito T, Sawada R, Fujiwara Y, Seyama Y, Tsuchiya T. FGF-2 suppresses cellular senescence of human mesenchymal stem cells by down-regulation of TGF-beta2. Biochem Biophys Res Commun 2007; 359(1):108-114.

(65) Guillot PV, Gotherstrom C, Chan J, Kurata H, Fisk NM. Human first trimester fetal mesenchymal stem cells (MSC) express pluripotency markers, grow faster, and have longer telomeres compared to adult MSC. Stem Cells 2006.

(66) Gotherstrom C, West A, Liden J, Uzunel M, Lahesmaa R, Le Blanc K. Difference in gene expression between human fetal liver and adult bone marrow mesenchymal stem cells. Haematologica 2005; 90(8):1017-1026.

(67) HAYFLICK L, MOORHEAD PS. The serial cultivation of human diploid cell strains. Exp Cell Res 1961; 25:585-621.

(68) Heo JY, Jing K, Song KS, Seo KS, Park JH, Kim JS et al. Downregulation of APE1/Ref-1 Is Involved in the Senescence of Mesenchymal Stem Cells. Stem Cells 2009; 27(6):1455-1462.

(69) Kurz DJ, Decary S, Hong Y, Erusalimsky JD. Senescence-associated (beta)-galactosidase reflects an increase in lysosomal mass during replicative ageing of human endothelial cells. J Cell Sci 2000; 113 (Pt 20):3613-3622.

(70) Dimri GP, Lee X, Basile G, Acosta M, Scott G, Roskelley C et al. A biomarker that identifies senescent human cells in culture and in aging skin in vivo. Proc Natl Acad Sci U S A 1995; 92(20):9363-9367.

(71) Roura S, Farre J, Soler-Botija C, Llach A, Hove-Madsen L, Cairo JJ et al. Effect of aging on the pluripotential capacity of human CD105+ mesenchymal stem cells. Eur J Heart Fail 2006; 8(6):555-563.

(72) Banfi A, Bianchi G, Notaro R, Luzzatto L, Cancedda R, Quarto R. Replicative aging and gene expression in long-term cultures of human bone marrow stromal cells. Tissue Eng 2002; 8(6):901-910.

(73) Wright WE, Piatyszek MA, Rainey WE, Byrd W, Shay JW. Telomerase activity in human germline and embryonic tissues and cells. Dev Genet 1996; 18(2):173-179.

(74) Shay JW, Wright WE. Telomerase activity in human cancer. Curr Opin Oncol 1996; 8(1):66-71.

(75) Amit M, Carpenter MK, Inokuma MS, Chiu CP, Harris CP, Waknitz MA et al. Clonally derived human embryonic stem cell lines maintain pluripotency and proliferative potential for prolonged periods of culture. Dev Biol 2000; 227(2):271-278.

(76) Zimmermann S, Voss M, Kaiser S, Kapp U, Waller CF, Martens UM. Lack of telomerase activity in human mesenchymal stem cells. Leukemia 2003; 17(6):1146-1149.

(77) Masutomi K, Yu EY, Khurts S, Ben Porath I, Currier JL, Metz GB et al. Telomerase maintains telomere structure in normal human cells. Cell 2003; 114(2):241-253.

(78) Zhao YM, Li JY, Lan JP, Lai XY, Luo Y, Sun J et al. Cell cycle dependent telomere regulation by telomerase in human bone marrow mesenchymal stem cells. Biochem Biophys Res Commun 2008; 369(4):1114-1119.

(79) Atkinson SP, Hoare SF, Glasspool RM, Keith WN. Lack of telomerase gene expression in alternative lengthening of telomere cells is associated with chromatin remodeling of the hTR and hTERT gene promoters. Cancer Res 2005; 65(17):7585-7590.

(80) Serakinci N, Hoare SF, Kassem M, Atkinson SP, Keith WN. Telomerase promoter reprogramming and interaction with general transcription factors in the human mesenchymal stem cell. Regen Med 2006; 1(1):125-131.

(81) Simonsen JL, Rosada C, Serakinci N, Justesen J, Stenderup K, Rattan SI et al. Telomerase expression extends the proliferative life-span and maintains the osteogenic potential of human bone marrow stromal cells. Nat Biotechnol 2002; 20(6):592-596.

(82) Abdallah BM, Haack-Sorensen M, Burns JS, Elsnab B, Jakob F, Hokland P et al. Maintenance of differentiation potential of human bone marrow mesenchymal stem cells immortalized by human telomerase reverse transcriptase gene despite [corrected] extensive proliferation. Biochem Biophys Res Commun 2005; 326(3):527-538.

(83) Serakinci N, Guldberg P, Burns JS, Abdallah B, Schrodder H, Jensen T et al. Adult human mesenchymal stem cell as a target for neoplastic transformation. Oncogene 2004; 23(29):5095-5098.

(84) Kassem M, Burns JS, Garcia CJ, Rubio MD. Adult stem cells and cancer. Cancer Res 2005; 65(20):9601.

(85) Bernardo ME, Zaffaroni N, Novara F, Cometa AM, Avanzini MA, Moretta A et al. Human bone marrow derived mesenchymal stem cells do not undergo transformation after long-term in vitro culture and do not exhibit telomere maintenance mechanisms. Cancer Res 2007; 67(19):9142-9149.

(86) Wu C, Wei Q, Utomo V, Nadesan P, Whetstone H, Kandel R et al. Side population cells isolated from mesenchymal neoplasms have tumor initiating potential. Cancer Res 2007; 67(17):8216-8222.

(87) Lee HW, Blasco MA, Gottlieb GJ, Horner JW, Greider CW, DePinho RA. Essential role of mouse telomerase in highly proliferative organs. Nature 1998; 392(6676):569-574.

(88) Samper E, Fernandez P, Eguia R, Martin-Rivera L, Bernad A, Blasco MA et al. Long-term repopulating ability of telomerase-deficient murine hematopoietic stem cells. Blood 2002; 99(8):2767-2775.

(89) Blasco MA, Lee HW, Hande MP, Samper E, Lansdorp PM, DePinho RA et al. Telomere shortening and tumor formation by mouse cells lacking telomerase RNA. Cell 1997; 91(1):25-34.

(90) Liu L, Digirolamo CM, Navarro PA, Blasco MA, Keefe DL. Telomerase deficiency impairs differentiation of mesenchymal stem cells. Exp Cell Res 2004; 294(1):1-8.

(91) Bonab MM, Alimoghaddam K, Talebian F, Ghaffari SH, Ghavamzadeh A, Nikbin B. Aging of mesenchymal stem cell in vitro. BMC Cell Biol 2006; 7:14.

(92) Shelton DN, Chang E, Whittier PS, Choi D, Funk WD. Microarray analysis of replicative senescence. Curr Biol 1999; 9(17):939-945.

(93) Sharpless NE, Bardeesy N, Lee KH, Carrasco D, Castrillon DH, Aguirre AJ et al. Loss of p16Ink4a with retention of p19Arf predisposes mice to tumorigenesis. Nature 2001; 413(6851):86-91.

(94) Herbig U, Jobling WA, Chen BP, Chen DJ, Sedivy JM. Telomere shortening triggers senescence of human cells through a pathway involving ATM, p53, and p21(CIP1), but not p16(INK4a). Mol Cell 2004; 14(4):501-513.

(95) Bellantuono I, Keith WN. Stem cell ageing: does it happen and can we intervene? Expert Rev Mol Med 2007; 9(31):1-20.

(96) Park JS, Kim HY, Kim HW, Chae GN, Oh HT, Park JY et al. Increased caveolin-1, a cause for the declined adipogenic potential of senescent human mesenchymal stem cells. Mech Ageing Dev 2005; 126(5):551-559.

(97) Griffiths-Jones S, Grocock RJ, van Dongen S, Bateman A, Enright AJ. miRBase: microRNA sequences, targets and gene nomenclature. Nucleic Acids Res 2006; 34(Database issue):D140-D144.

(98) Lafferty-Whyte K, Cairney CJ, Jamieson NB, Oien KA, Keith WN. Pathway analysis of senescence-associated miRNA targets reveals common processes to different senescence induction mechanisms. Biochim Biophys Acta 2009; 1792(4):341-352.

(99) Porter D, Polyak K. Cancer target discovery using SAGE. Expert Opin Ther Targets 2003; 7(6):759-769.

(100) Porter D, Lahti-Domenici J, Keshaviah A, Bae YK, Argani P, Marks J et al. Molecular markers in ductal carcinoma in situ of the breast. Mol Cancer Res 2003; 1(5):362-375.

(101) Polyak K, Riggins GJ. Gene discovery using the serial analysis of gene expression technique: implications for cancer research. J Clin Oncol 2001; 19(11):2948-2958.

(102) Zhang L, Zhou W, Velculescu VE, Kern SE, Hruban RH, Hamilton SR et al. Gene expression profiles in normal and cancer cells. Science 1997; 276(5316):1268-1272.

(103) Jones SJ, Riddle DL, Pouzyrev AT, Velculescu VE, Hillier L, Eddy SR et al. Changes in gene expression associated with developmental arrest and longevity in Caenorhabditis elegans. Genome Res 2001; 11(8):1346-1352.

(104) Boheler KR, Tarasov KV. SAGE analysis to identify embryonic stem cell-predominant transcripts. Methods Mol Biol 2006; 329:195-221.

(105) Silva WA, Jr., Covas DT, Panepucci RA, Proto-Siqueira R, Siufi JL, Zanette DL et al. The profile of gene expression of human marrow mesenchymal stem cells. Stem Cells 2003; 21(6):661-669.

(106) Velculescu VE, Zhang L, Vogelstein B, Kinzler KW. Serial analysis of gene expression. Science 1995; 270(5235):484-487.

(107) Jia L, Young MF, Powell J, Yang L, Ho NC, Hotchkiss R et al. Gene expression profile of human bone marrow stromal cells: high-throughput expressed sequence tag sequencing analysis. Genomics 2002; 79(1):7-17.

(108) Lash AE, Tolstoshev CM, Wagner L, Schuler GD, Strausberg RL, Riggins GJ et al. SAGEmap: a public gene expression resource. Genome Res 2000; 10(7):1051-1060.

(109) Boon K, Osorio EC, Greenhut SF, Schaefer CF, Shoemaker J, Polyak K et al. An anatomy of normal and malignant gene expression. Proc Natl Acad Sci U S A 2002; 99(17):11287-11292.

(110) Saha S, Sparks AB, Rago C, Akmaev V, Wang CJ, Vogelstein B et al. Using the transcriptome to annotate the genome. Nat Biotechnol 2002; 20(5):508-512.

(111) Matsumura H, Reich S, Ito A, Saitoh H, Kamoun S, Winter P et al. Gene expression analysis of plant host-pathogen interactions by SuperSAGE. Proc Natl Acad Sci U S A 2003; 100(26):15718-15723.

(112) Lu J, Lal A, Merriman B, Nelson S, Riggins G. A comparison of gene expression profiles produced by SAGE, long SAGE, and oligonucleotide chips. Genomics 2004; 84(4):631-636.

(113) Ye SQ, Zhang LQ, Zheng F, Virgil D, Kwiterovich PO. miniSAGE: gene expression profiling using serial analysis of gene expression from 1 microg total RNA. Anal Biochem 2000; 287(1):144-152.

(114) Peters DG, Kassam AB, Yonas H, O'Hare EH, Ferrell RE, Brufsky AM. Comprehensive transcript analysis in small quantities of mRNA by SAGE-lite. Nucleic Acids Res 1999; 27(24):e39.

(115) Datson NA, van der Perk-de Jong, van den Berg MP, de Kloet ER, Vreugdenhil E. MicroSAGE: a modified procedure for serial analysis of

gene expression in limited amounts of tissue. Nucleic Acids Res 1999; 27(5):1300-1307.

(116) Wei CL, Ng P, Chiu KP, Wong CH, Ang CC, Lipovich L et al. 5' Long serial analysis of gene expression (LongSAGE) and 3' LongSAGE for transcriptome characterization and genome annotation. Proc Natl Acad Sci U S A 2004; 101(32):11701-11706.

(117) Shiraki T, Kondo S, Katayama S, Waki K, Kasukawa T, Kawaji H et al. Cap analysis gene expression for high-throughput analysis of transcriptional starting point and identification of promoter usage. Proc Natl Acad Sci U S A 2003; 100(26):15776-15781.

(118) Chen J, Sun M, Lee S, Zhou G, Rowley JD, Wang SM. Identifying novel transcripts and novel genes in the human genome by using novel SAGE tags. Proc Natl Acad Sci U S A 2002; 99(19):12257-12262.

(119) Margulies M, Egholm M, Altman WE, Attiya S, Bader JS, Bemben LA et al. Genome sequencing in microfabricated high-density picolitre reactors. Nature 2005; 437(7057):376-380.

(120) Shendure J, Ji H. Next-generation DNA sequencing. Nat Biotechnol 2008; 26(10):1135-1145.

(121) Ibrahim AF, Hedley PE, Cardle L, Kruger W, Marshall DF, Muehlbauer GJ et al. A comparative analysis of transcript abundance using SAGE and Affymetrix arrays. Funct Integr Genomics 2005; 5(3):163-174.

(122) Sun M, Zhou G, Lee S, Chen J, Shi RZ, Wang SM. SAGE is far more sensitive than EST for detecting low-abundance transcripts. BMC Genomics 2004; 5(1):1.

(123) Oien KA, Vass JK, Downie I, Fullarton G, Keith WN. Profiling, comparison and validation of gene expression in gastric carcinoma and normal stomach. Oncogene 2003; 22(27):4287-4300.

(124) Zhou G, Chen J, Lee S, Clark T, Rowley JD, Wang SM. The pattern of gene expression in human CD34(+) stem/progenitor cells. Proc Natl Acad Sci U S A 2001; 98(24):13966-13971.

(125) Richards M, Tan SP, Tan JH, Chan WK, Bongso A. The transcriptome profile of human embryonic stem cells as defined by SAGE. Stem Cells 2004; 22(1):51-64.

(126) Williams C, Wirta V, Meletis K, Wikstrom L, Carlsson L, Frisen J et al. Catalog of gene expression in adult neural stem cells and their in vivo microenvironment. Exp Cell Res 2006; 312(10):1798-1812.

(127) Georgantas RW, III, Tanadve V, Malehorn M, Heimfeld S, Chen C, Carr L et al. Microarray and serial analysis of gene expression analyses identify known and novel transcripts overexpressed in hematopoietic stem cells. Cancer Res 2004; 64(13):4434-4441.

(128) Kronenwett R, Butterweck U, Steidl U, Kliszewski S, Neumann F, Bork S et al. Distinct molecular phenotype of malignant CD34(+) hematopoietic

stem and progenitor cells in chronic myelogenous leukemia. Oncogene 2005; 24(34):5313-5324.

(129) Gal H, Amariglio N, Trakhtenbrot L, Jacob-Hirsh J, Margalit O, Avigdor A et al. Gene expression profiles of AML derived stem cells; similarity to hematopoietic stem cells. Leukemia 2006; 20(12):2147-2154.

(130) Reya T, Morrison SJ, Clarke MF, Weissman IL. Stem cells, cancer, and cancer stem cells. Nature 2001; 414(6859):105-111.

(131) Rao RR, Stice SL. Gene expression profiling of embryonic stem cells leads to greater understanding of pluripotency and early developmental events. Biol Reprod 2004; 71(6):1772-1778.

(132) Sato N, Meijer L, Skaltsounis L, Greengard P, Brivanlou AH. Maintenance of pluripotency in human and mouse embryonic stem cells through activation of Wnt signaling by a pharmacological GSK-3-specific inhibitor. Nat Med 2004; 10(1):55-63.

(133) Ramalho-Santos M, Yoon S, Matsuzaki Y, Mulligan RC, Melton DA. "Stemness": transcriptional profiling of embryonic and adult stem cells. Science 2002; 298(5593):597-600.

(134) Okita K, Ichisaka T, Yamanaka S. Generation of germline-competent induced pluripotent stem cells. Nature 2007; 448(7151):313-317.

(135) Wernig M, Meissner A, Foreman R, Brambrink T, Ku M, Hochedlinger K et al. In vitro reprogramming of fibroblasts into a pluripotent ES-cell-like state. Nature 2007; 448(7151):318-324.

(136) Maherali N, Sridharan R, Xie W, Utikal J, Eminli S, Arnold K et al. Directly reprogrammed fibroblasts show global epigenetic remodeling and widespread tissue contribution. Cell Stem Cell 2007; 1(1):55-70.

(137) Okita K, Nakagawa M, Hyenjong H, Ichisaka T, Yamanaka S. Generation of mouse induced pluripotent stem cells without viral vectors. Science 2008; 322(5903):949-953.

(138) Wagner W, Wein F, Seckinger A, Frankhauser M, Wirkner U, Krause U et al. Comparative characteristics of mesenchymal stem cells from human bone marrow, adipose tissue, and umbilical cord blood. Exp Hematol 2005; 33(11):1402-1416.

(139) Katz AJ, Tholpady A, Tholpady SS, Shang H, Ogle RC. Cell surface and transcriptional characterization of human adipose-derived adherent stromal (hADAS) cells. Stem Cells 2005; 23(3):412-423.

(140) Jeong JA, Hong SH, Gang EJ, Ahn C, Hwang SH, Yang IH et al. Differential gene expression profiling of human umbilical cord blood-derived mesenchymal stem cells by DNA microarray. Stem Cells 2005; 23(4):584-593.

(141) Phinney DG, Hill K, Michelson C, Dutreil M, Hughes C, Humphries S et al. Biological Activities Encoded by the Murine Mesenchymal Stem Cell Transcriptome Provide a Basis for Their Developmental Potential and Broad Therapeutic Efficacy. Stem Cells 2005.

(142) Panepucci RA, Siufi JL, Silva WA, Jr., Proto-Siquiera R, Neder L, Orellana M et al. Comparison of gene expression of umbilical cord vein and bone marrow-derived mesenchymal stem cells. Stem Cells 2004; 22(7):1263-1278.

(143) Prockop DJ, Sekiya I, Colter DC. Isolation and characterization of rapidly self-renewing stem cells from cultures of human marrow stromal cells. Cytotherapy 2001; 3(5):393-396.

(144) Song L, Webb NE, Song Y, Tuan RS. Identification and functional analysis of candidate genes regulating mesenchymal stem cell self-renewal and multipotency. Stem Cells 2006; 24(7):1707-1718.

(145) Reyes M, Lund T, Lenvik T, Aguiar D, Koodie L, Verfaillie CM. Purification and ex vivo expansion of postnatal human marrow mesodermal progenitor cells. Blood 2001; 98(9):2615-2625.

(146) Zeng L, Rahrmann E, Hu Q, Lund T, Sandquist L, Felten M et al. Multipotent adult progenitor cells from swine bone marrow. Stem Cells 2006; 24(11):2355-2366.

(147) Ylostalo J, Smith JR, Pochampally RR, Matz R, Sekiya I, Larson BL et al. Use of differentiating adult stem cells (marrow stromal cells) to identify new downstream target genes for transcription factors. Stem Cells 2006; 24(3):642-652.

(148) Chen SL, Fang WW, Ye F, Liu YH, Qian J, Shan SJ et al. Effect on left ventricular function of intracoronary transplantation of autologous bone marrow mesenchymal stem cell in patients with acute myocardial infarction. Am J Cardiol 2004; 94(1):92-95.

(149) Aggarwal S, Pittenger MF. Human mesenchymal stem cells modulate allogeneic immune cell responses. Blood 2005; 105(4):1815-1822.

(150) Sotiropoulou PA, Perez SA, Gritzapis AD, Baxevanis CN, Papamichail M. Interactions between human mesenchymal stem cells and natural killer cells. Stem Cells 2005.

(151) Poncelet AJ, Vercruysse J, Saliez A, Gianello P. Although pig allogeneic mesenchymal stem cells are not immunogenic in vitro, intracardiac injection elicits an immune response in vivo. Transplantation 2007; 83(6):783-790.

(152) Nauta AJ, Westerhuis G, Kruisselbrink AB, Lurvink EG, Willemze R, Fibbe WE. Donor-derived mesenchymal stem cells are immunogenic in an allogeneic host and stimulate donor graft rejection in a nonmyeloablative setting. Blood 2006; 108(6):2114-2120.

(153) Vasa M, Fichtlscherer S, Aicher A, Adler K, Urbich C, Martin H et al. Number and migratory activity of circulating endothelial progenitor cells inversely correlate with risk factors for coronary artery disease. Circ Res 2001; 89(1):E1-E7.

(154) Kondo T, Hayashi M, Takeshita K, Numaguchi Y, Kobayashi K, Iino S et al. Smoking cessation rapidly increases circulating progenitor cells in

peripheral blood in chronic smokers. Arterioscler Thromb Vasc Biol 2004; 24(8):1442-1447.

(155) Brouilette SW, Moore JS, McMahon AD, Thompson JR, Ford I, Shepherd J et al. Telomere length, risk of coronary heart disease, and statin treatment in the West of Scotland Primary Prevention Study: a nested case-control study. Lancet 2007; 369(9556):107-114.

(156) Wexler SA, Donaldson C, Denning-Kendall P, Rice C, Bradley B, Hows JM. Adult bone marrow is a rich source of human mesenchymal 'stem' cells but umbilical cord and mobilized adult blood are not. Br J Haematol 2003; 121(2):368-374.

(157) Stenderup K, Justesen J, Eriksen EF, Rattan SI, Kassem M. Number and proliferative capacity of osteogenic stem cells are maintained during aging and in patients with osteoporosis. J Bone Miner Res 2001; 16(6):1120-1129.

(158) Thompson LF, Eltzschig HK, Ibla JC, Van De Wiele CJ, Resta R, Morote-Garcia JC et al. Crucial role for ecto-5'-nucleotidase (CD73) in vascular leakage during hypoxia. J Exp Med 2004; 200(11):1395-1405.

(159) Barry F, Boynton R, Murphy M, Haynesworth S, Zaia J. The SH-3 and SH-4 antibodies recognize distinct epitopes on CD73 from human mesenchymal stem cells. Biochem Biophys Res Commun 2001; 289(2):519-524.

(160) Barry FP, Boynton RE, Haynesworth S, Murphy JM, Zaia J. The monoclonal antibody SH-2, raised against human mesenchymal stem cells, recognizes an epitope on endoglin (CD105). Biochem Biophys Res Commun 1999; 265(1):134-139.

(161) Gang EJ, Hong SH, Jeong JA, Hwang SH, Kim SW, Yang IH et al. In vitro mesengenic potential of human umbilical cord blood-derived mesenchymal stem cells. Biochem Biophys Res Commun 2004; 321(1):102-108.

(162) Liu F, Akiyama Y, Tai S, Maruyama K, Kawaguchi Y, Muramatsu K et al. Changes in the expression of CD106, osteogenic genes, and transcription factors involved in the osteogenic differentiation of human bone marrow mesenchymal stem cells. J Bone Miner Metab 2008; 26(4):312-320.

(163) Gronthos S, Franklin DM, Leddy HA, Robey PG, Storms RW, Gimble JM. Surface protein characterization of human adipose tissue-derived stromal cells. J Cell Physiol 2001; 189(1):54-63.

(164) Le Blanc K. Immunomodulatory effects of fetal and adult mesenchymal stem cells. Cytotherapy 2003; 5(6):485-489.

(165) Sotiropoulou PA, Perez SA, Salagianni M, Baxevanis CN, Papamichail M. Cell culture medium composition and translational adult bone marrow-derived stem cell research. Stem Cells 2006; 24(5):1409-1410.

(166) Tondreau T, Lagneaux L, Dejeneffe M, Delforge A, Massy M, Mortier C et al. Isolation of BM mesenchymal stem cells by plastic adhesion or

negative selection: phenotype, proliferation kinetics and differentiation potential. Cytotherapy 2004; 6(4):372-379.

(167) Gronthos S, Graves SE, Ohta S, Simmons PJ. The STRO-1+ fraction of adult human bone marrow contains the osteogenic precursors. Blood 1994; 84(12):4164-4173.

(168) von Zglinicki T. Oxidative stress shortens telomeres. Trends Biochem Sci 2002; 27(7):339-344.

(169) Ksiazek K, Passos JF, Olijslagers S, Saretzki G, Martin-Ruiz C, von Zglinicki T. Premature senescence of mesothelial cells is associated with non-telomeric DNA damage. Biochem Biophys Res Commun 2007; 362(3):707-711.

(170) Gowda M, Jantasuriyarat C, Dean RA, Wang GL. Robust-LongSAGE (RL-SAGE): a substantially improved LongSAGE method for gene discovery and transcriptome analysis. Plant Physiol 2004; 134(3):890-897.

(171) Silva AP, De Souza JE, Galante PA, Riggins GJ, De Souza SJ, Camargo AA. The impact of SNPs on the interpretation of SAGE and MPSS experimental data. Nucleic Acids Res 2004; 32(20):6104-6110.

(172) Khattra J, Delaney AD, Zhao Y, Siddiqui A, Asano J, McDonald H et al. Large-scale production of SAGE libraries from microdissected tissues, flow-sorted cells, and cell lines. Genome Res 2007; 17(1):108-116.

(173) Dinel S, Bolduc C, Belleau P, Boivin A, Yoshioka M, Calvo E et al. Reproducibility, bioinformatic analysis and power of the SAGE method to evaluate changes in transcriptome. Nucleic Acids Res 2005; 33(3):e26.

(174) Anisimov SV, Sharov AA. Incidence of "quasi-ditags" in catalogs generated by Serial Analysis of Gene Expression (SAGE). BMC Bioinformatics 2004; 5:152.

(175) Emmersen J, Heidenblut AM, Hogh AL, Hahn SA, Welinder KG, Nielsen KL. Discarding duplicate ditags in LongSAGE analysis may introduce significant error. BMC Bioinformatics 2007; 8:92.

(176) Mironov AA, Fickett JW, Gelfand MS. Frequent alternative splicing of human genes. Genome Res 1999; 9(12):1288-1293.

(177) Chen J, Lee S, Zhou G, Wang SM. High-throughput GLGI procedure for converting a large number of serial analysis of gene expression tag sequences into 3' complementary DNAs. Genes Chromosomes Cancer 2002; 33(3):252-261.

(178) Kuo BY, Chen Y, Bohacec S, Johansson O, Wasserman WW, Simpson EM. SAGE2Splice: unmapped SAGE tags reveal novel splice junctions. PLoS Comput Biol 2006; 2(4):e34.

(179) Pauws E, Van Kampen AH, van de Graaf SA, de Vijlder JJ, Ris-Stalpers C. Heterogeneity in polyadenylation cleavage sites in mammalian mRNA sequences: implications for SAGE analysis. Nucleic Acids Res 2001; 29(8):1690-1694.

(180) Ewing B, Green P. Base-calling of automated sequencer traces using phred. II. Error probabilities. Genome Res 1998; 8(3):186-194.

(181) Ewing B, Hillier L, Wendl MC, Green P. Base-calling of automated sequencer traces using phred. I. Accuracy assessment. Genome Res 1998; 8(3):175-185.

(182) Akmaev VR. Correction of technology-related artifacts in serial analysis of gene expression. Methods Mol Biol 2008; 387:133-142.

(183) Madden SL, Galella EA, Zhu J, Bertelsen AH, Beaudry GA. SAGE transcript profiles for p53-dependent growth regulation. Oncogene 1997; 15(9):1079-1085.

(184) Audic S, Claverie JM. The significance of digital gene expression profiles. Genome Res 1997; 7(10):986-995.

(185) Kal AJ, van Zonneveld AJ, Benes V, van den BM, Koerkamp MG, Albermann K et al. Dynamics of gene expression revealed by comparison of serial analysis of gene expression transcript profiles from yeast grown on two different carbon sources. Mol Biol Cell 1999; 10(6):1859-1872.

(186) Man MZ, Wang X, Wang Y. POWER_SAGE: comparing statistical tests for SAGE experiments. Bioinformatics 2000; 16(11):953-959.

(187) Ruijter JM, Van Kampen AH, Baas F. Statistical evaluation of SAGE libraries: consequences for experimental design. Physiol Genomics 2002; 11(2):37-44.

(188) Ingman M, Kaessmann H, Paabo S, Gyllensten U. Mitochondrial genome variation and the origin of modern humans. Nature 2000; 408(6813):708-713.

(189) Oien KA, McGregor F, Butler S, Ferrier RK, Downie I, Bryce S et al. Gastrokine 1 is abundantly and specifically expressed in superficial gastric epithelium, down-regulated in gastric carcinoma, and shows high evolutionary conservation. J Pathol 2004; 203(3):789-797.

(190) MacFadyen JR, Haworth O, Roberston D, Hardie D, Webster MT, Morris HR et al. Endosialin (TEM1, CD248) is a marker of stromal fibroblasts and is not selectively expressed on tumour endothelium. FEBS Lett 2005; 579(12):2569-2575.

(191) Zannettino AC, Paton S, Arthur A, Khor F, Itescu S, Gimble JM et al. Multipotential human adipose-derived stromal stem cells exhibit a perivascular phenotype in vitro and in vivo. J Cell Physiol 2008; 214(2):413-421.

(192) Shaulian E, Karin M. AP-1 in cell proliferation and survival. Oncogene 2001; 20(19):2390-2400.

(193) Hu Y, Jin X, Snow ET. Effect of arsenic on transcription factor AP-1 and NF-kappaB DNA binding activity and related gene expression. Toxicol Lett 2002; 133(1):33-45.

(194) Yoon IK, Kim HK, Kim YK, Song IH, Kim W, Kim S et al. Exploration of replicative senescence-associated genes in human dermal fibroblasts by cDNA microarray technology. Exp Gerontol 2004; 39(9):1369-1378.

(195) Tanaka H, Horikawa I, Kugoh H, Shimizu M, Barrett JC, Oshimura M. Telomerase-independent senescence of human immortal cells induced by microcell-mediated chromosome transfer. Mol Carcinog 1999; 25(4):249-255.

(196) Lossos IS, Czerwinski DK, Wechser MA, Levy R. Optimization of quantitative real-time RT-PCR parameters for the study of lymphoid malignancies. Leukemia 2003; 17(4):789-795.

(197) de Kok JB, Roelofs RW, Giesendorf BA, Pennings JL, Waas ET, Feuth T et al. Normalization of gene expression measurements in tumor tissues: comparison of 13 endogenous control genes. Lab Invest 2005; 85(1):154-159.

(198) Anisimov SV, Tarasov KV, Stern MD, Lakatta EG, Boheler KR. A quantitative and validated SAGE transcriptome reference for adult mouse heart. Genomics 2002; 80(2):213-222.

(199) Fukami J, Anno K, Ueda K, Takahashi T, Ide T. Enhanced expression of cyclin D1 in senescent human fibroblasts. Mech Ageing Dev 1995; 81(2-3):139-157.

(200) Lucibello FC, Sewing A, Brusselbach S, Burger C, Muller R. Deregulation of cyclins D1 and E and suppression of cdk2 and cdk4 in senescent human fibroblasts. J Cell Sci 1993; 105 (Pt 1):123-133.

(201) Kinoshita A, Wanibuchi H, Imaoka S, Ogawa M, Masuda C, Morimura K et al. Formation of 8-hydroxydeoxyguanosine and cell-cycle arrest in the rat liver via generation of oxidative stress by phenobarbital: association with expression profiles of p21(WAF1/Cip1), cyclin D1 and Ogg1. Carcinogenesis 2002; 23(2):341-349.

(202) Kortlever RM, Higgins PJ, Bernards R. Plasminogen activator inhibitor-1 is a critical downstream target of p53 in the induction of replicative senescence. Nat Cell Biol 2006; 8(8):877-884.

(203) Narita M, Narita M, Krizhanovsky V, Nunez S, Chicas A, Hearn SA et al. A novel role for high-mobility group a proteins in cellular senescence and heterochromatin formation. Cell 2006; 126(3):503-514.

(204) Narita M, Nunez S, Heard E, Narita M, Lin AW, Hearn SA et al. Rb-mediated heterochromatin formation and silencing of E2F target genes during cellular senescence. Cell 2003; 113(6):703-716.

(205) Yoshiko Y, Son A, Maeda S, Igarashi A, Takano S, Hu J et al. Evidence for stanniocalcin gene expression in mammalian bone. Endocrinology 1999; 140(4):1869-1874.

(206) Ito D, Walker JR, Thompson CS, Moroz I, Lin W, Veselits ML et al. Characterization of stanniocalcin 2, a novel target of the mammalian

unfolded protein response with cytoprotective properties. Mol Cell Biol 2004; 24(21):9456-9469.

(207) Dasari A, Bartholomew JN, Volonte D, Galbiati F. Oxidative stress induces premature senescence by stimulating caveolin-1 gene transcription through p38 mitogen-activated protein kinase/Sp1-mediated activation of two GC-rich promoter elements. Cancer Res 2006; 66(22):10805-10814.

(208) Volonte D, Zhang K, Lisanti MP, Galbiati F. Expression of caveolin-1 induces premature cellular senescence in primary cultures of murine fibroblasts. Mol Biol Cell 2002; 13(7):2502-2517.

(209) Elchuri S, Oberley TD, Qi W, Eisenstein RS, Jackson RL, Van Remmen H et al. CuZnSOD deficiency leads to persistent and widespread oxidative damage and hepatocarcinogenesis later in life. Oncogene 2005; 24(3):367-380.

(210) Ebert R, Ulmer M, Zeck S, Meissner-Weigl J, Schneider D, Stopper H et al. Selenium supplementation restores the antioxidative capacity and prevents cell damage in bone marrow stromal cells in vitro. Stem Cells 2006; 24(5):1226-1235.

(211) Blander G, de Oliveira RM, Conboy CM, Haigis M, Guarente L. Superoxide dismutase 1 knock-down induces senescence in human fibroblasts. J Biol Chem 2003; 278(40):38966-38969.

(212) Moiseeva O, Mallette FA, Mukhopadhyay UK, Moores A, Ferbeyre G. DNA damage signaling and p53-dependent senescence after prolonged beta-interferon stimulation. Mol Biol Cell 2006; 17(4):1583-1592.

(213) Kasperkovitz PV, Verbeet NL, Smeets TJ, van Rietschoten JG, Kraan MC, van der Pouw Kraan TC et al. Activation of the STAT1 pathway in rheumatoid arthritis. Ann Rheum Dis 2004; 63(3):233-239.

(214) Miguel RF, Pollak A, Lubec G. Metalloproteinase ADAMTS-1 but not ADAMTS-5 is manifold overexpressed in neurodegenerative disorders as Down syndrome, Alzheimer's and Pick's disease. Brain Res Mol Brain Res 2005; 133(1):1-5.

(215) West MD, Shay JW, Wright WE, Linskens MH. Altered expression of plasminogen activator and plasminogen activator inhibitor during cellular senescence. Exp Gerontol 1996; 31(1-2):175-193.

(216) Miyakoshi K, Murphy MJ, Yeoman RR, Mitra S, Dubay CJ, Hennebold JD. The identification of novel ovarian proteases through the use of genomic and bioinformatic methodologies. Biol Reprod 2006; 75(6):823-835.

(217) Liu J, Sukhova GK, Sun JS, Xu WH, Libby P, Shi GP. Lysosomal cysteine proteases in atherosclerosis. Arterioscler Thromb Vasc Biol 2004; 24(8):1359-1366.

(218) Nakagawa TY, Brissette WH, Lira PD, Griffiths RJ, Petrushova N, Stock J et al. Impaired invariant chain degradation and antigen presentation and

diminished collagen-induced arthritis in cathepsin S null mice. Immunity 1999; 10(2):207-217.

(219) Horikawa I, Oshimura M, Barrett JC. Repression of the telomerase catalytic subunit by a gene on human chromosome 3 that induces cellular senescence. Mol Carcinog 1998; 22(2):65-72.

(220) Michishita E, Garces G, Barrett JC, Horikawa I. Upregulation of the KIAA1199 gene is associated with cellular mortality. Cancer Lett 2006; 239(1):71-77.

(221) Kulkarni NH, Karavanich CA, Atchley WR, Anholt RR. Characterization and differential expression of a human gene family of olfactomedin-related proteins. Genet Res 2000; 76(1):41-50.

(222) Caballero M, Borras T. Inefficient processing of an olfactomedin-deficient myocilin mutant: potential physiological relevance to glaucoma. Biochem Biophys Res Commun 2001; 282(3):662-670.

(223) Kobayashi D, Koshida S, Moriai R, Tsuji N, Watanabe N. Olfactomedin 4 promotes S-phase transition in proliferation of pancreatic cancer cells. Cancer Sci 2007; 98(3):334-340.

(224) Meijer L, Skaltsounis AL, Magiatis P, Polychronopoulos P, Knockaert M, Leost M et al. GSK-3-selective inhibitors derived from Tyrian purple indirubins. Chem Biol 2003; 10(12):1255-1266.

(225) Tseng AS, Engel FB, Keating MT. The GSK-3 inhibitor BIO promotes proliferation in mammalian cardiomyocytes. Chem Biol 2006; 13(9):957-963.

(226) Etheridge SL, Spencer GJ, Heath DJ, Genever PG. Expression profiling and functional analysis of wnt signaling mechanisms in mesenchymal stem cells. Stem Cells 2004; 22(5):849-860.

(227) Gregory CA, Gunn WG, Reyes E, Smolarz AJ, Munoz J, Spees JL et al. How wnt signaling affects bone repair by mesenchymal stem cells from the bone marrow. Ann N Y Acad Sci 2005; 1049:97-106.

(228) Ambrosino C, Nebreda AR. Cell cycle regulation by p38 MAP kinases. Biol Cell 2001; 93(1-2):47-51.

(229) Sun P, Yoshizuka N, New L, Moser BA, Li Y, Liao R et al. PRAK is essential for ras-induced senescence and tumor suppression. Cell 2007; 128(2):295-308.

(230) Iwasa H, Han J, Ishikawa F. Mitogen-activated protein kinase p38 defines the common senescence-signalling pathway. Genes Cells 2003; 8(2):131-144.

(231) Ito K, Hirao A, Arai F, Takubo K, Matsuoka S, Miyamoto K et al. Reactive oxygen species act through p38 MAPK to limit the lifespan of hematopoietic stem cells. Nat Med 2006; 12(4):446-451.

(232) Davis T, Baird DM, Haughton MF, Jones CJ, Kipling D. Prevention of accelerated cell aging in Werner syndrome using a p38 mitogen-

activated protein kinase inhibitor. J Gerontol A Biol Sci Med Sci 2005; 60(11):1386-1393.

(233) Rogakou EP, Pilch DR, Orr AH, Ivanova VS, Bonner WM. DNA double-stranded breaks induce histone H2AX phosphorylation on serine 139. J Biol Chem 1998; 273(10):5858-5868.

(234) d'Adda dF, Reaper PM, Clay-Farrace L, Fiegler H, Carr P, von Zglinicki T et al. A DNA damage checkpoint response in telomere-initiated senescence. Nature 2003; 426(6963):194-198.

(235) Ali AS, Chopra R, Robertson J, Testa NG. Detection of hTERT protein by flow cytometry. Leukemia 2000; 14(12):2176-2181.

(236) Kovarik P, Stoiber D, Eyers PA, Menghini R, Neininger A, Gaestel M et al. Stress-induced phosphorylation of STAT1 at Ser727 requires p38 mitogen-activated protein kinase whereas IFN-gamma uses a different signaling pathway. Proc Natl Acad Sci U S A 1999; 96(24):13956-13961.

(237) Zer C, Sachs G, Shin JM. Identification of genomic targets downstream of p38 mitogen-activated protein kinase pathway mediating tumor necrosis factor-alpha signaling. Physiol Genomics 2007; 31(2):343-351.

(238) Tenhunen O, Rysa J, Ilves M, Soini Y, Ruskoaho H, Leskinen H. Identification of cell cycle regulatory and inflammatory genes as predominant targets of p38 mitogen-activated protein kinase in the heart. Circ Res 2006; 99(5):485-493.

(239) Zdanov S, Debacq-Chainiaux F, Remacle J, Toussaint O. Identification of p38MAPK-dependent genes with changed transcript abundance in H2O2-induced premature senescence of IMR-90 hTERT human fibroblasts. FEBS Lett 2006; 580(27):6455-6463.

(240) Bilsland AE, Stevenson K, Atkinson S, Kolch W, Keith WN. Transcriptional repression of telomerase RNA gene expression by c-Jun-NH2-kinase and Sp1/Sp3. Cancer Res 2006; 66(3):1363-1370.

(241) Rane MJ, Coxon PY, Powell DW, Webster R, Klein JB, Pierce W et al. p38 Kinase-dependent MAPKAPK-2 activation functions as 3-phosphoinositide-dependent kinase-2 for Akt in human neutrophils. J Biol Chem 2001; 276(5):3517-3523.

(242) Cabane C, Coldefy AS, Yeow K, Derijard B. The p38 pathway regulates Akt both at the protein and transcriptional activation levels during myogenesis. Cell Signal 2004; 16(12):1405-1415.

(243) Graves JD, Gotoh Y, Draves KE, Ambrose D, Han DK, Wright M et al. Caspase-mediated activation and induction of apoptosis by the mammalian Ste20-like kinase Mst1. EMBO J 1998; 17(8):2224-2234.

(244) Zaragosi LE, Wdziekonski B, Fontaine C, Villageois P, Peraldi P, Dani C. Effects of GSK3 inhibitors on in vitro expansion and differentiation of human adipose-derived stem cells into adipocytes. BMC Cell Biol 2008; 9:11.

(245) Ye X, Zerlanko B, Kennedy A, Banumathy G, Zhang R, Adams PD. Downregulation of Wnt signaling is a trigger for formation of facultative heterochromatin and onset of cell senescence in primary human cells. Mol Cell 2007; 27(2):183-196.

(246) Liu H, Fergusson MM, Castilho RM, Liu J, Cao L, Chen J et al. Augmented Wnt signaling in a mammalian model of accelerated aging. Science 2007; 317(5839):803-806.

(247) Solchaga LA, Penick K, Porter JD, Goldberg VM, Caplan AI, Welter JF. FGF-2 enhances the mitotic and chondrogenic potentials of human adult bone marrow-derived mesenchymal stem cells. J Cell Physiol 2005; 203(2):398-409.

(248) Buhring HJ, Battula VL, Treml S, Schewe B, Kanz L, Vogel W. Novel markers for the prospective isolation of human MSC. Ann N Y Acad Sci 2007; 1106:262-271.

(249) Tominaga S, Yamaguchi T, Takahashi S, Hirose F, Osumi T. Negative regulation of adipogenesis from human mesenchymal stem cells by Jun N-terminal kinase. Biochem Biophys Res Commun 2005; 326(2):499-504.

(250) Baird DM, Davis T, Rowson J, Jones CJ, Kipling D. Normal telomere erosion rates at the single cell level in Werner syndrome fibroblast cells. Hum Mol Genet 2004; 13(14):1515-1524.

(251) Wiktor A, Rybicki BA, Piao ZS, Shurafa M, Barthel B, Maeda K et al. Clinical significance of Y chromosome loss in hematologic disease. Genes Chromosomes Cancer 2000; 27(1):11-16.

(252) Wong AK, Fang B, Zhang L, Guo X, Lee S, Schreck R. Loss of the Y chromosome: an age-related or clonal phenomenon in acute myelogenous leukemia/myelodysplastic syndrome? Arch Pathol Lab Med 2008; 132(8):1329-1332.

(253) Miura M, Miura Y, Padilla-Nash HM, Molinolo AA, Fu B, Patel V et al. Accumulated chromosomal instability in murine bone marrow mesenchymal stem cells leads to malignant transformation. Stem Cells 2006; 24(4):1095-1103.

(254) Zhou YF, Bosch-Marce M, Okuyama H, Krishnamachary B, Kimura H, Zhang L et al. Spontaneous transformation of cultured mouse bone marrow-derived stromal cells. Cancer Res 2006; 66(22):10849-10854.

(255) Dominguez C, Powers DA, Tamayo N. p38 MAP kinase inhibitors: many are made, but few are chosen. Curr Opin Drug Discov Devel 2005; 8(4):421-430.

9 Appendix

Symbol	Gene Name	Function	Process	Cytoband
ACTB	actin, beta	Cytoskeletal protein, Actin family cytoskeletal protein, Actin and actin related protein	Intracellular protein traffic, Exocytosis, Endocytosis, Cell cycle, Mitosis, Cytokinesis, Cell structure and motility	7p15-p12
ADAMTS1	ADAM metallopeptidase with thrombospondin type 1 motif, 1	Signalling molecule, Protease, Metalloprotease	Protein metabolism and modification, Proteolysis, Signal transduction, Cell communication	21q21.2
AKRC1,2	aldo-keto reductase family 1, member C1 (dihydrodiol dehydrogenase 1; 20-alpha (3-alpha)-hydroxysteroid dehydrogenase)	Oxido-reductase	Other metabolism	10p15-p14
ANXA2	annexin A2	Select calcium binding protein, Annexin, Transfer/carrier protein	Intracellular protein traffic, Mesoderm development, Cell structure and motility	15q21-q22
APLP2	amyloid beta (A4) precursor-like protein 2	Receptor	Cell surface receptor mediated signal transduction, Neuronal activities	11q23-q25; 11q24
ARPC2	actin related protein 2/3 complex, subunit 2, 34kDa	Actin family cytoskeletal protein	Cell structure and motility	2q36.1
ATP5G3	ATP synthase, H+ transporting, mitochondrial F0 complex, subunit C3 (subunit 9)	Hydrogen transporter, Synthase and synthetase, ATP synthase	Nucleotide and nucleic acid metabolism, Ion transport	2q31.1
BLVRB	biliverdin reductase B (flavin reductase (NADPH))	Oxido-reductase	Electron transport, Coenzyme and prosthetic group metabolism	19q13.1-q13.2
BSCL2, HNRPUL2	Bernardinelli-Seip congenital lipodystrophy 2 (seipin),heterogeneous nuclear ribonucleoprotein U-like 2	Molecular function unclassified	Biological process unclassified	11q12.3
CALM1,2	calmodulin 1 (phosphorylase kinase, delta),calmodulin 2 (phosphorylase kinase, delta)	Select calcium binding protein	Intracellular signalling cascade, Calcium mediated signalling, Cell cycle, Cell proliferation and differentiation	2p21
CAV1	caveolin 1, caveolae protein, 22kDa	Membrane traffic protein	Intracellular protein traffic	7q31.1
CCND1	cyclin D1	Select regulatory molecule, Kinase modulator, Kinase activator	Cell cycle control, Cell proliferation and differentiation	11q13
CCT7	chaperonin containing TCP1, subunit 7 (eta)	Chaperone	Protein metabolism and modification	2p13.2
CD44	CD44 molecule (Indian blood group)	Receptor, Cell adhesion molecule, Cell junction protein	Intracellular signalling cascade, MAPKKK cascade, Cell communication, Cell adhesion-mediated signalling, Immunity and defence, Oncogenesis, Inhibition of apoptosis, Cell structure and motility, Cell adhesion	11p13
CD63	CD63 molecule	Signalling molecule	Signal transduction, Cell communication, Cell adhesion-mediated signalling, Immunity and defence	12q12-q13
CDKN1A	cyclin-dependent kinase inhibitor 1A (p21, Cip1)	Select regulatory molecule, Kinase inhibitor	Oncogenesis, Tumour suppressor, Cell cycle control, Cell proliferation and differentiation	6p21.2
CDKN1B	cyclin-dependent kinase inhibitor 1B (p27, Kip1)	Select regulatory molecule, Kinase inhibitor	Oncogenesis, Tumour suppressor, Cell cycle control, Cell proliferation and differentiation	12p13.1-p12
CDKN2A	cyclin-dependent kinase inhibitor 2A (melanoma, p16, inhibits CDK4)	Select regulatory molecule, Kinase inhibitor, Molecular function unclassified	Oncogenesis, Tumour suppressor, Cell cycle control, Biological process unclassified	9p21
CEECAM1	cerebral endothelial cell adhesion molecule 1	Cell adhesion molecule, Other cell adhesion molecule	Cell adhesion	9q34.11
CLIC1	chloride intracellular channel 1	Ion channel, Voltage-gated ion channel	Biological process unclassified	6p22.1-p21.2
COL1A1	collagen, type I, alpha 1	Extracellular matrix structural protein	Mesoderm development, Skeletal development, Cell structure and motility, Cell adhesion	17q21.33
COL1A2	collagen, type I, alpha 2	Extracellular matrix structural protein	Mesoderm development, Skeletal development, Cell structure and motility, Cell adhesion	7q22.1
COL3A1	collagen, type III, alpha 1 (Ehlers-Danlos syndrome type IV, autosomal dominant)	Extracellular matrix structural protein	Cell structure and motility	2q31
COL5A1	collagen, type V, alpha 1	Extracellular matrix structural protein	Cell structure and motility	9q34.2-q34.3
COTL1	coactosin-like 1	Molecular function	Biological process unclassified	16q24.1

	(Dictyostelium)	unclassified		
COX5B	cytochrome c oxidase subunit Vb	Oxido-reductase	Electron transport, Oxidative phosphorylation	2cen-q13
CST3	cystatin C (amyloid angiopathy and cerebral haemorrhage)	Select regulatory molecule, Cysteine protease inhibitor	Protein metabolism and modification, Proteolysis	20p11.21
CTGF	connective tissue growth factor, Gene hCG22108 Celera Annotation	Signalling molecule, Growth factor, Cell adhesion molecule	Cell surface receptor mediated signal transduction, Cell communication, Ligand-mediated signalling, Immunity and defence, Stress response, Oncogenesis, Mesoderm development, Angiogenesis, Cell structure and motility	6q23.1
CTSS	Cathepsin S	Protease, Cysteine protease	Protein metabolism and modification, Proteolysis	1q21
DEGS1	degenerative spermatocyte homolog 1, lipid desaturase (Drosophila)	Oxido-reductase	Other metabolism	1q42.11
DPYSL3	dihydropyrimidinase-like 3	Hydrolase,	Nucleotide and nucleic acid metabolism	5q32
DSP	desmoplakin	Cytoskeletal protein, Intermediate filament,	Cell structure and motility, Cell adhesion	6p24
DUSP6	dual specificity phosphatase 6	Protein phosphatase, Kinase inhibitor	Protein metabolism and modification, Intracellular signalling cascade, MAPKKK cascade, Immunity and defence, Stress response, Antioxidation and free radical removal	12q22-q23
DVL1	dishevelled, dsh homolog 1 (Drosophila)	Select regulatory molecule	Ectoderm development, Neurogenesis, Mesoderm development, Heart development	1p36
ELN	elastin (supravalvular aortic stenosis, Williams-Beuren syndrome)	Extracellular matrix protein, Structural protein	Blood circulation and gas exchange, Cell structure and motility, Cell proliferation and differentiation	7q11.23
FBXO18	F-box protein, helicase, 18	Nucleic acid binding, Helicase	Biological process unclassified	10p15.1
FOS	v-fos FBJ murine osteosarcoma viral oncogene homolog	Transcription factor	Nucleotide and nucleic acid metabolism, mRNA transcription, Immunity and defence, Oncogenesis, Mesoderm development, Skeletal development, Cell cycle control, Cell proliferation and differentiation	14q24.3
FOXO3A	forkhead box O3A	Transcription factor	Nucleotide and nucleic acid metabolism, mRNA transcription, Cell cycle control, Induction of apoptosis	6q21
GAPDH	glyceraldehyde 3-phosphate dehydrogenase	Molecular function unclassified	Biological process unclassified	12p13.3
GARS	glycyl-tRNA synthetase	Synthase and synthetase, Aminoacyl-tRNA synthetase, Ligase	Protein metabolism and modification, Amino acid activation	7p15
GPX4	glutathione peroxidase 4 (phospholipid hydroperoxidase)	Oxido-reductase, Peroxidase	Lipid, fatty acid and steroid metabolism, Immunity and defence, Stress response, Detoxification, Antioxidation and free radical removal	19p13.3
HMGA1	high mobility group AT-hook 1	Molecular function unclassified	Biological process unclassified	6p21
HMOX1	heme oxygenase (decycling) 1	Oxido-reductase	Coenzyme and prosthetic group metabolism, Porphyrin metabolism	22q12; 22q13.1
HNF4A	hepatocyte nuclear factor 4	Receptor, Transcription factor, Nuclear hormone receptor, Nucleic acid binding	Lipid, fatty acid and steroid metabolism, Nucleoside, nucleotide and nucleic acid metabolism, mRNA transcription, Signal transduction, Cell communication, Developmental processes	20q12-q13.1
HSPA8	heat shock 70kDa protein 8	Hsp 70 family chaperone	Protein metabolism and modification, Immunity and defence, Stress response	11q24.1
HTRA1	HtrA serine peptidase 1	Serine protease	Protein metabolism and modification, Proteolysis, Intracellular signalling cascade, Cell communication	10q26.3
IFI30	interferon, gamma-inducible protein 30	Oxido-reductase	Immunity and defence	19p13.1
IGFBP4	insulin-like growth factor binding protein 4	Miscellaneous function	Signal transduction, Cell communication, Extracellular matrix protein-mediated signalling, Homeostasis, Growth factor homeostasis	17q12-q21.1
IL6ST	interleukin 6 signal transducer (gp130, oncostatin M receptor)	Cytokine receptor, Interleukin receptor	Cell surface receptor mediated signal transduction, Cytokine and chemokine mediated signalling pathway, Intracellular signalling cascade, MAPKKK cascade, JAK-STAT cascade, Cell communication, Ligand-mediated signalling,	5q11

			Immunity and defence, Mesoderm development, Haematopoiesis	
ITGA1	integrin, alpha 11	Receptor, Cell adhesion molecule,	Signal transduction, Cell surface receptor mediated signal transduction, Cell communication, Cell adhesion	15q23
KDELR2	KDEL (Lys-Asp-Glu-Leu) endoplasmic reticulum protein retention receptor 2	Receptor, Membrane traffic regulatory protein	Intracellular protein traffic, Exocytosis	7p22.1
KIAA1199	KIAA1199	Molecular function unclassified	Biological process unclassified	15q24
KLF9	Kruppel-like factor 9	Zinc finger transcription factor, KRAB box transcription factor	Nucleoside, nucleotide and nucleic acid metabolism, mRNA transcription,	9q13
LMO7	LIM domain 7	Molecular function unclassified	Biological process unclassified	13q22.2
LOC401152	HCV F-transactivated protein 1	Molecular function unclassified	Biological process unclassified	4q26
LOXL1	lysyl oxidase-like 1	Extracellular matrix, Oxido-reductase	Oncogenesis, Tumour suppressor	15q24-q25; 15q22
LUM	Lumican	Extracellular matrix	Signal transduction, Cell communication, Cell adhesion-mediated signalling	12q21.3-q22
MRC2	mannose receptor, C type 2	Receptor	Intracellular protein traffic, Endocytosis, Phagocytosis,	17q23.2
MVP	major vault protein	Nucleic acid binding, Ribonucleoprotein	Biological process unclassified	16p13.1-p11.2
MYL9	myosin, light chain 9, regulatory	Select calcium binding protein	Muscle contraction, Mesoderm development, Muscle development, Cell structure and motility	20q11.23
MYO10	myosin X	Cytoskeletal protein	Cell structure and motility	5p15.1-p14.3
OAZ2	ornithine decarboxylase antizyme 2	Select regulatory molecule, enzyme inhibitor, Miscellaneous function	Protein metabolism and modification, Proteolysis, Oncogenesis, Gametogenesis, Spermatogenesis and motility, Apoptosis	15q22.31
OLFML3	olfactomedin-like 3	Extracellular matrix glycoprotein	Sensory perception, Olfaction	1p13.2
PEA15	phosphoprotein enriched in astrocytes 15	Molecular function unclassified	Biological process unclassified	1q21.1
PLAT	plasminogen activator, tissue	Tyrosine protein kinase receptor, Serine protease	Protein metabolism and modification, Proteolysis, Cell surface receptor mediated signal transduction, Receptor protein tyrosine kinase signalling pathway, Immunity and defence, Blood clotting, Ectoderm development, Neurogenesis	8p12
POLR2A	polymerase (RNA) II (DNA directed) polypeptide A, 220kDa	Nucleic acid binding, DNA-directed RNA polymerase, Nucleotidyltransferase	Nucleoside, nucleotide and nucleic acid metabolism, mRNA transcription,	17p13.1
PRG1	proteoglycan 1, secretory granule			10q22.1
PRSS23	protease, serine, 23	Serine protease, Hydrolase	Protein metabolism and modification, Proteolysis	11q14.1
PSAP	prosaposin (variant Gaucher disease and variant metachromatic leukodystrophy)	Miscellaneous function	Lipid, fatty acid and steroid metabolism, Lipid and fatty acid transport	10q21-q22
PTGS2	prostaglandin-endoperoxide synthase 2 (prostaglandin G/H synthase and cyclooxygenase)	Synthase and synthetase, Oxido-reductase, Peroxidase	Lipid, fatty acid and steroid metabolism, Fatty acid biosynthesis,	1q25.2-q25.3
ROR1	receptor tyrosine kinase-like orphan receptor 1	Tyrosine protein kinase receptor	Protein metabolism and modification, Cell surface receptor mediated signal transduction, Receptor protein tyrosine kinase signalling pathway, Ectoderm development, Neurogenesis	1p32-p31
RPLP0	Ribosomal protein, large, P0	Nucleic acid binding, Ribosomal protein	Protein metabolism and modification	12q24.2
RTN4	reticulon 4	Miscellaneous function, Transmembrane receptor regulatory/adaptor protein	Intracellular protein traffic	2p16.3
S100A6	S100 calcium binding protein A6	Signalling molecule, Growth factor, Select calcium binding protein,	Signal transduction, Cell cycle control, Cell proliferation and differentiation	1q21
SERPINE1	serpin peptidase inhibitor, clade E (nexin, plasminogen activator inhibitor type 1), member 1	Select regulatory molecule, Serine protease inhibitor	Protein metabolism and modification, Proteolysis, Immunity and defence	7q21.3-q22
SERPINE2	serpin peptidase inhibitor, clade E (nexin, plasminogen activator inhibitor type 1), member 2	Select regulatory molecule, Serine protease inhibitor	Protein metabolism and modification, Proteolysis, Neuronal activities	2q33-q35
SHC1	SHC (Src homology 2 domain containing) transforming protein 1	Signalling molecule	Signal transduction, Cell surface receptor mediated signal transduction, Receptor protein	1q21

			tyrosine kinase signalling pathway, Intracellular signalling cascade, MAPKKK cascade, Oncogenesis, Cell cycle control	
SLC38A2	solute carrier family 38, member 2	Transporter	Amino acid metabolism and transport	12q
SOD1	superoxide dismutase 1, soluble (amyotrophic lateral sclerosis 1 (adult)),Gene hCG1748590 Celera Annotation	Oxido-reductase	Immunity and defence	21q22.1; 21q22.11
SPARC	secreted protein, acidic, cysteine-rich (osteonectin)	Extracellular matrix glycoprotein	Immunity and defence, Cell proliferation and differentiation	5q31.3-q32
SRM	spermidine synthase	Synthase and synthetase, Transferase	Other metabolism	1p36-p22
STAT1	signal transducer and activator of transcription 1, 91kDa	Transcription factor, Nucleic acid binding	Nucleoside, nucleotide and nucleic acid metabolism, mRNA transcription, mRNA transcription termination, Intracellular signalling cascade, JAK-STAT cascade, Immunity and defence, Stress response, Oncogenesis, Mesoderm development, Haematopoiesis, Cell cycle control, Inhibition of apoptosis, Cell proliferation and differentiation	2q32.2
STC2	stanniocalcin 2	Signalling molecule, Peptide hormone	Signal transduction, Cell surface receptor mediated signal transduction, Ion transport, Calcium ion homeostasis	5q35.2
TGFBI	transforming growth factor, beta-induced, 68kDa	Signalling molecule, Cell adhesion molecule	Signal transduction, Cell communication, Extracellular matrix protein-mediated signalling, Sensory perception, Vision, Mesoderm development, Skeletal development, Cell proliferation and differentiation, Cell adhesion	5q31
TGM2	transglutaminase 2 (C polypeptide, protein-glutamine-gamma-glutamyltransferase)	Select calcium binding protein, Annexin, Transferase, Acyltransferase	Protein metabolism and modification	20q12
THY1	Thy-1 cell surface antigen	Membrane-bound signalling molecule	Signal transduction, Cell communication, Ligand-mediated signalling	11q22.3-q23
TM4SF1	transmembrane 4 L six family member 1	Molecular function unclassified	Oncogenesis	3q21-q25
TMEM47	transmembrane protein 47	Miscellaneous function	Apoptosis	Xp11.4
TRAM2	translocation associated membrane protein 2	Molecular function unclassified	Biological process unclassified	6p21.1-p12
TUBB6	tubulin, beta 6	Cytoskeletal protein, Microtubule family	Intracellular protein traffic, Cell cycle, Mitosis, Chromosome segregation, Cell structure and motility	18p11.21
UBC	ubiquitin C	Molecular function unclassified	Protein metabolism and modification	12q24.3
VCP	valosin-containing protein	Hydrolase	Protein metabolism and modification, Intracellular protein traffic, Exocytosis, Protein targeting and localization	9p13.3
VIM	Vimentin	Cytoskeletal protein, Intermediate filament	Cell structure and motility	10p13
WBSCR1	Williams-Beuren syndrome chromosome region 1	Nucleic acid binding, Translation factor, Translation initiation factor	Protein metabolism and modification, Protein biosynthesis	7q11.23
YIPF5	Yip1 domain family, member 5	Molecular function unclassified	Biological process unclassified	5q32
YWHAB	tyrosine 3-monooxygenase/tryptophan 5-monooxygenase activation protein, beta polypeptide	Miscellaneous function	Non-vertebrate process	20q13.1

Table 8 Characteristics of genes on the TLDA

Long Tag	Unigene	Gene	Tags			O.R 25P9: 25P2	P	O.R 25P9: 12P2	P	O.R 25P2: 12P2	P
			12P2	25P2	25P9						
GCTTTATTTGTTTTTTT	Hs.520640	ACTB[4,11]	13	189	179	0.98	n.s	14.39	***	15.11	***
TACTTTATAAGTATTGG	Hs.643357	ADAMTS1[1,15]	7	2	28	14.44	***	4.18	***	0.30	n.s
AGGTCTGCCAGAAGGCC	Hs.567256	AKR1C2[1]	1	1	14	14.44	***	14.63	***	1.04	n.s
CTTCCAGCTAACAGGTC	Hs.511605	ANXA2[2,15]	123	61	137	2.32	***	1.16	n.s	0.52	***
AATAGGGTCAAAGGGGA	Hs.370247	APLP2[1,15]	4	2	18	9.28	***	4.70	***	0.52	n.s
CAGGAGTTCAAAGAAGG	Hs.529303	ARPC2[2]	29	9	39	4.47	***	1.41	n.s	0.32	***
GGAATGTACGTTATTTC	Hs.429	ATP5G3	17	4	23	5.93	***	1.41	n.s	0.24	**
AGGAGCAAAGGAAGGGG	Hs.515785	BLVRB[1]	3	4	25	6.44	***	8.71	***	1.39	n.s
AAGCTGAATCTCTGGGG	Hs.533709	BSCL2[1]	1	1	6	6.19	*	6.27	n.s	1.04	n.s
TTGTTGTTGAAGTGTGG	Hs.643483	CALM2[2,15]	46	14	35	2.58	***	0.80	n.s	0.32	***
TCCTGTAAAGGTTACAA	Hs.74034	CAV1[2,9]	14	2	12	6.19	**	0.90	n.s	0.15	**
AAAGTCTAGAAATAAAA	Hs.523852	CCND1[1,15]	2	4	21	5.41	***	10.97	***	2.08	n.s
GCTGGCTGGCTGCTGGG	Hs.368149	CCT7[2]	14	5	19	3.92	***	1.42	n.s	0.37	*
ATATGTATATTGCTGAG	Hs.502328	CD44[1,15]	4	3	12	4.12	*	3.14	*	0.78	n.s
TCGAAGAACCGAGTCCC	Hs.445570	CD63[2]	55	17	50	3.03	***	0.95	n.s	0.32	***
TGTCCTGGTTCCCGTTT	Hs.370771	CDKN1A[10]	1	1	1	1.03	n.s	1.05	n.s	1.04	n.s
TTTTGTGCATTTGTAAA	Hs.238990	CDKN1B[10]	1	1	1	1.03	n.s	1.05	n.s	1.04	n.s
AAGAGAAGCAATTTTGG	Hs.238990	CDKN1B[10]	1	2	1	0.52	n.s	1.05	n.s	2.08	n.s
CCCGCATAGATGCCGCG	Hs.512599	CDKN2A[10]	2	1	1	1.03	n.s	0.52	n.s	0.52	n.s
GCCACTCTGCCCTCTGG	Hs.495230	CEECAM1	1	2	12	6.19	**	12.54	***	2.08	n.s
GTACTGTGGCTCAAGGG	Hs.414565	CLIC1[2]	39	5	25	5.16	***	0.67	n.s	0.13	***
ACCAAAAACCAAAAGTG	Hs.172928	COL1A1[1,2,8,15]	138	289	177	0.63	***	1.34	**	2.18	***
CCGGGGGAGCCACCAGC	Hs.172928	COL1A1[2,8,15]	7	40	14	0.36	***	2.09	n.s	5.94	***
GACCAGCAGACTGGCAA	Hs.172928	COL1A1[3,8,15]	17	21	10	0.49	*	0.61	n.s	1.25	n.s
TGGAAATGACCCAAACA	Hs.172928	COL1A1[1,8,15]	22	17	6	0.36	*	0.29	***	0.80	n.s
GGAGGAGAGCGTGTGCG	Hs.172928	COL1A1[1,8,15]	8	14	1	0.07	***	0.13	*	1.82	n.s
GGCCCCCCTGGATTGGC	Hs.172928	COL1A1[3,8,15]	4	9	1	0.11	*	0.26	n.s	2.28	n.s
GACTTTGGAAAATATTT	Hs.172928	COL1A1[2,8,15]	1	8	1	0.13	*	1.05	n.s	8.32	*
GATGAGGAGACTGGCAA	Hs.489142	COL1A2[1,8,15]	97	101	58	0.59	***	0.62	***	1.08	n.s
TTTGGTTTTCCAAAAGA	Hs.489142	COL1A2[1,2,8,15]	42	83	34	0.42	***	0.85	n.s	2.05	***
TTTGGTTTTCCAAAAAA	Hs.489142	COL1A2[2,8,15]	12	27	3	0.11	***	0.26	*	2.34	**
CCGTGACTTGAGACTCA	Hs.489142	COL1A2[2,8,15]	1	14	1	0.07	***	1.05	n.s	14.55	***
GTTCCACAGAAGCTTTG	Hs.489142	COL1A2[1,8,15]	17	17	1	0.06	***	0.06	***	1.04	n.s
CCACAGGGGATTCTCCT	Hs.443625	COL3A1[1,2]	29	47	4	0.09	***	0.14	***	1.68	*
GATCAGGCCAGTGGAAA	Hs.443625	COL3A1[1]	33	29	15	0.53	*	0.48	**	0.91	n.s
CCAGGTCCTAGGGGAAG	Hs.443625	COL3A1[2]	1	7	1	0.15	*	1.05	n.s	7.28	*
CCTCCAGCCCCCCAGCT	Hs.210283	COL5A1[1]	6	13	1	0.08	***	0.17	*	2.25	n.s
TGATTCTGTTTTCATTT	Hs.210283	COL5A1[2]	4	16	4	0.26	**	1.05	n.s	4.16	**
AGCACATTTGATATAGC	Hs.289092	COTL1[3]	17	9	23	2.64	**	1.41	n.s	0.55	n.s
CTGGCTGCAAAGAAGGG	Hs.1342	COX5B[1]	11	5	23	4.74	***	2.19	*	0.47	n.s
TGCCTGCACCAGGAGAC	Hs.304682	CST3[3,15]	14	7	24	3.54	***	1.79	n.s	0.52	n.s
TTTGCACCTTTCTAGTT	Hs.591346	CTGF[2,8,15]	101	141	89	0.65	***	0.92	n.s	1.45	***
CCTGTAATCCCAGCTAC	Hs.181301	CTSS[3,15]	12	6	18	3.09	**	1.57	n.s	0.52	n.s
GGAGGCTGAGGTGGGAG	Hs.299878	DEGS1[2]	12	3	16	5.50	***	1.39	n.s	0.26	*
GGCTGCCCTGGGCAGCC	Hs.519659	DPYSL3[1]	11	10	2	0.21	*	0.19	*	0.95	n.s
ACAGCGGCAATCTTTTC	Hs.519873	DSP[3]	4	1	9	9.28	*	2.35	n.s	0.26	n.s
GGTACCCATTTGATAAG	Hs.712581	DUSP6[3]	1	1	6	6.19	*	6.27	n.s	1.04	n.s
GCCCGCAGGGTCAAGGG	Hs.74375	DVL1[1]	5	1	13	13.40	***	2.72	*	0.21	n.s

CAGTACTGTATACCCCC	Hs.647061	ELN[3,15]	25	15	34	2.34	***	1.42	n.s	0.62	n.s
AGGCCCTGCTCTTCCTC	Hs.498543	FBXO18[7,14]	1	1	1	1.03	n.s	1.05	n.s	1.04	n.s
TGGAAAGTGAATTTGAA	Hs.25647	FOS[1,12,13,15]	11	37	7	0.20	***	0.67	n.s	3.50	***
TAAATAAAGCATCAGTG	Hs.220950	FOXO3A[7,12,14]	3	2	2	1.03	n.s	0.70	n.s	0.69	n.s
TACCATCAATAAAGTAC	Hs.544577	GAPDH[2,11]	76	125	207	1.71	***	2.85	n.s	1.71	***
GGCTGATGTGGAGGCCA	Hs.404321	GARS[1]	17	14	3	0.22	**	0.18	***	0.86	n.s
GCCTGCTGGGCTTGGCT	Hs.433951	GPX4[1,15]	17	9	1	0.11	*	0.06	***	0.55	n.s
ATTTGTCCCAGCCTGGG	Hs.518805	HMGA1[1,12,15]	6	2	33	17.01	***	5.75	***	0.35	n.s
CGTGGGTGGGGAGGGAG	Hs.517581	HMOX1[1,15]	11	8	26	3.35	***	2.47	**	0.76	n.s
TGTATATAAAGCCTCAC	Hs.116462	HNF4A[7,12,14]	1	1	1	1.03	n.s	1.05	n.s	1.04	n.s
CCAGGAGGAATGCCTGG	Hs.180414	HSPA8[1,2]	54	17	83	5.03	***	1.61	***	0.33	***
TTTCCCTCAAAGACTCT	Hs.501280	HTRA1[2]	7	15	2	0.14	***	0.30	n.s	2.23	*
ATCAAGAATCCTGCTCC	Hs.14623	IFI30[3,15]	4	2	10	5.16	*	2.61	n.s	0.52	n.s
ATGTCTTTTCTTCTTTT	Hs.462998	IGFBP4[4,6]	14	85	85	1.03	n.s	6.35	***	6.31	***
TGCTAATTGTAACCACA	Hs.532082	IL6ST[6,9]	12	11	8	0.75	n.s	0.70	n.s	0.95	n.s
CCCGCCAGTGCACAGGG	Hs.436416	ITGA11[1]	14	24	4	0.17	***	0.30	*	1.78	n.s
AAAGGCATCAGTCCCCC	Hs.436416	ITGA11[2]	10	24	11	0.47	*	1.15	n.s	2.50	**
ATACCTTCCGAGTGGAG	Hs.654552	KDELR2[1,15]	3	5	18	3.71	**	6.27	***	1.73	n.s
AACAAAGATATATTTTC	Hs.459088	KIAA1199[1]	1	1	14	14.44	***	14.63	***	1.04	n.s
CTTCTCTTGAGAATTCT	Hs.150557	KLF9[3,12]	5	1	6	6.19	*	1.25	n.s	0.21	n.s
GTTTGTATACTAGAAGT	Hs.207631	LMO7[1,3]	8	6	18	3.09	**	2.35	*	0.78	n.s
ACTTGTTCGCTGATATC	Hs.173705	LOC401152[2]	11	1	8	8.25	*	0.76	n.s	0.09	***
CACCTCTCATACCCAGG	Hs.65436	LOXL1[2,15]	45	17	38	2.30	***	0.88	n.s	0.39	***
TTATGTTTAATAAGCTA	Hs.406475	LUM[2]	4	17	2	0.12	***	0.52	n.s	4.42	**
GCCCTTTCTCTGTAGTT	Hs.7835	MRC2[2]	13	51	5	0.10	***	0.40	n.s	4.08	***
GCCGTGGAGAGCACCGG	Hs.632177	MVP[3,15]	5	1	12	12.37	***	2.51	n.s	0.21	n.s
GGAGTGTGCTCAGGAGT	Hs.504687	MYL9[5]	108	118	104	0.91	n.s	1.01	n.s	1.14	n.s
CAAAACTGTTTGTTGGC	Hs.481720	MYO10[1]	1	1	11	11.34	***	11.50	**	1.04	n.s
GCCTGGAGGGCTGGTGG	Hs.74563	OAZ2[3,15]	6	1	10	10.31	**	1.74	n.s	0.17	n.s
TCAACAAATTTCAGGCT	Hs.9315	OLFML3[1]	19	24	5	0.21	***	0.28	**	1.31	n.s
AACTGTCCTTCCATTTG	Hs.517216	PEA15[2,15]	12	4	14	3.61	*	1.22	n.s	0.35	*
TTAGTTTTTACTTTCTG	Hs.491582	PLAT[1,15]	1	1	8	8.25	*	8.36	*	1.04	n.s
TCTCCCAGCTACTCGCC	Hs.270017	POLR2A[7,11]	1	2	1	0.52	n.s	1.05	n.s	2.08	n.s
GCCATAAAATGGCTTTA	Hs.1908	PRG1[4,9]	1	8	9	1.16	n.s	9.41	n.s	8.32	*
TTCTTATTTTAGGAGAG	Hs.25338	PRSS23[1]	4	4	30	7.73	***	7.84	***	1.04	n.s
AAGTTGCTATTAAATGG	Hs.523004	PSAP[1,15]	6	7	19	2.80	**	3.31	**	1.21	n.s
CTGTTCCTTTTCTTTTC	Hs.196384	PTGS2[9]	4	1	3	3.09	n.s	0.78	n.s	0.26	n.s
GACACACCGAATCTATG	Hs.654491	ROR1[12,14]	1	1	1	1.03	n.s	1.05	n.s	1.04	n.s
CTCAACATCTCCCCCTT	Hs.546285	RPLP0[6,11]	42	35	31	0.91	n.s	0.77	n.s	0.87	n.s
TGTTCATCATCTTAAGT	Hs.645283	RTN4[1]	2	2	10	5.16	*	5.23	*	1.04	n.s
AAATGCCACACACATAG	Hs.645283	RTN4[3]	2	1	7	7.22	*	3.66	n.s	0.51	n.s
CCCCCTGGATCAGGCCA	Hs.275243	S100A6[1,2]	48	13	29	2.30	**	0.63	*	0.28	***
GGTTATTTTGGAGTGTA	Hs.414795	SERPINE1[1,2,15]	13	3	44	15.12	***	3.54	***	0.24	*
TATTCACTAAAATAAAA	Hs.38449	SERPINE2[1,2,15]	8	23	56	2.51	***	7.32	***	2.99	**
GAGGGGAAACGCAAAAC	Hs.433795	SHC1[3]	4	1	9	9.28	***	2.35	n.s	0.26	n.s
CTTAATCCTGAAAAAAA	Hs.221847	SLC38A2	8	10	1	0.10	*	0.13	*	1.30	n.s
AAAAAGCAGATGACTTG	Hs.443914	SOD1[2]	12	1	16	16.50	***	1.39	n.s	0.09	***
ATGTGAAGAGTTTCACA	Hs.111779	SPARC[2,8,15]	72	226	76	0.35	***	1.10	n.s	3.26	***
TTAGTGTCGTATTTTGA	Hs.111779	SPARC[3,8,15]	13	22	8	0.37	*	0.64	n.s	1.72	n.s
GGTGGACACGGATCTGC	Hs.111779	SPARC[1,8,15]	11	11	1	0.09	**	0.10	**	1.04	n.s
GAGCATTGCACCACCCG	Hs.111779	SPARC[1,8,15]	8	12	1	0.09	***	0.13	*	1.56	n.s

CTGTGCAGCAAGAACCC	Hs.76244	SRM[2]	11	2	13	6.70	**	1.24	n.s	0.19	*
CAAATGCTGTATTCTTC	Hs.655132	STAT1[2,9,12,15]	8	1	14	14.44	***	1.83	n.s	0.13	*
CCCGAGGCAGAGTCGGG	Hs.233160	STC2[1,2]	53	14	82	6.04	***	1.62	***	0.27	***
GTGTGTTTGTAATAATA	Hs.369397	TGFBI[2,8]	34	143	72	0.52	***	2.21	n.s	4.37	***
GGAAGTCCTGGCACAGT	Hs.369397	TGFBI[2,8]	6	17	6	0.36	*	1.05	n.s	2.95	*
GGCCGCACCATAATGAG	Hs.369397	TGFBI[1,8]	1	10	1	0.10	**	1.05	**	10.40	n.s
TATATTTTCTCTATACA	Hs.517033	TGM2[1,9]	3	2	12	6.19	**	4.18	*	0.69	n.s
GAGTGAGACCCAGGAGC	Hs.653181	THY1[2]	42	24	53	2.28	***	1.32	n.s	0.59	*
GGGACGAGTGACGGCAG	Hs.715499	TM4SF1[3]	14	5	17	3.51	**	1.27	n.s	0.37	n.s
AAGTCATCTATGTGGAA	Hs.8769	TMEM47[1]	1	1	10	10.31	**	10.45	**	1.04	n.s
TAAAAAAGGGTTGGGGG	Hs.520182	TRAM2[1,15]	3	2	11	5.67	*	3.83	*	0.69	n.s
TCTGCAAATTAGGAGGG	Hs.193491	TUBB6[2,15]	18	3	24	8.25	***	1.39	n.s	0.17	***
GGGTCCCGGGTCCGCCT	Hs.520348	UBC[11]	1	1	1	1.03	n.s	1.05	n.s	1.04	n.s
TTGTAAAAGGACAATAA	Hs.529782	VCP[1]	3	2	11	5.67	*	3.83	*	0.69	n.s
TCCAAATCGATGTGGAT	Hs.642813	VIM[1,8,15]	131	73	166	2.34	***	1.32	**	0.58	n.s
CATCTAAACTGCTGGGC	Hs.520943	WBSCR1[3]	15	8	25	3.22	***	1.74	n.s	0.55	n.s
CAGAGTTGTATATAGCC	Hs.372050	YIPF5[1]	3	4	17	4.38	**	5.92	***	1.39	n.s
CTTTTTGTGCCTGTCAC	Hs.651212	YWHAB[2]	11	1	8	8.25	*	0.76	n.s	0.09	**

Table 9 SAGE results matching genes on the TLDA

[1]Genes differentially expressed 25P2v25P9 and found in 12P2v25P9 (F=1, p<0.05)
[2]Genes differentially expressed 25P2v25P9 and found in 25P2v12P2 (F=1, p<0.05)
[3]Genes differentially expressed 25P2v25P9 (F=1, p<0.05)
[4]Genes not differentially expressed 25P2v25P9 but significantly different 12P2 and 25P2 and P9 (F=1, p<0.05)
[5]Gene matching a high abundance tag in SAGE
[6]Gene matching moderate abundance tags in SAGE
[7]Gene matching low abundance tags in SAGE
[8]Gene abundant in MSC's from other studies
[9]Potential p38 target gene
[10]Cell cycle control gene
[11]Endogenous control gene
[12]Trancription factor
[13]Component of AP-1 transcription factor
[14]Wild card gene
[15]Gene identified on the regulatory network from Metacore™

O.R - Odds Ratio
P - P value, * ≤ 0.05, ** ≤0.01, *** ≤0.001 and n.s, not significant

Gene	25 P2 RQ	25 P2 RQ Min	25 P2 RQ Max	25 P5 RQ	25 P5 RQ Min	25 P5 RQ Max	25 P9 RQ	25 P9 RQ Min	25 P9 RQ Max
GAPDH	1	0.832	1.202	1.119	0.798	1.570	1.024	0.783	1.340
ACTB	1	0.825	1.211	0.804	0.779	0.831	0.687	0.512	0.920
ADAMTS1	1	0.693	1.443	2.326	2.310	2.341	3.107	2.159	4.469
AKR1C1,2	1	0.824	1.213	0.594	0.535	0.658	2.818	1.957	4.057
ANXA2	1	0.826	1.211	1.351	1.040	1.756	1.482	1.054	2.083
APLP2	1	0.793	1.261	1.466	0.998	2.154	2.369	1.872	3.000
ARPC2	1	0.752	1.329	0.898	0.740	1.091	1.398	1.057	1.849
ATP5G3	1	0.834	1.199	0.859	0.673	1.097	2.391	1.877	3.046
BLVRB	1	0.853	1.172	0.970	0.808	1.165	1.791	1.421	2.258
BSCL2	1	0.902	1.109	0.934	0.924	0.944	1.260	0.828	1.918
CALM1,2	1	0.781	1.280	1.177	0.688	2.014	1.413	1.064	1.876
CAV1	1	0.728	1.374	1.475	1.136	1.916	3.696	2.580	5.296
CCND1	1	0.834	1.199	4.292	3.055	6.030	9.625	7.607	12.18
CCT7	1	0.856	1.168	0.984	0.979	0.988	1.757	1.193	2.588
CD44	1	0.871	1.148	2.931	2.448	3.509	4.547	3.473	5.953
CD63	1	0.897	1.115	1.007	0.979	1.035	1.375	0.988	1.914
CDKN1A	1	0.899	1.112	0.852	0.851	0.853	1.054	0.781	1.423
CDKN1B	1	0.838	1.194	0.629	0.628	0.631	0.572	0.441	0.740
CDKN2A	1	0.891	1.122	0.686	0.636	0.740	1.139	0.822	1.579
CEECAM1	1	0.894	1.118	0.818	0.754	0.886	0.910	0.710	1.165
CLIC1	1	0.852	1.174	1.202	1.157	1.249	1.465	1.087	1.975
COL1A1	1	0.537	1.862	0.570	0.271	1.197	0.268	0.208	0.345
COL1A2	1	0.850	1.177	0.535	0.195	1.467	0.312	0.239	0.406
COL3A1	1	0.855	1.169	0.382	0.327	0.447	0.240	0.187	0.308
COL5A1	1	0.899	1.113	0.442	0.367	0.533	0.405	0.304	0.541
COTL1	1	0.836	1.196	1.257	1.218	1.297	1.764	1.319	2.359
COX5B	1	0.902	1.109	0.889	0.778	1.016	1.466	1.159	1.854
CST3	1	0.821	1.218	0.908	0.807	1.022	1.006	0.785	1.289
CTGF	1	0.866	1.154	0.668	0.665	0.671	0.821	0.649	1.039
CTSS	1	0.691	1.446	0.414	0.230	0.743	0.336	0.258	0.438
DEGS1	1	0.901	1.110	1.283	1.039	1.584	1.401	1.103	1.780
DPYSL3	1	0.902	1.108	0.429	0.362	0.508	0.292	0.194	0.440
DSP	1	0.901	1.110	1.770	1.374	2.280	2.418	1.864	3.137
DUSP6	1	0.728	1.373	1.611	1.071	2.423	2.554	1.873	3.484
DVL1	1	0.485	2.063	1.081	0.896	1.305	1.475	1.103	1.973
ELN	1	0.609	1.642	2.309	1.754	3.039	1.920	1.451	2.540
FBXO	1	0.787	1.271	0.913	0.892	0.935	0.776	0.601	1.002
FOS	1	0.838	1.193	0.850	0.769	0.940	0.683	0.534	0.874
FOXO3A	1	0.762	1.313	0.604	0.469	0.776	0.492	0.219	1.109
GARS	1	0.901	1.110	0.420	0.302	0.585	0.499	0.353	0.706
GPX4	1	0.820	1.220	0.816	0.692	0.962	0.577	0.282	1.181
HMGA1	1	0.155	6.465	2.037	1.116	3.716	6.245	4.291	9.087
HMOX1	1	0.795	1.258	1.087	1.022	1.156	0.701	0.530	0.928
HNF4A	Not detected after 40 cycles								
HSPA8	1	0.872	1.146	1.007	0.730	1.389	1.602	1.200	2.138
HTRA1	1	0.89	1.124	0.302	0.297	0.306	0.255	0.166	0.391
IFI30	1	0.817	1.223	1.127	1.072	1.185	1.624	1.050	2.511
IGFBP4	1	0.896	1.116	1.174	1.085	1.269	1.167	0.907	1.501
IL6ST	1	0.893	1.120	0.938	0.888	0.991	1.282	0.950	1.731
ITGA11	1	0.896	1.116	0.627	0.549	0.718	0.170	0.127	0.226
KDELR2	1	0.881	1.135	0.976	0.971	0.982	1.149	0.663	1.991
KIAA1199	1	0.792	1.263	5.292	4.771	5.870	3.916	2.733	5.612
KLF9	1	0.898	1.113	0.999	0.948	1.053	0.621	0.492	0.783
LMO7	1	0.872	1.146	0.913	0.563	1.480	1.106	0.788	1.551

LOC401152	1	0.765	1.307	0.708	0.678	0.739	0.703	0.557	0.888
LOXL1	1	0.831	1.204	0.652	0.512	0.831	0.708	0.543	0.923
LUM	1	0.509	1.965	0.736	0.716	0.757	0.233	0.182	0.299
MRC2	1	0.899	1.112	0.578	0.521	0.642	0.340	0.242	0.477
MVP	1	0.901	1.110	1.169	0.978	1.398	1.702	1.347	2.151
MYL9	1	0.549	1.821	1.666	1.287	2.157	1.458	1.017	2.089
MYO10	1	0.815	1.227	1.060	1.013	1.109	1.932	1.500	2.489
OAZ2	1	0.820	1.220	0.855	0.833	0.877	1.004	0.759	1.327
OLFML3	1	0.879	1.137	0.324	0.323	0.324	0.205	0.128	0.327
PEA15	1	0.475	2.106	1.052	0.797	1.389	1.401	0.751	2.616
PLAT	1	0.597	1.676	1.912	1.719	2.125	9.789	7.575	12.651
POLR2A	1	0.638	1.566	0.872	0.480	1.584	0.913	0.723	1.154
PRG1	1	0.740	1.351	2.622	2.554	2.691	4.392	3.393	5.687
PRSS23	1	0.834	1.199	2.114	1.805	2.475	2.142	1.669	2.749
PSAP	1	0.759	1.318	1.230	1.064	1.423	1.171	0.828	1.656
PTGS2	1	0.629	1.590	1.808	1.674	1.952	1.924	1.365	2.712
ROR1	1	0.884	1.131	1.460	1.334	1.599	1.777	1.323	2.387
RPLP0	1	0.901	1.109	0.507	0.488	0.527	0.815	0.583	1.138
RTN4	1	0.872	1.147	1.280	1.118	1.466	2.092	1.381	3.168
S100A6	1	0.649	1.542	2.028	1.642	2.506	2.030	1.539	2.678
SERPINE1	1	0.640	1.562	2.046	1.887	2.219	2.591	1.857	3.615
SERPINE2	1	0.902	1.108	1.808	1.492	2.190	1.471	0.940	2.303
SHC1	1	0.795	1.258	0.803	0.719	0.896	1.132	0.887	1.444
SLC38A2	1	0.718	1.393	0.584	0.348	0.981	0.638	0.496	0.822
SOD1	1	0.902	1.109	1.212	1.075	1.366	2.429	1.573	3.751
SPARC	1	0.882	1.134	0.490	0.442	0.544	0.284	0.223	0.362
SRM	1	0.727	1.376	1.179	0.799	1.739	1.761	1.281	2.421
STAT1	1	0.659	1.519	1.891	0.969	3.692	3.348	2.342	4.786
STC2	1	0.834	1.199	1.720	1.298	2.280	2.335	1.812	3.009
TGFBI	1	0.901	1.109	0.615	0.553	0.684	0.675	0.254	1.795
TGM2	1	0.877	1.141	1.224	1.125	1.331	1.302	0.923	1.836
THY1	1	0.897	1.115	1.229	1.100	1.373	0.974	0.748	1.267
TM4SF1	1	0.846	1.183	2.477	2.178	2.817	5.859	4.579	7.497
TMEM47	1	0.808	1.237	0.818	0.544	1.229	0.890	0.568	1.396
TRAM2	1	0.834	1.199	1.363	1.342	1.384	1.429	1.112	1.835
TUBB6	1	0.830	1.204	1.340	0.983	1.826	1.170	0.404	3.386
UBC	Control								
VCP	1	0.902	1.108	1.121	1.024	1.228	1.624	1.040	2.535
VIM	1	0.889	1.125	0.877	0.795	0.966	0.839	0.635	1.107
WBSCR1	1	0.886	1.128	2.613	2.381	2.868	3.323	2.629	4.201
YIPF5	1	0.857	1.167	0.996	0.946	1.049	1.374	1.065	1.771
YWHAB	1	0.879	1.138	1.099	0.805	1.500	1.300	0.911	1.855

Table 10 TLDA results for donor 25 MSC's

Gene	Mean RQ P5 (n=8)	Std Dev.	P value	Mean RQ P9 (n=8)	Std Dev.	P value	P value RQ P5 v P9
ACTB	0.781	0.092	***	0.574	0.252	***	*
ADAMTS1	2.315	0.832	***	2.643	0.799	***	n.s
AKR1C1,2	1.231	0.358	n.s	2.169	1.563	n.s	n.s
ANXA2	1.049	0.486	n.s	0.866	0.359	n.s	n.s
APLP2	1.942	0.956	*	2.131	0.992	**	n.s
ARPC2	1.069	0.238	n.s	1.057	0.332	n.s	n.s
ATP5G3	1.114	0.182	n.s	1.402	0.530	*	n.s
BLVRB	0.972	0.133	n.s	0.999	0.415	n.s	n.s
BSCL2	1.035	0.109	n.s	1.184	0.298	n.s	n.s
CALM1,2	1.535	0.741	n.s	1.358	0.533	n.s	n.s
CAV1	2.430	0.669	***	4.026	1.759	***	*
CCND1	2.836	1.090	***	4.889	2.308	***	*
CCT7	1.041	0.179	n.s	1.129	0.393	n.s	n.s
CD44	2.605	0.870	***	3.490	1.462	***	n.s
CD63	1.276	0.253	**	1.495	0.394	**	n.s
CDKN1A	1.049	0.409	n.s	1.329	0.353	*	n.s
CDKN1B	0.823	0.141	**	0.761	0.189	**	n.s
CDKN2A	1.656	0.605	**	1.979	1.250	*	n.s
CEECAM1	1.207	0.256	*	1.196	0.286	n.s	n.s
CLIC1	1.149	0.264	n.s	1.123	0.230	n.s	n.s
COL1A1	1.217	0.469	n.s	0.976	0.683	n.s	n.s
COL1A2	1.551	0.627	*	1.287	0.951	n.s	n.s
COL3A1	0.922	0.331	n.s	0.947	0.454	n.s	n.s
COL5A1	1.246	0.548	n.s	1.620	2.033	n.s	n.s
COTL1	0.969	0.376	n.s	0.961	0.559	n.s	n.s
COX5B	0.969	0.118	n.s	1.034	0.290	n.s	n.s
CST3	1.229	0.288	*	1.573	0.603	*	n.s
CTGF	1.700	0.770	*	1.699	0.714	*	n.s
CTSS	0.283	0.314	***	0.356	0.293	***	n.s
DEGS1	1.179	0.156	**	1.197	0.384	n.s	n.s
DPYSL3	0.982	0.370	n.s	0.592	0.492	*	n.s
DSP	2.011	0.760	**	2.300	0.994	**	n.s
DUSP6	1.201	0.784	n.s	1.579	0.979	n.s	n.s
DVL1	1.376	0.327	**	1.445	0.445	*	n.s
ELN	1.283	0.582	n.s	1.216	0.804	n.s	n.s
FBXO18	1.037	0.190	n.s	0.957	0.165	n.s	n.s
FOS	0.549	0.206	***	0.582	0.229	***	n.s
FOXO3A	0.807	0.163	**	0.654	0.166	***	n.s
GAPDH	1.028	0.250	n.s	0.914	0.340	n.s	n.s
GARS	0.988	0.291	n.s	1.123	0.721	n.s	n.s
GPX4	1.016	0.173	n.s	0.836	0.194	*	n.s
HMGA1	2.295	1.479	*	3.249	2.699	*	n.s
HMOX1	0.743	0.371	n.s	0.502	0.107	***	n.s
HNF4A	Not detected after 40 cycles						
HSPA8	1.216	0.143	***	1.318	0.419	*	n.s
HTRA1	0.827	0.356	n.s	0.652	0.629	n.s	n.s
IFI30	0.731	0.390	n.s	0.845	0.620	n.s	n.s
IGFBP4	0.695	0.208	***	0.649	0.241	**	n.s

IL6ST	1.078	0.288	n.s	1.421	0.473	*	n.s
ITGA11	0.841	0.323	n.s	0.506	0.361	**	n.s
KDELR2	1.062	0.265	n.s	1.115	0.348	n.s	n.s
KIAA1199	4.951	1.516	***	4.621	2.534	**	n.s
KLF9	0.954	0.235	n.s	0.844	0.282	n.s	n.s
LMO7	1.395	0.406	*	1.400	0.428	*	n.s
LOC401152	0.954	0.297	n.s	0.806	0.163	**	n.s
LOXL1	1.025	0.292	n.s	1.102	0.694	n.s	n.s
LUM	0.870	0.085	***	0.900	0.576	n.s	n.s
MRC2	0.716	0.167	***	0.507	0.161	***	*
MVP	1.290	0.256	**	1.499	0.259	***	n.s
MYL9	1.727	0.712	*	1.625	0.528	**	n.s
MYO10	1.323	0.185	***	1.706	0.344	***	*
OAZ2	0.957	0.144	n.s	1.008	0.165	n.s	n.s
OLFML3	0.480	0.173	***	0.166	0.061	***	***
PEA15	1.279	0.218	**	1.300	0.259	**	n.s
PLAT	3.726	2.438	**	14.722	7.640	***	**
POLR2A	0.871	0.120	**	0.955	0.147	n.s	n.s
PRG1	1.818	0.536	**	2.812	1.076	***	*
PRSS23	1.944	0.579	**	3.223	2.110	*	n.s
PSAP	1.339	0.248	**	1.520	0.550	*	n.s
PTGS2	1.215	1.118	n.s	1.178	0.744	n.s	n.s
ROR1	1.948	0.316	***	2.161	0.576	***	n.s
RPLP0	1.178	0.429	n.s	1.054	0.469	n.s	n.s
RTN4	1.392	0.240	***	1.605	0.430	**	n.s
S100A6	1.644	0.428	***	2.005	1.063	*	n.s
SERPINE1	2.060	0.426	***	2.860	1.161	***	n.s
SERPINE2	2.274	0.773	***	1.943	1.315	n.s	n.s
SHC1	1.212	0.353	n.s	1.369	0.507	n.s	n.s
SLC38A2	1.221	0.375	n.s	1.003	0.484	n.s	n.s
SOD1	1.693	0.534	**	2.047	0.566	***	n.s
SPARC	1.030	0.505	n.s	0.773	0.332	n.s	n.s
SRM	1.250	0.377	n.s	1.266	0.569	n.s	n.s
STAT1	2.048	0.584	***	3.378	1.743	**	n.s
STC2	2.287	1.778	n.s	2.305	1.558	*	n.s
TGFBI	0.904	0.470	n.s	0.967	0.473	n.s	n.s
TGM2	0.919	0.553	n.s	1.303	1.262	n.s	n.s
THY1	1.282	0.200	**	1.086	0.627	n.s	n.s
TM4SF1	2.596	1.225	**	5.215	3.351	**	n.s
TMEM47	1.769	0.660	**	2.047	0.850	**	n.s
TRAM2	1.359	0.227	***	1.593	0.437	**	n.s
TUBB6	1.082	0.262	n.s	0.823	0.389	n.s	n.s
UBC	Control						
VCP	1.216	0.334	n.s	1.323	0.317	*	n.s
VIM	1.011	0.181	n.s	0.876	0.194	n.s	n.s
WBSCR1	1.651	1.153	n.s	1.716	0.913	*	n.s
YIPF5	1.319	0.389	*	1.334	0.496	n.s	n.s
YWHAB	1.220	0.207	**	1.224	0.223	**	n.s

Table 11 TLDA results for eight MSC cultures at passage five and nine

P - P value, * ≤ 0.05, ** ≤0.01, *** ≤0.001 and n.s, not significant

Gene	Mean RQ P9 DMSO Control (n=5)	Std Dev.	Mean RQ P9 SB203580 (1μM) (n=5)	Std Dev.	P value
ACTB	0.359	0.058	0.485	0.090	*
ADAMTS1	2.753	1.776	2.785	0.876	n.s
AKR1C1,2	1.249	0.498	1.067	0.787	n.s
ANXA2	0.786	0.288	1.063	0.264	n.s
APLP2	6.053	5.423	6.586	5.394	n.s
ARPC2	1.168	0.599	1.426	0.414	n.s
ATP5G3	1.225	0.540	1.568	0.615	n.s
BLVRB	0.666	0.149	0.837	0.064	*
BSCL2;HNRPUL2	1.084	0.214	0.887	0.168	n.s
CALM1,2	1.908	1.325	2.298	1.243	n.s
CAV1	5.619	5.076	3.646	1.054	n.s
CCND1	9.607	10.316	7.501	3.348	n.s
CCT7	1.105	0.423	1.294	0.316	n.s
CD44	3.884	2.783	4.796	0.964	n.s
CD63	1.895	0.704	1.786	0.431	n.s
CDKN1A	2.610	2.185	2.238	1.721	n.s
CDKN1B	0.967	0.598	1.305	0.783	n.s
CDKN2A	6.808	6.163	4.496	4.384	n.s
CEECAM1	1.811	1.106	1.860	1.036	n.s
CLIC1	1.168	0.478	1.386	0.264	n.s
COL1A1	1.553	1.436	1.336	0.986	n.s
COL1A2	2.160	1.859	1.948	1.520	n.s
COL3A1	1.104	0.938	0.869	0.626	n.s
COL5A1	6.230	9.970	4.700	6.717	n.s
COTL1	0.845	0.294	1.397	0.164	**
COX5B	0.676	0.230	0.763	0.420	n.s
CST3	1.622	0.558	1.726	0.585	n.s
CTGF	3.771	3.508	3.958	3.799	n.s
CTSS	0.255	0.295	0.211	0.227	n.s
DEGS1	1.414	0.669	1.365	0.420	n.s
DPYSL3	1.289	1.301	1.299	0.968	n.s
DSP	4.540	2.928	7.893	4.736	n.s
DUSP6	1.324	0.617	1.423	1.065	n.s
DVL1	2.377	1.487	2.908	1.722	n.s
ELN	1.006	0.672	1.190	1.122	n.s
FBXO18	1.006	0.247	1.096	0.309	n.s
FOS	0.452	0.486	0.484	0.323	n.s
FOXO3A	0.934	0.457	1.171	0.669	n.s
GAPDH	0.508	0.287	0.677	0.368	n.s
GARS	1.377	0.844	1.116	0.504	n.s
GPX4	0.593	0.247	0.552	0.074	n.s
HMGA1	4.638	5.436	10.445	9.350	n.s
HMOX1	0.471	0.227	0.501	0.290	n.s
HNF4A	Not detected after 40 cycles				
HSPA8	0.830	0.150	1.167	0.332	n.s
HTRA1	1.583	1.735	1.577	1.270	n.s
IFI30	0.692	0.489	0.786	0.375	n.s
IGFBP4	0.793	0.370	0.826	0.336	n.s
IL6ST	1.104	0.447	1.082	0.173	n.s
ITGA11	1.040	0.536	0.635	0.348	n.s
KDELR2	1.155	0.222	1.060	0.081	n.s
KIAA1199	7.833	6.631	12.194	10.958	n.s
KLF9	0.846	0.140	1.128	0.277	n.s
LMO7	1.840	0.850	2.329	1.154	n.s

LOC401152	0.971	0.480	1.214	0.404	n.s
LOXL1	2.054	1.547	2.578	1.643	n.s
LUM	1.032	0.391	0.549	0.109	*
MRC2	0.638	0.258	0.663	0.168	n.s
MVP	2.282	1.281	2.880	1.238	n.s
MYL9	2.165	0.964	2.333	0.872	n.s
MYO10	1.826	0.569	2.325	0.436	n.s
OAZ2	0.843	0.225	0.845	0.314	n.s
OLFML3	0.228	0.275	0.334	0.213	n.s
PEA15	2.381	1.216	2.498	1.286	n.s
PLAT	27.046	31.410	17.032	10.702	n.s
POLR2A	1.060	0.153	1.045	0.101	n.s
PRG1	3.313	2.194	2.698	0.807	n.s
PRSS23	3.717	1.694	2.365	1.245	n.s
PSAP	2.431	2.153	1.445	0.609	n.s
PTGS2	0.832	0.446	1.407	0.928	n.s
ROR1	2.324	1.109	2.534	1.142	n.s
RPLP0	1.429	1.418	1.801	1.406	n.s
RTN4	2.561	1.650	2.075	1.051	n.s
S100A6	1.819	0.745	1.462	0.469	n.s
SERPINE1	5.430	4.277	6.325	4.035	n.s
SERPINE2	4.468	3.560	1.866	1.442	n.s
SHC1	2.045	1.082	2.215	0.923	n.s
SLC38A2	1.295	0.847	1.244	0.873	n.s
SOD1	2.570	1.362	3.137	1.393	n.s
SPARC	1.576	1.458	1.222	0.793	n.s
SRM	1.303	0.758	1.560	0.636	n.s
STAT1	6.286	5.243	3.649	1.944	n.s
STC2	5.029	3.617	4.082	3.026	n.s
TGFBI	1.850	1.453	1.788	0.831	n.s
TGM2	2.398	1.990	5.029	4.798	n.s
THY1	1.262	0.282	2.113	0.440	***
TM4SF1	3.903	2.728	3.856	1.600	n.s
TMEM47	5.000	3.066	3.698	2.725	n.s
TRAM2	1.543	0.492	1.669	0.502	n.s
TUBB6	0.943	0.631	1.398	0.509	n.s
UBC	Control				
VCP	1.567	0.723	1.625	0.515	n.s
VIM	0.984	0.345	1.287	0.124	n.s
WBSCR1	2.143	1.282	2.225	0.720	n.s
YIPF5	1.300	0.434	1.331	0.282	n.s
YWHAB	1.156	0.299	1.339	0.087	n.s

Table 12 TLDA results for late passage MSC's treated with DMSO or SB203580

P - P value, * ≤ 0.05, ** ≤0.01, *** ≤0.001 and n.s, not significant